Molybdenum-containing oxidases and their application in cascade synthesis

Thesis submitted in accordance with the requirements of the University of Liverpool for the degree of Doctor in Philosophy

By

Shane Matthew McKenna

Table of Contents

Abstract

Molybdenum-dependent xanthine oxidoreducatases (XOR) are a family of well characterized enzymes which are known to oxidise purines, imines and aldehydes in cellular metabolism. Despite significant studies relating to drug metabolism, application to chemical synthesis is relatively unexplored..

Herein we report the first use of XORs in the cascade synthesis of carboxylic acids from activated and unactivated alcohols by the combination of the mutant alcohol oxidase GOase$M_{3\text{-}5}$ and XOR (*E.coli* XDH & PaoABC). Twenty five carboxylic acids were obtained in quantitative conversion and the methodology compares very well with state-of-the-art catalytic chemical oxidation methods. The reactions were performed in water at ambient temperature and pH using oxygen as the terminal oxidant with the only by-product being H_2O_2. The oxidation system was also applied to the synthesis of the biomass-derived platform chemical FDCA starting from HMF. The biocatalysts used were able to tolerate a substrate concentration of 100 mM, 20 times higher than previous reported methods with 74% isolated yield of FDCA. Although XORs exhibited a wide substrate scope, no chiral selectivity could be demonstrated.

The application of XOR enzymes was also demonstrated in the synthesis of lactams from amino alcohols *via* an *in situ* generated imine intermediate. Although pyrrolidone was obtained in 85% yield from its corresponding amino alcohol, longer chain amino alcohols were not well tolerated with either poor or no conversion observed. Although currently limited in substrate scope, this novel biomimetic oxidative cyclisation represents an interesting synthetic approach to lactams, found in a wide variety of biologically interesting target molecules.

Acknowledgements

I would like to thank Prof. Andrew Evans for offering me a position within his research group and also Dr. Andrew Carnell for allowing me join his research group in my second year of my PhD when Andy moved to Canada.

Andrew's encouragement, guidance and patience have been invaluable to me and has allowed me to become the chemist I am today. Your eagerness to help and your approachable nature, made working on the project a great joy! I really could not have done it without all our brainstorming sessions over coffee in your office. In addition I would like to thank Prof. Nick Turner, Prof. Silke Leimkühler and Prof. Rick Cosstick for helpful discussions and providing us with the enzymes used in this project.

I would also like to thank Dr. Sam Oliver, Dr. Ryan O' Connor, Dr. Tomas Baikstiss, Dr. Dan Tetlow and past members of the Evans group who showed me the ropes in Liverpool. The experience and work ethic I gained from working with you was vital to the success in my new project. The sink or swim philosophy worked! To my gym buddies Chris Riley and Paul McGillian, both of you took my mind off my research when times were tough. You were always willing to go for a quick pint or a sneaky gym session to relax (but it was never a sneaky leg session!). My masters students Shaun Hughes and Yannick Gama, it gave me great pleasure to watch you develop into very efficient chemists!

Additional thanks goes to Stephanie Yip. We both were in a similar situation with Andy moving to Canada and it was great to talk to someone that was going through the same thing as me. You were always there to listen to me moan about chemistry or if equipment was broken. Other members of the Carnell group, Cosstick group and Aïssa group and of course Adam Rolt, I could not of remained sane without you all!

I would like to thank my Mum, Dad and Evan for their unwavering support, love and encouragement. Thank you for pushing me to reach my goals. All those times you forced me to study when I was young paid off! All the Skype calls and Whats App messages really gave me a boost.

Finally Daisy, I really don't know how I would have done this without you. You constantly encourage me and supported me throughout my PhD. You always showed interest in what I was doing and would listen to me moan when chemistry didn't work. Your solution of adding Magnesium or when you told me enantiomers were overated still makes me laugh to this day. You always push me so I can reach my goals. For everything you have done for me I am eternally grateful.

Abbreviations

2-HA	2-Hydroxyacids
AAO	Aryl alcohol oxidase
ABTS	2,2'-Azino-bis(3-ethylbenzothiazoline-6-sulphonic acid)
AcOH	Acetic acid
ADH	Alcohol dehydrognenase
$AlCl_3$.	Aluminium chloride
aldDH	Aldehyde dehydrogenase
AldO	Alditol oxidase
AMOs	Alkane monooxygenases
AO	Aldehyde oxidase
AOX	Alcohol oxidases
ATP	Adenosine triphosphate
AZADO	2-Azaadamantane N-oxyl
BVMOs	Baeyer-Villiger monoxygenases
CALB	Candida antarctica Lipase B
CHMO	Cyclohexanone monooxygenase
CPMO	Cyclopentanone monooxygenase
CPO	Chloroperoxidase
CSA	Camphorsulphonic acid
D-AAO	D-amino acid oxidase
DCM	Dichloromethane
DCPIP	Dichlorophenolindophenol
DFF	Diformyl furan
DHIQ	Dihydroisoquinoline

DIBAL-H	Diisobutylaluminium hydride
DKR	Dynamic kinetic resolution
DMPU	3,3-Dimethyl-3,4,5,6-tetrahydro-2-pyrimidinone
DMSO	Dimethyl sulfoxide
E. coli XDH	Xanthine oxidase
epPCR	Error-prone PCR
EtOH	Ethanol
FAD	Flavin adenine dinucleotide
FCC	Flash column chromatography
FDCA	Furan-2,5-dicarboxylic acid
FFCA	5-formylfuran-2-carboxylic acid
GC	Gas Chromatography
GDH	Glycerol dehydrogenase
GOase	Galactose oxidase
HAPMO	4-Hydroxyacetophenone monooxygenase
HBT	*N,N'*-Bis-(1*H*-tetrazol-5-yl)-hydrazine
HCl	Hydrochloric acid
HCN	Hydrogen cyanide
Hex	Hexane
HMF	Hydroxymethyl furfural
HMFCA	Hydroxymethyl furan carboxylic acid
HMFO	Hydroxymethylfufural oxidase
IBX	2-Iodoxybenzoic acid
IPA	Isopropyl alcohol
KMnO4	Potassium permangante
KOH	Potassium hydroxide
KPi	Potassium phosphate

L-AAO	L-amino acid oxidase
LMS	Laccase mediator system
LC-MS	Liquid chromatography-Mass Spectrometry
LDA	Lithium diisopropylamide
LiAlH4	Lithium aluminium Hhydride
$LiBH_4$	Lithium borohydride
LiCl	Lithium chloride
LiH	Lithium Hydroxide
MAO-N	Monoamine oxidase
mCPBA	*meta*-Chloroperoxybenzoic acid
MeCN	Acetonitirile
MeOH	Methanol
MTBE	Methyl tert-butyl ether
$NaBH_4$	Sodium borohydride
NaCN	Sodium cyanide
NAD	Nicotinamide adenine dinucleotide
NADP	Nicotinamide adenine dinucleotide phosphate
NaH	Sodium hydride
NaOH	Sodium hydroxide
NMR	Nuclear magnetic resonance
NOX	NADPH oxidase
OYE	Old yellow enzyme
PAMO	Phenylacetone monoxygenase
PaoABC	Periplasmic aldehyde oxidase
PCR	Polymerase Chain Reaction
PET	Polyethylene terephthalate
RP-HPLC	Reverse phase high pressure liquid chromatography

SOD	Superoxide Dismutase
StyAB	Styrene monooxygenase
t-BuOK	Potassium tert-butoxide
TA	Transaminase
TBDMS	Tert-butyldimethylsilyl
TEMPO	2,2,6,6-Tetramethylpiperidinyloxy
TFA	Trifluoroacetic acid
THF	Tertahydrofuran
THIQ	Tetrahydroisoquinolines
TLC	Thin layer chromatography
TMSCN	Trimethylsilyl cyanide
UPO	Unspecific peroxygenase
UV	Ultra-violet

Chapter 1

1.0 Introduction

1.1 Biocatalysts in pharmaceutical and fine chemical industries

Biocatalysts are increasingly being used to catalyse key steps in synthetic routes to complex molecules of industrial interest[1-4]. Enzymes facilitate the synthesis of complex organic molecules by chemo- regio- and stereoselective bond forming and breaking reactions. The enantioselective and regioselective power of enzymes make them an ideal match for the pharmaceutical and fine chemical industry.

Thirty years ago the scope of biocatalysis did not extend far beyond esterification or hydrolysis. This was mainly due to the fact that the availability of enzymes was limited as efficient cloning systems were not available. However, today with the emergence of enabling technologies such as genome mining, directed evolution and homology modeling, this is no longer the case. Powerful C-C, C-N, C-O forming enzymes such as aldolases, hydroxynitralases, lyases and redox enzymes such as oxidases and reductases are now generally available[5-8].

The pharmaceutical market is one of the most important driving forces for innovation in biocatalysis. 54% of drug molecules are chiral and resolution remains an important and cost effective approach to chiral molecules[9]. With the emergence of enabling technologies such as large scale DNA sequencing, structural biology, protein expression, high throughput screening, directed evolution and metabolic engineering, biocatalysts can contribute significantly to the synthesis of active pharmaceutical ingredients (APIs)[10-12]. Incorporating biocatalysts can provide more efficient, atom economical and less hazardous synthetic routes, thus reducing capital costs.

Second generation manufacturing processes for pharmaceuticals requires substantial resources and so efficient catalytic methods are highly desirable. The first generation manufacturing process for the anticonvulsant drug, pregabalin (**1**) was executed as a racemic

synthesis, followed by a late stage classical resolution with mandelic acid. This was required to obtain the API in high optical purity (99.5%)[13]. Although this route was cost effective, there were possibilities for improvement such as the use of an early (as opposed to late stage) resolution of enantiomers but also recycling of the unwanted enantiomer. To this end, a chemo-biocatalytic route was developed for the second generation manufacturing process (Scheme 1).

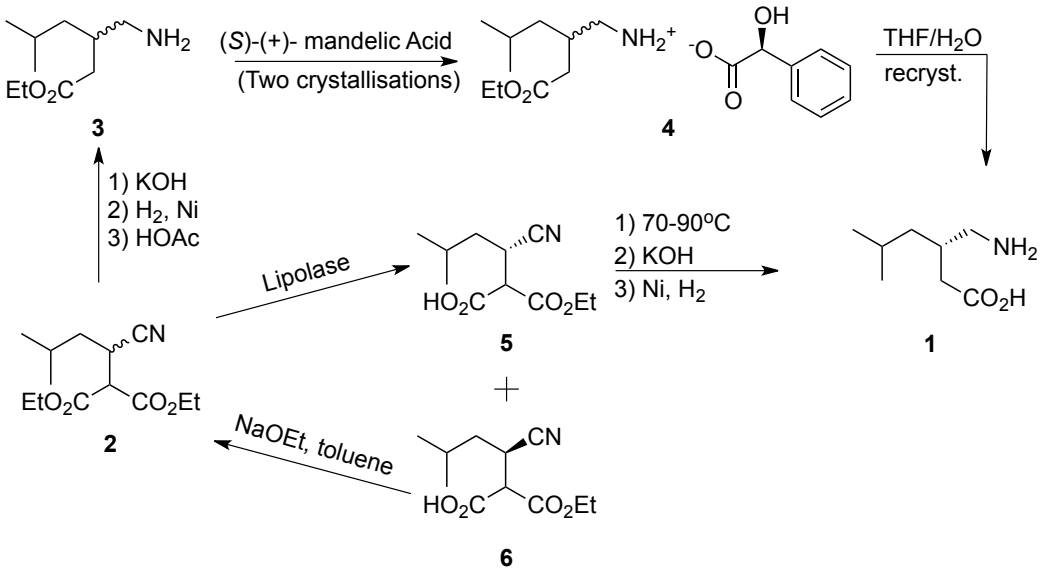

Scheme 1: Chemical *vs* biocatalytic synthesis of Pregabalin[13].

For the first generation synthesis, compound **2** was identified as a key intermediate which was converted to racemic ester **3** in a three step reaction sequence that includes hydrolysis, reduction and a decarboxylation step. The racemic pregabalin ester **3** was then resolved using (*S*)-(+) mandelic acid in a three-stage crystalisation procedure. However, due to the resolution step being carried out on a late stage intermediate, the overall efficiency of the process was poor. The use of hydrolases for the synthesis of chiral compounds has been extensively reviewed and their application at large scale has also been reported[14,15]. To increase efficiency, an enzymatic kinetic resolution using the commercially available Lipolase® was developed using the same key intermediate **2** previously used in the first generation synthesis. Stereospecific hydrolysis of **2** led to the mono acid **5** with 45% conversion and > 98% ee. With the kinetic resolution being carried out at an earlier stage, the unwanted enantiomer **6** could be

recycled by base-assisted racemisation of the nitrile. The elegance of this process is that the diastereoselectivity in the desymmetrisation at the prochiral C-2 center is irrelevant as the stereochemistry at C-2 is destroyed while converting **5** to Pregabalin **1**. Therefore the enatioselectivity of the kinetic resolution is more important. This new bio-chemo based synthesis combined with the recycling of unwanted enantiomer **6** resulted in higher yields of Pregabalin (40-45%), compared to the first generation manufacturing process (18-21%).

Another example of process improvement using biocatalysis was for the synthesis of atorvastatin **11**. Atorvostatin is the active ingredient in Lipitor. The key building block in the synthesis of atorvastatin (**11**) is ethyl (*R*)-4-cyano-3-hydroxybutyrate **7** (Scheme 2).

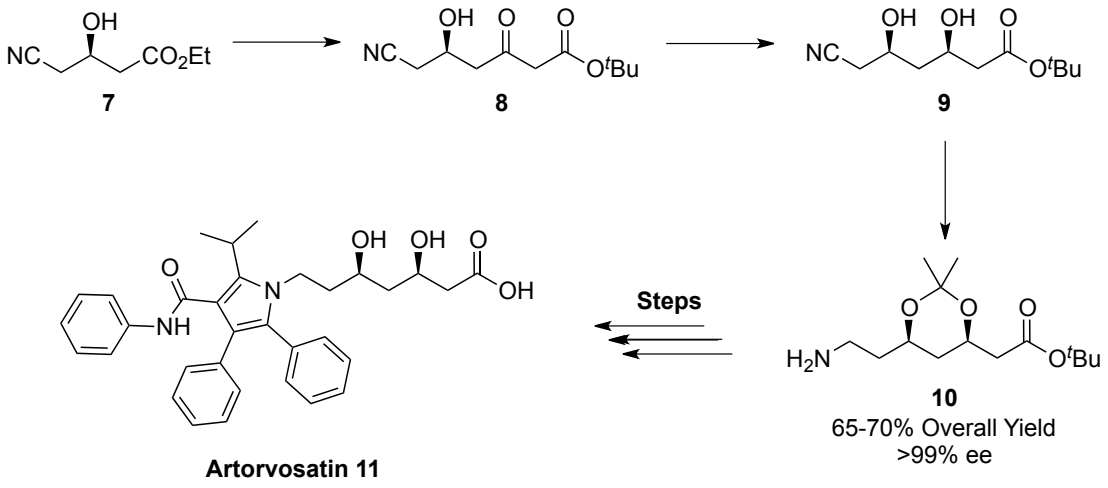

Scheme 2: Lipitor Synthesis[16]

First generation synthesis of **10** started with Claisen condensation of **7** to **8**, borane-chelation controlled reduction of **8** to **9** with both steps under cryogenic conditions, followed by acetal protection of the two hydroxyl groups and subsequent Ni-catalysed nitrile reduction to form **10**. Paal-Knorr condensation of **10** with a diketone provided the final API[16]. To replace the hazardous reagents, cryogenic conditions and mixed solvents used to furnish **9** from **8**, a reductase Ox-28 from *Candida magnoliae* was used as a lysate stabilized with IPA for the biotransformation. Upon reduction, the atorvastatin intermediate **9** was formed with 100%

diastereoselectivity compared to chemical methods, which furnished a mixture of *cis* and *trans* products (Scheme 3)[17].

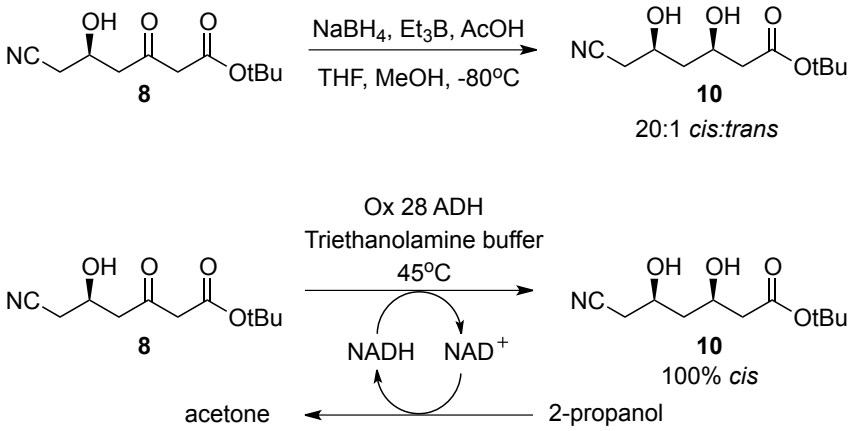

Scheme 3 Enzymatic reduction of intermediate **8**[17]

Further improvements of this process were made with the biocatalytic installation of the stereocenter and cyano functionality of the key building block hydroxy ester **7**. Although the original synthesis of **7** was high yielding, many toxic reagents such as sodium cyanide and HBr were used as well as harsh hydrogenation conditions[16]. To circumvent these harsh conditions, Dowpharma exploited the inexpensive starting material, epichlorohydrin **12** leading to an enzymatic desymetrisation of bisnitrile **13** (Scheme 4). The nitrilase was able to tolerate substrate concentration of 3M and the stereoselectivity of the biocatalyst was able to be tuned to 99% by applying gene site saturation mutagenisis[18]. This method led to a significant reduction of by-products, toxic wastes and organic solvents associated with chemical routes.

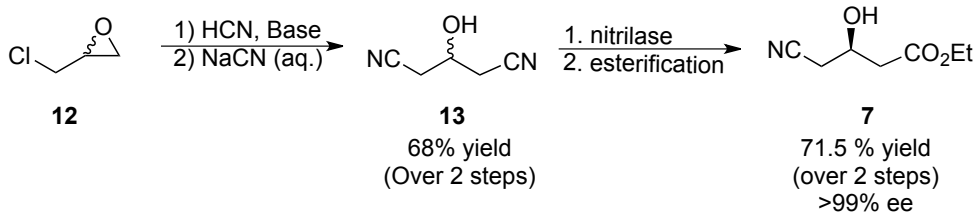

Scheme 4: Biocatalytic alternative to key intermediate **7**[18]

Biotransformations are also used to manufacture products on a scale of several 100s to 10,000 tons per year. Acrylamide is an important example where the chemical route has been abandoned and replaced by a biocatalytic approach. The chemical process for acrylamide involves the hydration of acrylonitrile by using copper catalysis at 70-120°C, resulting in large amounts of waste, including HCN. Under these conditions acrylamide tends to polymerise and undergo further hydrolysis to the acid. A hydralase of *Rhodococcus rhodochrous* J1 was able to produce acrylamide in higher yield at a concentration of 400g L^{-1} at 10°C. [19,20].

Overall the substitution of chemocatalysis by biocatalysis has many advantages in industry. Enzyme reactions are usually carried out at ambient temperature and pH. Organic solvents can be replaced with water and thus may provide a greener process. However, wild type enzymes often exhibit low industrial applicability as a natural enzyme often lacks substrate promiscuity and also will tolerate only low substrate concentrations. Moreover, enzymes can provide new synthetic routes by exposing synthons which cannot be obtained by classical chemical methods[21]. High chemoselectivity can circumvent the use of protection and deprotection stratagies and so atom economy can be satisfied as additional chemical steps are not required.

It is evident that a major driving force in biocatalytic innovation stems from the pharmaceutical and fine chemical industry. Green alternatives to chemocatalysts are required to provide sustainable synthesis of commercial products. However, extensive enzyme modifications are necessary to fine tune wild type enzymes for a chemical process by expanding their substrate scope or increasing their stability. To accomplish this task, it is necessary to understand the biological and chemical properties of these biocatalysts.

1.2 Biocatalysts

1.2.1 Enzyme Structure.

Enzymes are protein macromolecules that have an amino acid sequence, which is determined by the DNA sequence of the encoding gene. There are four distinct levels of protein structure; primary, secondary, tertiary and quaternary (Figure 1). The primary structure of the

enzyme consists of a defined sequence of α-amino acids linked together by amide bonds. Due to amino acids possessing both hydrogen bond donors and acceptors, hydrogen bonding occurs between residues and side chains giving rise to higher order secondary structure (α-helix and β-Sheet). The 3D structure of the protein is determined by its tertiary structure in which the protein adopts the conformation with the lowest ΔG in which the secondary structures are folded into a compact globular structure. This folding is driven by the burial of hydrophobic residues (aryl, alkyl chains) within the protein thus pushing the hydrophilic residues (-COOH, -OH, - NH_2, -SH, $CONH_2$) to the surface of the enzyme. Other non-covalent interactions such as salt bridges, van der walls interactions, π-π stacking and also covalent disulfide bonds contribute to the stability of the proteins tertiary structure.

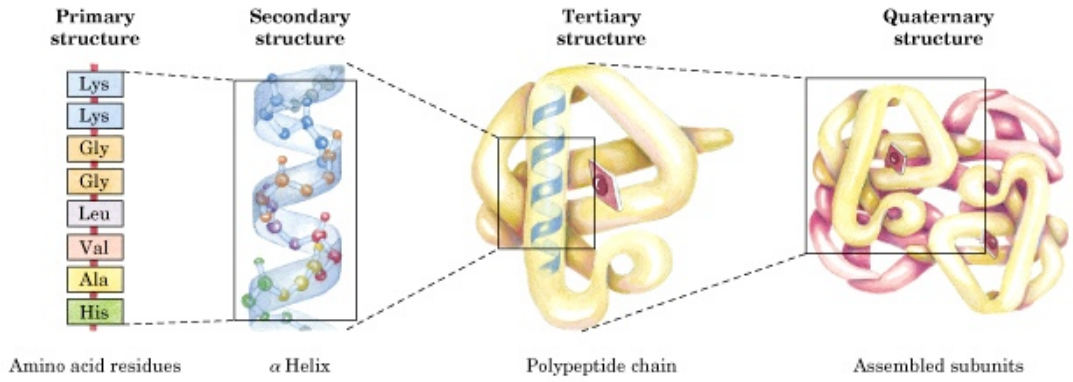

Figure 1 Illustration of primary, secondary, tertiary and quaternary structure.[22]

Finally, some enzymes possess quaternary structure. Quaternary structure is the three dimensional structure of a multi subunit enzyme and how it fits together. These subunits interact with each other with the same non-covalent interactions and disulfide bonds as tertiary structure.

Due to the weak forces holding the enzyme together, they are unstable in solution and can be deactivated easily by denaturation as a result of high temperature, salt concentration and extreme pH[23]. Functional groups of amino acid side chains asparagine and glutamine can be hydrolytically cleaved to give aspartic acid and glutamic acid respectively. As a result a new

negative charge is created from a neutral group of the enzyme ie $–COO^-$ from $–CONH_2$ and in order to become hydrated it forces a rearrangement of the enzyme's structure. Thiol groups may also interchange with disulfide groups and finally elimination and oxidation reactions will also force permanent conformational change in the enzyme resulting in irreversible deactivation. Many enzymes are stable to high temperature and also to organic solvents[24]. These enzymes possess fewer asparagine and more salt or disulfide bridges, which increase their stability.

1.2.2 Mechanistic aspects of biotransformations

Enzymes are remarkable catalysts and their rate enhancements range 5-17 orders of magnitude. The distinguishing feature of an enzyme catalysed reaction is that the reaction takes place in a confined space in the enzyme called an active site. The surface of the active site is lined with different amino acid residues and sometimes metals and organic cofactors which interact with the substrate and catalyse chemical reactions.

As in every catalytic reaction, an enzyme accelerates the rate of reaction without affecting the equilibrium. A simple enzymatic reaction can be seen in Figure 2.

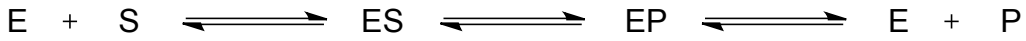

Figure 2 Simple enzymatic reaction where E = Enzyme, S = Substrate, ES = Enzyme-substrate complex, EP = Enzyme-product complex and P = Product

Any reaction, chemical or biocatalytic, can be described by a reaction coordinate diagram (Figure 3). The starting point for either the forward or reverse reaction is called the ground state. If the difference between the free energies of the substrate and product is negative then reaction favors product formation. However, favourable equilibrium does not necessarily mean conversion will occur at a detectable rate.

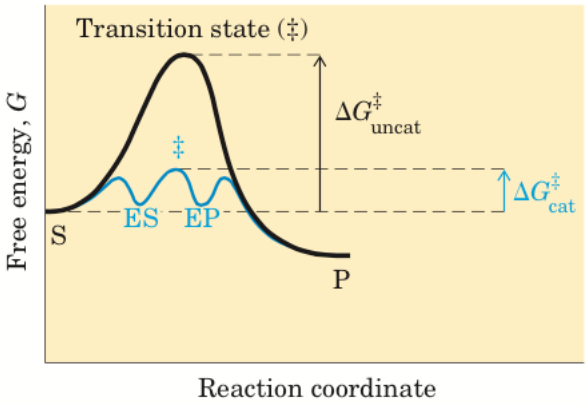

Figure 3 Reaction coordinate diagram comparing enzyme catalyzed and uncatalysed reaction[22]

Enzymes lower the activation energy by stabilising the transition states or by supplying an alternative reaction pathway. Lowering the activation energy of the system will allow the reaction to progress faster, increasing the reaction rate. Computational models suggest that transition state stabilisation is the largest contribution to catalysis by enzymes[25].

In 1984, Emil Fischer proposed the lock and key mechanism[26]. He believed that enzymes are structurally complementary to their substrate. Given his rationale, substrates smaller than the natural substrate should have a higher rate of reaction due to a larger active site. However this is not the case. Furthermore an enzyme completely complementary to its substrate would be a very poor enzyme as shown in Figure 4 (a). In order to accommodate the transition state, covalent bonds need to rearrange. However, this would not be possible and the substrate may not be able to escape the ES complex which has a negative ΔG. A more feasible mechanism in which enzyme must be complementary to the transition state was proposed by Haldau (1930). The new [ES] has a positive ΔG and so will not be trapped in the active site. Additional energy is required however to turn S into P. This energy requirement is paid for in binding energy.

Binding energies are a major source of free energy used by enzymes to lower the activation energies of reactions. Enzymes are at least 100 times larger than common chemical catalysts. This allows enzymes to totally engulf their substrate and position their catalytically active residues close to the substrates reactive group, thus reducing entropy

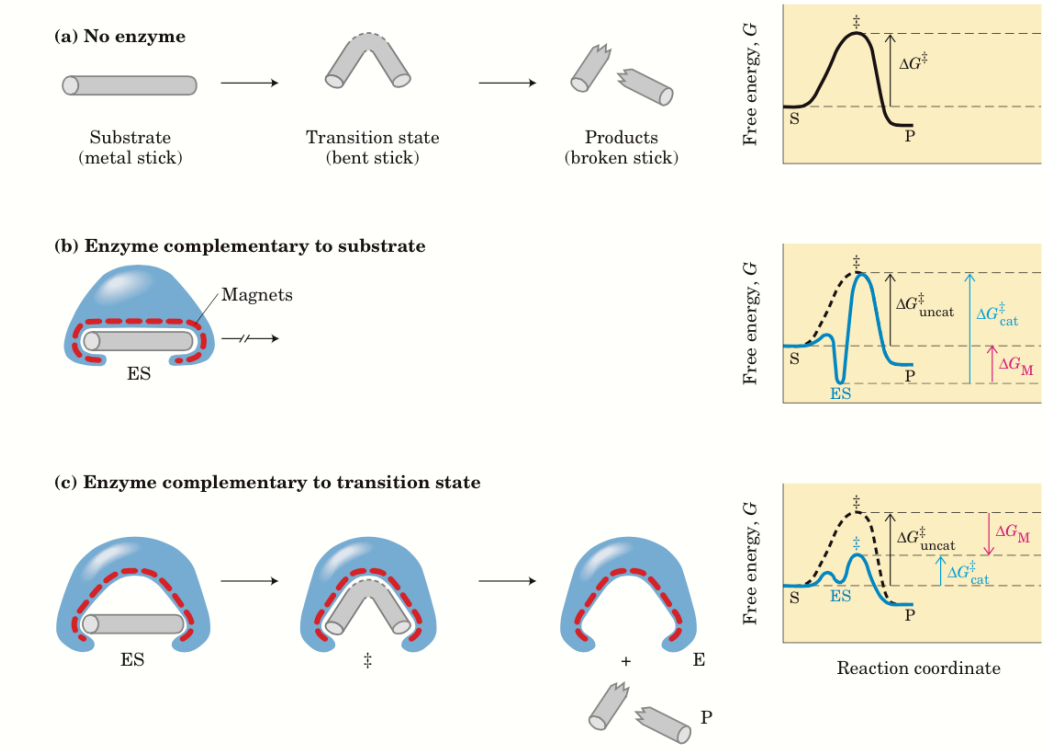

Figure 4 A) Representation of an uncatalysed reaction. B) Enzyme with active site complementary to substrate. C) Enzyme with active site complementary to transition state[22]

Constraining the motion of reactants has many rate enhancement affects. A chemical example of this is intramolecular vs intermolecular substitution reactions. Also the formation of weak bonds between substrate and enzyme results in desolvation of the substrate. Enzyme-substrate interactions replace most or all hydrogen bonds between substrate and water. Finally the enzyme itself can undergo a conformational change. On approach of the substrate, the enzyme can change its conformation and make the binding site more complementary to the substrate. This is known as the induced fit model and was postulated by Daniel Koshland[27]. Induced fit serves to bring specific functional groups of the enzyme into contact with substrate to catalyse the reaction (Figure 5).

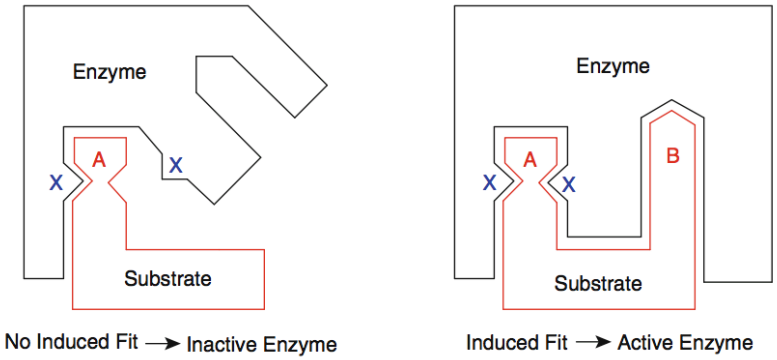

Figure 5 Induced fit model

Once a substrate is bound to an enzyme, properly positioned catalytic functional groups aid the cleavage and formation of bonds. These interactions provide an alternative low energy reaction path which lowers the activation energy further. Amino acid residues such as Glu, Asp, Cys, His, Ser and Tyr can participate in acid-base catalysis and also as nucleophiles or electrophiles creating transient covalent bonds. The active site can also contain metals that can stablise the transition state via ionic interactions or can participate directly in oxidation or reduction pathways.

The binding energy that provides energy for catalysis discussed previously also gives rise to the enzyme specificity. Anabolic enzymes are known to have quite high substrate specificity whereas catabolic and detoxification enzymes tend to be broader.

The space restriction imposed by enzymes in their active site also give rise to high chemo- regioselectivity but also enantiodescrimination which has been rationalized by three point attachment rule first postulated by O. G Ogston[3]. In the active site, the substrate has to be positioned to ensure spatial recognition and high enantioselectivity. As a result, three points of contact with stabilising groups on the active site is required (Figure 5). Enantiomer A represents an sp^3 carbon atom and enantiomer B its mirror image. If the active site is complementary to the substrate then optimal binding of the reactive group and efficient catalysis due to the stabilisation of its transition state will be observed as shown by enantiomer A. However, if the there is uncomplementary binding as is the case of enantiomer B, then poor catalysis will be

observed as the activation energy can not be sufficiently decreased and the reaction of one enantiomer will dominate over the other. Prochiral, sp^2 carbons[28] and also sp^3 heteroatoms such as phosphorous or sulfur can be subject to this principle [29].

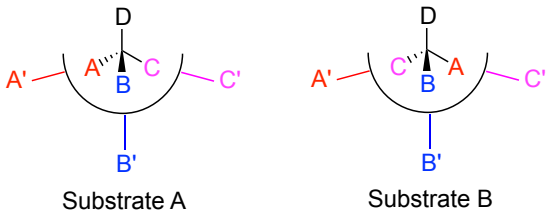

Figure 5 Illustration of enantiomeric recognition by enzyme active site.

1.2.3 Isolated enzymes *versus* whole cell biocatalysts

Biocatalysts can be applied in many forms, either as pure isolated enzymes or as part of a whole cell system. Enzymes utilized in the 1960s were largely restricted to use in whole cells. However, with the emergence of efficient protein purification techniques, the possibility of using purified enzymes was realised. The final decision on which biocatalyst preparation to employ depends on the type of reaction, the co-factors required, reaction scale and price.

A proportion of synthetically useful enzymes require co-factors that provide redox equivalents (NAD^+/$NADP^+$, NADH/NADPH) or chemical energy (ATP)[3]. When co-factor dependent enzymes are employed as biocatalysts, the stoichiometric addition of their respective co-factor is required when using isolated enzymes. However, this addition is expensive and the stability of NADPH in solution is low. To this end a whole cell biocatalyst has the distinct advantage in that cofactors are regenerated within the cell by microbial metabolism. Other important protecting enzymes are also present within the cell which act as a shield against toxic side products such as hydrogen peroxide which may destroy the activity of isolated enzymes[3].

Isolated enzymes are easy to use, often as either lyophilized powder or as a solution. Reactions generally proceed with significantly higher reaction rate when compared with whole cell reactions. This advantage, when coupled with easy product removal (due to the elimination of cell debris), can make the use of isolated enzymes extremely efficient. For redox enzymes, a

number of cofactor regeneration strategies have been developed so that only catalytic amounts of the cofactor is required[30,31].

$NAD(P)^+$ is required in many enzymatic oxidation processes and its regeneration is crucial when using isolated enzymes. When using ADHs, an excess of sacrificial ketone allows sufficient regeneration of $NAD(P)^+$ however with the generation of large amounts of alcohol co-product[32]. More elegent and atom economical alternatives however have also been developed using NADH oxidase as the regeneration catalyst[33]. NADH oxidases utilise oxygen as the terminal oxidant and thus the generates water and hydrogen peroxide as the co-product (Scheme 5).

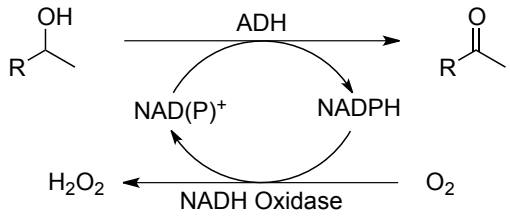

Scheme 5 Co-factor regeneration stratagy using NADH Oxidase with an ADH

1.2.4 Limitations of biocatalysts

As mentioned previously enzymes can possess extraordinary chemo-, regio- and enantioselectivity. However, there are a number of drawbacks associated with the use of wild type enzymes.

Most enzymes function at ambient temperature and pH, which can be a limitation. For example, the reaction rate of a chemical reaction is too slow at a given temperature. Increasing temperature or extreme pH can have a detrimental affect and lead to denaturation although there are exceptions where this can be beneficial[34].

The use of water as solvent allows enzymes to display their highest catalytic activity but the majority of organic molecules are poorly soluble and so only very low substrate concentrations are possible. The use of organic solvents is desirable to allow high concentrations of substrate but at a loss in catalytic activity[35].

Enzymes are prone to substrate and product inhibition phenomenon, which causes a

drop in reaction rate at high substrate and/or product concentration. Substrate inhibition can be easily addressed by keeping substrate concentration low, however product inhibition is much more difficult to address.

Despite enzymes showing remarkable enantioselectivity for a single enantiomer it is often very difficult to obtain the opposite enantiomer. In chemical asymmetric catalysis, switching the chiral ligand from (*S*) to (*R*) will allow a switch in enantioselectivity. However, this approach is not possible for enzyme reactions.

To combat these limitations, protein engineering has emerged as a useful and efficient tool to optimize and remove the limitations of wild type enzymes. Substrate scope, reaction rate, enantioselectivity, regioselectivity, chemoselectivty and enzyme stability can all be improved by protein engineering.

1.3 Enzyme optimization

Despite the clear advantages of enzymes, further improvement of their substrate scope, activity, stereoselectivity are paramount to their broader appliciations on an industrial scale. To address these challenges, protein engineering by rational design has provided numerous successful solutions. Directed evolution has become a method of choice in tackling many of these issues however genome mining is becoming an increasingly popular alternative.

1.3.1 Directed Evolution

Directed evolution involves repeating cycles of gene mutagenesis, expression and screening of mutant enzyme libraries in an overall process that simulates natural evolution (Figure 6)[36]. The availability of a suitable high throughput screening of mutants is critical to the success of this approach, particularly when using random or semi-random approaches that result in large libraries of mutants.

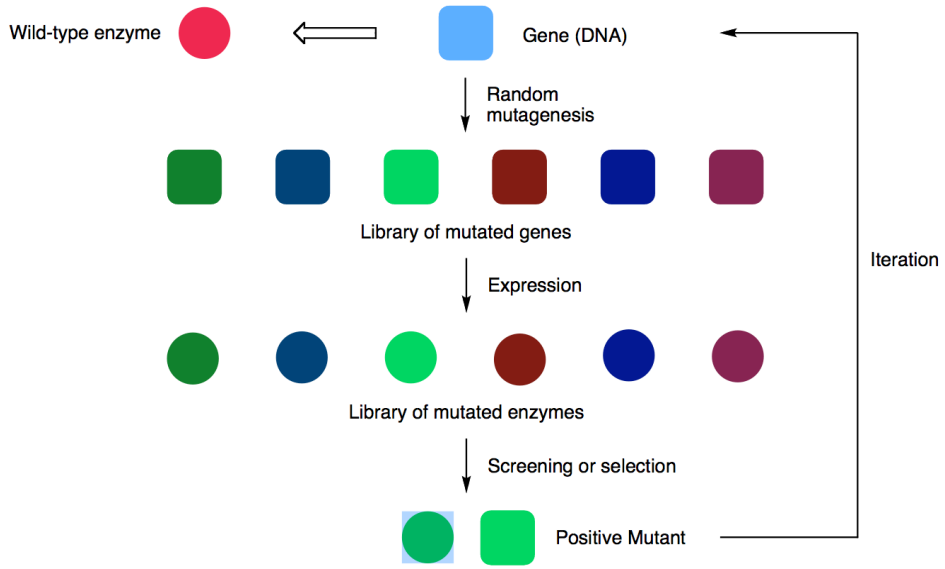

Figure 6 General directed evolution strategy[36].

1.3.1.1 Directed evolution techniques

The Polymerase Chain Reaction (PCR) has emerged as a very powerful gene amplification technique and can be modified for the introduction of random or specific mutations into a target gene[36].

When the experimental conditions of PCR are altered with the addition of $MnCl_2$ or increasing $MgCl_2$ concentration, 2-3 wrong base pairs are incorporated into each replicated DNA strand. This technique is called error-prone PCR (epPCR) which targets the entire gene. Additionally bacterial mutator strains can be used in which natural mutation is enhanced. These approaches have the advantage that structural data for the enzyme is not required.

In contrast to epPCR, oligonucleotide-based saturation mutagenesis involves combinatorial randomization at predetermined sites. However, this requires structural information on the enzyme. For improvement of enantio-, regioselectivity and substrate scope, the enzyme's active site is the logical choice for mutations.

Another gene mutagenesis method is termed DNA shuffling. A family of homologous mutated genes are digested by DNase to provide double stranded oligonucleotide fragments that

are then ligated to reassemble full length mutant genes (figure 7.0). This allows back shuffling for recombination of mutually beneficial mutations

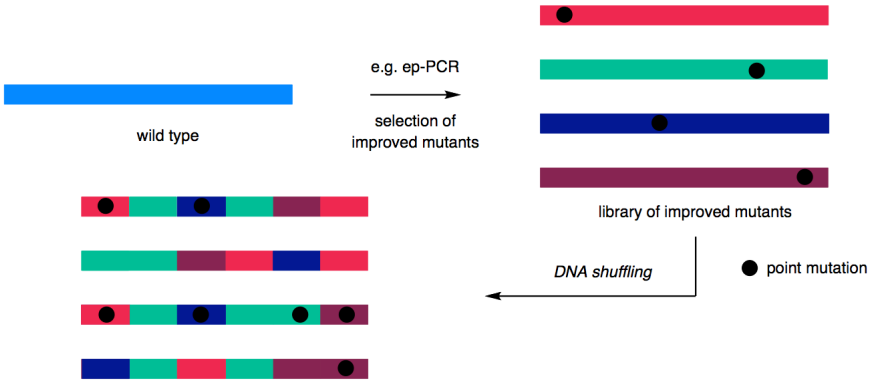

Figure 7 Illustration of DNA shuffling techniques[36]

1.3.2.2 Selected examples of directed evolution

Low thermostability is a major limiting factor for industrial application of biocatalysts. Using epPCR and adding thermal stress to screening processes, mutant laccases were identified with improved thermostability[37]. The thermostability of CALB was also improved by rational mutations based on the crystal structure. Hotspot residues were identified by using B-Fit analysis which resulted in improved thermostability at 60°C[38].

Fine tuning enzyme enantioselectivity is challenging considering the small relative differences in energy barriers for the activated enzyme-substrate complex between stereoisomers. Therefore, rationally designing the enzyme active site through successive single amino acid mutations may not provide the desired results. In general, simultaneous mutations tend to show synergistic effects rather than additive and so pairs of amino acids are altered in a process known as CASTing. By applying this methodology, CALB was evolved to hydrolyse stereocomplementary α-substituted carboxylic esters such as 2-arylpropionic acids[39]. CASTing was also used to engineer alcohol dehydrogenase for the asymmetric reduction of prochiral ketones such as 4-alkylidene cyclohexanones to produce axially chiral (*R)*-configured alcohols in excellent ee (>99%)[40].

1.3.2 Genome mining.

Database mining is another promising strategy to discover new enzymes based on genomic and enzyme structure information[41]. Large amounts of sequence information have been deposited in public databases, for example NCBI has more than 6000 genomes and 110 million protein sequences. Systematic mining of such databases with bioinformatics tools allows the identification of additional enzymes and homologs of characterized enzymes. In addition, software such as 3DM has been developed for the accurate homolog-based structure prediction[42].

1.4 Enzymatic oxidations

Oxidation reactions represent a cornerstone of organic chemistry providing access to functional groups such as aldehydes, ketones carboxylic acids, imines and amides. Traditionally, many of these oxidation reactions have been performed using stoichiometric amounts of toxic transition metal based oxidants[43]. Despite the high selectivity and product purity associated with these methods, the applicability of stoichiometric toxic and dangerous reagents in fine chemicals and pharmaceutical industry is low, as the modern world shifts to green manufacturing[44].

The term green chemistry was coined in the early 1990s and the concept is paraphrased in the following 12 principles[45].

1) Waste Prevention

2) Atom efficiency

3) Less hazardous/toxic chemicals

4) Safer products by design

5) Innocuous solvents and auxiliaries

6) Energy efficient by design

7) Preferably renewable materials

8) Shorter Synthesis

9) Catalytic reagents

10) Design products for degradation

11) Analytical methods for pollution prevention

12) Inherently safer process

Green chemistry efficiently utilizes raw materials, eliminates waste and avoids the use of toxic and hazardous reagents and solvents. To be able to compare the greenness of a reaction, the E-Factor developed by Sheldon, represents a simple metric to initially assess the environmental impact.

Biocatalysts have many benefits to offer green chemisty especially for oxidations. Reactions are performed under mild reaction conditions (physiological pH and ambient temperature and pressure) with a biodegradable biocatalyst using oxygen as a terminal oxidant and producing water as by-product. In addition reactions of multifunctional molecules proceed with chemo-, -regio and stereoselectivity generally without the need of protecting groups. This can afford a process that is much more step economic with less waste generated resulting in better E-Factor ratings. This being said, a general green claim cannot be made for biocatalysis since the environmental impact has to be assessed on a case by case basis.

Enzymatic oxidations have been extensively explored in the last 20 years with many green alternatives emerging when compared with classical oxidation methods[46,47]. Alcohol, aldehyde and amine oxidations are all possible using a range of metal free biocatalysts. Additionally, selective C-H activation is now possible using heavily engineered cytochrome P450 hydroxylases.

1.4.1 Enzymatic alcohol oxidation

Oxidation of primary and secondary alcohols to their corresponding aldehydes, ketones and carboxylic acids are among the most important reactions in organic chemistry. Classical chemical oxidising reagents employ toxic metals and include Jones, Sarrette and Collin's reagents. Explosive hypervalent organoiodine reagents (Dess-Martin, IBX) and sulphur

oxidations (Swern, Corey-Kim) are available as a metal-free alternative. Other limitations of these oxidants include poor regioselectivity and stereoselectivity[4].

With green principles [45,48] in mind, developments have been made to provide more environmentally friendly oxidations. Extensive research has been carried out in the use of gold nanoparticles and also *N*-oxo-ammonium salts such as TEMPO and its derivatives. State of the art oxidation of unactivated alcohols has been reported recently by Milstein[49] with a novel Ru based catalyst in refluxing water. Despite being inherently green the reaction suffers from high temperature, tricky experimental set up, expensive catalyst and side reactions which limit its generality. Molecular oxygen is an ideal oxidant but the application of chemocatalysis to realize this at ambient temperature and pressure has not yet been realized[50].

A variety of different enzymes (dehydrogenases, oxidases, laccases, peroxidases) are available for biooxidation of alcohols. Alcohol dehydrogenases (ADHs) are the most extensively studied catalyst for the oxidation of alcohols[3,51]. Dehydrogenases are $NAD(P)^+$/NAD(P)H dependent oxidoreductases that catalyse freely reversible redox processes in which both oxidized or reduced products are obtainable, depending on the cofactor present. For oxidation processes, excess $NAD(P)^+$ is necessary. The nicotinamide pyridinium is the active oxidant in abstracting a hydride from the carbinol group. (Scheme 6).

In many cases however ADHs have been used in reduction mode for the generation of enantiomerically pure alcohols[2,3,52]. Another class of oxidation enzymes is the alcohol oxidases (AOX), although they are not widely distributed in nature. Galactose oxidase (GOase) is a Cu^{2+} oxidase requiring molecular oxygen as its terminal oxidant[53,54]. However, this enzyme displays limited substrate scope without protein engineering. The flavin-dependent alcohol oxidases are much more prevalent in the literature and accept a variety of aromatic and aliphatic alcohols[55-57].

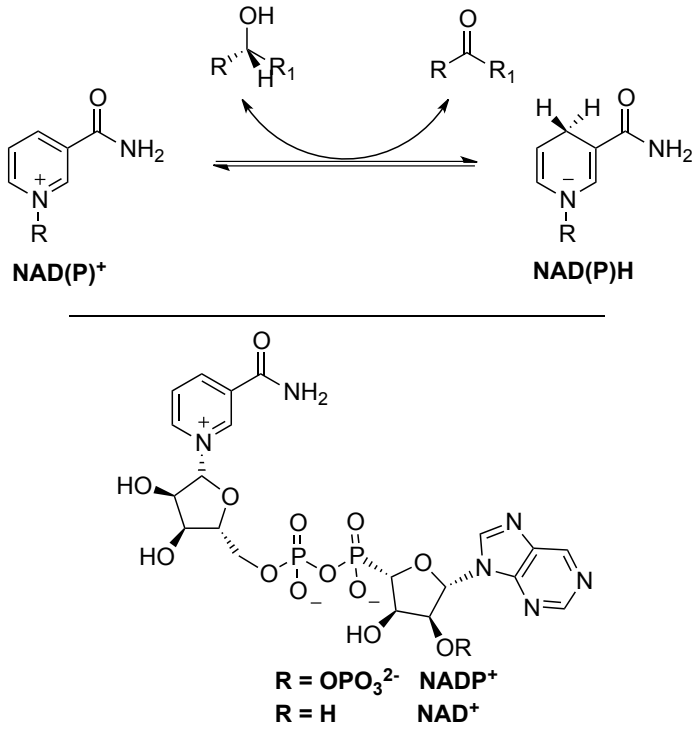

Scheme 6 Reversible redox chemistry of NAD(P)H cofactor used by alcohol dehydrogenases

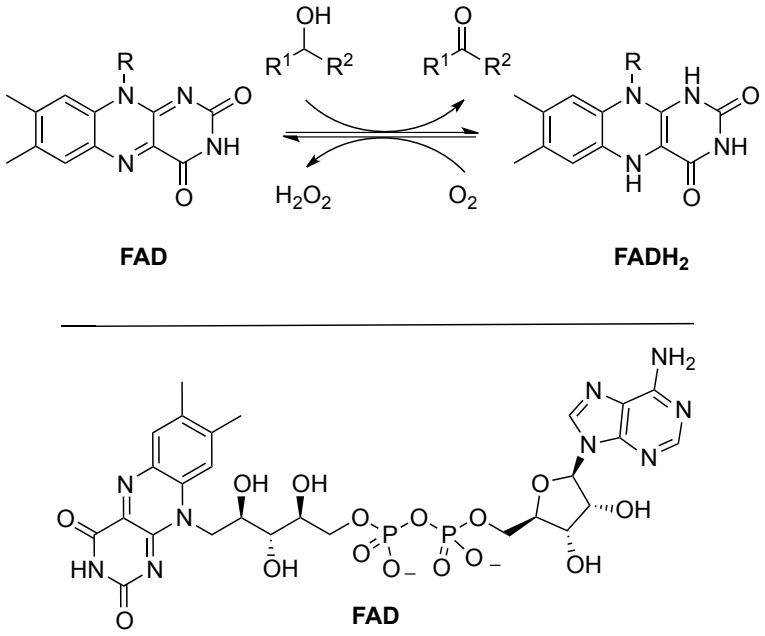

Scheme 7 Interconversion of reduced and oxidised FAD

The flavin moiety acts as a primary hydride acceptor in which excess reducing equivalents are shuttled to molecular oxygen (Scheme 7). Oxidases have the advantage over dehydrogenases in

that molecular oxygen is used as the terminal oxidant. Finally, laccases belonging to the blue copper oxidases and catalyse hydrogen abstraction reactions from phenoxy radicals[58]. These phenoxy radicals can regenerate an oxidized mediator which then carries out subsequent oxidation reactions.

1.4.1.1 Biooxidation of primary alcohols to carboxylic acids.

The 'through' oxidations of primary alcohols to carboxylic acids has been dominated by the use of microbial whole cells rather than isolated enzymes perhaps due to the fact that whole cells guarantee the regeneration of $NAD(P)^+$ which is necessary to shift equilibrium to oxidized products. *Acetobacter* possessing alcohol dehydrogenase (ADH III), has been utilized in a number of alcohol oxidations. The Orleans process, for the production wine acetic acid from ethanol was the first example of such a biotransformation in 1670. Ethanol is oxidized by ADH III into acetaldehyde and an additional cell bound enzyme, aldehyde dehydrogenase (aldDH) immediately oxidises the aldehyde to acetate. This process was applied to the preparation of a number of carboxylic acids starting from the corresponding primary alcohol on a multigram scale (Scheme 8)[59,60]. Interestingly, these fermentation reactions showed chiral selectivity for certain substrates and thus kinetic resolution of racemic primary alcohols including solketal [61,62], glycidol[62] and 2-phenyl-propanol[63] have been performed using whole cells expressing ADHs (Scheme8) .

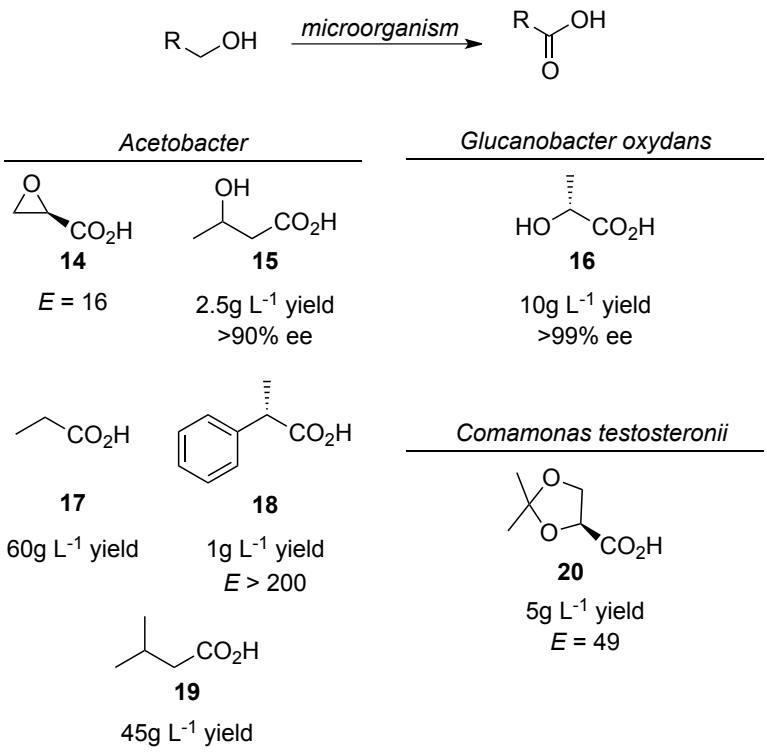

Scheme 8 Selected examples of products obtained on a gram scale through oxidation and kinetic of various alkyl and aromatic alcohols catalyzed by whole cell biocatalysts[61,62,64,65]

Isolated alditol oxidase (AldO) from *Streptomyces coelicolor*, an FAD dependent oxidase, has successfully facilitated the oxidation of a number alditol substrates[66] to their corresponding aldehydes, however in the case of aromatic and aliphatic 1,2 diols, hydroxy acids were formed, showing remarkable regioselectivity albeit with low conversion. AldO does provide an attractive alternative to glycerol dehydrogenase[67] for the kinetic resolution of diols as the reaction does not require expensive co-factors and uses molecular oxygen. The main limitation of such a kinetic resolution process is that the maximum yield of the desired enantiomer is limited to 50%.

Another interesting application of through oxidations is shown in the oxidative lactonisation of symmetrical diols using purified ADH. This desymmetrisation approach has an advantage over classical kinetic resolutions as potentially 100% yield of the required enantiomer is possible. The purified ADH is not active towards aldehydes. However, if intramolecular hydroxyl groups are present, lactol formation can occur followed by oxidation to

the lactone (Scheme 9). A number of 1,4 and 1,5 symmetrical diols have been desymmetrised using isolated ADH[68,69] and more recently valerolactone derivative **25**[70] have been prepared using horse liver ADH (HLADH) and the appropriate $NADP^+$ regeneration system. These examples highlight how the meso-trick can result in high conversions and enantioselecivity.

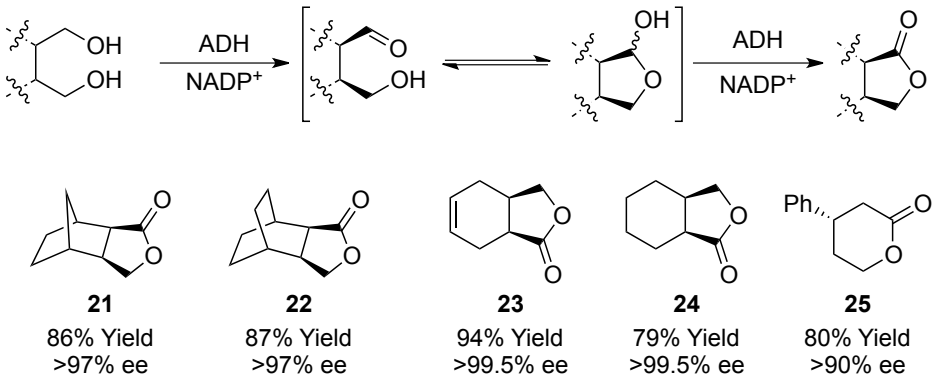

Scheme 9 Desymmeterisation of 1,4 and 1,5 diols by isolated ADH[68,69]

1.4.1.2 Oxidation of primary alcohols to aldehydes

Molinari[63,64] has published many papers documenting whole cell ADH-catalysed biotransformations of alcohols. However, it is difficult to stop the oxidation at the aldehyde stage due to the presence of other enzymes including aldehyde dehydrogenases. Microbial screening of various acetic acid bacteria identified a strain, *Gluconobacter oxydans* R, in which aldehyde oxidation was diminished, however limited substrate specificity was observed[64]. In addition, large scale microbial screening of various bacterial and yeast strains has been a powerful tool in identifying novel biocatalysts for the chemoselective oxidation of primary alcohols[71]. 218 lyophilised microbial strains have been tested for their ability to oxidise benzyl alcohol in buffer and the result was an extremely powerful chemoselective biocatalyst *Janibacter terrae* DSM 13953 with no benzoic acid being observed. Lyophilised cells from *Janibacter terrae* have since been employed for the oxidation of substituted benzyl alcohols, *n*-alkanols, and allylic alcohols in excellent conversions >95% of high substrate concentration (96mM) using acetaldehyde as hydrogen acceptor. However, steric interactions have a major

affect on conversions with *o*-substituted benzyl alcohols giving poor conversions in most cases[72]. The screening of microbes with diminished aldehyde oxidising activity is a labour intensive task and to this end simpler approaches have been developed to counteract 'through' oxidation.

Reaction engineering can avoid the through oxidation of alcohols, namely by the addition of a second hydrophobic organic layer to remove the aldehyde intermediate. The biphasic system allowed a range of primary aldehydes to be prepared in good conversion by acetic acid bacteria (Scheme 10) [73]. Moreover, the carboxylic acids could be obtained in high conversions if the biphasic system was substituted for the regular buffered aqueous system. However, the major limitation that the substrate scope is extremely narrow and no aromatic substrates are accepted. As mentioned previously, aldehyde oxidation is a result of endogenous aldehyde oxidases/dehydrogenase and good results have been obtained from microbial screening of strains with diminished oxidase activity. An alternative to finding 'what nature has provided' is by using genetically modified whole cells which have the problematic enzymes knocked out. This would allow alcohol oxidation only. However, as demonstrated by Wu, genetically modified *Gluconobacter oxydens* benefited from both the biphasic system and genetic modification, oxidizing the aromatic benzyl alcohol to benzaldehyde in 100% conversion after 1 hour[74] and so the combination of multiple solutions to this problem seems promising.

The use of isolated ADHs eliminates the over oxidation alcohols but NAD(P)H regeneration strategies need to be incorporated into the biocatalytic process to drive the equilibrium towards oxidation products. After seminal work by Bryan Jones[75], alcohol dehydrogenase from horse liver (HLADH) was identified as an exciting enzyme with great synthetic potential. As already shown, HLADH shows high selectivity towards meso diols (Scheme 9), however it also boasts higher activity and substrate scope when compared with 33 other commercially available ADHs, showing remarkable chemoselectivity for alcohol functionality[71].

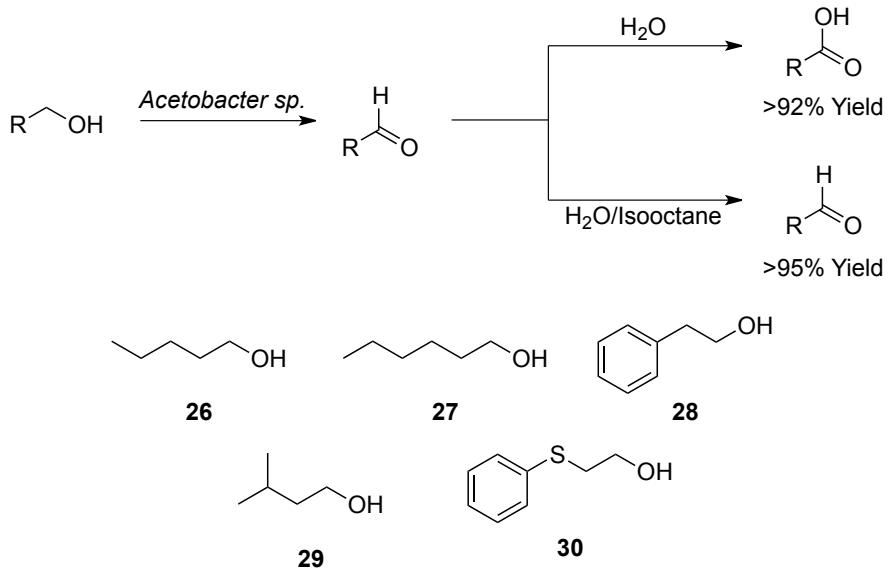

Scheme 10 Control of selectivity of acetic acid bacteria catalyzed oxidation of primary alcohols by choice of reaction conditions[73].

The use of isolated oxidases has the distinct advantage over dehydrogenases in that oxygen is used as the terminal electron acceptor and in turn is reduced to H_2O_2. H_2O_2 is detrimental to the activity of many isolated enzymes and its removal is necessary. The simple addition of catalase can circumvent the effects associated with H_2O_2 by its decomposition into water and additional equivalents of O_2.

Flavin-dependent alcohol oxidase (AlcO) from the yeast *Pichia pastoris* has been shown to provide a number of interesting unbranched aldehydes including propargyl aldehyde, 2-chloroethanal and 2-cyano ethanol however increased chain length and additional hydroxyl functionality are not tolerated[54,56]. Enantioselective oxidations have also been reported using AlcOx[76] from different yeast strains. However, poor enantioselectivity and limited substrate range (2-methyl-1-pentanol) limit its practical application. Another interesting oxidase which has recently been discovered by Fraaije is hydroxymethylfufural oxidase (HMFO)[77]. HMFO shows a broad substrate scope accepting, aromatic alcohols such as benzyl alcohol, cinammyl alcohol and vanillyl alcohol. HMFO also accepts aldehyde hydrates which is not a common feature of oxidases. The main limiting factors are low substrate concentration and reaction rates, but directed evolution strategies have been employed to make HMFO more general[78]. Oxidases

may therefore represent an important tool for the oxidation of alcohols with more directed evolution and genome mining facilitating enzyme discovery and optimisation

The Cu^{2+} dependent galactose oxidase (GOase) is another alternative for the oxidation of primary alcohols to aldehydes. WT GOase shows remarkable selectivity for substrates possessing a D-galactose moiety such as melibiose, raffinose, lactose and lacticol, however no activity for hydrophobic alcohols was observed[54]. Much research has been carried out on the development of GOase mutants to circumvent poor substrate specificity. The $GOaseM_{3-5}$ mutant has been reported for the oxidation of a number of secondary and primary alcohols, both in high conversion and enantioselectivity[53] and this interesting development will be discussed in more detail later.

Finally, laccases offer a chemo-enzymatic alternative for the oxidation of primary alcohols to aldehydes. Laccases generally have a redox potential in the range of 0.5-0.8 V and so cannot directly oxidise primary alcohols. This can be overcome by using a redox mediator (LMS) in catalytic amounts which is kept in its oxidized form by a laccase and oxygen as the terminal oxidant.[79]. HBT **32**, ABTS **33** and TEMPO **31** have all been demonstrated as redox mediators[80], with TEMPO most often employed[81]. Additionally, the laccase mediated system (LMS) produces water rather than H_2O_2 produced by oxidases, which may be preferable (Scheme 11).

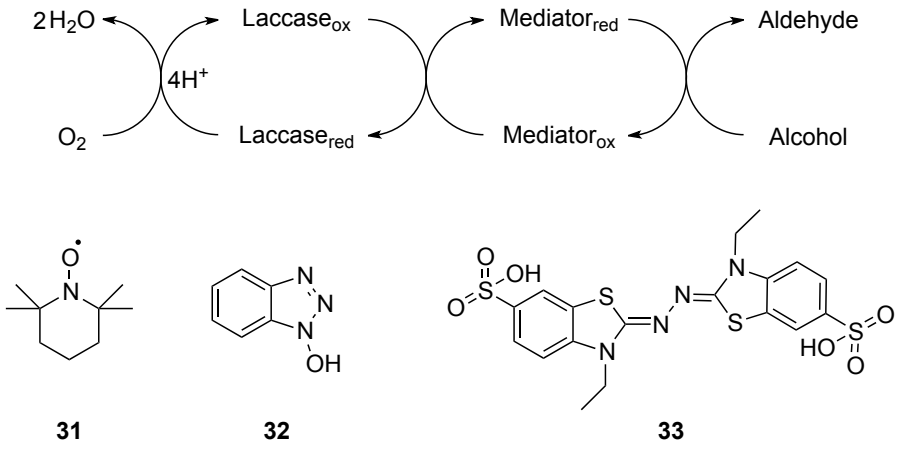

Scheme 11 Laccase-catalysed substrate oxidation in presence of chemical mediator[80,82].

This type of biotransformation has been applied to the oxidation of a number of benzylic[82,83], allylic[82], propargylic[84] and aliphatic alcohols[82] however with variable conversions depending on the reactivity of the alcohol. Recently, a new chemical mediator AZADO (2-azaadamantane N-oxyl) was reported for the selective and mild oxidation[85] of primary alcohols providing excellent yields and broad substrate scope, even with highly functionalised alcohols containing sensitive functional groups. The major limitation of the LMS is poor regioselectivity as reactivity is dictated by the oxidised mediator and not the active site of the enzyme. Low mediator turnovers also limit applicability for preparative scale reactions[86].

1.4.1.3 Enzymatic secondary alcohol oxidation

Oxidation of secondary alcohols is often considered less interesting from a synthetic point of view because chiral information is destroyed in the transformation. Using enantioselective ADHs in the oxidation direction allows the accumulation of a single enantiomer secondary alcohol, however with the inherent disadvantage of a maximum 50% yield. Nevertheless, a range of oxidative kinetic resolutions have been reported using both whole cell and isolated alcohol oxidases and dehydrogenases yielding enantiopure alcohols in moderate yields (>40%)[87-91].

To overcome this intrinsic limitation of maximum 50% conversion symmetrical prochiral alcohols can be used in desymmetrisation reactions. This has been shown to be very efficient in the oxidation of *syn*-cyclohexanediol[92] and 2,3-butanediol[65] using isolated glycerol dehydrogenase (GDH) and whole cell *Acetobacter* respectively, providing enantiopure hydroxy ketones. Faber *et al.* have also reported the desymmetrisation of *meso*-2,5 hexanediol[93] using recombinant ADH-A in *E.coli* utilising acetone as hydrogen acceptor, in 88% conversion and >99% ee. The recombinant enzyme is able to withstand a maximum acetone concentration of 50% and so remarkably high substrate concentrations up to 1.8 mol/L are tolerated. However, despite the efficiency of desymmetrisation reactions, the number of *meso*-compounds and their uses are few and so using the *meso*-trick is not a viable solution for the limitations set by kinetic resolutions. Deracemisation by stereoinversion is a more effective solution to this problem.

This includes a two step interconversion reaction in which the first step includes a stereospecific oxidation of one enantiomer or a non-specific oxidation of both, followed by a selective reduction (Scheme 12).

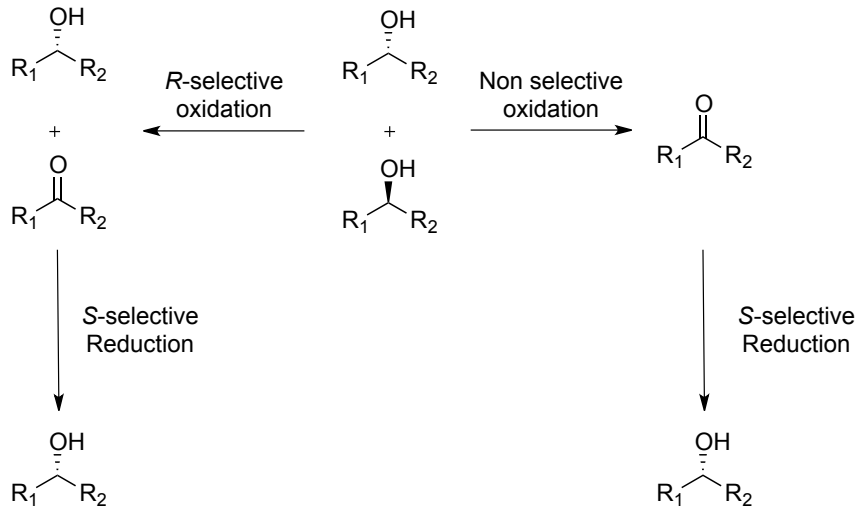

Scheme 12 Approaches for deracemisation of secondary alcohols using combined enzymatic oxidations and reductions.

Sodium borohydride ($NaBH_4$) has been used to facilitate the chemical deracemisation of secondary alcohols and in combination with immobilised *Geotrichum candidum*[94] has provided a number of aromatic and aliphatic alcohols in varied ee and conversion (Scheme 13). Despite the elegance of this one pot chemo-enzymatic redox process, incomplete reduction and low yields are major drawbacks to this methodology.

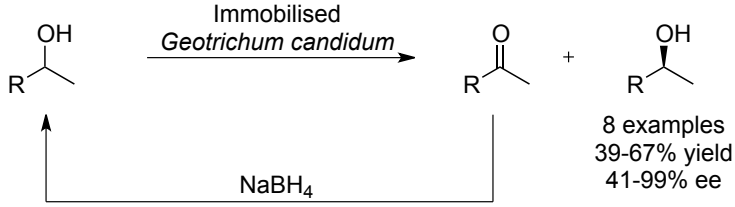

Scheme 13 Chemo enzymatic racemization of secondary alcohols with $NaBH_4$[94]

More recently, highly efficient cascade enzymatic systems have shown great promise for deracemisation processes. The application of two stereocomplementary reduction and oxidation catalysts is extremely attractive as only one redox cycle is necessary for total de-racemisation of secondary alcohols. Kroutil and co-workers have demonstrated this concept using whole cell *Alcaligenes faecalis* DSM 13975 for the (*R*) selective oxidation step and isolated RE-ADH from *Rhodicoccum erythropolis* for the *S*-selective reduction (Scheme 14)[95]. With this dual enzymatic system a number of aliphatic, allylic and aromatic secondary alcohols were provided in quantitative conversion however ee is heavily affected by bulky substituents near the reaction centre, ie **38**. In addition, the applicability of this methodology was demonstrated on preparative scale to furnish enantiopure 4-phenyl-2-butanol in 91% isolated yield and >99% ee

The use of two isolated enzymes for this process has an inherent disadvantage in that an efficient oxidation and reduction process is not possible if both dehydrogenases require the same phosphorylated or non phosphorylated co-factor (NADPH or NADH). As mentioned, oxidation and reduction by dehydrogenases is an equilibrium process and co-factor regeneration is required for complete oxidation or reduction. If two enzymes require the same co-factor then only one regeneration strategy can be used and as a result only oxidation or reduction can take place efficiently. To circumvent this major problem, two co-factor independent dehydrogenases can be used. This has been demonstrated again by Kroutil[96] utilizing an NADPH-specific (*R*) selective ADH and a NADH specific (*S*)-selective ADH with two separate regeneration strategies working in tandem, for the de-racemisation of secondary alcohols (Scheme 15).

This compared very well with the whole cell-isolated ADH process discussed previously, providing similar enantiopurity and conversions on the same substrates, albeit with longer reaction times. It is notable that in both these processes the other enantiomer could be obtained by switching the selectivity of the biocatalysts.

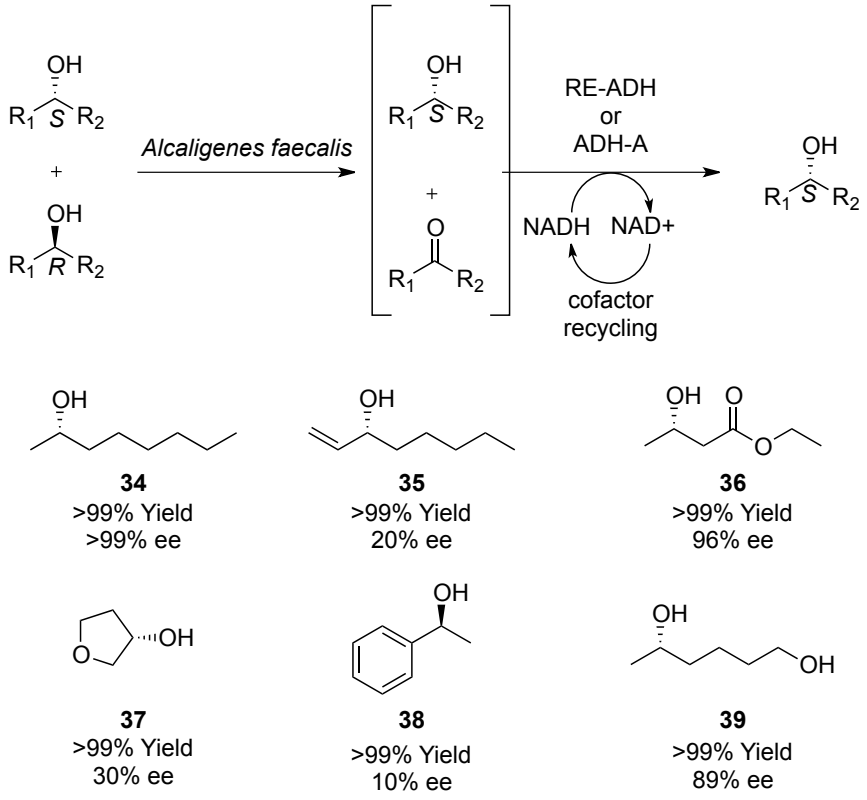

Scheme 14. Tandem biocatalysis for the deracemisation of racemic secondary alcohols[95].

Dual whole cells with complementary enantioselectivity are viable alternative to isolated enzymes and has the advantage of *in situ* co-factor regeneration. An alcohol dehydrogenase from *Microbacterium oxydans* and a ketone reductase with complementary stereoselectivity from *Rhodotorula sp.* have been used to obtain many secondary aryl alcohols with in high yield and excellent optical purity.[97]

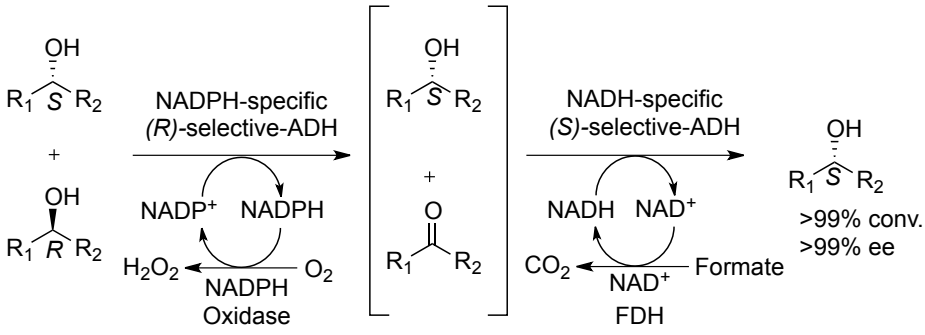

Scheme 15. Cascade combing four enzymes with opposite co-factor and stereopreference to access 10 enantiopure (*S*)-alcohols by biocatalytic deracemisation[96]

Recently, the deracemisation of racemic 3-aryl-2-hydroxyacids (2-HA) to (*R*)-2-HA have been reported by employing two resting-cell biocatalysts (Scheme 16)[98]. *Pseudomonas aeruginosa* CCTCC M 2011394 was shown to possess an extremely active ADH for the enantioselective oxidation of (*S*)-2-HAs and when combined with *S. cerevisiae* ZJB5074, which possesses an *R* selective ADH for the reduction of 2-ketoacids, provided an extremely powerful deracemisation system. Substituted enantiopure (*R*)-2-hydroxy acids were provided in good yield (>90%) using this one-pot tandom redox process. However, electron donating substituents on the aromatic ring decreased conversion.

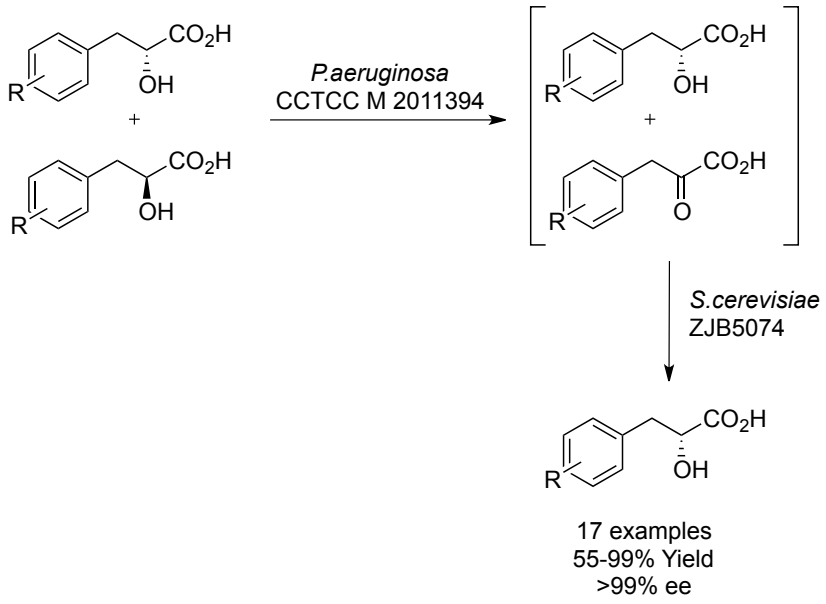

Scheme 16 Biocatalytic deracemisation of racemic 2-hydroxy acids[98]

Interestingly, the above process can be used for the stereoinversion of enantioenriched secondary alcohols which in organic chemistry is performed using the Mitsunobu inversion which requires toxic and expensive reagents. *Geotrichium candidum*[99], *Cyanidioschyzon merolae* [100] and *Candida albicans*[101] have all been evaluated for the stereoinversion of substituted aryl ethanols and more recently the stereoinversion of α- and β- tetralone alcohols by *Chaemtomium sp*. KCh 6651 has been reported[102], however compared to deracemisations little attention has been paid to this green methodology.

1.4.1.4 Regioselective alcohol oxidation

For the chemical oxidation of polyol containing compounds, protection strategies are inevitable to allow the regioselective oxidation of specific alcohol groups. These strategies add two additional steps to the synthesis and thus the overall yield will be decreased. Polyol dehydrogenases and oxidases show remarkable regioselectivity and thus are an attractive alternative to protection strategies.

The ideal substrates to showcase the regioselective power of enzymes is the polyol containing sugars. *Gluconobacter oxydans* whole cells facilitated the stereo and regioselective oxidation of a number of polyol containing compounds to provide important chemical intermediates and products from glycerol (**42**)[103], *N*-butylglucamine (**44**)[104], glucose (**40**) [105] and ribitol (**43**)[106]. Other different biocatalytic approaches have been developed for the transformation of ribitol into L-ribulose such as the use of isolated ribitol dehydrogenase[107] and a mutant of mannitol-dehydrogenase[108] to provide the large scale production of L-ribulose.

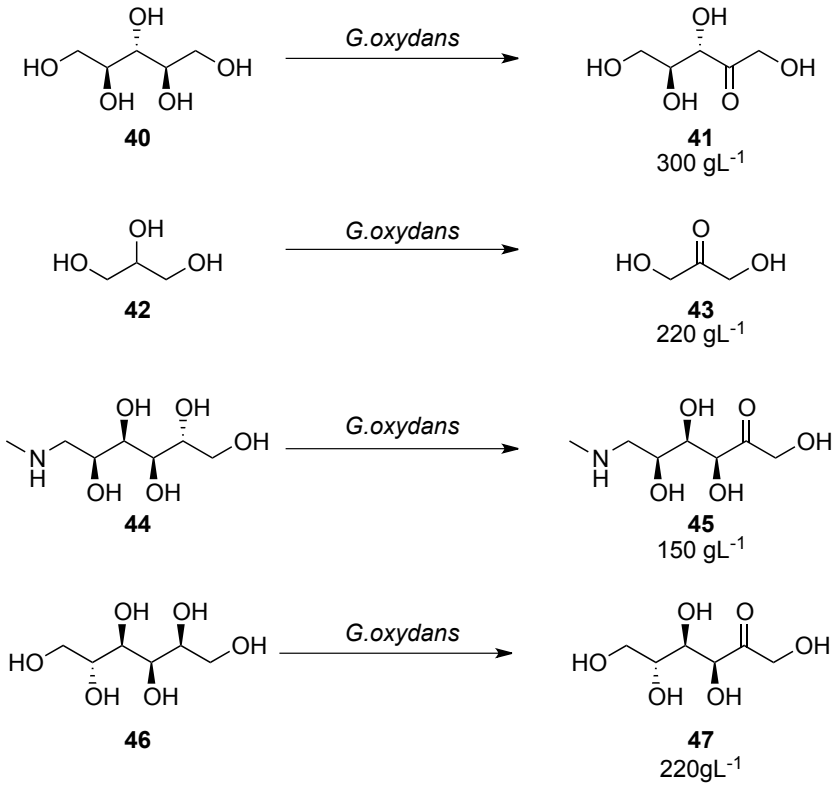

Scheme 17 Preparative scale applications of *Gluconobacter oxydans* for the regioselective oxidation of polyols[104-106].

1.4.2 Amine Oxidation

The principal enzymes used to carry out amine oxidations belong to the flavin-dependent oxidases and include amino acid oxidase, D-amino acid oxidase and monoamine oxidases. The use of enzymes to catalyse the oxidation of C-N to C=N bonds is an extremely attractive prospect, as many chemical methods require aggressive conditions let alone stoichiometric reagents. Selectivity is also an issue with the chemical oxidation of amines as multiple oxidized side products such as N-oxides, nitroso and nitro compounds can be formed. Imines, although less reactive than aldehydes, are versatile synthetic intermediates in redox chemistry and their formation has been exploited in a number of desymmetrisation and deracemisation reactions to form optically pure amines.

1.4.2.1 Deracemisations and stereoinversion of amines

D-amino acid oxidase (D-AAO) has been used in conjunction with the non-selective reductant sodium borohydride to facilitate the stereoinversion of D-alanine and L-alanine to the corresponding enantiomers[109]. Subsequently this methodology was furthered in the deracemisation of DL-proline and DL-pipecolic acid[110,111]. Turner *et al.* furthered this research and demonstrated that the deracemisation process could be applied to compounds containing two stereocenters such as isoleucine (**48**) to provide products in high yield and diasteromeric excess.[112] (Scheme 18)

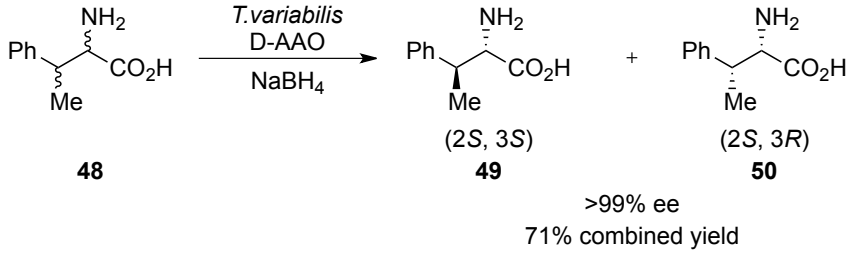

Scheme 18 Stereoinversion of β-substituted α-amino acids[112].

In addition, amino acid oxidase based deracemisation has been cleverly combined with the asymmetric hydrogenation of dehydroamino acids to provide all 4 diasteroisomers of β-arylalanines with yields ranging from 68-92% and excellent ees (>98%)[113] (Scheme 19). Although AAOs are extremely efficient at providing enantiopure products in excellent conversion, the inherent limitation is substrate specificity. D-AAO and L-AAO only accept substrates with an α-carboxy group which limits their synthetic application.

To this end, alternative biocatalysts such as monoamine oxidase have been developed. The FAD dependent monoamine oxidase (MAO-N) from *Aspergillus niger* represents an alternative to D and L amino acid oxidases, as the α-carboxy group is not required for amine oxidation. There are currently three mechanistic proposals for MAO catalysis[114,115] which include single electron transfer, direct hydride transfer and a concerted polar nucleophilic mechanism.

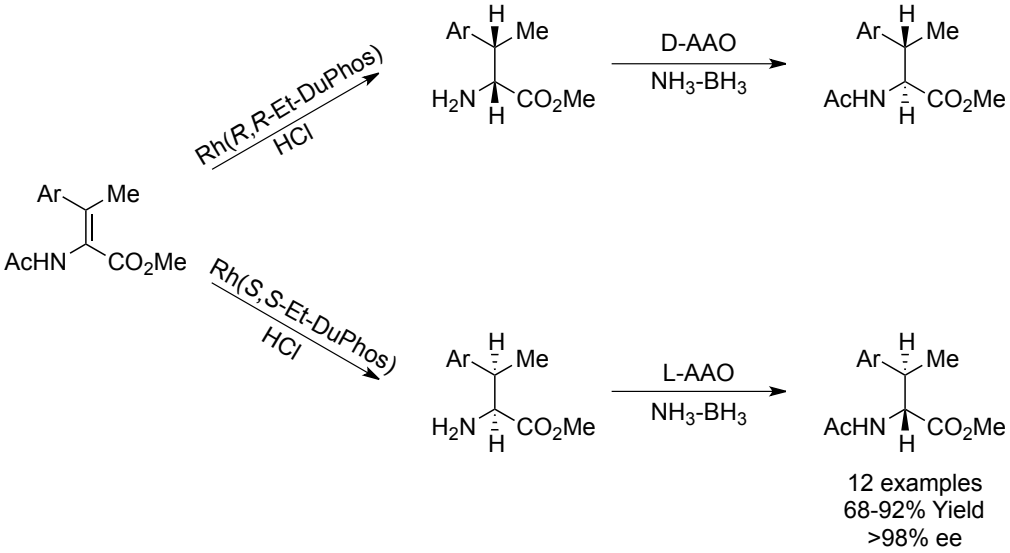

Scheme 19 Asymmetric hydrogenation and subsequent enzymatic stereoinversion to provide all diastereoisomers of β-branched α-amino acids[113]

However, thus far there has been no agreement concerning the mechanism of these enzymes. The wild-type MAO-N substrate scope is rather limited to simple amines such as butylamine, amylamine and benzylamine[116], and to this end MAO-N has been subjected to a series of rounds

of directed evolution[117-119] which provided a toolbox of MAO-N variants (MAO-N D3, D5, D9, D11) that display complementary substrate specificity. For example, MAO-N variants D3 to D11 are able to facilitate the chemoenzymatic deracemisation of secondary and tertiary cyclic amines with broad structural features. Acyclic imines however undergo problematic hydrolysis to provide unwanted ketones/aldehydes that cannot be recycled and thus are not suitable for general chemoenzymatic deracemisation.

Recently, MAO-N D9 and D11, which exhibit high activity and enantioselectivity towards substrates containing bulky aryl substituents have been developed. Late stage intermediates in the synthesis of the generic APIs levocetirizine and solifenacin[119] have been provided by MAO-N D11 catalysed deracemisation. In addition, these variants have enjoyed great success in the preparative deracemisation of tetrahydro-β-carbolines[120] to provide optically pure secondary amines (Scheme 20). Interestingly, a switch in enantioselectivity (*S* to *R*) is observed as the nature of the C1 substituent is varied from small substituents (methyl) to bulky (isopropyl). Furthermore, the sterically unhindered substrates displayed lower ee (R = ethyl, 36% ee) as a result of poor enantiodiscrimination by MAO-N between enantiomers.

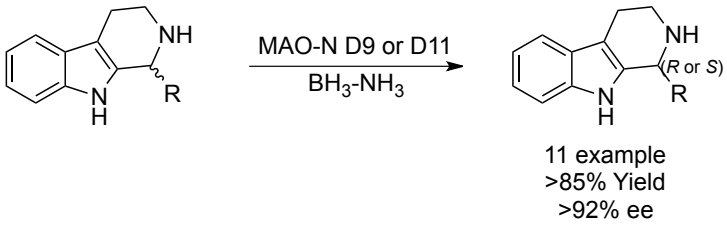

Scheme 20 Deracemisation of bulky amines by the combination of an enantioselective amine oxidase with a non selective reducing agent[120]

Lately, the chemoenzymatic deracemisation of benzylisoquinoline alkaloids[121] by MAO-N D11 has been coupled with another enzyme, the flavin dependent berberine bridge enzyme (BBE), to provide (*S*)-berbines (Scheme 21)[122]. This concept combines the interconversion of **51** by MAO-N to the opposite enantiomer **ent-51**, with a kinetic resolution by BBE and affords conversions of up to 98%, with up to 93% of the optically pure product being isolated.

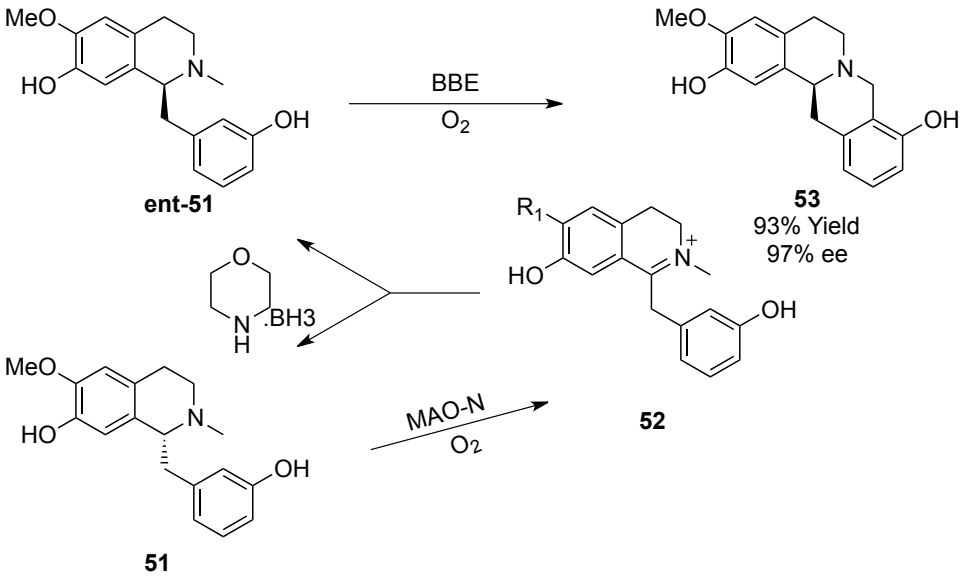

Scheme 21. Deracemization of benzylisoquinolines to berberines by a MAO/BBE/borane redox cascade[121]

The natural product harmicine can be obtained in four linear steps with an overall yield of 59% using a MAO-N D9 facilitated deracemisation [119]. Interestingly, MAO-N provides an alternative route to harmicine *via* a Pictet-Spengler type cyclisation using a tryptophan derivative as the starting material in a single step (Scheme 22). The intermediate iminium ion **55** undergoes nonstereoselective cyclisation to form racemic harmicine **57**. The (*S*) enantiomer was then further oxidized to the corresponding iminium ion and upon reduction with BH_3-NH_3 is fully converted to (*R*)-harmicine **ent-57** in >99% ee and 83% conversion.

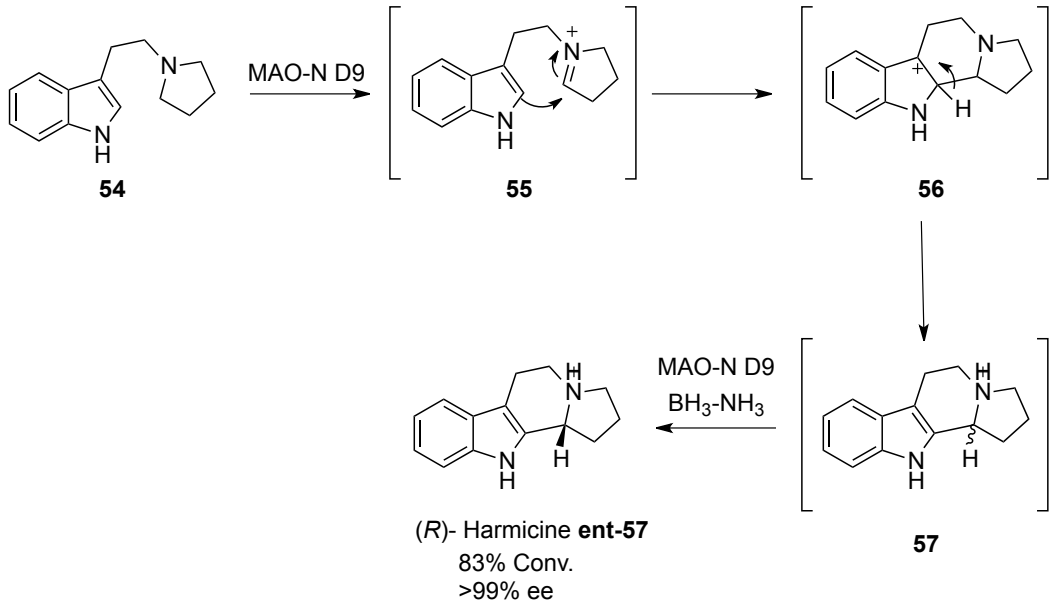

Scheme 22. Biocatalytic Oxidative Pictet−Spengler Approach to the Synthesis of (*R*)-Harmicine[119]

Despite the elegance of the previously described chemoenzymatic deracemisations, their utility with acyclic structures is limited by competing hydrolysis of the imine under aqueous conditions. Turner *et al*[123] has addressed this issue by employing a ω-transaminase to regenerate the chiral amine from the hydrolysed imine (Scheme 23). The approach relies on selective MAO-N mediated oxidation of one enantiomer of the amine to the imine, which undergoes spontaneous hydrolysis to the corresponding ketone. Subsequent amination mediated by ω-TA provided optically pure *R* amines in excellent conversions without the use of chemical reductants.

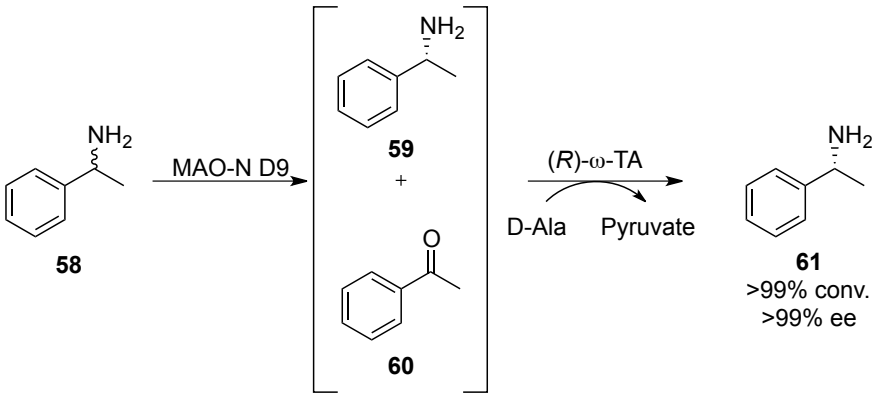

Scheme 23. Deracemisation of 1-phenylethanamine using a MAO-N/ ω-TA cascade process[123]

1.4.2.2 Desymmetrisation of amines.

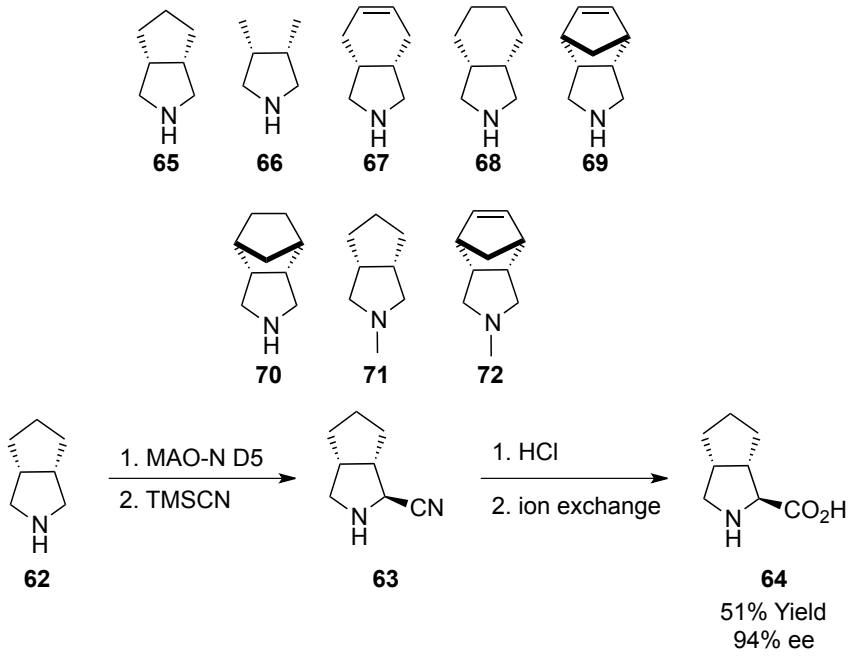

Scheme 24 Stereoselective synthesis of amino acid **64** and other accepted substrates for the biotransformation[124].

Desymmetrisation has a significant advantage over deracemisation in that no chemical or enzymatic reductant is required to obtain in theory over 50% yield of a single enantiomer. The variant MAO-N D5 has been applied to the selective desymmetrisation of a range of 3,4 substituted meso pyrollidines in >98% ee and excellent yield (Scheme 24)[124]. The

corresponding pyrrolines were found to serve as useful building blocks for the synthesis of L-proline analogues and R amino nitriles of high enantiomeric purity. In addition, the oxidized **63** was subjected to HCN resulting in the highly diastereoselective *trans*-addition of cyanide to form the amino nitrile, which was then hydrolised to the corresponding proline analogue **64**. Such proline analogues are components of the hepatitis C viral protease inhibitor telepavir and bocepravir.

1.4.3 Enzyme-catalysed Baeyer Villiger oxidations

The Baeyer-Villiger oxidation involves the oxidative cleavage of a carbon-carbon bond adjacent to a carbonyl group and subsequent insertion of an oxygen atom between these two carbons (Scheme 25).

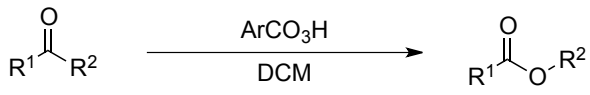

Scheme 25 Classical Baeyer villiger oxidation

Classical Baeyer villiger oxidations lack the high chemo-, and enantioselectivity which are needed in organic synthesis[125]. The waste associated with the use of peracid is one equivalent of carboxylic acid salt per ester formed, which in an atom economic world is not efficient. In addition many of the peracids used are intrinsically unstable, costly, shock sensitive or explosive in condensed form. To this end, a number of transition metal complexes have become available to perform this transformation in a highly enantio-, chemo and regioselective fashion but employ toxic and expensive precious metals[126,127]. A bio-based alternative to the abiotic Baeyer villigar oxidation would be of importance as reactions could be conducted at ambient temperature, in water and with a biodegradable catalyst.

1.4.3.1 Baeyer Villiger monooxygenases

Baeyer-Villiger monooxygenases (BVMOs) are most suited to Baeyer-Villiger oxidations. These enzymes are part of the class B subgroup of the larger class of flavoprotein monooxygenases[128]. BVMOs possess the ability to catalyse the insertion of oxygen with both high regio- and enantioselectivity. Cyclohexanone monooxygenase from *Acinetobacter calcoaceticus* (CHMO) [129,130] is the most studied BVMO.

BVMOs use a flavin cofactor for catalysis, which after coenzyme-mediated reduction by NADPH and reaction with molecular oxygen, forms a peroxyflavin intermediate (Scheme 26)[128]. The reactivity of the peroxy intermediate does not depend on substrate binding, which explains the broad substrate scope of BVMOs. Despite BVMOs being promiscuous enzymes, they instil remarkable enantioselectivity and provide access to unexpected Baeyer-Villiger products due to space restrictions in the active site of the enzyme. This has been exploited in a number of desymmetrisation reactions and kinetic/dynamic resolutions[131-133].

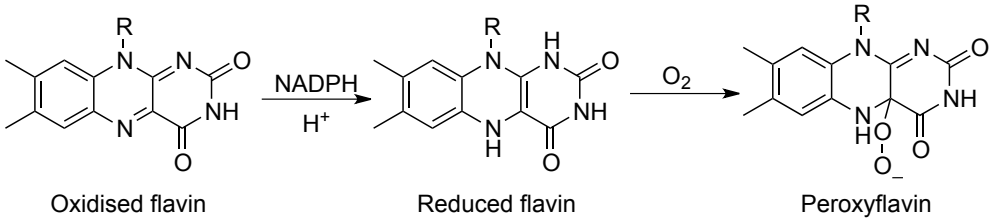

Scheme 26 Peroxyflavin formation by NADPH and O_2 in BVMOs

Cyclopentanone monooxygenase from *Comamonas sp* ($CPMO_{Coma}$) is an enzyme believed to be complementary to CHMO with many examples of opposite regio- or stereoisomers being formed depending on which enzyme is used[134]. This can be seen in the desymmetrisation of bridged cycloketones. For almost all ketones tested in this work, enantiodivergent behavior of both enzymes was observed with CPMO catalyzed reactions providing (+) lactones and CHMO forming (-) lactones (Scheme 27)

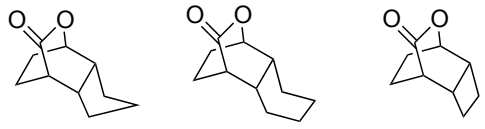

	73	**74**	**75**
$CHMO_{Acineto}$	100% Conv. 97% (-) ee	100% Conv. 97% (-) ee	100% Conv. 84% (-) ee
$CPMO_{Coma}$	100% Conv. 91% (+) ee	100% Conv. 93% (+) ee	56% Conv. 86% (-) ee

Scheme 27 Enantiodivergent behavior of CHMO and CPMO on selected bridged cycloketones[134]

Another example of the complementary nature of these enzymes can be seen in the formation of abnormal lactones. Sterics, conformation and electronic effects govern the migration of the carbon centre in the Baeyer-Villiger oxidation. Due to the addition of the peroxy group from the flavin moiety occurring in the active site of the enzyme, steric factors play a larger role in migration and so depending on substrate, the least substituted carbon can migrate providing abnormal lactones. For example, Baeyer-Villiger reaction of (-) *trans* dihydrocarvone (**76**) catalyzed by CHMO type enzymes led to the formation of expected lactones **77**[135]. However, when the catalyst is substituted for CPMO type enzyme, unexpected lactones **78** were formed albeit in low yield (Scheme 28). These reactions highlight nicely how CPMO and CHMO complement each other with opposite enantiomers and regioisomers being accessible from a common starting material.

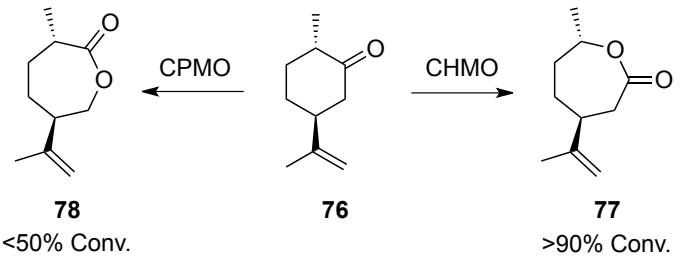

Scheme 28 Formation of abnormal and expected lactones from CPMO and CHMOs[135].

BVMOs display remarkable chemoselectivity. Chemical oxidants such as mCPBA can lead to multiple oxidation products if there are more than one oxidisable group, such as alkenes. With the use of BVMOs this chemical limitation is overcome as the active site of enzymes is specific. However, that being said, reactions of BVMOs usually employ whole cells reactions (to regenerate NADPH) and multiple enzymes such as alcohol dehydrogenase (ADH) and old yellow enzyme (OYE) may be present in the expression system[136]. This can lead to side reactions such as ketone reduction and also alkene hydrogenations. This limitation is illustrated in the whole cell oxidation of Wieland-Miescher ketone **79** in which the alcohol **80** is formed as a result of indigenous ADHs (Scheme 29)[136]. Isolated BVMOs would circumvent this problem however cofactor regeneration strategies such as the $[Cp^*Rh(bpy)(H_2O)]^{2+}$ flavin regeneration system developed by Fraiije[137], would be required to make the process cost effective.

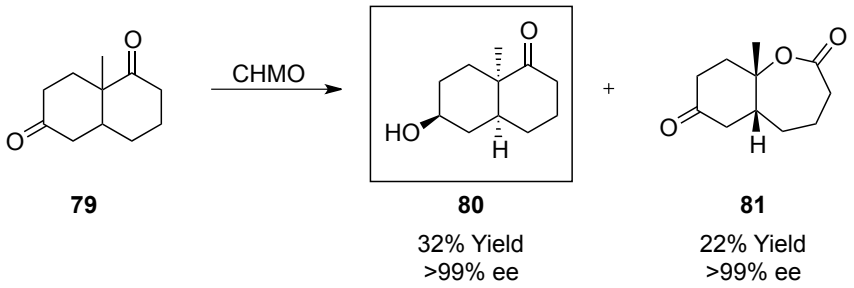

Scheme 29 Formation of side products resulting from additional enzymes in whole cell biocatalysts[136].

1.4.3.2 Kinetic resolutions of racemic ketones catalysed by BVMOs

Many kinetic resolutions of cyclic ketones have been reported to provide enantiopure chiral building block chemicals. A key chiral starting material in prostanoid synthesis was obtained in the kinetic resolution of a fused hetero bicylic ketone (Scheme 30)[138]. Recombinant *E.coli* expressing gene Rv3049c ($BVMO_{Mtb5}$) displayed excellent kinetic resolution for the formation of abnormal lactone **84** and at 50% conversion the ketone **83** was obtained in its enantiopure form. When the reaction was allowed to proceed further, a steady decrease in enantiopurity was observed as the unwanted enantiomer was converted.

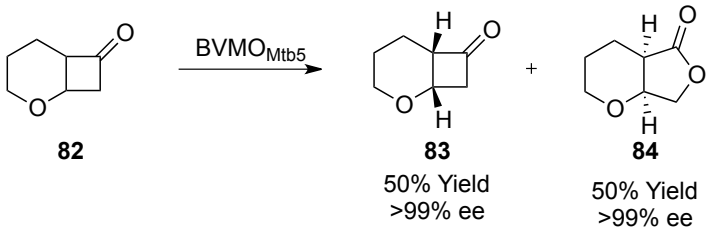

Scheme 30 Kinetic resolution of lactone 88 catalysed by $BVMO_{mtb5}$[138]

Initially kinetic resolutions were limited to cyclic ketones however, with the discovery of a BVMO from *P. fluorescens* DSM 50106, this methodology has been expanded to acylic ketones (Scheme 31)[139]. The new BVMO shows little activity towards cyclic substrates however it accepts a variety of acyclic β hydroxyl ketones. Under the reaction conditions, β-hydroxy acetates were furnished in >90% ee and overall (*S*) configuration in every case using recombinant whole cells *E.coli* expressing the BVMO.

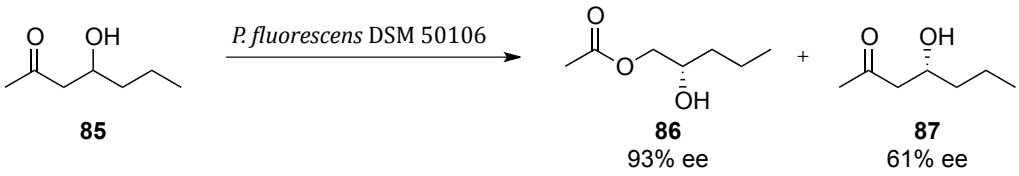

Scheme 31 Enzymatic Baeyer Villiger oxidation of racemic 4-hydroxy-2 ketone 91 by BVMOs[139].

Recently, the gram scale kinetic resolution of chiral building block **89** was demonstrated[140]. BVMO M014 was expressed in *E.coli* in a 2L bioreactor (Scheme 32). At 50% conversion the ketone **89** was formed with 96% ee and this example illustrates the applicability of BVMOs to industrial processes.

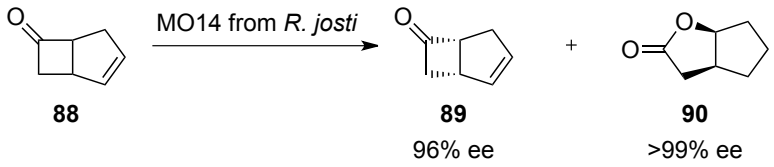

Scheme 32 Enzymatic Baeyer Villiger oxidation of racemic ketone 90 by MO14[140].

1.4.3.3 Dynamic kinetic resolutions of racemic ketones catalysed by BVMOs

Due to the inherent limitation associated with kinetic resolutions of 50% maximum yield, dynamic kinetic resolutions are of much interest. DKR was first described for the selective oxidation of racemic 2-benzyoxymethylcyclopenanone **91** (Scheme 33)[141]. The substrate posses an enolisable proton and thus under high pH would racemise the unwanted enantiomer. Using whole cells expressing CHMO, the desired lactone **92** was formed in 75% yield and 98% ee. This proved that DKR was possible, however at high pH BVMOs are known to lose activity. To circumvent this issue, anionic exchange resins have been used to facilitate racemisation at neutral pH which resulted in higher conversion[142].

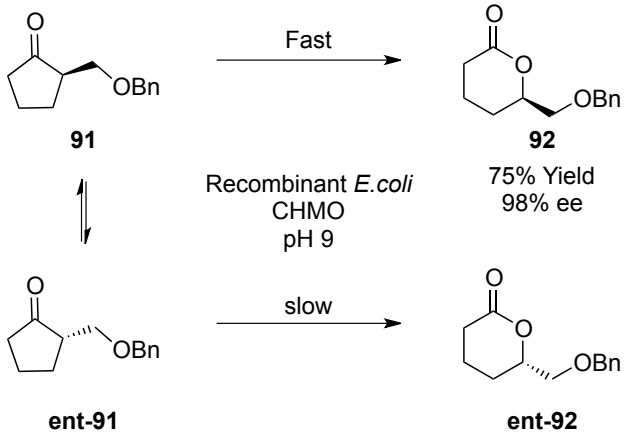

Scheme 33 Dynamic kinetic resolution of racemic **91** using a recombinant *E. coli*. expressing CHMO[142]

4-Hydroxyacetophenone monooxygenase (HAPMO) represents the first BVMO to be primarily active on aromatic ketones. Dynamic kinetic resolution of substituted benzyl ketones was

performed using an isolated HAPMO and the anion exchange resin DOWEX MWA-1, thus expanding DKR methodology to acylic compounds (Scheme 34)[132]. However, this reaction was plagued with long reaction times (>116hr), modest conversions (>46%) and ee's (58-84). The optimal substrate **93** was afforded in high conversion and optical purities (84%, 86% ee).

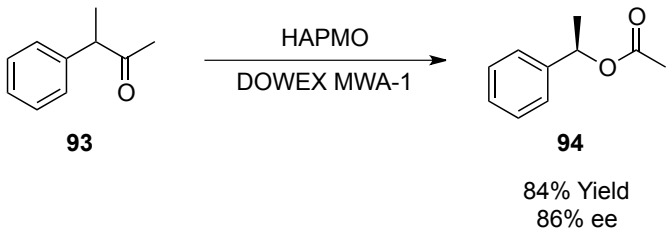

93 **94**

84% Yield
86% ee

Scheme 34 HAPMO-catalyzed DKR of **93** employing anion exchange resins[1]

Fraaije also demonstrated that BVMOs can catalyse the oxidation of β-ketoesters to form acylated hydroxyl esters[143], whose hydrolysed products are of importance to the pharmaceutical and cosmetics industry[144] (Scheme 35). β-Keto esters posses an acidic α-proton and require only slightly basic pH for enolisation, which eliminates the need for anion exchange resins. Therefore DKR was carried out using isolated phenylacetone monoxygenase (PAMO) from *Thermobifida fusca* and 5% MTBE as co-solvent. These conditions afforded the final ester in conversions close to 100% and >99% ee. PAMO was chosen as it has shown increased stability at high pH values[145]. Chemical hydrolysis of the ester furnished the desired hydroxyl acid **97** without affecting the enantiopurity.

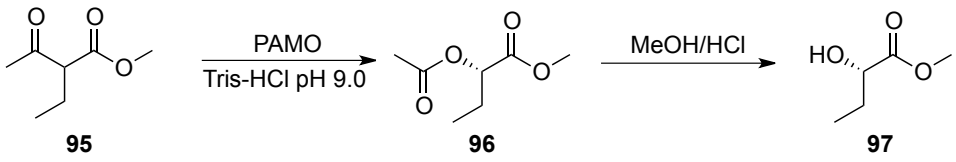

95 **96** **97**

Scheme 35 BVMO-catalyzed dynamic kinetic resolution of aliphatic α-alkyl-β-ketoesters and subsequent hydrolysis of the diesters to obtain the corresponding enantioenriched α-hydroxy esters[143].

1.4.4 Enzymatic epoxidation reactions

Enantiopure epoxides are extremely important building blocks in the fine chemical industry[146]. The versatility of the epoxide is attributed to the oxirane functionality that can be opened by various nucleophiles or undergo rearrangements or reductions to more elaborate intermediates.[147]

The most prominent catalytic reaction for epoxide formation is the transition metal catalyzed Sharpless epoxidation which allows the asymmetric epoxidation of prochiral allylic alcohols[148,149]. Katsuki-Jacobson epoxidation of *cis*-substituted alkenes[150] and Shi's epoxidation[151] of *trans* substituted alkenes are other transition metal protocols that have been developed. However, not all substrates are accepted by chemical methods and thus biological alternatives have been explored.

A number of enzymes from microorganisms, plants and animals are capable of catalyzing the asymmetric epoxidation reaction in a regio-, diastereo and enantioselective fashion. The most common biocatalysts are either monooxygenases and peroxidases. However, these enzymes lack flexibility in their substrate scope, which is a major limitation. Often many microbial strains are screened or engineered to carry out the desired biotransformation.

1.4.4.1 Enzyme-catalysed epoxidations of aliphatic alkenes.

The non-heme diiron alkane monooxygenases (AMOs) are very powerful epoxidation catalysts. Diiron monooxygenases catalyse the reductive activation of molecular oxygen resulting in high valent metal oxo complexs which are excellent oxidising agents[152,153]. Since these enzymes are complex and relatively unstable, the majority of studies are focused on whole cell biotransformations.

A number of microbial oxidation systems harboring AMOs have been reported for the epoxidation of a number aliphatic alkenes but with moderate ee (>86%)(Scheme 36).[154,155].

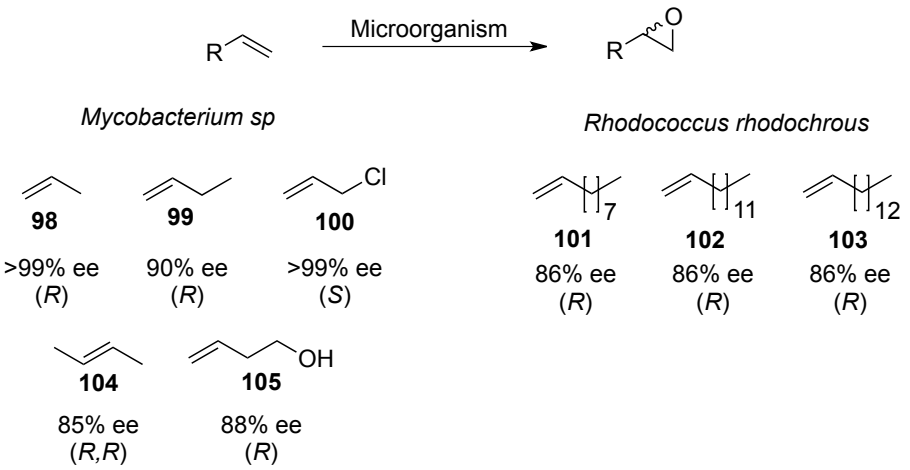

Scheme 36 Examples of selective microbial alkene epoxidations[155]

Nocardia corallina B-276, catalysed the epoxidation of a broad range of terminal alkenes to their (*R*) epoxides with optical purities reaching 90% in product titers 80 g L^{-1} [156,157], however optical purities decrease with alkyl chain length.

Interestingly, depending on bacterial growth conditions, enantioselectivity varies. This indicates stereocomplementary epoxidation systems are active within the cell, which is a major limitation of whole cell epoxidation systems. A further limitation of using whole cells is the extreme toxicity of epoxides. This issue can be easily circumvented using biphasic mixtures and concentrations of 150 g L^{-1} have been reported[158]. Despite AMOs being an extremely effective biocatalyst for epoxidation, their presence in recent literature is lacking. With the development of molecular biology techniques the more interesting and powerful cytochrome P450s and chloroperoxidases (CPO) have gained considerable interest in aliphatic alkene oxidation.

P450 monooxygenases contain a heme-iron complex. The catalytically active oxyferryl species is formed through a sequence of NAD(P)H reduction and O_2 activation (Scheme 37).

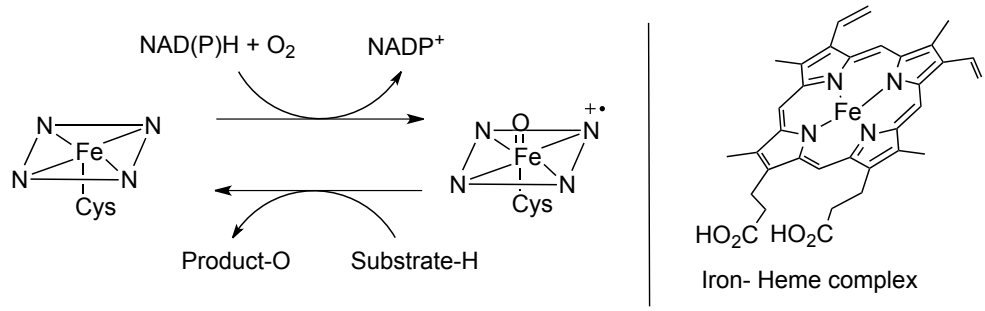

Scheme 37 Structure and simplified redox chemistry of P450 monoxygenases.

Bacillus megaterium was the first organism reported to catalyse the P450-dependent epoxidation of alkenes. This system facilitated the epoxidation of a number of unsaturated fatty acids, however poor conversion to the desired epoxides was observed <34%[159]. The responsible enzyme was identified as P450 monooxygenase BM3 ($P450_{BM3}$) and has since undergone a series of rounds of directed evolution to expand its substrate scope[160]. The mutant $P450_{BM3}$ G4 was capable of providing artemisinic- 11S, 12- epoxide (**107**) an important intermediate in the synthesis of the antimalarial drug artemisinin at titers of 250 mg L^{-1} in *E. coli,*(Scheme 38)[161].

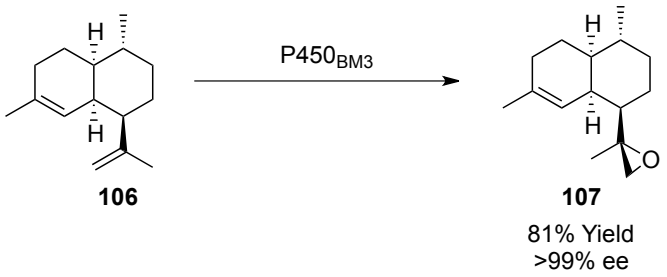

Scheme 38 Enantioselective epoxidation by $P450_{BM3}$ furnishing artemisinic - 11*S*, 12-epoxide[161]

The use of P450 monooxygenases however is hampered by their general low activity. In the conversion of limonene, pinene and valencene (**108**), a number of unwanted side reactions such as hydroxylation and overoxidation have been reported(Scheme 39) [162,163].

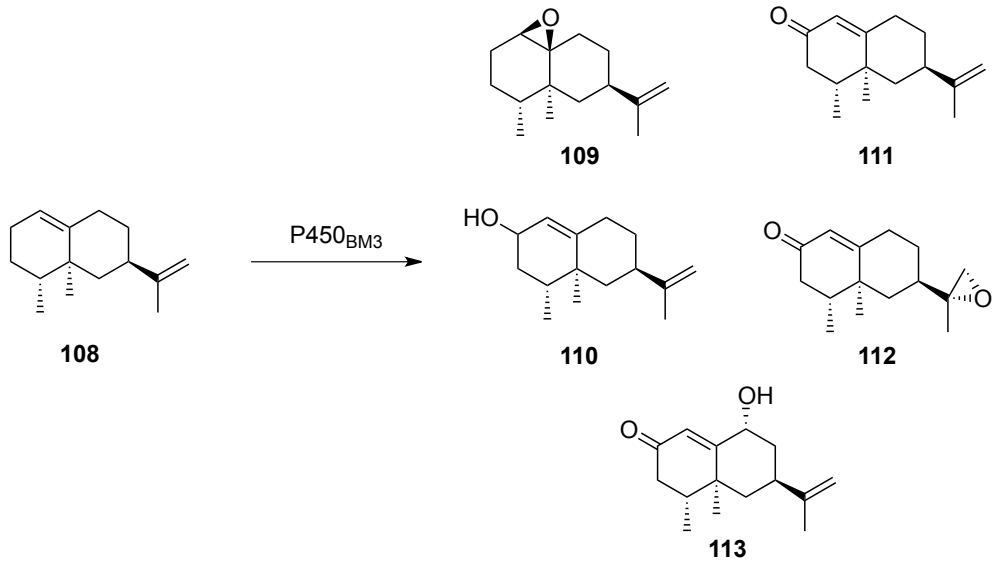

Scheme 39 Product distributions of P450-catalysed transformation of valencene **108**[162]

This inherent limitation can be overcome with excessive rounds of directed evolution as demonstrated recently by Reetz[164]. The natural product (+)-nootkatone (**121**) has a number of C-H oxidation sites and carbonyl functionality and thus makes it a challenging substrate for selective epoxidation. The heavily engineered variant of $P450_{BM3}$ provided the epoxide product in 96% conversion (Scheme 40) eliminating the formation of side products through extensive directed evolution. Although P450 monooxygenases remain a powerful force in C-H activation their application as off the shelf biocatalysts is low due to their poor chemoselectivity without protein engineering.

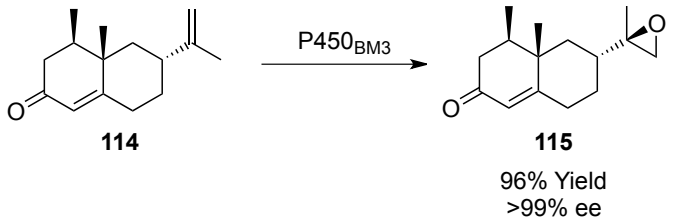

Scheme 40 Chemoselective oxidation of (+)-nooketone by the highly engineered $P450_{BM3}$ variant[1].

Finally, peroxidases such as chloroperoxidase from *Caldariomyces fumago* (CPO) are known to catalyse epoxidation of double bonds. Chloroperoxidase is heme containing glyco protein that requires H_2O_2 to regenerate its oxidised catalytically active protoporphyrin prosthetic group. Compared to P450s, CPO may be considered a better candidate as a practical epoxidation catalyst since it utilizes H_2O_2 whereas the P450 systems utilize molecular oxygen but also require NAD(P)H. This allows CPOs to be used as isolated enzymes and thus stereocomplementary epoxidation systems are no longer an issue that could be present within the cell.

A number of *cis* alkenes and *gem*-substituted alkenes have been efficiently epoxidised by CPO reaching high enantiopurities (Scheme 41) [165-167]. However, low enantioselectivity is observed with *trans*-alkenes. Recently, the successful epoxidation of chloropropene and allyl alcohol has been reported to provide the C3 building block chemicals epichlorohydrin (**123**) and glycidol (**124**) in excellent ee (>97%).[168]

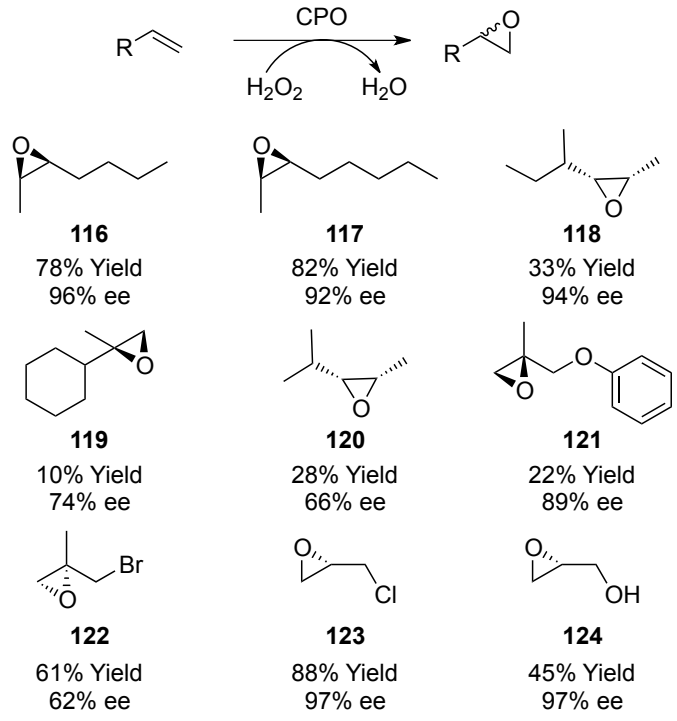

Figure 41 Epoxidation of different olefins catalysed by chloroperoxidase[165-168]

1.4.4.2 Styrene enzymatic epoxidation:

Due to the activated nature of aromatic alkenes a number of flavin and heme-dependent monoxygenases as well as peroxidases are suitable biocatalysts for epoxidation. Styrene monooxygenase (StyAB) from a *Pseudomonas sp.* strain is a two component enzyme consisting of a $FADH_2$-dependent oxygenase (StyA) which transforms its natural substrate styrene into (*S*)-epoxides with high enantioselectivity *via* reductive activation of molecular oxygen. The other reductase component (StyB) catalyses the transfer of hydrogen between the reduced NAD(P)H and oxidised flavin. As a result of SMOs cofactor dependence, whole cell biotransformations are the preferred medium however isolated enzymes coupled to co-factor regeneration systems have been reported with great success[169]. SMOs not only accept their natural styrene substrate but also a series of styrene derivatives with aromatic or carbon chain substitution, resulting in high (*S*) enantioselectivity in most cases (Scheme 42)[169-171].

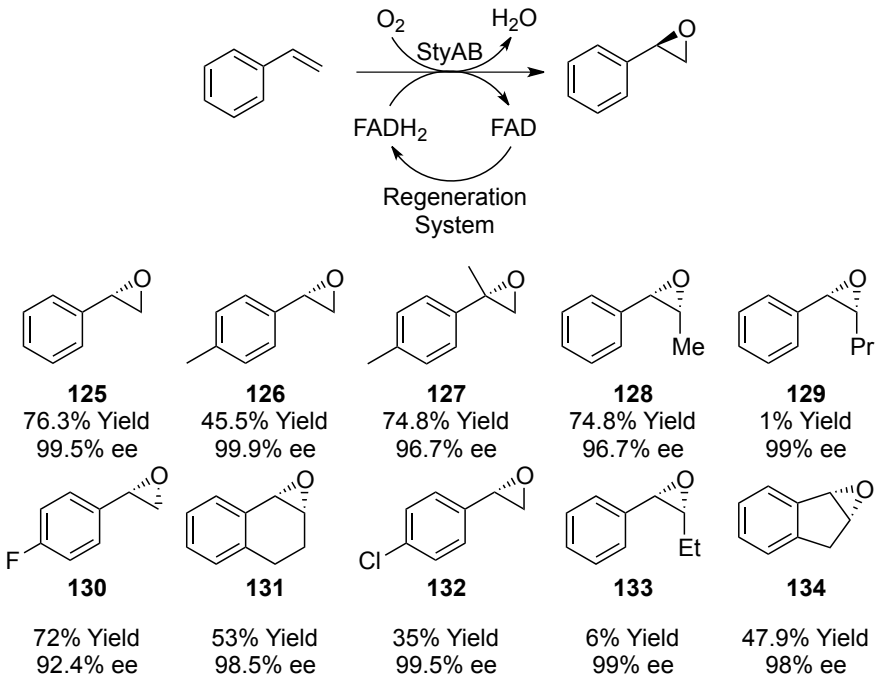

Scheme 42 Substrate scope of styrene monooxygenase (StyAB) [169-171]

Bulky substituents and/or electron withdrawing groups are associated with diminished enzyme activity. Formation of the (*R*) enantiomer of styrene epoxide is not possible using wild-type

StyAB. Directed evolution or genome mining strategies may provide a solution to this limitation, however this has not yet been realized.

1.4.5 Aldehyde Oxidations

Compared to the oxidation of alcohols, the oxidation of aldehydes is less popular. The Pinnick oxidation utilises sodium chlorite under mild acidic conditions to provide highly pure carboxylic acids from the corresponding aldehydes.[172] This remains the cornerstone of chemical green aldehyde oxidation. However, its intolerance to amines, pyroles and thioethers provides an inherent limitation. Protection strategies can circumvent this issue although the use of stoichiometric protecting groups does not coincide with green chemistry principles and thus alternative catalysts for chemo- and regioselectivie oxidations are required. Alcohol dehydrogenase (ADHs), aldehyde dehydrogenases (AldDH), Baeyer-Villiger monooxygenases (BVMOs) and members of the xanthine oxidase family all possess powerful aldehyde oxidation capabilities, yet comparably few biocatalytic procedures have been reported.

HLADH was the first reported ADH to catalyse the $NAD(P)^+$ dependent oxidation of aldehydes[173-176]. However, the NAD(P)H dependent aldehyde reduction represents a common side reaction. The so called aldehyde dismutase activity of some ADHs has been considered more of a curiosity than a viable synthetic method. Recently, Faber and co-workers[177] have exploited the dismutase activity of ADHs. They successfully demonstrated their biocatalytic equivalent to the Cannizzaro reaction to provide non racemic primary alcohols and α-chiral carboxylic acids, in equimolar amounts through a neutral redox process. Elegantly a dynamic kinetic resolution is possible *via* the easily enolisable aldehyde and so enantiopure products are possible. Interestingly, with increasing enzyme concentration, an increase in carboxylic acid is produced albeit with diminished ee values (Scheme 43).

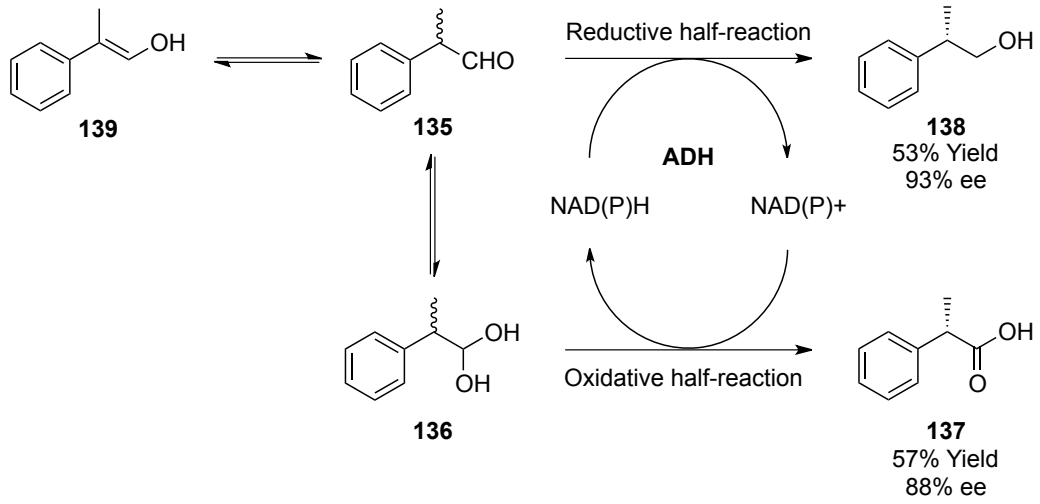

Scheme 43 Asymmetric Canizzaro-type reaction[177]

When a sufficient $NADP^+$ regeneration system is used, the dismutation activity can be switched into oxidative mode and predominantly the formation of carboxylic acid occurs. This has been exploited by Hollmann[178] in which an engineered recombinant ADH in *E.coli*, ADH9-V1 coupled with NADPH oxidase provided phenyl propionic acid in 97% ee and greater than 90% yield (Scheme 44). The preparative scale application was hindered however due to the instability of NOX under reaction conditions. A solution to this problem would be the use of an alternative regeneration system such as Laccase mediated system (LMS) or the use of an oxidase. However, these alternatives have yet to be explored.

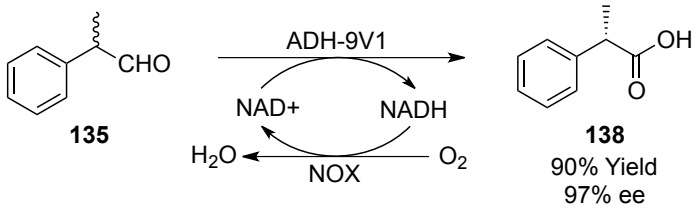

Scheme 44 Oxidative dynamic kinetic resolution of profen aldehydes

BVMOs such as CHMO have been known to transform aliphatic aldehydes into their respective carboxylic acids[179-181]. CHMOs are known to oxidise phenylacetaldehydes producing both the formate ester and carboxylic acid. The potential for BVMOs to carry out this

biotransformation in general is relatively unexplored. Recently, a newly characterised BVMO (BVMO4) from a strain of *Dietzia*[182], has displayed high activity for aldehydes containing a phenyl group and also for long chain aliphatic aldehydes with preference for carboxylic acid formation. BVMO4 is the first promising candidate for the practical synthesis of propionic acid drugs using BVMOs although it resulted in poor conversion and enantioselectivity (57% yield, 40% ee) (Scheme 45). Despite the modest performance, the aforementioned highlights that BVMOs could be applied to the asymmetric synthesis of α-substituted carboxylic acids after optimisation by protein engineering. Although interesting, it would need to compete with the highly developed alcohol dehydrogenase systems.

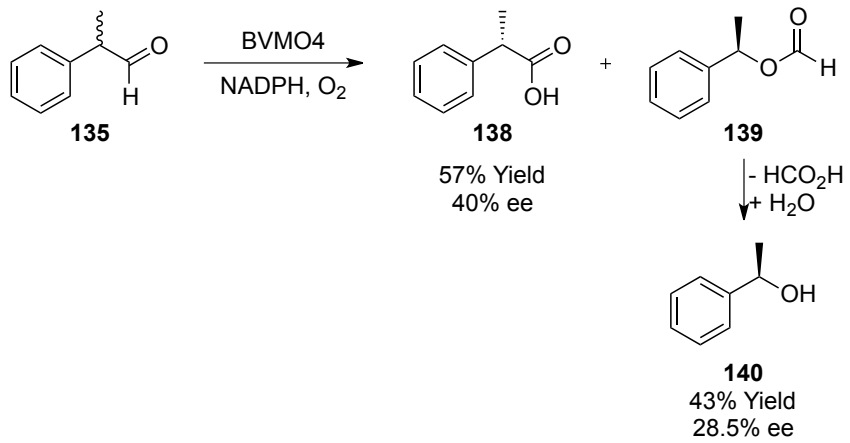

Scheme 45 2-Phenyl propionaldehyde oxidation by BVMO4

Finally, an attractive alternative to the aforementioned cofactor dependent oxidation is the use of oxidases. A family of molybdenum iron-sulphur flavoprotein hydroxylase such as xanthine oxidase (*E. coli* XDH)[183] and periplasmic aldehyde oxidase (PaoABC)[184] show promising activity. Although both XO and PaoABC show remarkable substrate promiscuity, and have the clear advantage of using molecular oxygen as the terminal oxidant, their use in synthetic applications is non-existent. These molybdenum-dependent enzymes are the subject of this work and will be discussed in detail later.

1.4 Enzyme cascade reactions

Single step enzyme biocatalysis has emerged as a powerful tool for the synthesis of chiral key intermediates with the main advantage of using mild reaction conditions in a chemo-, regio- and stereoselective manner. However, the isolation and purification of intermediates is associated with a decrease in yield.

In nature a large number of enzyme cascades can be found in different metabolic pathways inside the cell[185]. These enzymes work synergistically in cascade or multistep reactions, without isolation of intermediates to provide complex natural products. The utilization of such enzyme cascades *in vivo* or *in vitro* can provide efficient artificial synthetic pathways towards the generation of important complex molecules or building block chemicals from biomass in one pot. In addition, one-pot cascades of reaction sequences can substantially decrease the amount of chemicals used for each reaction as no isolation or purification of intermediates is required. Such cascades also eliminate the accumulation of unstable or toxic intermediates, which often hinder single step biotransformations. Depending on the catalysts, cascades can be classified into either chemo-bio or totally enzymatic bio-bio cascades.

1.4.1 Chemo-bio catalytic cascade reactions

An example of a chemo-bio cascade is represented by the work of Simon *et al*[186] in which all four diastereoisomers of disubstituted 2,6-piperidines were obtainable from asymmetrical 1,5 diketones (Scheme 46). The regio- and stereoselective monoamination of several 1,5 diketones was evaluated using 6 enantioselective whole cell transaminases. The reactions with **141**, were generally highly *S* selective using ω-TA from *C. violaceum* and the opposite enantiomer could be easily obtained using *Arthrobacter sp.* ω-TA. Diastereoselective hydrogenation of the resulting Δ1-piperideines provided enantiopure piperidines, however the chemical reductants proved incompatible in an aqueous environment and thus isolation of the intermediate was necessary. *Cis* piperidines were prepared with excellent de (>99%) from the enantiopure piperdines using H_2, Pd/C however, the preparation of *trans* piperdines occurred with poorer dr.

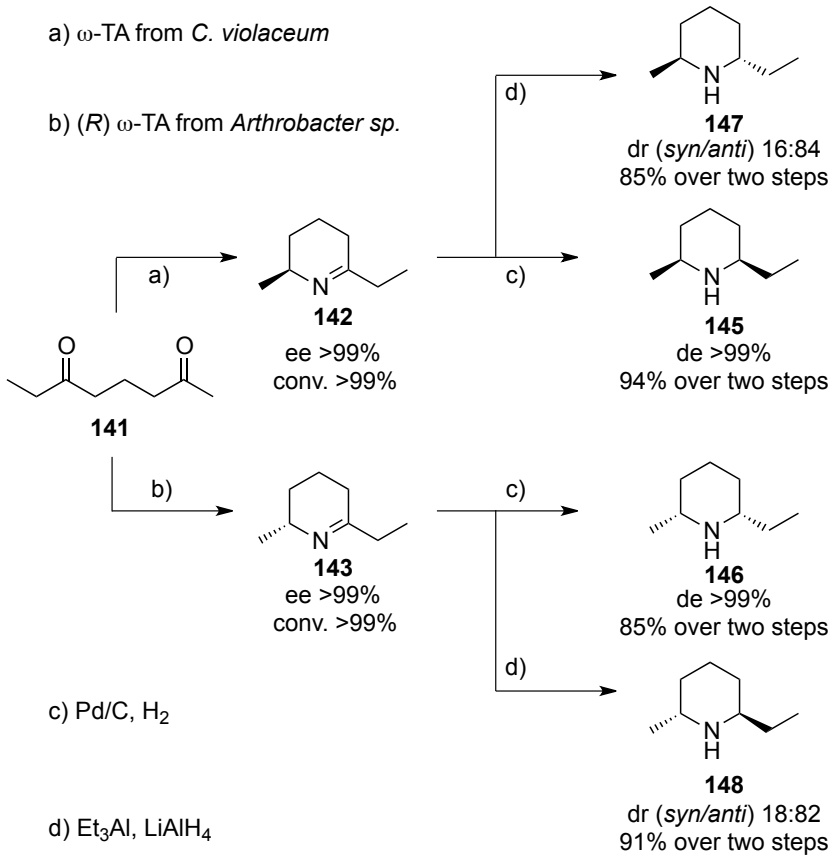

Scheme 46 Monoamination of **141** and subsequent hydrogenation providing all four diastereoisomers of disubstituted 2,6 piperidines[186].

Although the method described represents the highest yield and shortest chemical route to 2,6 di-substituted piperidines, the isolation of the unstable imine is an additional unwanted step.

One-pot two step reaction sequences are a common requirement in chemo-bio catalysis due to the incompatibility of reaction conditions for each step. Suzuki cross coupling of aryl boronic acid with aryl keto bromides was successfully combined with an enantioselective biocatalytic reduction by (*S*)-ADH from *Rhodococcus sp*. to provide biaryl substituted alcohols with high conversion of 91% and >99% ee[187]. However, subsequent adjustment of the reaction medium after the formation of the biaryl compound must occur to accommodate the biocatalyst and to ensure full conversion to the intermediate. Pd-catalysed Heck cross-coupling reactions combined with ADHs have also been reported by Cachi (Scheme 47)[188] but again a two-step one-pot reaction was required for successful conversion to the corresponding alcohols in yields

up to 92% and with >99% ee in all cases. This methodology has been successfully applied to the enantioselective one pot synthesis of (*R*)-rhododendrol (**151**) resulting in 90% yield and with >99% ee.[188]

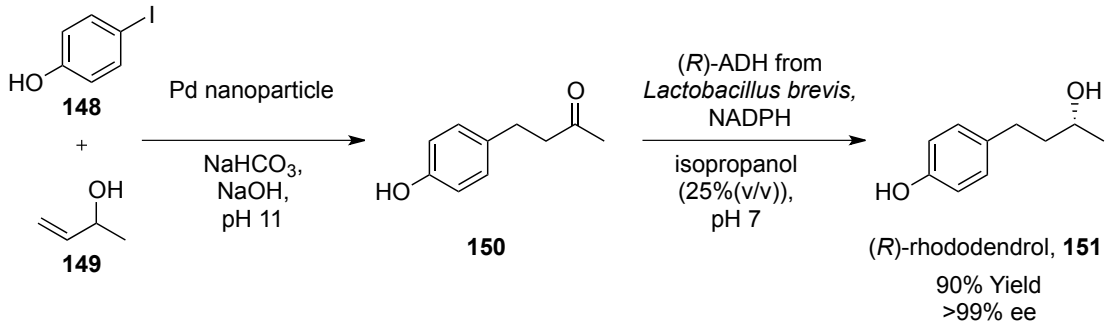

Scheme 47 One-pot chemoenzymatic synthesis of (*R*)-rhododendrol (157)[188]

The use of chemo-bio cascades can be very powerful tools to provide enantiopure products in high yields, often in which would not be possible if either catalysts are used alone. The major drawback of two-step sequential addition of either the biocatalyst or chemocatalyst is the time taken for the formation of the intermediate. To this end, much research has been devoted to the development of biocatalysts and chemocatalysts that are mutually compatible and can operate in a simultaneous manner rather than in a stepwise fashion.

Chemo-bio simultaneous catalysis has been demonstrated recently in which Turner *et al.*[189] reported a novel one-pot chemoenzymatic cascade for the regio and stereoselective synthesis of a panel of 2,5-substituted pyrollidines from their corresponding 1,4 diketones (Scheme 48). Commercially available ω-TA provided the mono transaminated product which spontaneously cyclises in excellent regioselectivity and ee (>99%). This has been demonstrated on a preparative scale in which both enantiomers were obtained using an (*S*) or (*R*) selective transaminase. Deracemisation of the resulting imine (**157**, **158**) with the mild unselective reducing agent $NH_3.BH_3$ and stereoselective oxidation by MAON-D5 or D9 provided the 2,5-substituted pyrrolidines in excellent conversion (>99%) and de (>99%) in a simultaneous one

pot manner. Unfortunately, not all diastereoisomers were obtainable in this work as a MAO-N mutant for the opposite enantiomer was not available.

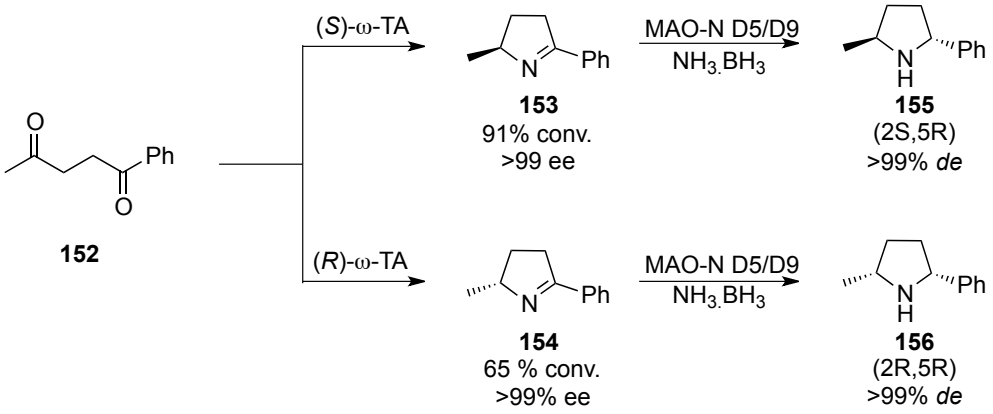

Scheme 48. Chemoenzymatic synthesis of 2,5 disubstituted pyrrolidines by employing ω-TA, MAO-N and an unselective reductant[189].

A more elaborate but interesting solution to the problem posed by chemical and biological incompatability involves the creation of artificial metalloenzymes.

The reaction scope of enzymes can be quite limiting when compared with transition metals such as Pd, Ru, and Rh. To some extent, this can be attributed to the poor bioavailability of these precious transition metals and so nature has not had the opportunity to explore the wealth of reactivity of these metals. Groups including Ward and Turner have tried to pick up where 'nature left off' by developing novel artificial biocatalysts that combine the richness of transition metal catalysis with the selectivity and rate enhancements of biocatalysis. These artificial enzymes are a step forward in reaching the goal of simultaneous chemo/bio catalysis as the reaction conditions when employing these hybrid biocatalysts often mimic those of natural enzymes but more importantly the incompatibility of the metal complex with the enzyme is eliminated.

Cp*Ir(Biot-p-L)Cl, an imine reduction catalyst was shown by Ward and Turner[190] *et al.* to completely inactivate monamine oxidase (MAO-N), which has enjoyed great success in the oxidation of a multitude of amines. To circumvent this inactivation, molecular compartmentalisation of the organometallic imine reduction catalyst within a protein scaffold

(Steptavidin) proved to shield it from the biocatalyst and in turn created a highly active artificial transfer hydrogenase metallozyme (ATHase). ATHase was compatible with several other co-factor dependent oxidases such as MAO-N, L-amino acid oxidase and D- amino oxidase in a simultaneous rather than a successive manner. The scope of the cascade reactions included reductions of prochiral imines with subsequent deracemisation[190], stereoinversion of nicotine[190] and also the synthesis of L-pipecolic acid[190]. Interestingly, the protein scoffold can be further improved by directed evolution to increase enantioselectivity or fine tune regioselectivity much like a natural enzyme.

Another cascade involving an artificial metallozyme was demonstrated in the Backväll[191] laboratory. Two catalysts, lipase CALB and palladium nanoparticles were co-immobilised in siliceous mesocellular foams to form a multifunctional hybrid catalyst. This artificial metallozyme was used in the dynamic kinetic resolution of primary amines affording the acylated amine product in quantitative yields and >99% ee. The main drawback is that this artificial "deracemase" metallozyme's activity decreases with each subsequent reaction due to the deactivation of CALB by denaturation. Despite this, Backvall has highlighted that chemo-bio cascades are possible by immobilising both a chemical and enzyme within a mesopourous material.

This relatively young discipline of using artificial metalloenzymes is very exciting as potentially any transition metal could be incorporated into the active site of a protein. This could give rise to a variety of powerful hybrid catalysts which may include Heckases, Suzukiases, Sonogashirases and perhaps novel carbocylases in the future.

1.4.2 Bio-Bio Catalytic cascades (*in vitro*)

The combination of two or more natural biocatalysts as either isolated enzymes, lyophilised whole cells or resting cells has received much attention in recent years[192]. The combination of multiple enzymes *in vitro* has the advantage in that mutually compatible reaction conditions are likely and so simultaneous catalysis is possible. However, problems can

occur when enzymes compete for the same substrate or are inhibited by an intermediate in the cascade[193-196].

In a recent example of a bio-bio cascade all four diastereoisomers of norephedrine [196] were obtained from benzaldehyde (**156**) and pyruvate (**157**) by the combined action of either multiple isolated enzymes or lyophilised whole cells (Scheme 49). In the first step, two enantiocomplementary carboligases recombinatly expressed from *E. coli*, were used to synthesise (*R*) and (*S*) phenylacetylcarbinol (**163**,**164**), which then underwent transamination by employing two stereocomplementary transaminases. However, simultaneous catalysis was not possible in this case as the benzaldehyde substrate can be transaminated by ω-TA and so the sequential addition of the biocatalysts was necessary. This two-step one-pot biotransformation provided (1*R*, 2*R*) and (1*R*,2*S*) norephedrine in >98% ee and de by employing the (*R*) selective carboligase AHAS-1 and either AT-(*R*) transaminase or Cv-(*S*) transaminase. The other diasteroisomers were accessed using a recently engineered carboligase from *Acetobacter pasteurianus* ApPDC (E469G) and so all four diastereomers were obtainable in titrs up 26g L^{-1} d^{-1}.

With clever biocatalytic retrosynthetic analysis[21], elegant multienzyme cascades have been developed in which the product formed by the action of the first enzyme becomes the starting material for the subsequent biotransformtion and thus competition between the enzymes is non-existent allowing simultaneous catalysis. This approach can also highlight suitable enzymes that would provide a neutral redox process in relation to co-factor regeneration and thus the process becomes self-sufficient. This approach was demonstrated in which the un-natural amino acid, L-phenylglycine (**168**) was obtained through a series of biotransformations using isolated enzymes starting from the readily available L-mandelic acid (**165)**(Scheme 50)[197]. Mandelate racemase was identified as suitable racemisation catalyst for the initial stereoinversion. The resulting D-enantiomer **166** was then oxidized by a novel D-mandelate dehydrogenase and subsequent reductive amination by L-amino acid oxidase provided the un-natural amino acid **168** in 86.5% yield and excellent ee in a 1 pot 1 step biotransformation.

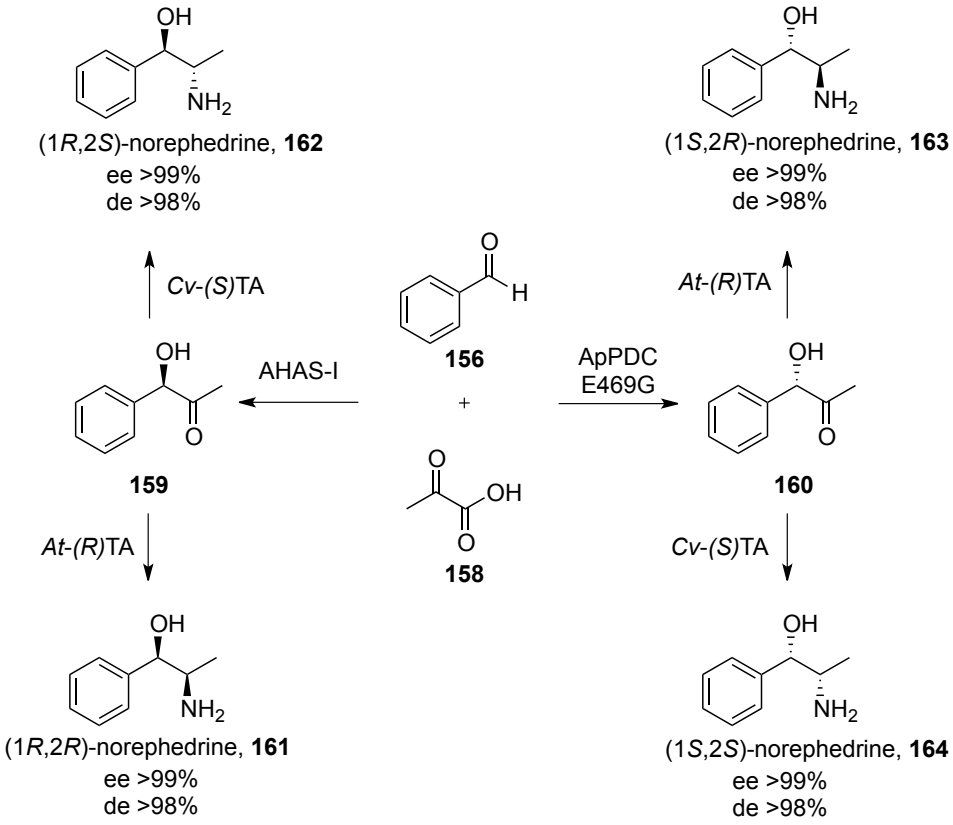

Scheme 49 Enzymatic synthesis of all 4 disastereoisomers of norephedrine[196]

All enzymes work cooperatively in this artificial synthetic *in vitro* pathway to provide the desired product without isolation. In addition, internal cofactor regeneration resulted in a redox neutral process and thus the use of these enzymes in tandem is beneficial as no external cofactor regeneration strategies are required and the process is self-sufficient. The use of redox self-sufficient biocatalyic systems is a very popular trend within the area of bio-bio *in vitro* cascades. Kroutil and co-workers[198] demonstrated a redox self-sufficient cascade for the amination of primary alcohols using three isolated enzymes (Scheme 51).

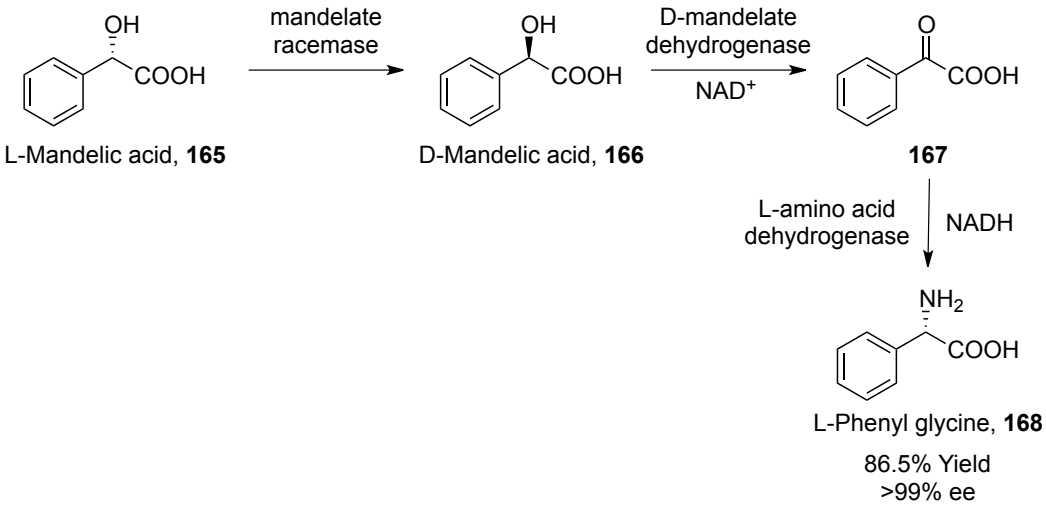

Scheme 50 Synthesis of L-phenyl glycine encompassing a redox neutral process NAD^+ is regenerated in the final transamination step[197].

The first step in the sequence was the oxidation of the alcohol **169** by an alcohol dehydrogenase (ADH-hT) that consumes NAD^+ leading to the formation of the aldehyde and NADH. In the second step, ω-transaminase (CV-ωTA) aminates the intermediate aldehyde **170**. L-Alanine was chosen as the amine donor which was regenerated by L-alanine dehydrogenase (AlaDH) at the expense of NADH from pyruvate. This redox neutral cascade was successfully applied to a range of aliphatic and aromatic alcohols however increased chain length was associated with a decrease in conversion.

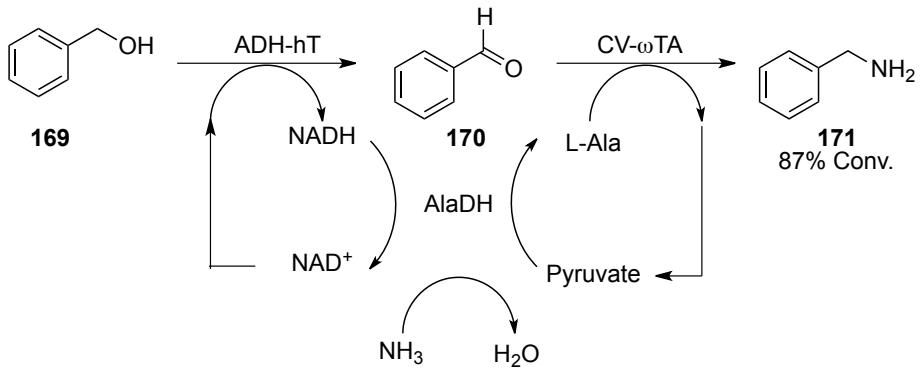

Scheme 51 Artificial redox neutral multi-enzyme network for the bioamination of primary alcohols[198]

Another cofactor recycling strategy has also been demonstrated recently by Bornschauer[193] in which the important building block chemical ε-caprolactone (ε-CL, **174**) was obtained from cyclohexanol (**172**), by combining ADH, CHMO and CAL-B in a single one-pot *in vitro* cascade reaction (Scheme 52). Although BVMOs are known to catalyse the formation of ε-caprolactone (ε-CL, **174**) from cyclohexanone (**173**), the reaction suffers from poor productivity as a result of enzyme instability, cofactor regeneration and also product inhibition. As before the use of NAD^+ dependent ADH and NADH dependent BVMO results in a redox neutral process. The toxicity effects of ε-CL on BVMO are eliminated by the utilization of the acetyltransferase activity of CAL-B to provide oligo- ε-CL **175** directly. With this artificial enzymatic pathway titers of up to 20 g L^{-1} of oligomeric ester have been obtained and highlights how multienzymatic cascades can be used in the synthesis of important polymer chemicals.

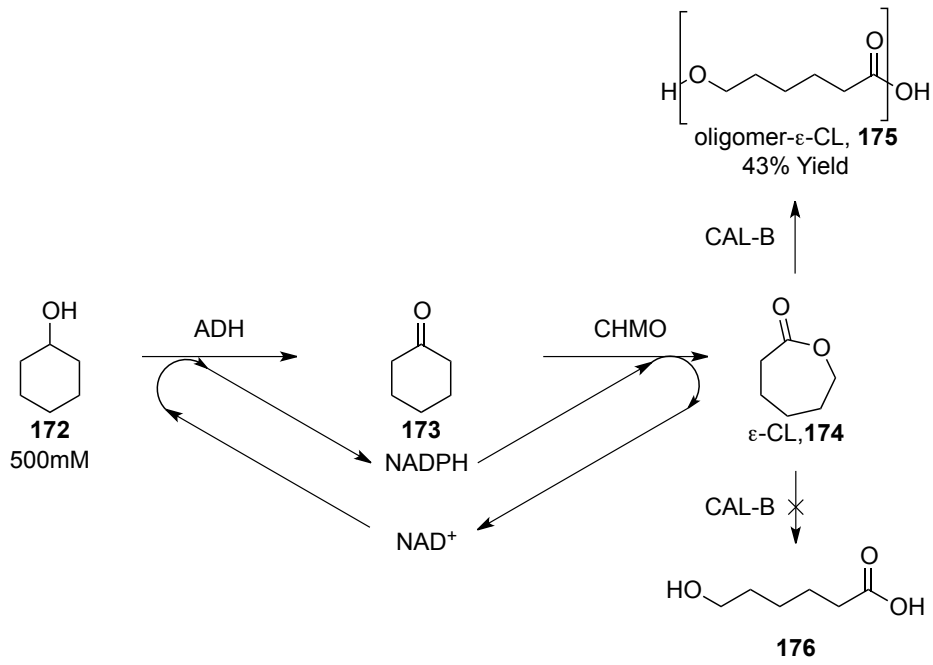

Scheme 52 Enzyme cascade synthesis of ε-CL and its oligomers[193].

The most sophisticated use of bioretrosynthetic analysis has recently been reported[194] in the six-enzyme isolated cascade for the synthesis of 6-aminohexanoic acid (**180**) from cyclohexanol (**172**)(Scheme 53). It was postulated that the use of two cofactor independent

enzymes could provide a self-sufficient biocatalytic system. Each module would involve an oxidation step requiring $NAD(P)^+$ and one step consuming NAD(P)H thus allowing two self sufficient redox cascades working independently from each other. The first module involved the production of ε-CL (**174**) from cyclohexanol (**172**) by the combination of the $NADP^+$ dependent ADH and the NADPH dependent BVMO mutant C376L M4001. The combination was successful and ε-CL (**174**) was formed in >99% conversion and titers up to 20 g L^{-1}. The more demanding second module involved transesterification of the ε-CL (**174**) with methanol by horse liver esterase followed by the NAD^+ dependent alcohol oxidation and subsequent NADH dependent transamination to provide the amino ester **179**. Horse liver esterase also catalysed the hydrolysis reaction of **179** to provide 6-amino hexanoic acid (**180**). Module two on its own provided 75% conversion within twenty hours and the preparative scale transformation of 1g of ε-CL was demonstrated. Despite the elegance of both modules, the combination of all six enzymes resulted in the poor conversion of cyclohexanol (**172**) to aminohexanoic acid (**176**) (24%) due the inactivation of BVMO by the high percentage of methanol required for the esterification reaction. Although low yielding, this study represents how clever biocatalytic synthesis can provide a highly atom efficient, two co-factor self sufficient multi enzymatic *in vitro* cascade for the synthesis of high value chemicals.

1.4.3 Metabolic engineering and bio-bio *in vivo* cascades

Microbes have long been adapted for the biosynthetic production of useful compounds. The concerted interaction of numerous enzymes within the cell allows exceptionally high conversions in multistep biosynthetic pathways. Many microbial primary metabolites (vitamins, nucleotides and ethanol) and also secondary metabolites (antibiotics, cholesterol lowering compounds and anti-tumor compounds) have a global market of several billion dollars. Now, we are seeing the assembly of microbial factories by combining diverse range of enzymes in a heterologous host and also improve pre-existing metabolic pathways to produce compounds that were previously unattainable.

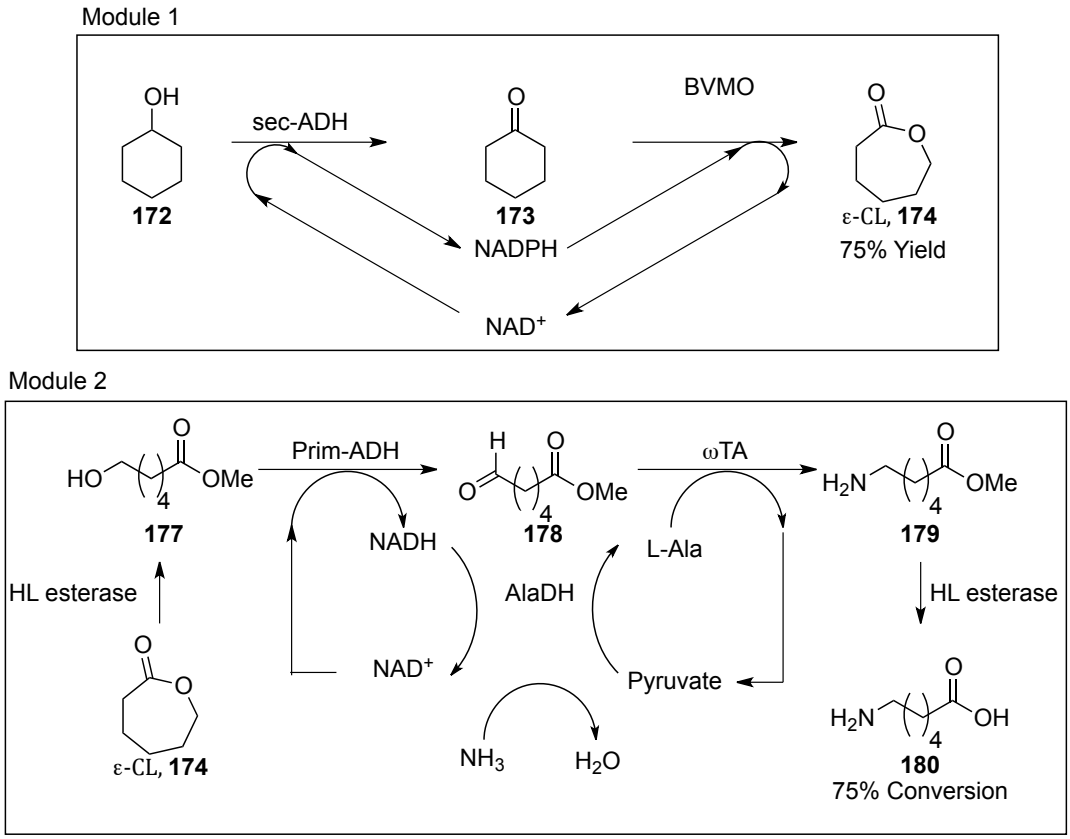

Scheme 53 Two co-factor independent enzyme cascades for the synthesis of 6-aminohexanoic acid, **180**[194]

Pre-existing metabolic pathways can be optimized by mediating strict control over the expression of the encoded pathway enzymes but also by engineering the enzymes to improve efficiency. This has been successfully demonstrated in which a novel *E.coli* strain was engineered to provide short chain alkanes by the manipulation of its own fatty acid biosynthesis and degradation pathways[199]. Similarly this approach has been successful in the production of 1,3 propane diol[200], 1,4-butane diol[201] and the artemisisin intermediate, artemisinic acid in titers up to 25 g L^{-1} [202]. With this approach, a detailed understanding and ability to control the host's metabolic pathway is required. Alternatively, host microorganisms may be used to recombinantly express a number of heterologous enzymes to generate unnatural metabolic pathways.

This concept was demonstrated by Schrewe[203], in which alkane monooxygenase AlkBGT from *Pseudomonas putida* GPo1 and w-TA CV2025 from *Chromobacterium*

violaceum were recombinatly expressed in *E.coli* BL21 for the direct amino functionalization of unactivated C-H bonds (Scheme 54). Dodecanoic acid methyl ester (**181**) was successfully converted to aldehyde **183** by alkBGT in a two step oxidation and subsequently transaminated by CV2025 with L-alanine serving as amine donor to provide the amino ester **184**. Poor mass transfer of the hydrophobic substrate over the cell membrane and competing enzyme reactions severely crippled the productivity and only 4% of the desired amino ester formed.

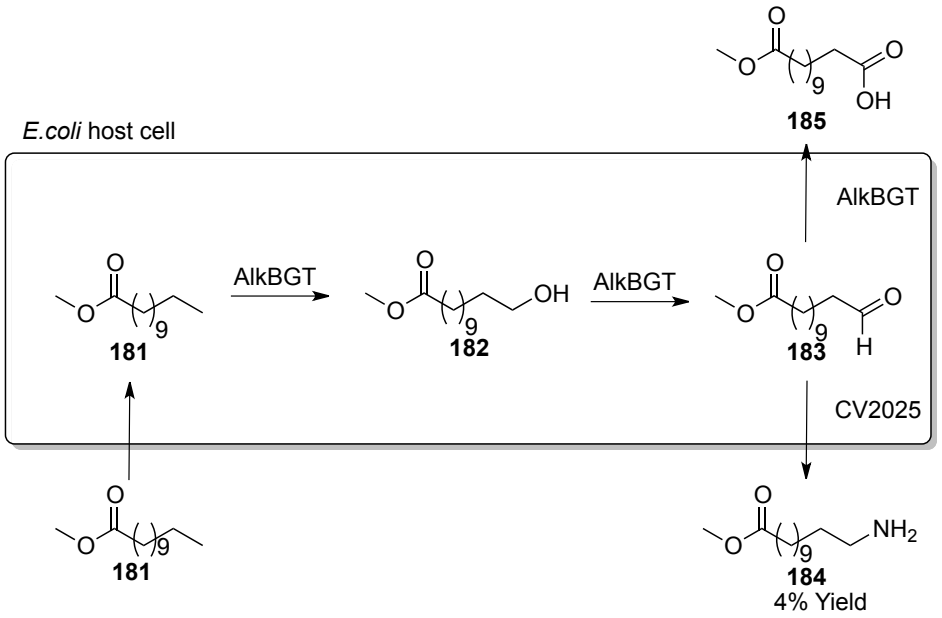

Scheme 54 Terminal amino functionalisation of dodecanoic acid methyl ester using an *in vivo* enzyme cascade[203].

Bornscheuer and coworkers[204] have recently demonstrated the application of *in vivo* enzyme cascades in desymmetrisation and kinetic resolutions. They developed an artificial mini metabolic pathway consisting of two ADHs, two enoate reductases and one BVMO recombinantly expressed in a single *E.coli* host to provide lactones from the corresponding allylic alcohols (Scheme 55). The first and second steps of the biotransformation are self-sustaining with respect to co-factor recycling but the final oxygenation step requires an additional equivalent of NADPH, which is provided by the host cell. The preparative capability of this artificial system was also shown in which 100 mg of carveol was successful transformed

into the desired lactone in 60% yield and >99% ee, albeit at low substrate concentration (4mM). The limited substrate concentration may reflect poor enzyme expression of one or more enzymes in the system although this issue is not commented on by the author.

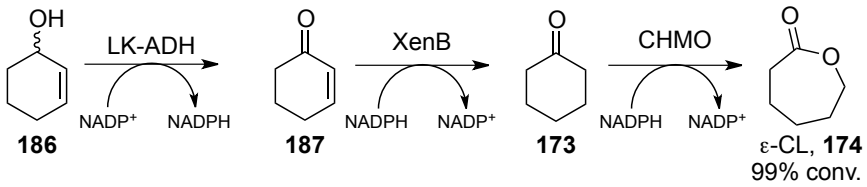

Scheme 55 An artificial metabolic pathway composed of an alcohol dehydro- genase (LK-ADH), an enoate reductase (XenB), and a Baeyer–Villiger-mono- oxygenase ($CHMO_{Acineto}$) starting from 2-cyclohexenol (**186**)[204]

Hollmann[205] has recently published a one-pot conversion of cycloalkanes to lactones using a similar recombinant system containing CYP450s, ADHs and BVMOs. However, in this study, poor expression of all enzymes was observed in the single *E.coli* host resulting in the desired lactone being obtained in low concentrations <1mM. The lower expression level was postulated to be a result of metabolic burden caused by the simultaneous expression of all three enzymes in a single host and represents a major limitation posed by multienzymatic *in vivo* cascades. This limitation was circumvented by the use of cell free lysates of separately expressed enzymes *in vitro*, which provided 23mM of caprolactone (**174**) from 30 mM cyclohexane.

Despite the inherent limitation of low substrate concentration, a number of whole cell *in vivo* enzyme cascades have been developed to provide a range of important building blocks chemicals from renewable resources. These include for example ω-amino fatty acids[203], ω-hydroxy fatty acids and dicarboxylic acids[206] and most recently azelic acid[207]. However, these reports are only proof of concept studies and are plagued with low yields with scarce industrial application. That being said further improvement *via* metabolic engineering to increase enzyme

expression and directed evolution may allow these strategies to become competitive in the future.

The prospect of a single whole cell designer biocatalyst to carry out multistep biotransformations *in vivo* is indeed highly desirable. However, low productivity as a result of low protein expression and substrate diffusion across the cell membrane are common problems associated with this type of catalysis. Although these issues can be engineered out, this is labour intensive and time consuming. Other drawbacks to using *in vivo* whole cells include lower chemoselectivity as unwanted enzyme activities may be present within the cells and also the control of the synthetic flux maybe difficult. In contrast, *in vitro* approaches are less complex and therefore reaction conditions are easier to control and optimize. In addition, higher purity products and substrate concentrations are possible. This may explain why, at this time, *in vitro* cascades is the method of choice for multienzyme cascade reactions.

Molybdenum-dependent oxidoreductases are a family of enzymes, which are relatively unexplored for their application in chemical synthesis. These enzymes catalyse the oxidation of imines and aldehydes to their corresponding amides and carboxylic acids. The use of these oxidoreductases for *in vitro* cascades is very appealing as aldehydes and imines can be generated by a variety of enzymes such as alcohol oxidases, and indirectly using transaminases

1.5 Molybdenum dependent oxidoreductases

Hydroxylation of either aromatic or aliphatic carbons is a common metabolic reaction. Many enzymes such as cytochrome P450 monoxygeneases have evolved to utilise molecular oxygen as the source of oxygen that is incorporated into the product. These require reducing equivalents as already discussed. In contrast, molybdenum hydroxylases use water as the source of oxygen for incorporation and also generate reducing equivalents such as NAD(P)H. These hydroxylases are known to accept a range of imines and aldehydes to provide the corresponding oxidation products[208].

The xanthine oxidoreductase (XOR) family consists of a number of well characterized molybdenum hydroxylases that include xanthine dehydrogenase (XDH), xanthine oxidase (XO)

and aldehyde oxidase (AO)[209,210]. XOR is recognised as the key enzyme in the catabolism of purines, oxidising hypoxanthine and xanthine to the terminal catabolite uric acid with concomitant reduction of NAD^+ (XDH) or O_2 (XO) [211,212]. The biological function of AO is still largely obscure but it is believed, due to its broad substrate specificity, to be involved in the elimination of xenobiotics. Periplasmic aldehyde oxidase (PaoABC) from *E.coli* has a preference for aromatic aldehydes and its suggested biological function is the detoxification of aromatic aldehydes in the periplasm[213].

1.5.1 Structure of molybdenum hydroxylases

Molybdenum is an essential component of this family of enzymes and is required for enzyme catalysis. Many molybdenum hydroxylases posses a similar overall architecture and contain a pair of [2Fe-2S] clusters, an FAD binding domain and a molybdenum binding domain[214,215] (Figure 8).

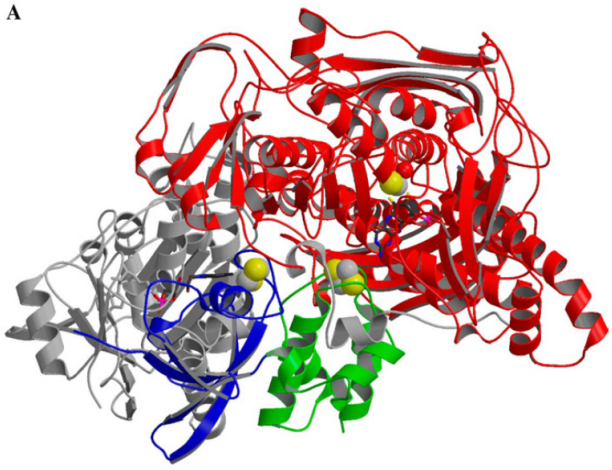

Figure 8: Crystal structure of bovine xanthine oxidase illustrating the major components in molybdenum hydroxylases: [Fe-S] clusters green and blue respectively, FAD domain (grey), molybdenum-binding portion (red)[216].

The Mo-binding domain consists of a pterin moiety which positions the catalytic Mo correctly within the active site of the enzyme and controls redox activity participating in electron transfer

to and from the Mo centre. For xanthine metabolising enzymes in this class, amino acid residues are highly conserved at positions; Phe914, Phe1009, Glu802, Glu1261 and Arg880 (Bovine XO numbering). Crystal structure analysis indicates that two glutamate residues lie on opposite sides of the substrate binding cleft that is defined by the phenylalanine residues. Glu802 is within H-bonding distance of the substrate and Glu1261 is in close proximity to the catalytic molybdenum (Figure 9). Interestingly, variants that favor aldehyde oxidation have tyrosine residues in place of phenylalanine residues. The Mo center itself consists of the metal in a distorted square pyramidal coordination geometry. The apical position is occupied by an Mo=O group, the four equatorial ligands are a terminal Mo=S, two sulfurs from the pterin moiety and a water derived hydroxide (Figure 10) [217].

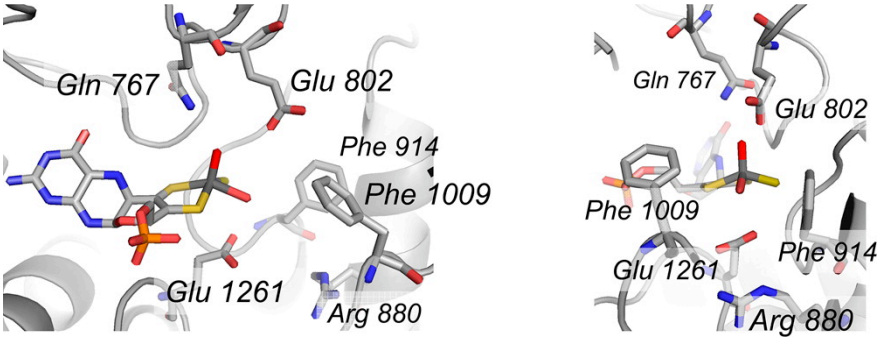

Figure 9 Active site structure of Bovine xanthine oxidoreductase. The orientation at right is rotated 90° about the vertical[217].

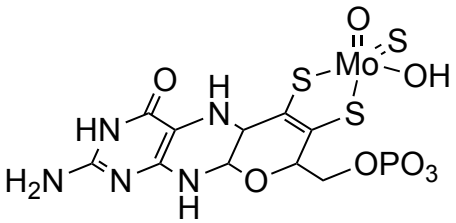

Figure 10 Structure of the pyranopterin cofactor bound Mo (MoCo)

1.5.2 Mechanism

The mechanism of oxidation of imines and aldehydes by molybdoenzymes has been determined using ^{18}O-labeling experiments, EPR analysis and also computational methods. The result of the experiments indicated that incorportated oxygen is derived from the water. The accepted mechanism is shown in Figure 11[216]. The initial step in the biotransformation is the base assisted (Glu1261) nucleophilic attack of the Mo-OH group leading to a tetrahedral Mo(VI) intermediate **189** that rapidly decays by hydride transfer to the Mo(VI)=S to yield reduced Mo(IV)-SH **190**. Water then displaces the bound product **191 (**Figure 11). Mo(VI) is then reformed by two-electron transfer out of the molybdenum center through the pterin moiety into the Fe/S cluster and finally to the FAD where molecular oxygen accepts the electrons and is subsequently reduced to H_2O_2 for XO.

1.5.3 Substrate scope of molybdenum hydroxylases

Extensive research has been conducted in the area of drug and other xenobiotic metabolism and it has been established that AO and XOR catalyse the oxidation of aldehydes to carboxylic acids, cyclic iminium ions to lactams and aromatic azaheterocyclic compounds to oxoheterocycles.

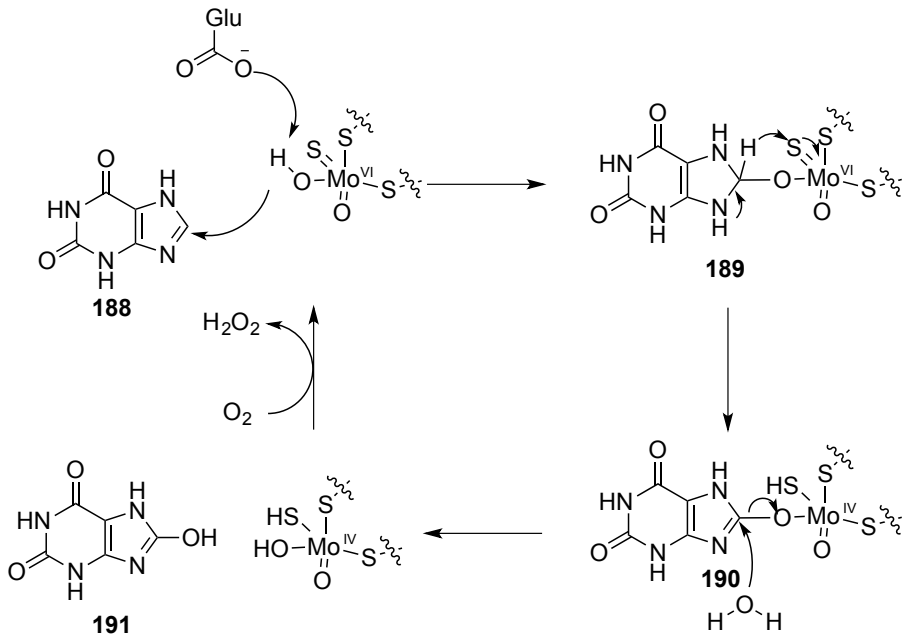

Figure 11. Proposed mechanism of molybdenum containing hydroxylases[216].

AO is known to metabolise a number of aliphatic and aromatic aldehydes to the corresponding carboxylic acids such as retinal into retinoic acid[218]. Secondary metabolites (**190-191**) derived from drug molecules such as Tamoxifen[219], Citalopram[220] and Tolbutamide[221] but also ethanol (**192**) are successfully oxidized, highlighting the wide substrate specificity of AO[208]. (Figure 12)

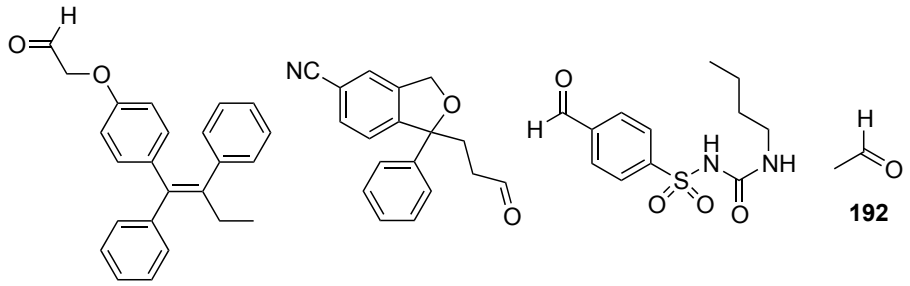

Figure 12. Aldehyde substrates for AO, metabolites derived from the drugs citralopram, tamoxifen and tolbutamide[208]

The hydroxylation of aromatic azaheterocycles is another important biotransformation carried out by molybdenum-dependent hydroxylases, especially XO and XDH. Quinazoline derivatives are metabolized to give their corresponding oxoheterocycles[222]. The sterically challenging selective dopamine D3 receptor antagonist SB-277011 (**197**)[223] and methotrexate (**196**) are metabolised by molybdoenzymes (Figure 13)[224].

Iminium ions are generated as intermediates during the metabolism of cyclic amines by P450 or MAO enzymes. These iminium ions are further metabolised to cyclic lactams by AO and XOR. Zapetin (**198)**[225], oxidized nicotine (**199)** [226], nicotinamide (**200)**[227] and prolintane (**201**)[228] all generate iminium ions during metabolism that are subsequently oxidized by XOR or AO to form lactam products. (Figure 14)

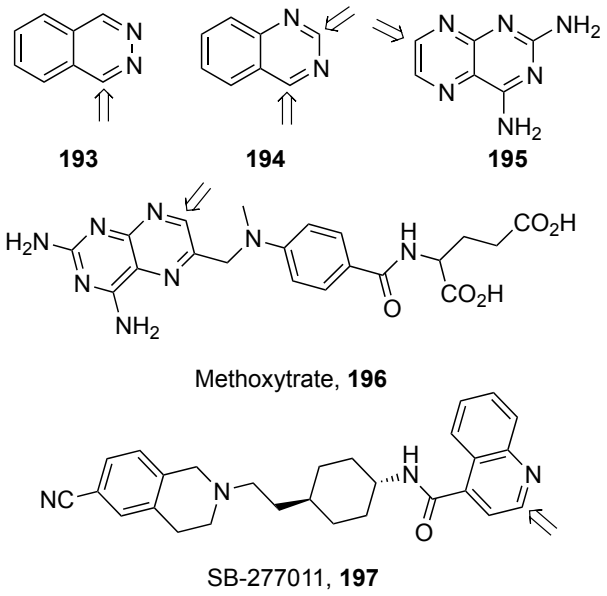

Figure 13 Aromatic azaheteroclic substrates for XOR type enzymes with arrows indicating oxidation site[208]

Despite the wide substrate specificity and interesting reactivity associated with molybdoenzymes, their synthetic application has not yet been explored. The regioselective and chemoselective hydroxylation of imines poses as an extremely interesting biotransformation as chemical methods in the literature for the regioselective oxidation of heterocycles are currently lacking. In addition, molybdoenzymes provide a distinct advantage over chemical oxidation methods which some employ toxic transition metals, as oxygen is used as the terminal oxidant and so may provide and selective, mild green alternative to traditional methods.

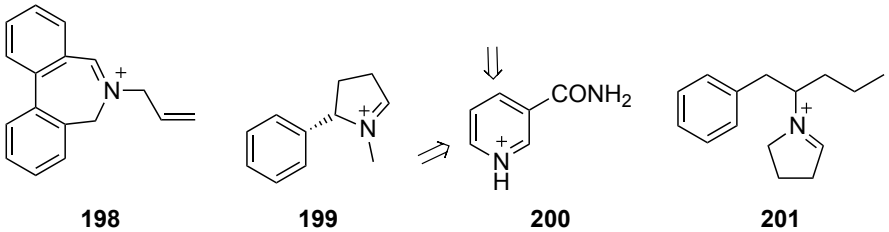

Figure 14 Iminium ion substrates for XOR[208]

1.6 Creation of Galactose Oxidase M_{3-5} ($GOaseM_{3-5}$)

Galactose oxidase (GOase) is a copper-containing free radical oxidase that can transform a range of primary alcohols into their corresponding aldehydes with reduction of molecular oxygen albeit with poor conversion. GOase has been applied in a broad range of areas including biosensors[229], cancer detection[230] and more recently, glycoprotein labeling[231]. Reports of its use in synthetic chemistry however, are limited in the literature. GOase is very efficient at oxidising substrates containing a β-galactose moiety such as melibiose, raffinose and lactose, however primary alcohols such a benzyl alcohol derivatives are poor substrates. To this end Turner[53] and Arnold[232,233] have developed novel GOase mutants to overcome this inherent limitation and to develop chiral variants.

1.6.1 Evolution of GOase for enantioselective secondary alcohol oxidation

Error prone PCR was conducted on WT GOase by Arnold[233] and after sufficient screening, a variant containing six mutations was discovered to provide a higher expression level and stability in *E.coli* ($GOaseM_1$). Additional mutations on $GOaseM_1$ using saturated mutagenesis provided an improved variant with a further three mutations[232]. The new variant ($GOaseM_3$) was capable of oxidizing D-Glucose but also showed low activity towards but-3-en-2-ol. $GOaseM_3$ exhibited low enantioselectivity towards 1-phenyl ethanol with the (*R*) enantiomer showing approximately 30-fold greater activity than the (*S*) enantiomer. Mutant libraries of $GOaseM_3$ were generated by epPCR with the aim to improve enantioselectivity and also broaden the substrate scope. The M_{3-5} variant was found to exhibit good activity against a range of substituted 1-phenylethanol analogues and provided these in high ee via kinetic resolution (Scheme 52).

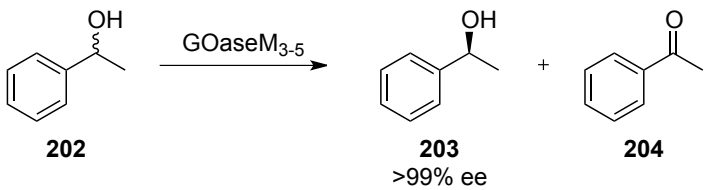

Scheme 52 Kinetic resolution of a 1-phenylethanol (202) using the $GOaseM_{3-5}$ variant[53].

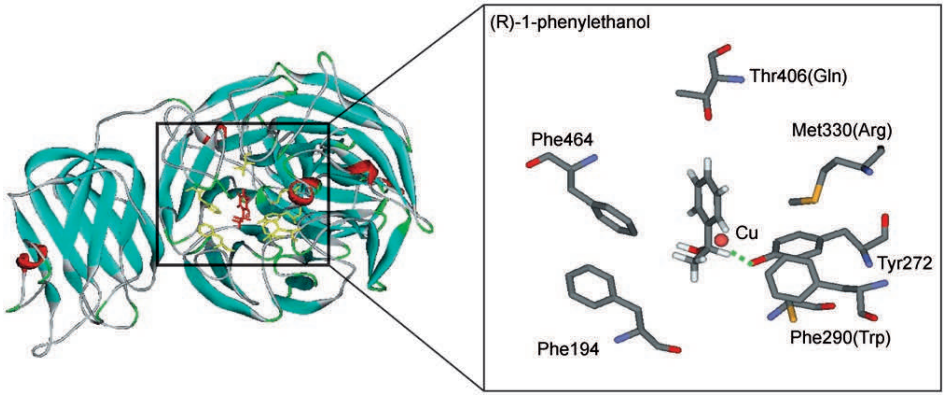

Figure 15 Active site structure of GOaseM_{3-5} showing (R)-1-phenylethanol 3 docked into active

The M_{3-5} variant contains a single mutation at position 330 compared to M_3 (Figure 15). This active site residue had previously been identified as important in controlling substrate recognition. Interestingly, this new variant has decreased activity towards its natural substrate galactose, indicating a switch in specificity with mutation of this residue. Recently GOaseM_{3-5} has been used in the redox desymmetrisation of biaryl atropisomers[234]

GOase has the advantage over the already established ADHs as no additional cofactors are required for oxidation. Oxidation only requires molecular oxygen and produces H_2O_2. As a result of the pioneering work by Arnold and Turner, a very stable and easily expressed GOase variant is available in which further directed evolution stratagies are possible with the already established screening methods. To this end the use of GOase mutants is very appealing in enzyme cascades as they can be fine tuned to meet further requirements.

Project Aim

Molybdenum-dependent oxidases have rarely seen use in synthetic chemistry. Their precedence in the literature remains limited to metabolic studies of xenobiotics, structural elucidation and more recently application in biosensors. *E. coli* XDH or PaoABC accept both aldehyde and imine functionalities to give the corresponding carboxylic acids and lactams. When compared with other oxidizing biocatalysts, molybdenum-dependent oxidoreductases have the advantage that molecular oxygen can often be used as the terminal oxidant and that $NAD(P)^+$ is not required as with alcohol dehydrogenases. Furthermore, the aldehyde and not the hydrate (as for FAD dependent oxidases) is the substrate for these oxidases and so oxidation is not dependent on hydrate formation. This has the benefit that electron rich aldehydes are accepted, which can prove problematic for FAD-dependent oxidases such as HMFO.

Herein, we attempt the design of enzyme cascade reactions, combining either *E. coli* XDH or PaoABC with $GOaseM_{3\text{-}5}$ to provide carboxylic acids from alcohols and also lactams from amino alcohols *via* an *in situ* generated imine. In addition, any chiral induction by the biocatalysts will be explored. Finally, we aim to apply this green methodology to the environmentally friendly synthesis of 2,4-furandicarboxylic (FDCA) from biobased 5-hydroxymethylfurfural (HMF).

Results and Discussion

Chapter 2

2.0 The oxidation of activated and unactivated alcohols to carboxylic acids *via* a two-enzyme one-pot cascade.

2.1 Introduction

The oxidation of alcohols to carboxylic acids often requires a stepwise process *via* the aldehyde intermediate and typically employs catalytic ruthenium or chromium and strong oxidants.[235] Biocatalytic processes using whole cells[60] and isolated enzymes[47,236] as already mentioned, are attractive tools for the synthesis of carboxylic acids due to the green attributes of biocatalysis. However, with whole cells, products often need to be removed from the reaction due to the toxicity of the intermediate aldehyde. To this end the use of isolated enzymes *in vitro* offers an attractive alternative. The use of alcohol dehydrogenases (ADH)[194] and aldehyde dehydrogenase (aldDH)[178] have been reported for this biotransformation but the use of $NAD(P)^+$ may limit their synthetic application as cofactor recycling is required. The use of two oxygen-dependent oxidases would have the advantage that no additional cofactors are required.

Galactose oxidase mutant $M_{3\text{-}5}$ ($GOaseM_{3\text{-}5}$) is known to accept a range of benzylic alcohols[53], converting them to their corresponding aldehydes at the expense of molecular oxygen as the terminal oxidant. Molybdenum-dependent hydroxylases, such as the commercially available *E. coli* XDH, have been documented to metabolise aldehyde xenobiotics converting them to the more polar carboxylic acids to facilitate elimination from the body[208]. However, the use of molybdenum hydroxylases to carry out this transformation for synthetic purposes has not been explored. The combination of both these enzymes in tandem would provide an extremely green synthetic route to carboxylic acids from alcohols as oxygen is used as the terminal oxidant with the only side product being hydrogen peroxide.

2.2 Oxidation of activated alcohols

2.2.1 Xanthine oxidase substrate scope

Molybdenum hydroxylases are known to metabolise various aldehyde containing drug molecules. The commercially available molybdoenzyme, xanthine oxidase (XDH) from *E. coli* was chosen as an ideal enzyme for the cascade due its availability. *E. coli* XDH uses O_2 as an electron acceptor in the absence of other mediators or co-factors. To quickly identify substrates for XDH, we believed it was necessary to develop a screening method in which oxidation of aldehydes could be observed by eye. The redox active dye, dichlorophenolindophenol (DCPIP, **205**) has been used routinely to assay XDH (Scheme 54).

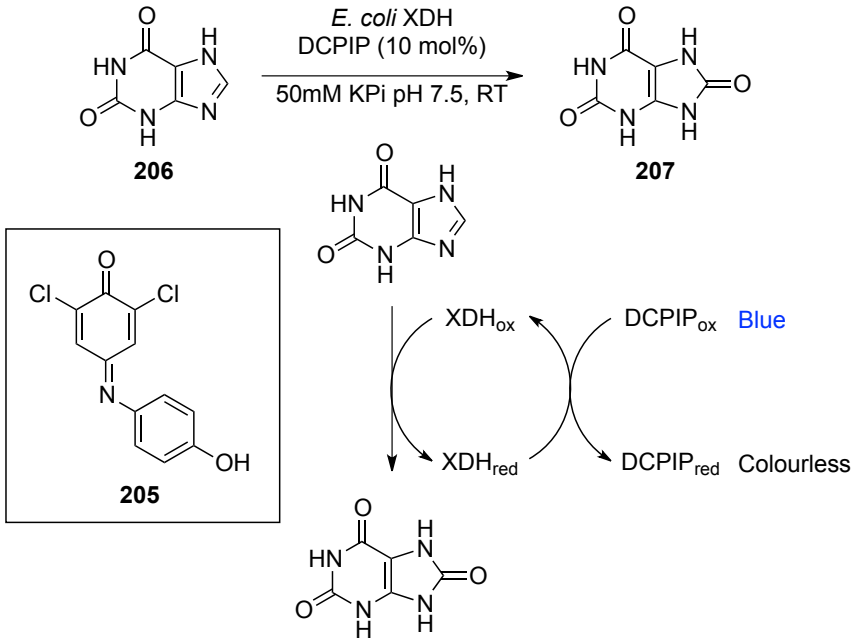

Scheme 54 DCPIP assay for XDH activity [184,237].

Using a 96 well plate a range of 56 aldehydes, were screened with the above method. *E. coli* XDH showed remarkable activity towards benzylic aldehydes with both electron withdrawing and donating groups in either ortho-, meta- and para positions. In addition, nitrogen, oxygen and sulphur containing heteroaromatic compounds were tolerated. The substrate specificity of *E. coli* XDH for aromatic aldehydes appeared to be dictated by enzyme substrate interactions, as no clear electronic effects were present (Scheme 55). Unfortunately,

the enzyme did not accept the less activated aldehydes such as phenylacetaldehyde (**231**) cinnamaldehyde (**232**) and alkyl aldehydes which was indicated by a negative result in our DCPIP screen (Scheme 56). This could be explained by the highly active nature of benzaldehyde derivatives to oxidation in air. Although the crystal structure of *E. coli* XDH is not known, the homologue *R.capsulatus* XDH contains two phenylalanine residues in the active site which may play an additional role[216]. The phenyl rings on the amino acids possibly pi stack with the benzyl aldehydes and so stabilize the transition state lowering the activation energy further. In the case of phenylacetaldehyde the reaction center may be too far from these interactions.

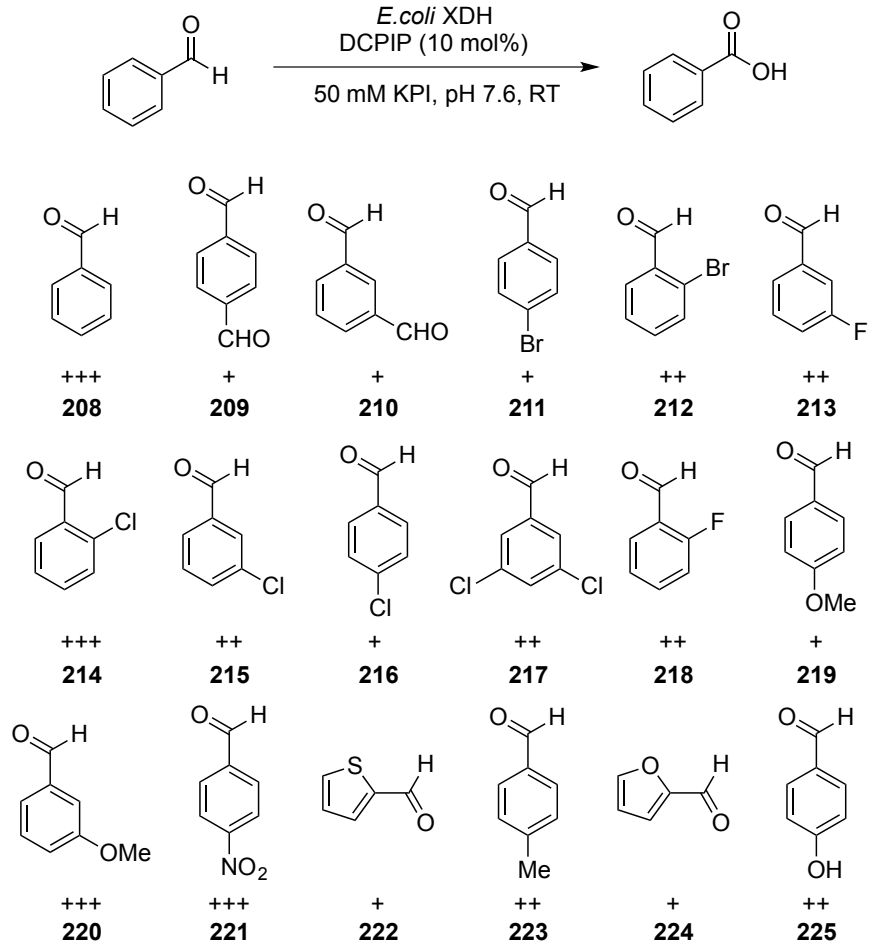

Scheme 55 Substrate scope of the *E. coli* XDH catalysed oxidation of benzylic alcohols as indicated by DCPIP screen. Activity as good as with natural substrate xanthine: +++; good activity: ++; moderate to low activity: +

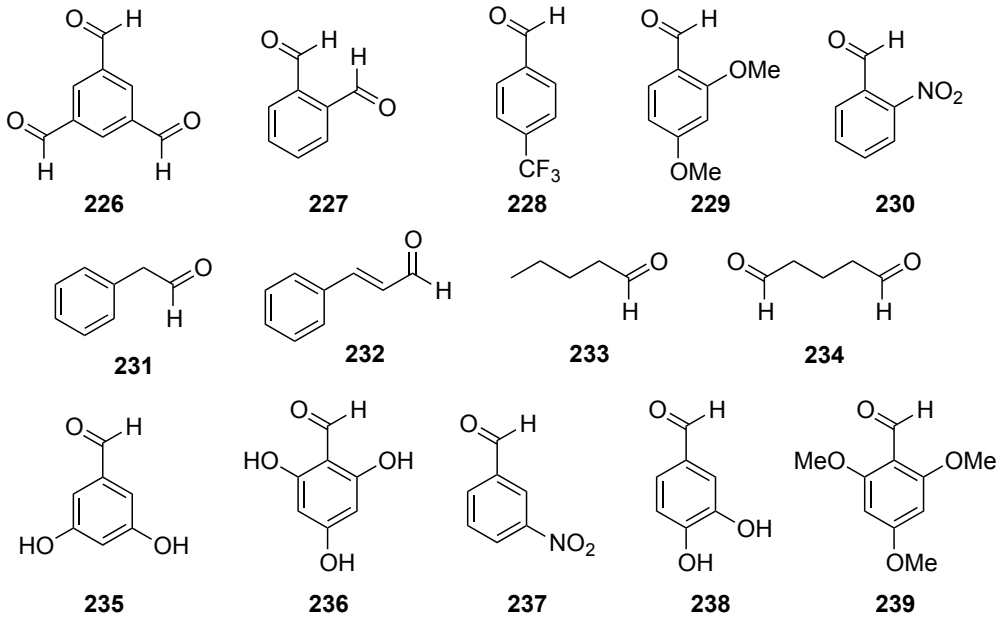

Scheme 56 Non-substrates for *E. coli* XDH as indicated by a negavite response in the DCPIP screen

2.2.2 Oxidation of selected benzaldehyde derivatives by *E. coli* XDH at 1mM substrate concentration

The major limitation posed by our substrate screen was that the extent of oxidation remained unknown. To this end, a selection of aldehydes was chosen and the conversion monitored by RP-HPLC to gain a detailed insight into the extent and rate of oxidation by *E.coli* XDH.

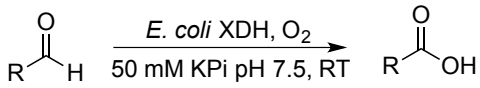

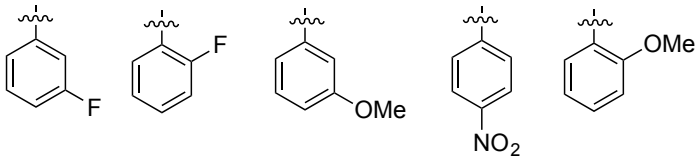

213 **218** **220** **221** **240**

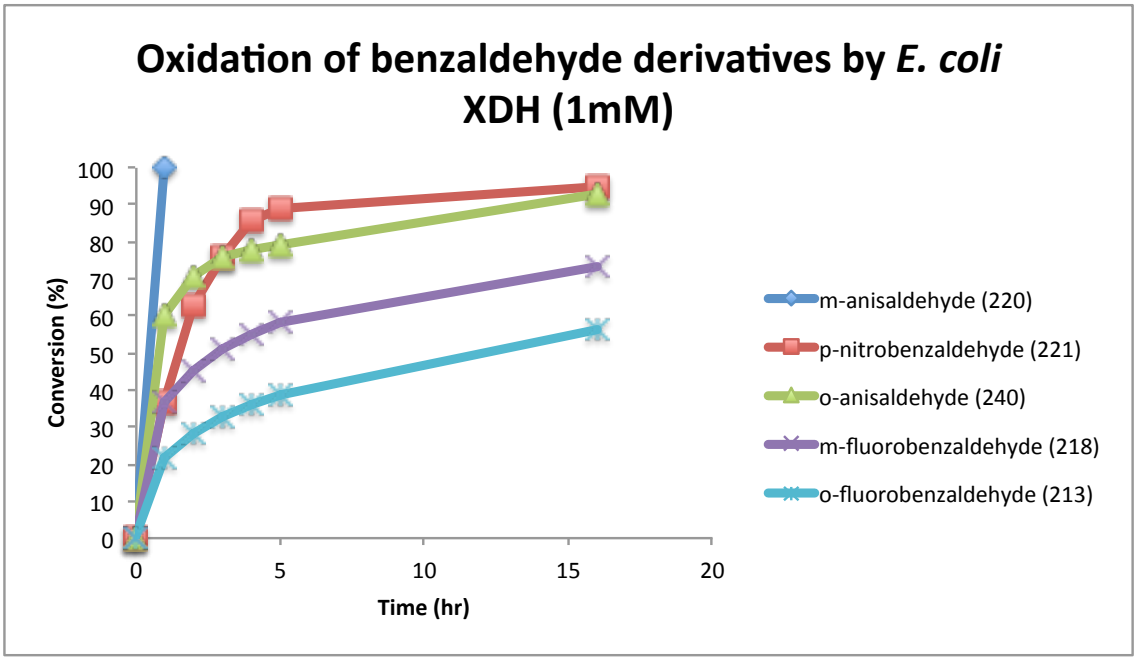

Figure 16 1 mM benzaldehyde derivatives oxidation time course. Reaction conditions: 3 µL substrate (100mM in MeCN), 297 µL 50 mM KPi buffer pH 7.6, RT. RP-HPLC conditions: ThermoFischer Hypurity C-18 column, flow rate 1.0 mL/min, UV 254 nm, Method A: 25% MeCN: 75% water + 0.1% TFA

Only full conversion was observed with *m*-anisaldehyde (**220**)(Figure 16). *p*-Nitrobenzaldeyde and *o*-anisaldehyde were also oxidised at a reasonable rate, albeit with a longer reaction time of 18 hours. However, the fluoro analogues were converted more slowly (73% for *m*-fluorobenzaldehyde (**213**) after 16 hours). We postulated that the low conversion and long reaction time was due to an inadequate supply of molecular oxygen dissolved in the buffer due

to the reaction being performed in sealed eppendorfs without agitation. The reactions were subsequently repeated with periodic opening of the reaction to air and subsequent shaking to allow oxygen to be dissolved in the buffer medium. Gratifyingly, with this modified procedure all the tested aldehydes were oxidized to the corresponding acid in excellent conversion (>92%) within one hour (Scheme 57). This observation highlights the importance of molecular oxygen in this catalytic system, as it is essential to re-activate the reduced molybdoenzyme. The different rates observed in Figure 10 presumably reflects differences in the K_m/K_{cat} under oxygen limiting conditions.

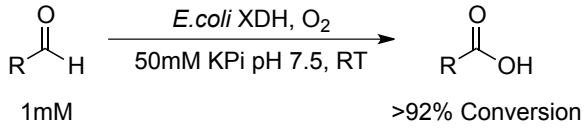

R = 4-NO_2-Ph, 4-Br-Ph, H, 4-Cl-Ph, 4-MeO-Ph, 2-MeO-Ph, 3-Cl-Ph, 3-Br-Ph, 4-Me-Ph, 2-F-Ph, 3-F-Ph, 2-Br-Ph, 3-MeO-Ph, 2,6-Cl_2-Ph, Ar = 2-thiophenyl, Ar = 2-furanyl

Scheme 57. Substrate scope for aromatic aldehyde oxidation by *E.coli* XDH

2.2.3 Oxidation of benzaldehydes at 10mM substrate concentration

p-Nitrobenzaldehyde (**221**) was chosen as a starting point for optimisation due to its activated nature (Table 1). At 1 mM the corresponding carboxylic acid was formed with quantitative conversion (Table 1, entry 1), however when the substrate concentration was increased beyond 10 mM a significant decrease in conversion was observed (Table 1, entry 2-4). *p*-Nitrobenzaldehyde is a solid and under our reaction conditions is poorly soluble in aqueous buffer. We considered this might be the reason behind the poor reactivity. The addition of co-solvents to aid solubility has enjoyed great success in many enzyme catalysed oxidations[47] and we believed we could incorporate this into our system.

Table 1 10mM substrate optimisation for the oxidation of benzaldehdye **220** and **221** using *E. coli* XDH[a]

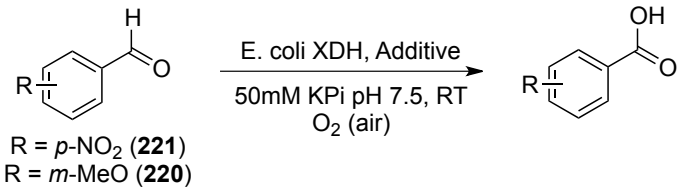

Entry	Compound	[Substrate] (mM)	Enzyme Volume (1 mg/mL)(µL)	Additive	Time (hr)	Conversion (%)[c]
1	**221**	1	20	None	1	100
2	"	10	"	"	"	15
3	"	30	"	"	"	7
4	"	50	"	"	"	6
5	"	1	"	10% IPA	1	46
6	"	30	"	"	"	0
7	**220**	"	15	None	16	9
8	"	"	20	"	"	11
9	"	"	50	"	"	12
10	"	"	70	"	"	19
11	"	"	100	"	"	11
12	"	"	120	"	"	18
13	"	10	50	None	"	53
14	"	"	"	SOD [b]	"	55
15	"	"	50	Catalase[b]	1	100
16	"	20	"	"	2	100

[a]Reaction conditions: X µL *E.coli* XDH (1.1 mg/mL), (3.3 mg/mL), X µL **221** or **222** (2 M in MeCN) in 50 mM pH 7.5 potassium phosphate buffer (300 µL final volume) 37°C. [b]Concentration of enzymes used was 1mg/ml). [c]Conversion calculated from peak areas of HPLC analysis using a Thermofisher hypurity C-18 column. Conversions were adjusted according to an NMR analysed 1:1 mix of aldehyde:acid and then analysed by RP-HPLC. SOD = Superoxide Dismutase

10% IPA did indeed help solubilise the substrate but it also reduced the activity of *E.coli* XDH (Table 1, entry 5-6). The next possibility we explored was substrate inhibition. We postulated if the substrate concentration remains low (1mM) by periodical addition of the substrate (**221**), this inhibition could be circumvented. However, decreased activity was observed after each subsequent addition of *p*-nitrobenzaldehyde (Figure 17).

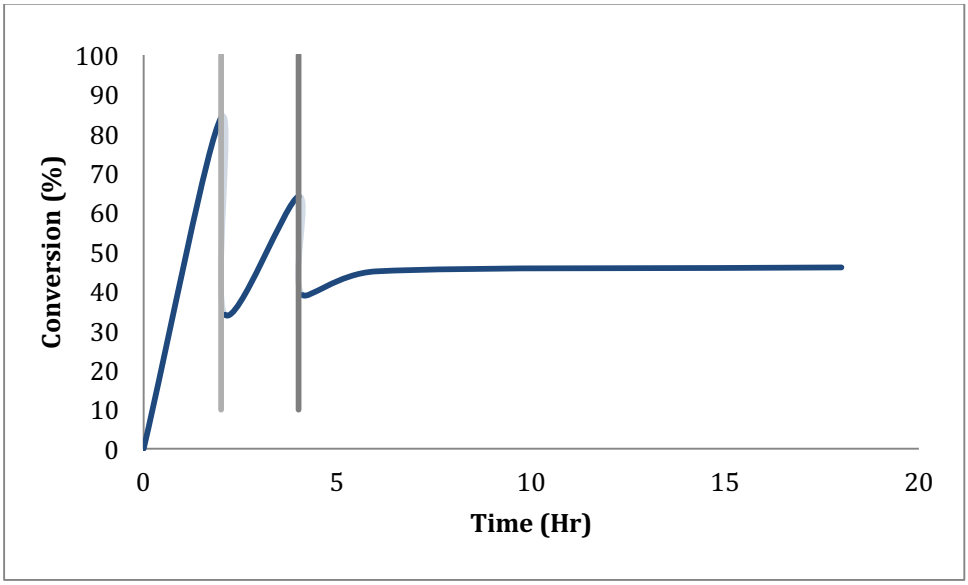

Figure 17 Periodic addition of 1mM p-nitrobenzaldehyde (**221**) to a final concentration of 3 mM

3-Methoxybenzaldehyde (**220**) was chosen as an alternative to *p*-nitrobenzaldehyde (**221**) as it showed high activity at 1mM but also it is a liquid and is more soluble in aqueous buffer. We believed that increasing enzyme concentration may overcome inhibition but this approach was met with no major increase in conversion even when 8 times the enzyme concentration was used (Table 1, entry 12). In the oxidation, molecular oxygen is reduced to H_2O_2 which is a known enzyme inhibitor[46]. In whole cell reactions, catalase is present as a protective enzyme that eliminates oxidative cell damage by this powerful oxidant. In our case the isolated enzyme has no protective enzymes and so can be subjected to oxidative damage by this side product. Two protective enzymes, superoxide dismutase and bovine catalase were employed, however only bovine catalase provided an increase in activity with quantitative conversion up to 20 mM in less than 2 hours (Table 1, entry 16). The use of catalase in isolated enzymatic oxidations is

often necessary if oxygen is the terminal oxidant. This has been documented by many groups working with oxidases[53]. However, this is the first time catalase has been reported to have a beneficial effect when using a molybdenum containing hydroxylase.

2.2.4 10mM GOaseM_{3-5}/XO cascade and preparative scale biotransformation

Our collaborator, Prof Nick Turner (University of Manchester, UK) has previously developed variants of *F. graminearum* galactose oxidase (GOase), such as GOase M_{3-5} that show remarkable ability to oxidise secondary and primary benzylic alcohols to their respective ketone and aldehyde products with H_2O_2 as by product[53]. We believed that by combining GOase M_{3-5} and *E.coli* XDH we could achieve direct and clean conversion of aryl alcohols to acids *via* an *in situ* generated aldehyde. The aryl alcohols corresponding to the best aldehyde substrates for *E. coli* XDH were selected for a one-pot-one step GOase M_{3-5}-XDH cascade approach. In all, quantitative conversion of the benzyl and heteroaryl alcohols (**241-257**) to the corresponding carboxylic acids (**258-274**) was observed within 16 hours (Scheme 58) using [S] = 10 mM.

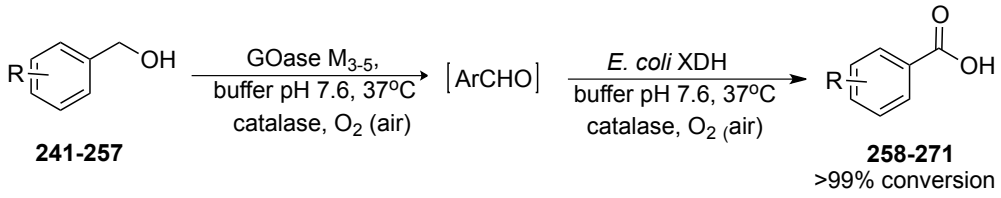

R = 4-NO_2-Ph, 4-Br-Ph, H, 4-Cl-Ph, 4-MeO-Ph, 2-MeO-Ph, 3-Cl-Ph, 3-Br-Ph, 4-Me-Ph, 2-F-Ph, 3-F-Ph, 2-Br-Ph, 3-MeO-Ph, 2,6-Cl_2-Ph, Ar = 2-thiophenyl, Ar = 2-furanyl

Scheme 58 Bio-bio cascade reaction for the conversion of alcohols to acids using GOaseM_{3-5} and *E.coli* XDH.

We next attempted to scale up the enzymatic cascade to [S] = 100 mM. 3-Methoxybenzylalcohol (**241**) was chosen as the most suitable candidate as it performed best in our cascade (Table 2). Increased substrate concentration up to 20 mM (Table 2, entry 2) was

tolerated, however when the concentration was increased to 40 mM a decrease in activity was observed (Table 2, entry 3). The addition of co-solvents to increase solubility was met with decreased activity as previously observed (Table 2, entries 4 & 5). As a result of higher substrate concentration an increase in H_2O_2 production would ensue and we postulated that the catalase concentration would need to be increased to provide sufficient protection. Gratifyingly, increasing catalase concentration provided the desired carboxylic acid in 94% conversion with 81% isolated yield after 5 hours (Table 2, entry 6). Increasing the substrate concentration further to 100 mM met with much lower conversion although no **241** was present after HPLC analysis (Table 2, entry 7).

Table 2 Optimisation of the GOaseM_{3-5}-*E. coli* XDH reaction for the formation of m-methoxy benzoic acid (**258**) from 3-methoxybenzyl alcohol (**241**) in a one step approach[a].

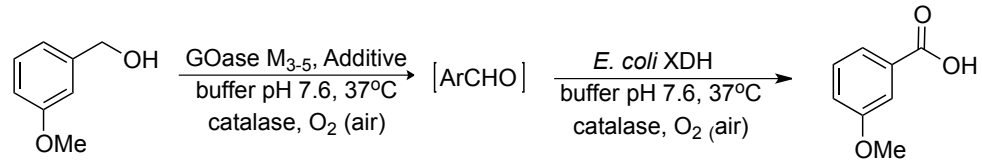

241 **220** **258**

Entry	[Substrate] mM	Additive	Catalase (1.1 mg/ml)	Time (Hr)	Conversion (%)
1	10	-	75 µL	1	100[b]
2	20	-	"	2	100[b]
3	40	-	"	16	82[b]
4	40	5% IPA	"	16	69[b]
5	40	15% IPA	"	16	21[b]
6	40	-	100 µL	5	94[b](81[c])
7	100	-	'	48	57[b](50[c])

[a]Reaction conditions: 103 µL GOaseM_{3-5} (3 mg/mL), 50 µL *E.coli* XDH (1.1 mg/mL), 33 µL catalase (3.3 mg/mL), X µL **241** (2 M in MeCN) in 50 mM pH 7.6 potassium phosphate buffer (300 µL final volume) 37°C, 16 hr [b]Conversion calculated from peak areas of HPLC analysis using a Thermofisher Hypurity C-18 column. Yields were adjusted according to an NMR analysed 1:1:1 mix of the aldehyde:acid:alcohol. [c]Isolated yields in parenthesis

The 10mM cascade reaction was further analysed by RP-HPLC by means of time course to identify relative rates of conversion by both enzymes (Figure 18). Clean and complete conversion to the aldehyde by GOase$M_{3\text{-}5}$ was observed after 10 minutes followed by a slower conversion to the acid by XDH.

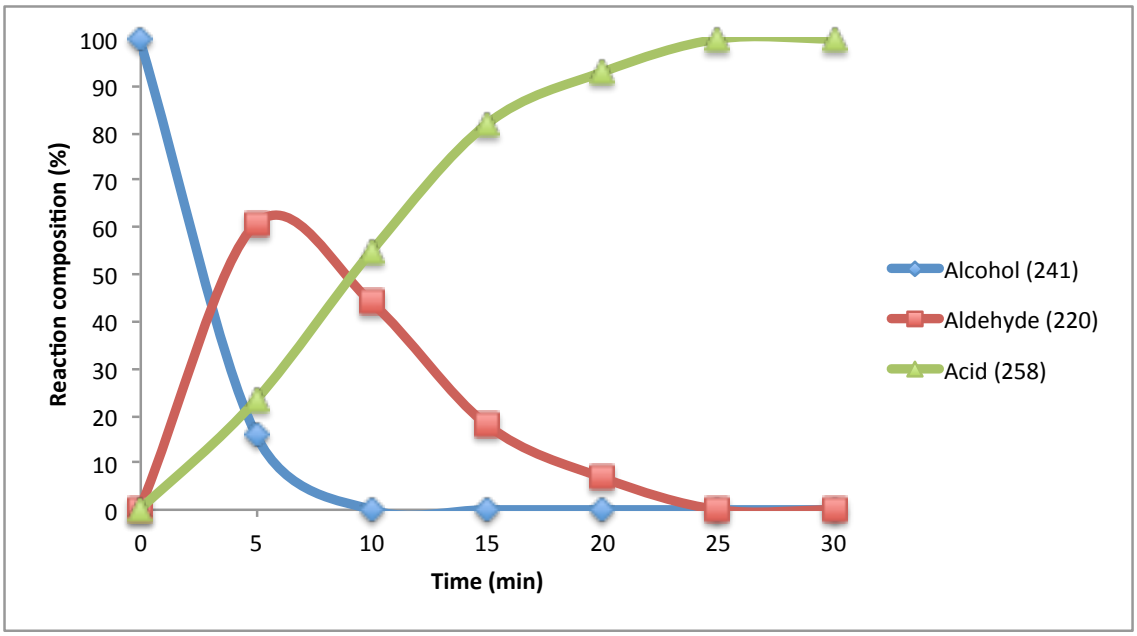

Figure 18 Time course 10 mM 3-Methoxybenzyl alcohol (**241**) to 3-methoxybenzoic acid (**258**) cascade with GOase$M_{3\text{-}5}$ and *E.coli* XDH

This experiment was repeated on 40 mM scale which indicated a similar reaction profile with an initial fast oxidation by GOase$M_{3\text{-}5}$ followed by a slower XDH catalysed oxidation of the intermediate aldehyde to reach 94% of the acid after 5 hours (Figure 19).

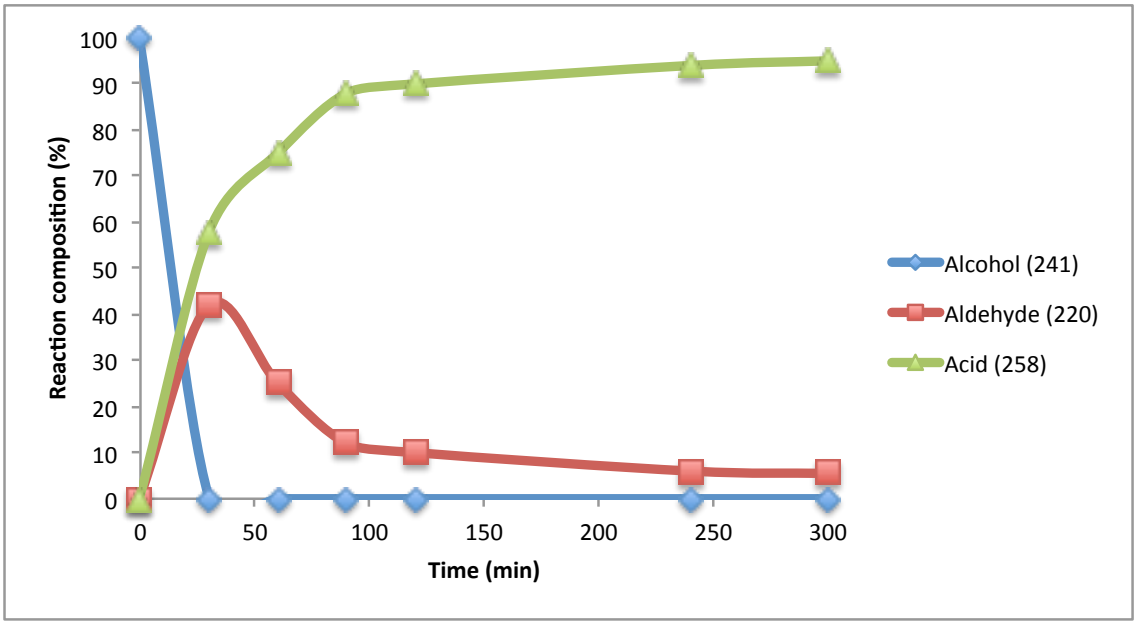

Figure 19 Time course 40 mM 3-Methoxybenzyl alcohol (**241**) to 3-methoxybenzoic acid (**258**) cascade with GOase$M_{3\text{-}5}$ and *E.coli* XDH

From the results it is clear that *E.coli* xanthine oxidase is the limiting factor in the cascade. GOase$M_{3\text{-}5}$ cleanly and efficiently converts aryl alcohols to their corresponding aldehydes up to 100mM substrate concentration. The major problem lies in the second oxidation step. *E.coli* XDH does not tolerate high substrate concentration (>40mM) possibly due to product or substrate inhibition. Alternative molybdoenzymes or immobilization of XDH may facilitate the scale up these cascades.

2.3 Enzyme cascades for the oxidation of unactivated alcohols to acids

2.3.1 PaoABC optimization and substrate screen

To expand the substrate scope of our cascades system an alternative molybdenum oxidase was required. Our collaborator Prof Silke Leimkühler (University of Potsdam) kindly donated a recently reported oxidase, periplasmic aldehyde oxidase (PaoABC) that uses oxygen as the terminal electron acceptor although this has not been reported[213]. PaoABC is a 135 kDa heterotrimer enzyme with a large (78.1 kDa) molybdenum cofactor containing PaoC subunit, a medium (33.9 kDa) FAD containing PaoB subunit and a small (21.0 kDa) [2Fe-2S] containing

PaoABC. Its is believed that *E.coli* PaoABC plays a role in the detoxification of aromatic aldehydes[213].

PaoABC has never been used for a synthetic application so it was unclear as to the optimum reaction conditions. To this end we decided to examine the effect of pH and buffer composition on the activity of PaoABC (Table 3).

Table 3 Optimisation of PaoABC-catalysed oxidation of to 3-methoxybenzaldehyde (**220)**

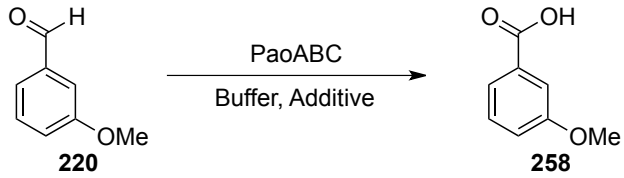

220 **258**

Entry	Molarity (mM)	PaoABC (13.3mg/mL)	Additive	Buffer (50 mM)	pH	Time (Min.)	Yield (%)[b]
1	1 mM	20 µL	None	Citrate	5	60	100
2	"	"	"	Phosphate	"	"	100
3	"	"	"	Acetate	"	"	100
4	"	10 µL	"	Phosphate	"	5	100
5	"	1 µL	"	"	5	30	100
6	"	"	"	"	5.5	5	70
7	"	"	"	"	6	"	85
8	"	"	"	"	6.5	"	100
9	"	"	"	"	7	"	86
10	"	"	"	"	7.5	"	65
11	10	5	"	"	6.5	60	41
12	"	"	Catalase	"	"	"	71

[a]Reaction conditions: X µL PaoABC (13.3 mg/mL), 3 µL **220** (1M in MeCN 10 mM final concentration) in 50 mM pH X potassium phosphate buffer (300 µL final volume) 37°C. [b]Yield was calculated by RP-HPLC on a ODS hypurity C-18 column with a flow rate 1mL/min and mobile phase 25% MeCN: 75% Water + 0.1%TFA

PaoABC is able to tolerate citrate, phosphate and acetate buffers. It was determined that pH 6.5 is the optimum pH for efficient catalysis (Table 3, entry 8). Catalase is also necessary for catalysis at higher substrate concentrations and this coincides with previous observations using *E.coli* XDH. The rate of oxidation of **220** was determined at different pH values in phosphate

buffer (Table 3, Entries 5-10) and it was shown that pH below 6 results in slower conversions (Figure 20).

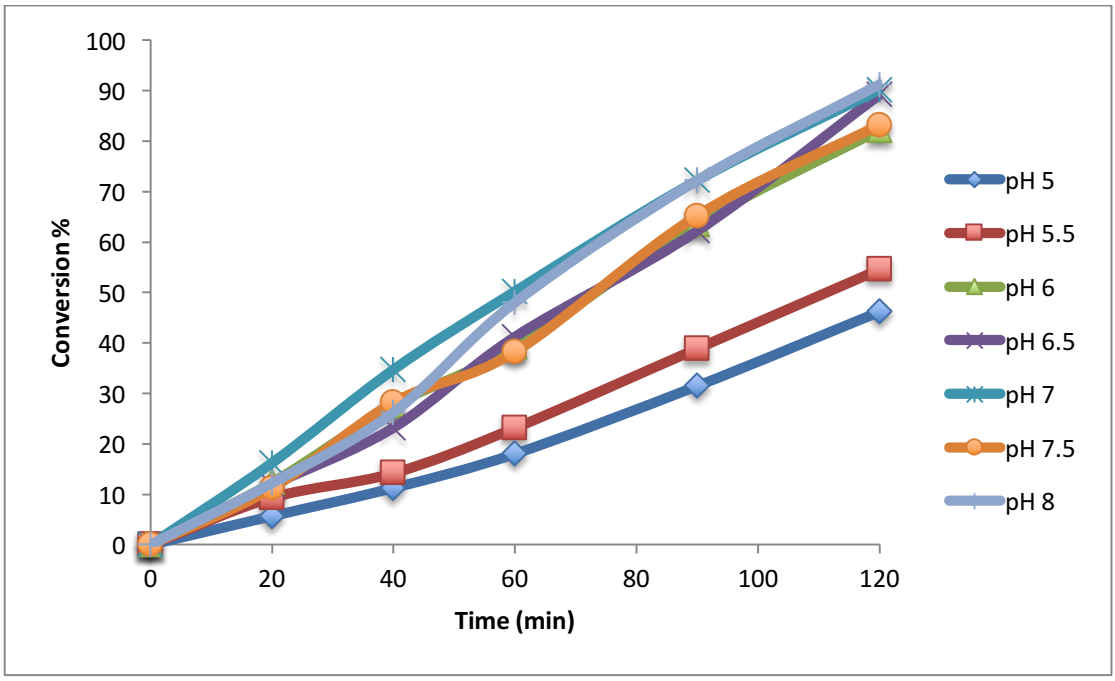

Figure 20 Rate of oxidation of 10mM to 3-methoxybenzaldehyde (**220**) by PaoABC in 100mM KPi buffer at different pHs.

Interestingly Leimkühler *et al.* reported that the optimum pH for PaoABC was pH 5.5 which contradicts these results. It is only recently that PaoABC was determined to be an oxidase, accepting oxygen as its terminal electron acceptor in the absence of other acceptor molecules. Previous work conducted by Leimkühler used ferricyanide as electron acceptor at pH 5.5[213] and also osmium complexes but at pH 9[238]. The ability of PaoABC to pass its electrons to an acceptor molecule appears to be dependent on pH and this may be the reason why we see higher activity at pH 7 as oxygen is now the electron acceptor.

With optimized conditions in hand we set out to identify additional substrates which could be used in new cascade reactions. Using the previously described DCPIP screen we found that a range of aldehydes were accepted by PaoABC which were not substrates for *E.coli* XDH. PaoABC had an expanded substrate scope accepting bulky, aromatic and aliphatic alcohols, not

oxidized by *E.coli* XDH (Scheme 59). Our collaborators working on the crystal structure of PaoABC have identified that the active site for PaoABC is extremely large and so it is no surprise that its substrate scope is wide. Interestingly, imine containing compounds such as DHIQ (**356**) and xanthine (**206**), the natural substrate for XDH are not accepted by PaoABC.

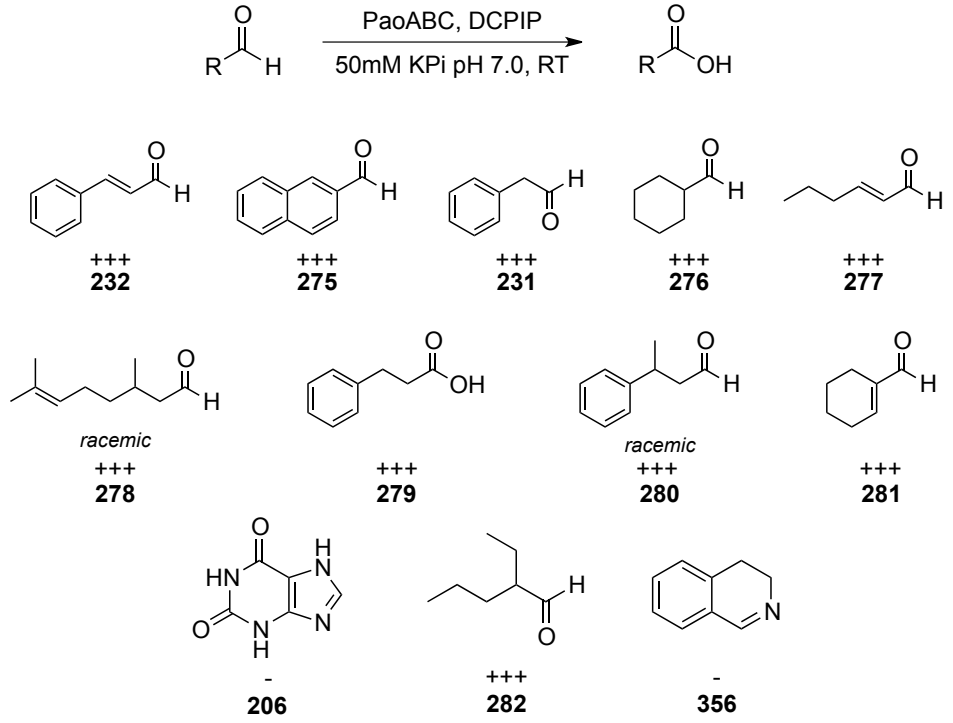

Scheme 59 Newly identified substrates for PaoABC as determined by a positive result from our DCPIP screen

2.3.2 Tempo-mediated alcohol oxidation

GOaseM_{3-5} has high activity towards benzyl alcohol derivatives but initial work by the Turner group indicated much lower activities towards unactivated aliphatic alcohols. For this reason we believed that a replacement oxidant was necessary. Alkyl alcohol oxidase or aryl alcohol oxidase was not available to us so we postulated that a chemo-bio oxidation would be a sufficient alternative. The laccase mediated TEMPO oxidation has enjoyed great success in many preparative scale transformations[82,239] and we anticipated that this system might allow us to obtain alkyl and bulky aldehydes that would not be possible using GOaseM_{3-5}. *m*-

Fluorobenzaldehyde was chosen as the test substrate for the chemo-bio cascade (Table 4). It was found to be necessary to lower the pH to 5, below the optimum pH of PaoABC, in order for sufficient oxidation of the alcohol to occur, albeit with poor subsequent conversion to the acid (Table 4, entry 2). Control reactions were conducted without PaoABC and it was seen that the addition of PaoABC has little affect on the formation of the carboxylic acid (Table 4, entry 2 and 5) which suggests PaoABC is being deactivated by TEMPO.

Table 4 Optimisation of TEMPO Laccase- PaoABC chemo-bio cascade for oxidation of 3-fluorobenzaldehyde[a]

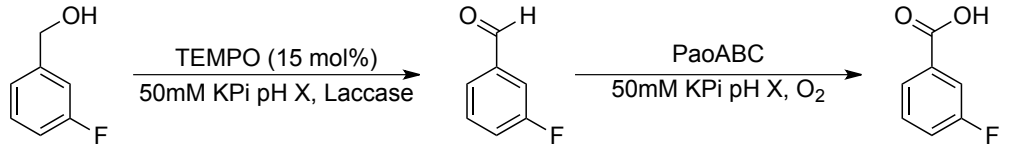

242 **213** **259**

Entry	[M]	pH	TEMPO (mol%)	Laccase (U)	Catalase (μL)	PaoABC (μL)	Yield (242:213:259)[b]
1	10 mM	6.5	15	1.5	100	5	100:0:0
2	"	5	"	"	"	"	5:79:14
3	"	"	"	-	"	"	69:10:20
4	"	"	"	1.5	-	"	4:84:10
5	"	"	"	"	100	-	1:82:16
6	"	"	"	"	-	-	1.5:80:17
7	"	"	"	-	-	-	62:37:0
8[c]	"	"	"	1.5	100	5	2:11:86
9[d]	"	"	"	"	"	"	4:5:89

[a]Reaction conditions: X μL PaoABC (13.2 mg/mL), X μL catalase (3.3 mg/mL), 3 μL **242** (1 M in MeCN 10 mM Final concentration) in 50mM pH X potassium phosphate buffer (300 μL final volume) 37°C, 16hr.[b]Yield was calculated by RP-HPLC on a ODS hypurity C-18 column with a flow rate 1mL/min and mobile phase 25% MeCN: 75% Water + 0.1% TFA.[c]After 4 hour the reaction was heated to 80°C for 5 minutes and allowed cool. After this time PaoABC was added. [d]After 4 hour the reaction was heated to 80°C for 5 minutes and allowed cool. After this time PaoABC was added and catalase.

Chemocatalysts are sometimes not compatible with biocatalysts for a variety of reasons. Reaction of the enzymes amino acids with the chemocatalyst can render the biocatalyst inactive as a result of a conformational change of the quaternary structure. This was observed by Turner and Ward in which they attempted to combine an iridium transfer hydrogenation catalyst with MAO-N[190] which resulted in deactivation of the biocatalyst. In these cases a one pot two step reaction sequence is required. Therfore after initial oxidation of the alcohol by TEMPO, the reaction was heated to 80°C to denature the laccase and to prevent TEMPO regeneration. PaoABC was then added which resulted in a significant increase of conversion to the acid (Table 4, entry 8). PaoABC is working below its pH optimum and so this may be a reason for incomplete conversion to the acid. However, when this system was applied to the oxidation of cinammyl alcohol, low conversion to the acid was observed with many additional uncharacterised side products. To this end, GOaseM_{3-5} was revisited which resulted in quantitative conversions of the alcohol to the acid over 16 hours (Table 5).

Table 5. Optimisation of GOaseM_{3-5}-PaoABC bio-bio enzymatic cascade for the oxidation of cinnamol.

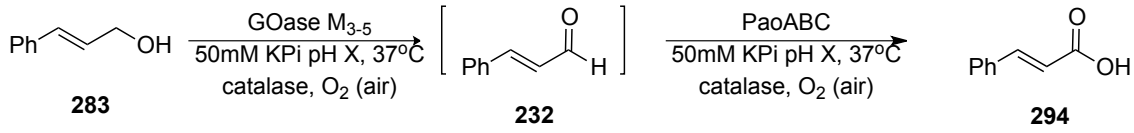

283 **232** **294**

Entry	pH	GoaseM$_{3-5}$ (3.7mg/mL)	Catalase (3.3mg/mL)	PaoABC (13.3mg/mL)	Yield[b] (283:232:294)
1	5	60µl	30µl	5µl	100:0:0
2	6.5	"	"	"	5:14:79
3	7.5	"	"	"	0:0:100

[a]Reaction conditions: X µL GOaseM_{3-5} (3 mg/mL), X µL PaoABC (13.2 mg/mL), X µL catalase (3.3 mg/mL), 3 µL X (1M in MeCN, 10 mM final concentration) in 50mM pH X potassium phosphate buffer (300 µL final volume) 37°C. [b]Yields calculated by GC

2.3.3 GOaseM_{3-5}/PaoABC cascade

The alcohols corresponding to the best aldehyde substrates (**283-293**) for PaoABC were selected for a one-pot-one step GOaseM_{3-5}-PaoABC cascade. This resulted in the successful conversion of all primary alcohols to carboxylic acids (**294-303**) with, in most cases, quantitative conversion at 10 mM substrate concentration (Table 6).

Table 6 Scope of the GOaseM_{3-5}-PaoABC enzymatic cascade[a]

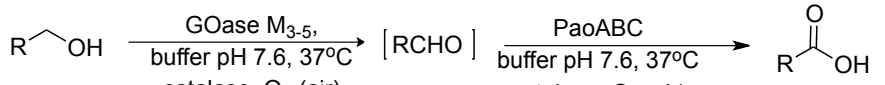

Product	Conversion[b]	Product	Conversion[b]
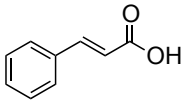 **294**	>99%	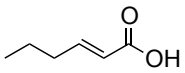 **298**	>99%
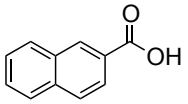 **295**	>99%	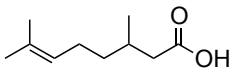 **299**	>99%
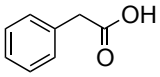 **296**	>99%	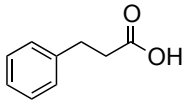 **300**	>99%
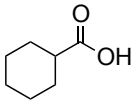 **297**	>99%	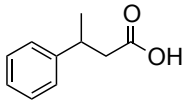 **301**	>99%
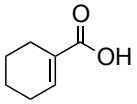 **302**	81%	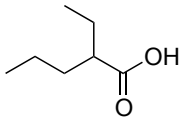 **303**	50%

[a]Reaction conditions: 103 µL GOaseM_{3-5} (3 mg/mL), 5 µL PaoABC (13.2 mg/mL), 33 µL catalase (3.3 mg/mL), 3 µL (1M in MeCN 10mM final concentration) in 50 mM pH 7.6 potassium phosphate buffer (159 µL), 37°C shaking overnight. [b]Conversions calculated by GC.

A time course study for the conversion of phenyl ethanol to phenyl acetic acid revealed no aldehyde intermediate (Figure 21), indicating that the second oxidation catalysed by PaoABC is extremely rapid.

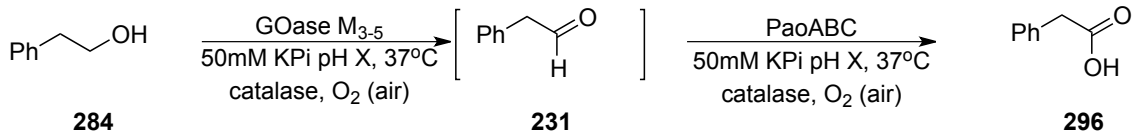

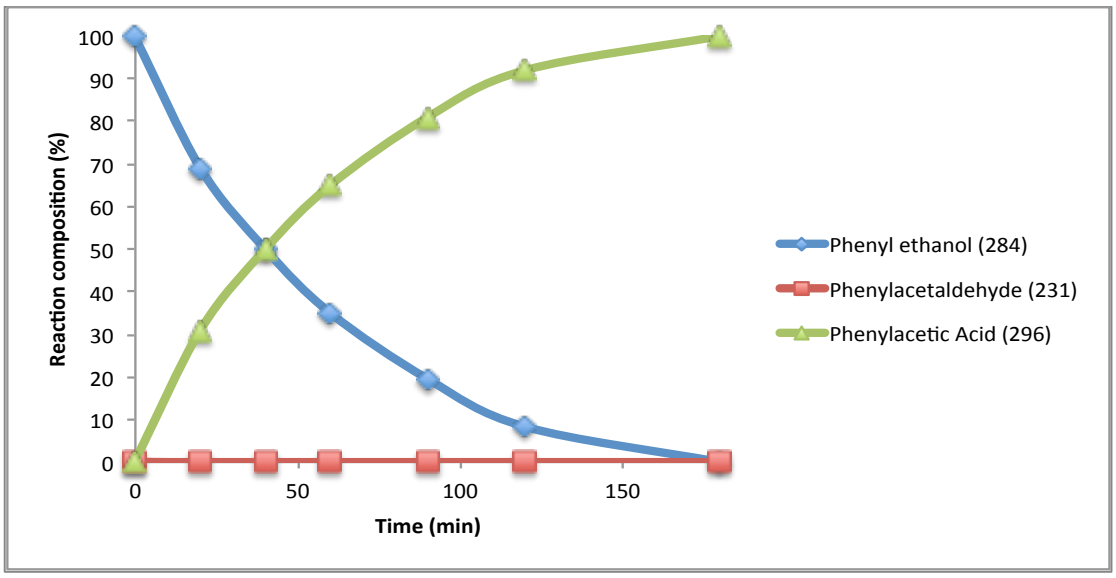

Figure 21. 10mM Phenyl ethanol GOaseM_{3-5}-PaoABC bio/bio cascade time course

This methodology compares very well against state-of-the-art chemical oxidations such as the ruthenium based method recently reported by Milstein[49]. Our catalytic system utilises molecular oxygen as the terminal oxidant and operates under mild conditions and is totally chemoselective. Milstein's procedure requires refluxing NaOH, argon atmosphere but is also plagued by side reactions such as hydrogenation of double bonds. Interestingly, in one substrate we obtained 50:50 aldehyde:carboxylic acid (Table 6, compound **303**) which suggests that PaoABC may be showing chiral selectivity. This will be explored in a later chapter (Chapter 4).

2.3.4 Preparative scale biotransformations.

We then set out to scale up our new catalytic system using 3-phenylbutan-1-ol (**285**) however increasing substrate concentration to [S] = 30 mM was met with decreased acitivity of GOase$M_{3\text{-}5}$ (Table 7, entry 1). Large quantities of GOase were required to obtain high conversions of 3-phenylbutan-1-ol (Table 7, entry 2). Interestingly, PaoABC showed a remarkable tolerance of high substrate concentration, as NMR of the crude reaction could identify no aldehyde intermediate. Since GOase$M_{3\text{-}5}$ currently represents the limiting activity it will be necessary to engineer GOase variants that are more tolerant to higher alcohol concentrations. Overall the GOase$M_{3\text{-}5}$-PaoABC one-pot conversion provides a highly green and direct method for the conversion of alcohols to carboxylic acids. However, if it is to become industrially relevant the limitation of low substrate concentration must be addressed.

Table 7 Optimisation of GOase$M_{3\text{-}5}$-PaoABC 30mM scale cascade oxidation of 3-phenylbutan-1-ol (**285**)[a].

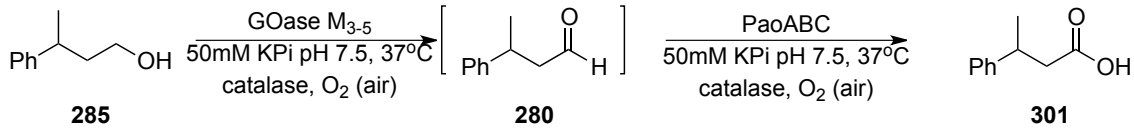

285 **280** **301**

Entry	Temp (°C)	Catalase (3.3 mg/mL)	GOase$M_{3\text{-}5}$ (1.3 mg/mL)	PaoABC (13.3 mg/ml)	Conversion (285:280:301)[a]
1	25	109 µL	268 µL	16.6 µL	62:0:38
2	37	"	400 µL	"	30:0:70
3	"	180 µL	"	"	12:0:88
4	"	"	500 µL	"	15:0:85

[a]Reaction conditions: X µL GOase$M_{3\text{-}5}$ (3 mg/mL), X µL PaoABC (13.2 mg/mL), X µL catalase (3.3 mg/mL), **285** µL (2 M in MeCN 30 mM final concentration) in 50 mM pH 7.6 ptassium phosphate buffer to a final volume of 1 mL, shaking overnight. [b]Conversions calculated by ^{1}H NMR of crude isolated product

2.4 GOase$M_{3\text{-}5}$ unusual activity with PaoABC (inhibition studies)

Interesting unpublished results from the Turner group indicate that many of the substrates such as phenylethanol (**284**), which were successful in our cascade, are not substrates for GOase$M_{3\text{-}5}$.

This led us to believe that perhaps the aldehyde product of the alcohol oxidations are inhibitors for GOaseM_{3-5}. However, in our system the PaoABC removes the aldehydes rapidly.

Benzyl alcohol has been shown by us to be a very good substrate for GOaseM_{3-5}. Therefore we tested if phenylacetaldehyde at different concentrations would act as an inhibitor (Table 8). Indeed phenylacetaldehyde did have an inhibitory affect even at concentrations as low as 1 mol% (Table 7, entry 2). However activity still remained, which does not account for total inactivity observed when phenyl ethanol is used as substrate.

We postulated that perhaps the phenylacetaldehyde that is formed from phenylethanol, in the active site, irreversibly binds to the protein and thus inactivating it. To simulate this we preincubated 1 mM phenylethanol with GOaseM_{3-5} (to form phenylacetaldehyde in the active site), prior to the addition of 10 mM benzyl alcohol.

Table 8 GOaseM_{3-5} inhibition by phenylacetaldehyde

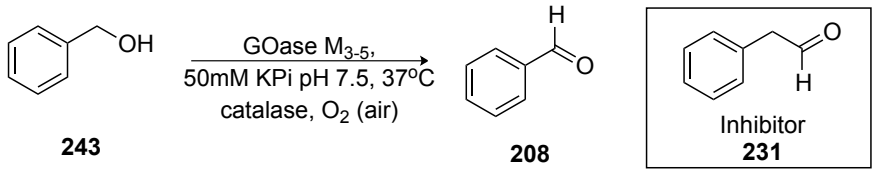

243 **208** **231**

Entry	Molarity [S]	Inhibitor (mM)	Conversion (%)[a]
1	10 mM	0	100
2	"	0.1	75
3	"	0.3	45
4	"	0.7	38
5	"	1	36

[a]Reaction conditions: 103 µL GOaseM_{3-5} (3 mg/mL), 5 µl PaoABC (13.2 mg/mL), 33 µL catalase (3.3 mg/mL), 3 µL benzyl alcohol (1 M in MeCN 10 mM Final concentration), X µL Phenylacetaldehyde (100 mM in MeCN), in 50 mM pH 7.6 ptassium phosphate buffer to a final volume of 1 mL, 1 hr. [a]Yield was calculated by RP-HPLC on a ODS hypurity C-18 column with a flow rate 1ml/min and mobile phase 25% MeCN: 75% Water + 0.1% TFA

Despite this preincubation benzyl alcohol was converted to 56% within an hour and although inhibition had taken place, this was not to the extent we had observed when phenylethanol was used on its own.

We then attempted to simulate cascade conditions by the addition of PaoABC to rescue the GOase in the previous reaction and to identify if we could obtain the carboxylic acid product. Only phenyl ethanol, benzyl alcohol and benzoic acid were present in the reaction mixture after a further hour, indicating that GOase$M_{3\text{-}5}$ has been inactivated as both alcohols have not been transformed to the corresponding aldehydes after this time. It is evident from this result, PaoABC must be present from the beginning of the reaction to instill its positive effect on GOase$M_{3\text{-}5}$

Thus it remains unclear why phenylethanol is a substrate for GOase$M_{3\text{-}5}$ only under cascade conditions. Phenylacetaldehyde is indeed an inhibitor although the extent of inhibition does not reflect the inactivity observed in the absence of PaoABC. To this end we believe that there is some sort of potentiation of GOase$M_{3\text{-}5}$ by PaoABC. This could be a result of a conformational change of GOase$M_{3\text{-}5}$ by protein-protein interactions[240] between both oxidases or perhaps the presence of reactive oxygen species[241] generated by PaoABC, that activates the GOase active site. Ongoing studies are being conducted to determine the mechanism of this apparent potentiation.

2.5 Conclusion

We have demonstrated a one-pot, single stage tandem cascade for the quantitative conversion of 26 alcohols directly to their corresponding carboxylic acids, including aliphatic examples, employing three oxygen-dependent enzymes, GOase$M_{3\text{-}5}$, PaoABC and *E.coli* XDH. This is the first time XOR enzymes have been applied in preparative biocatalysis and the two we have used have the distinct advantage in that they do not require addition of cofactors.

A novel enzymatic screening method was developed, utilising artificial electron acceptors DCPIP to facilitate the transfer of electrons out of the molybdenum centre resulting in a colour change, indicating oxidation. This concept of using artificial electron acceptors[238] is exciting as water soluble metal catalysts could potentially be used to facilitate electron transport

which could subsequently carry out a chemical transformation such as hydrogenation in novel bio-chemo cascade.

The major limitation of the discovered bio-bio cascades is the relatively low substrate concentration in which one of the combined enzymes tolerate. In the first benzyl alcohol cascades, *E.coli* XDH was highlighted as the limiting factor. When substrate concentrations above 50 mM were employed, a decrease in aldehyde conversion was observed but GOase$M_{3\text{-}5}$ remained highly active. PaoABC may circumvent the issues of scale up associated with *E.coli* XDH as the new enzyme is much more active than the commercially available XDH. Utilising PaoABC and GOase$M_{3\text{-}5}$ in tandem one-pot oxidation of benzyl alcohols could tolerate much higher substrate concentrations and this work is ongoing in our laboratory.

In contrast, the cascades using inactivated alcohols indicated the alcohol oxidase was now the limiting factor. When substrate concentrations were increased past 30 mM, the activity of GOase$M_{3\text{-}5}$ decreased most likely as a result of substrate inhibition. Unfortunately, this could not be addressed by increasing GOase$M_{3\text{-}5}$ concentration. Interestingly, no aldehyde intermediate was present in the reaction mixtures indicating rapid oxidation of the aldehyde intermediates by PaoABC. Evaluation of PaoABC, GOase$M_{3\text{-}5}$ and *E.coli* XDH stability, immobilisation and creation of additional mutants will facilitate scale up of these cascade processes.

In addition, we have observed a novel potentiation effect by combining GOase$M_{3\text{-}5}$ and PaoABC. We have successfully expanded the substrate scope of GOase$M_{3\text{-}5}$ by combining the alcohol oxidase with PaoABC. Substrates previously believed to be not accepted by GOase$M_{3\text{-}5}$ furnished carboxylic acids in cascade conditions. Although the mechanism of this potentiation is unknown at this time it may be key to unlocking a potentially very powerful alcohol oxidase with a wide substrate scope.

Chapter 3

3.0 Steps towards the dynamic kinetic resolution of α-substituted aldehydes

3.1 Introduction

With the growing demand for homochiral active pharmaceutical ingredients, environmentally friendly synthetic routes to enantiomerically pure compounds are being increasingly investigated[242-246].

There are many chemical methods for the synthesis of carboxylic acids from alcohols. These methods can also be applied to the of synthesis of α-substituted carboxylic acids such as profens, however only from an enantiomerically enriched starting material. Traditional chemical methods employing chromium reagents[247], potassium permanganate[248], palladium[249], ruthenium[250] often operate at high temperature and use strongly basic or acidic conditions which have the further drawback of racemisation of enantiopure intermediates. For this reason alternative routes have been explored. The use of chiral auxiliaries to install the chiral methyl group on profen drugs have been reported[242] but installation and hydrolysis of the auxiliary are required leading to unwanted extra steps, lower yields and lack of green chemistry credentials.

To this end numerous biological approaches have been developed applying lipases in both the kinetic and dynamic kinetic resolution of profen esters[251]. Recently Holmann[178] has reported an oxidative dynamic kinetic resolution of profen aldehydes using ADH-9VI with *in situ* NAD^+ regeneration to promising ees, albeit at low substrate concentration (Scheme 59).

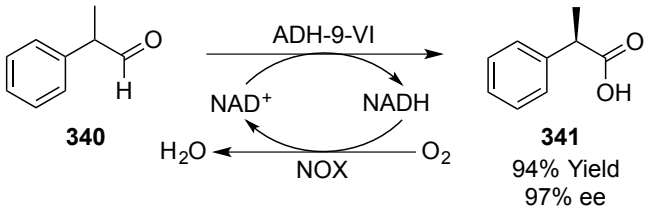

340 **341**
94% Yield
97% ee

Scheme 59 Oxidative dynamic kinetic resolution of profen aldehydes by ADH.

With the seminal work by Holmann in mind, we believe our recently developed GOase$M_{3\text{-}5}$-PaoABC could be applied to the synthesis of enantiopure α-substituted carboxylic acids *via* an enzymatic dynamic kinetic resolution one pot cascade.

3.2 Dynamic kinetic resolution of profen esters

Results from the previous cascade indicated that one particular chiral substrate **303** was only converted to 50% of the carboxylic acid (Table 6, substrate **303**) suggesting that perhaps PaoABC was showing enantioselectivity. To this end a range of α-substituted aldehydes including profen precursors were synthesized to explore the extent of enantioselectivity exhibited by PaoABC and to assess its applicability in the synthesis of enantiopure profens via dynamic kinetic resolution (DKR) (Scheme 60).

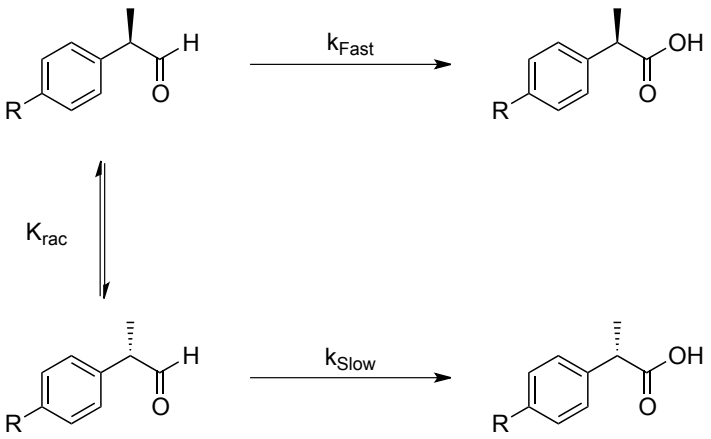

Scheme 60 Dynamic Kinetic resolution of profen aldehydes**.**

In a DKR, as with a classical kinetic resolution, one enantiomer reacts slowly under the reaction conditions. In addition, the rate of racemisation of the starting material is fast relative to the rate of the asymmetric transformation. Therefore using DKR it is possible to convert 100% of racemic starting material to enantiopure product due to equilibrating racemisation of starting material.

3.2.1 Synthesis of profen aldehydes and kinetic resolution.

Flurbiprofenal (**304**), ibuprofenal (**305**) and ketoprofenal (**306**) were synthesised via their corresponding methyl esters by di*iso*butyl aluminium hydride reduction (DIBAL-H) as test substrates for the biotransformation (Scheme 51).

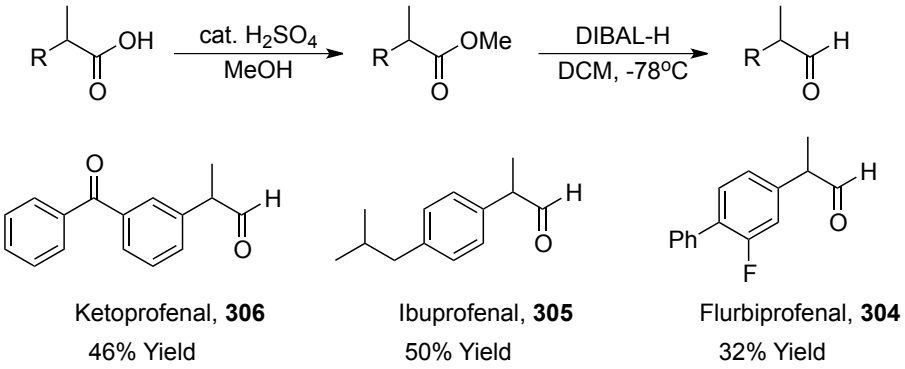

Scheme 51 Synthesis of profen aldehydes.

The profen aldehydes were indeed substrates for PaoABC as determined by the previous DCPIP screening method. However, HPLC analysis indicated that no enantioselectivity was observed at 50% conversion. The initial substrate 2-ethyl hexanol, which indicated potential enantioselectivity posses a bulkier α-substituent compared to the methyl substituent of the profens. We believe this steric bulk may be required for the enzyme to discriminate between enantiomers and so we set out to examine this hypothesis by synthesising a variety of α-substituted aldehydes to determine the E value for each substrate.

3.3 Kinetic resolution of α-substituted aldehydes

3.3.1 Synthesis of substrates

A range of aldehyde substrates and carboxylic acid standards were synthesised using a three step reaction sequence from methyl 2-phenylacetate (**307**) as starting material (Scheme 52). We postulated that increasing R group chain length may provide additional bulk in which enantiomers may be easily differentiated by the enzyme active site. Additionally, benzyl and

allyl substrates were chosen as π-stacking interactions may allow them to adopt a conformation not possible with alkyl chains and may lead to increased enantioselectivities.

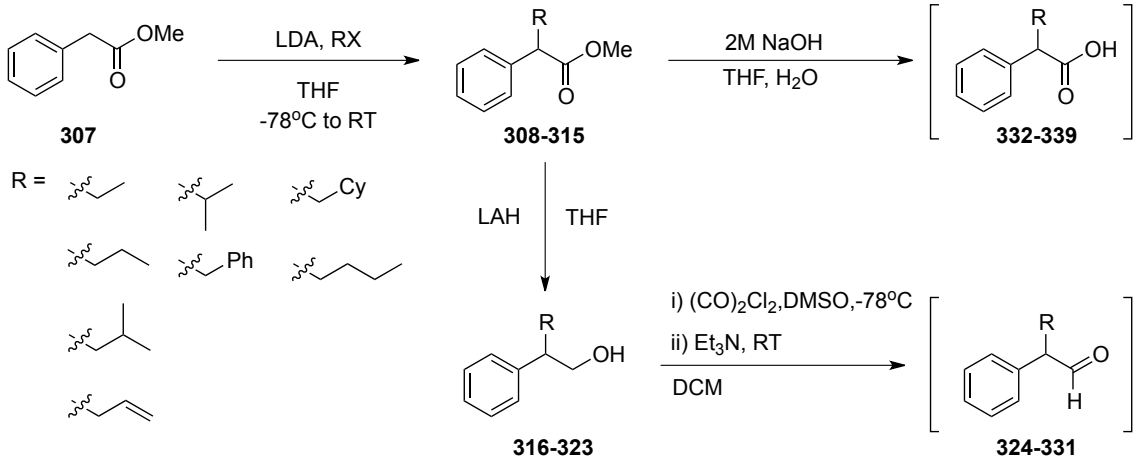

Scheme 52 Reaction sequence for the synthesis of substrates and racemic standards (for yields see Chapter 6).

The strong sterically bulky lithium disopropylamide (LDA) was chosen as a suitable base for ester alkylation over other strong bases such as NaOH or sodium hydride (NaH) to avoid unwanted dialkylation of the starting material[252]. In the case of the unreactive secondary halide isopropyl bromide, alternative reaction conditions employing the lithium de-aggregator 1,3-Dimethyl-3,4,5,6-tetrahydro-2-pyrimidinone (DMPU) was used to facilitate efficient alkylation by increasing reactivity of the resulting lithium enolate[253], albeit with low conversion to **315**. Base hydrolysis of the resulting esters provided the α-substituted carboxylic acid standards in quantitative conversion in all cases. The aldehyde substrates were synthesised via Lithium aluminium hydride ($LiAlH_4$) reduction of the corresponding esters followed by subsequent Swern oxidation[254] to yield the desired racemic α-substituted aldehydes.

3.3.2 Kinetic resolution of alpha substituted aldhehydes (Calculation of E values)

When a racemic substrate is subjected to an enzymatic reaction, chiral discrimination between the can enantiomers occur. As a consequence, each of the enantiomers can be obtained in only 50% yield. For an efficient kinetic resolution the rate of oxidation of one enantiomer must be much faster than the rate of the other enantiomer. In an extreme case the reaction will only proceed on one enantiomer leaving the other enantiomer unreacted. However this is not the case in many enzymatic reactions and in practice one a decrease in reaction rate beyond 50% conversion. In such cases the velocity of the transformation of each enantiomer varies with the degree of conversion and the optical purity of both substrate (ee_S) and product (ee_p) becomes a function of conversion[3].

For irreversible reactions such as oxidation, selectivity is expressed as Enantiomeric Ratio (*E*) and can be mathematically linked to the conversion (c) of the reaction and the optical purities of substrate (ee_S) and product (ee_p). The dependence of enantioselectivity and conversion can be expressed in the following equation, which is used to obtain all the *E* values relating to PaoABC with each subsequent α-substituted aldehyde oxidation[3].

$$E = \frac{\mathrm{In}[1 - \mathrm{c}(1 + \mathrm{ee_p})]}{\mathrm{In}[1 - \mathrm{c}(1 - \mathrm{ee_p})]}$$

Using the previous DCPIP screen, all our synthesised aldehydes were confirmed as substrate for PaoABC. The oxidations were initially performed for 5 hours and the conversions and any ees were determined by chiral HPLC (Table 9).

Table 9 Initial PaoABC catalysed oxidation of α-substituted aldehydes[a]

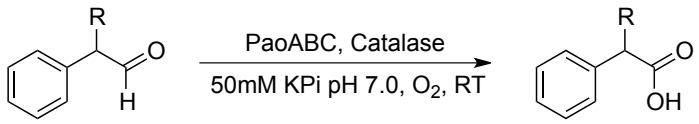

324-331 **323-339**

Entry	Substrate R =	Time (hr)	Conversion to acid[b] (%)	ee of acid[c]
1		5	91	16
2	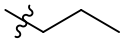	"	86	23
3	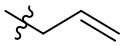	"	97	7
4	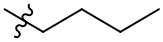	"	65	25
5	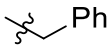	"	36	0
6		"	90	9
7	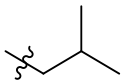	"	56	5
8	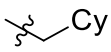	"	13	3

[a]Reaction conditions: 2 µL PaoABC (13.2 mg/mL), 33 µL catalase (3.3 mg/mL), 3 µL (1 M in MeCN 10mM final concentration) in 50 mM pH 7.5 potassium phosphate buffer (262 µL). [b]Conversions determined by HPLC using a chiracell AD-H column 95:5 hex:IPA, flowrate (1 mL/min). Conversions adjusted by the comparison of a 1:1 NMR authenticated standard of aldehyde and acid. [c]ee calculated by chiral HPLC

All substrates except **328 (**Table 9, entry 5) showed some selectivity and also straight chain aliphatics were converted faster than the bulky substrates (Table 6, entry 5,7,8). To this end the E value of all substrates was calculated and the best substrates were examined in detail *via* timecourse analysis to identify if any substrates could potentially be used in DKR (Table 11).

Table 10 E value of α-substituted aldehydes[a]

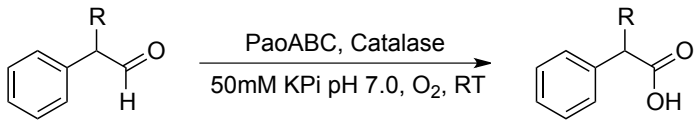

324-331 **323-339**

Entry	R	E[a]
1	Me	3
2	Et	6
3	Pr	4
4	Bu	2
5	$CH_2{}^{i}Pr$	1
6	CH_2Cy	1
7	Bn	1
8	$CH_2C(H)CH_2$	2
9	^{i}Pr	11

[a]Reaction conditions: 2 µL PaoABC (13.2 mg/mL), 33 µL catalase (3.3mg/mL), 3 µL substrate (1M in MeCN 10 mM Final concentration) in 50 mM pH 7.0 potassium phosphate buffer (262 µL) [b] E value was calculated using the above equation .

It is accepted that an E value of less than 15 for a specific substrate indicates poor enantioselectivity[3]. The E values of PaoABC for all aldehydes were below 15 indicating that PaoABC's enantioselectivity is generally very low. This signifies that the active site of PaoABC is large which is not surprising as we have yet to find an aldehyde it will not oxidise. This large active site results in each enantiomer of the racemic aldehyde substrate having a similar binding interaction with the appropriate amino acid residues in the binding site leading to low enzyme enantioselectivity.

The effect of chain length of the R group on the enantioselectivity is unclear. Although increasing the chain length from a methyl group to an ethyl group doubled the E value from 3-6 (Table 10, entries 1 & 2), further chain length had a negative effect (Table 10, entries 3 & 4). This implies that there may not be a steric influence on the enantioselectivity or in the transition state, the freely rotating alkyl chains can position themselves away from the reaction centre.

Additionally, the presence of sterically demanding groups (Table 10, entries 5 & 6) showed no enantioselectivity and we believe these large groups are positioned too far away from the reaction site to influence the rate of the enantiomers reactivity. The potentially π stacking substrates also exhibited poor enantioselectivity (Table 10, entries 7 & 8). Encouragingly, the isopropyl aldehyde (Table 10, entry 9) provided a slightly imporoved E value of 11. The greater degree of substitution on the R group may limit the binding for one enantiomer.

Table 11 Conversion, ee, calculated E value and time course analysis of the oxidation of α-substituted aldehydes by PaoABC[a].

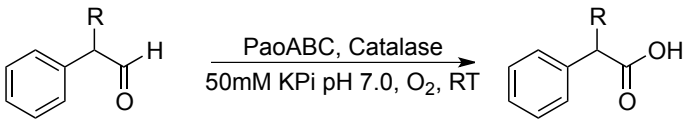

R = Me (**340**)
Et (**324**)
Pr (**325**)
iPr (**331**)

R = Me (**341**)
Et (**332**)
Pr (**333**)
iPr (**339**)

Entry	Substrate	Time (min)	Conv (%)[b]	ee of acid[c]	E[d]
1	**340**	60	43	39	3
2	**324**	20	23	62	6
3	**325**	60	26	50	4
4	**331**	60	44	70	11

[a]Reaction conditions: 2 µL PaoABC (13.2 mg/mL), 33 µL catalase (3.3 mg/mL), 3 µL substrate (**340**, **324**, **325**, **321**) (1M in MeCN 10 mM final concentration) in 50 mM pH 7.0 potassium phosphate buffer (262 µL). [b]Conversion determined by normal phase HPLC. Conversion was adjusted by comparison of a 1:1 mix of aldehyde and acid. [c]ee was calculated by chiral HPLC using a chiracel AD-H column with eluent 98:2 Hexane:IPA with a flow rate 1 mL/min. [d]E value calculated via the above equations

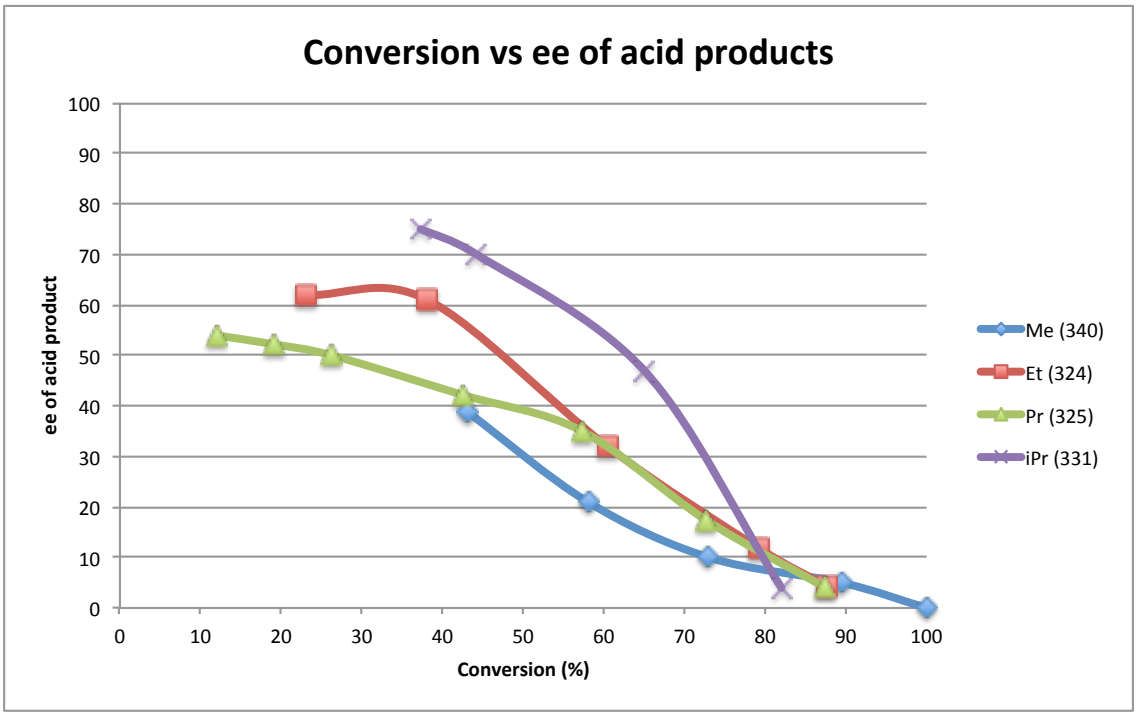

Figure 22 Analysis of the reaction mixture of the 10 mM oxidation of α-substituted aldehdyes **340**, **324**, **325** and **331** showing a decrease in ee with increasing conversion.

We then set out to optimise the reaction conditions using the best substrate, isopropyl substituted aldehyde (**331**). We believed that changes in pH might alter the protonation state of key active site residues of paoABC. Higher pH may also facilitate enolisation of the α substituted aldehyde and may lead to better enantioselectivity if the rate of enolisation is faster than the oxidation of the unfavoured enantiomer[239]. Upon alteration of the pH (Table 12) no significant increase in the E value was observed although pH 10 (Table 16, entry 4) did provide conditions in which an E value of 14 was obtained. The pH optimum of PaoABC is between 6-8 as we have shown (Figure 5) and when subjected to conditions outside this range, a decrease in activity is observed (Table 12, entry 1,4,5). Interestingly, PaoABC remains active even at extreme pHs albeit with lower conversions (Table 12, entry 5).

Table 12 Effect of pH on the E value associated with the oxidation of 331 with PaoABC[a]

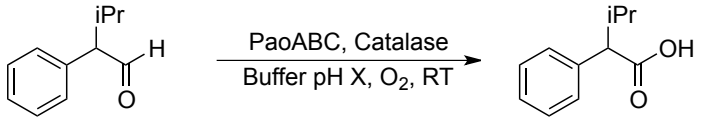

331 **339**

Entry	pH	Time (min)	Conversion (%)[b]	ee[c]	E[d]
1	5	120	43.4	64	7
2	7	60	44.3	70	10
3	8	40	41	70	9
4	10	120	40	79	14
5	11	120	38.6	75	11

[a]Reaction conditions: 2 µL PaoABC (13.2 mg/mL), 33 µL catalase (3.3 mg/mL), 3 µL substrate (1M in MeCN 10 mM final concentration) in 50mM pH X buffer (262 µL). [b]Conversion determined by normal phase HPLC. Conversion was adjusted by comparison of a 1:1 mix of aldehyde and acid. [c]ee was calculated by chiral HPLC using a chiracel AD-H column with eluent 98:2 Hexane:IPA with a flow rate 1mL/min. [d]E value calculated via the above equations

3.4 Second Generation substrate.

With the success of the isopropyl aldehyde (**331**) we postulated that substrates with side chain groups that could interact with the active site may show increased enantioselectivity. To this end we proposed the synthesis of the lactol (**346**), which in an aqueous medium, would be in equilibrium with its aldehyde-alcohol (**347**). The free hydroxyl group could coordinate *via* hydrogen bonding which may lead to better enantiodiscrimination[255]

3.4.1 Synthesis of second generation substrate

A four step synthetic route was designed for the synthesis of alcohol **347** (Scheme 53), which comprised firstly of the alkylation of phenylacetaldehyde with the TBDMS protected hydroxy bromide, reduction of the alkylated product and subsequent Swern oxidation to furnish

the protected hydroxy aldehyde. Final deprotection of the TBDMS protected alcohol would afford the desired lactol **346**.

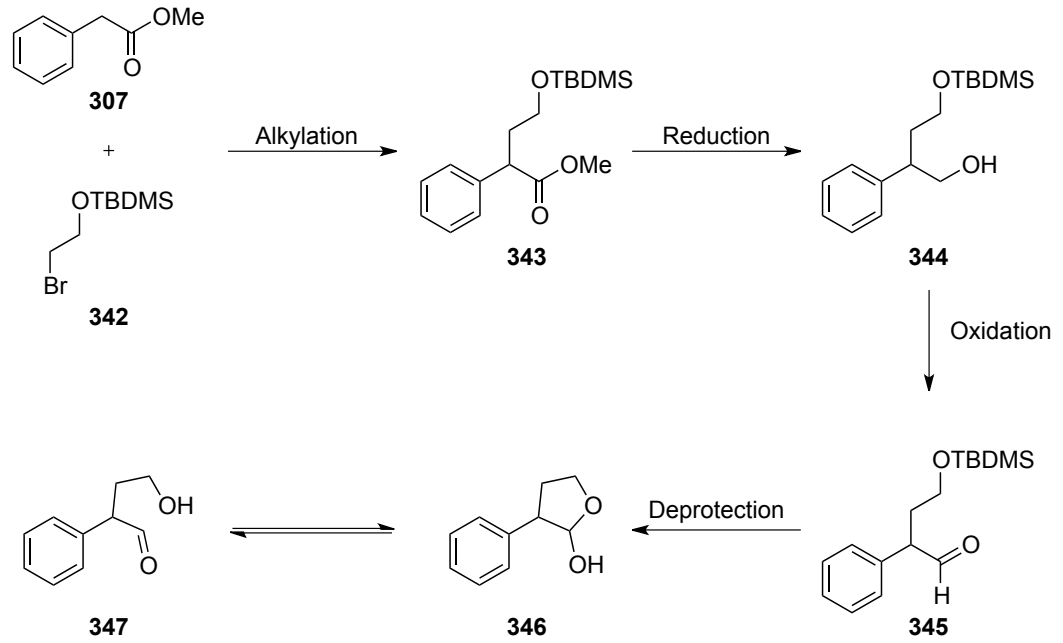

Scheme 53 Synthetic route to compound second generation substrate

Initial attempts to alkylate phenylacetaldehyde (**307**) with the TBDMS protected alcohol (**342**) were unsuccessful using our previously established alkylating procedure employing LDA. To this end a solvent and base screen was initiated to determine optimum reaction conditions for the transformation (Table 13).

Three bases were tested, LDA, NaH and t-BuOK. Only t-BuOK furnished the desired alkylated ester in 60% isolated yield. Further improvements were met by employing the polar aprotic solvent DMF, which provided the alkylated ester in 95% isolated yield (Table 13, entry 4).

Table 13 Base and solvent screen for the alkylation of methyl phenylacetaldehyde

307 **342** **343**

Entry	Base	Solvent	Temperature	Time	Yield[a]
1	LDA	THF	-78°C to RT	16Hr	Decomp.
2	NaH	‘	0°C to RT	‘	Decomp.
3	t-BuOK	‘	‘	‘	60%
4	‘	DMF	‘	‘	95%

[a]Isolated yield of product

The previously employed $LiAlH_4$ reduction step was again unsuitable with substrate **343** as although the ester functional group was reduced, the protecting group was also cleaved to provide the deprotected diol (Table 14, entry 1). A possible explanation for this cleavage is the nucleophilic attack by hydride on the electrophilic silicon centre cleaving the Si-O bond in the process. This is surprising as TBDMS ethers are generally stable in the presence of $LiAlH_4$[256]. Using either of the milder reducing agents DIBAL-H and lithium borohydride furnished the pure alcohol **344**.

Table 14 Screening of chemical reductants

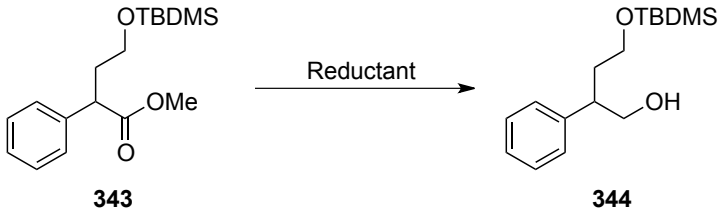

343 **344**

Entry	Reductant	Solvent	Temperature	Yield (%)[a]
1	$LiAlH_4$	THF	0°C	0
2	DIBAL-H	DCM	-78°C	50
3	$LiBH_4$	THF	0°C	65

[a]Reaction was stopped when all starting material was consumed as determined by TLC. Isolated yield of product.

Swern oxidation of the mono protected alcohol **344** was successful in providing the protected aldehyde (**345,** 78% yield) and subsequent TBAF deprotection furnished the lactol (**346**) in 75% yield (Scheme 54).

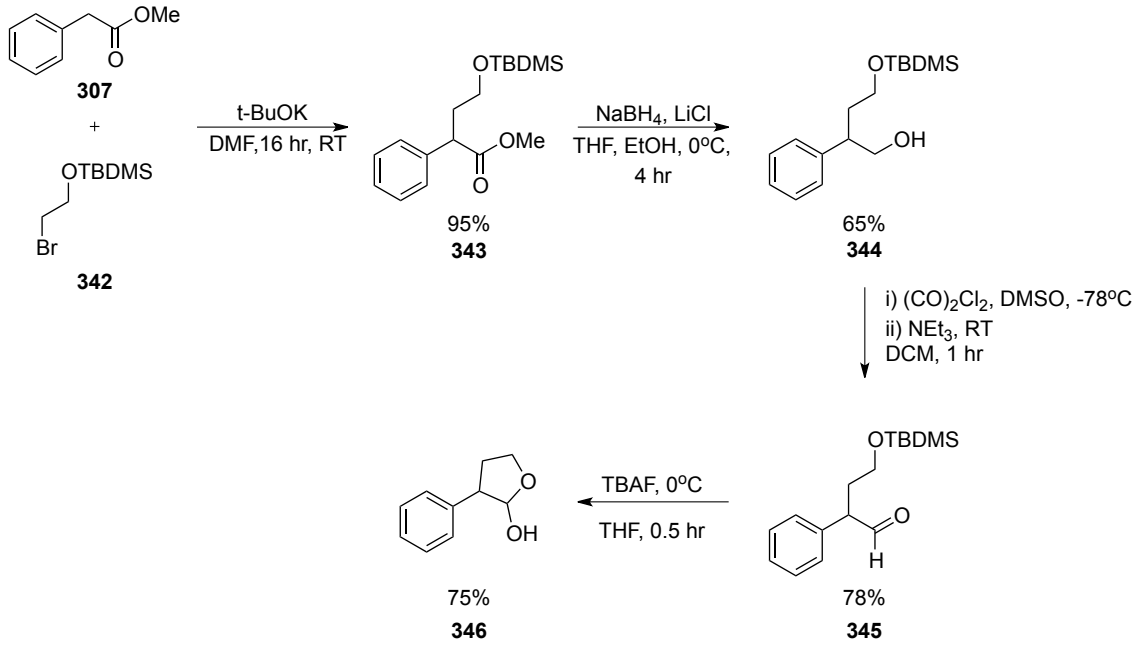

Scheme 54 Successful synthesis of lactol substrate

The carboxylic acid standard was synthesised through a two step reaction sequence from the alkylated ester (Scheme 55).

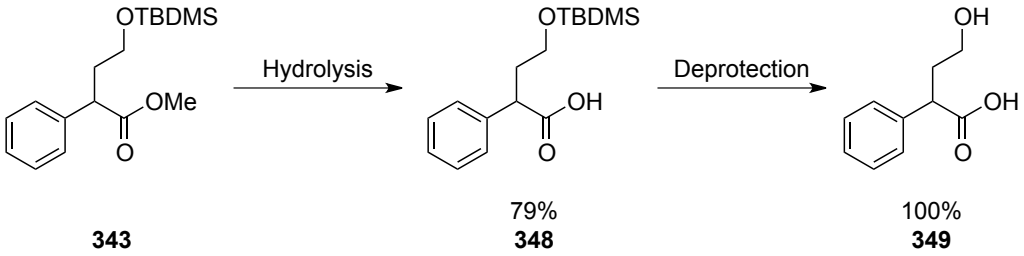

Scheme 55 Proposed synthesis of carboxylic acid standard

Base catalaysed hydrolysis of the protected ester (**343**) would provide the protected carboxylic acid (**348**). However, mild conditions were necessary to avoid the deprotection and subsequent cyclisation to form the unwanted lactone (**350**). Initially, a 2M aqueous lithium hydroxide solution in a 3:1 methanol: water mixture at room temperature was attempted but was met with the formation of the unwanted lactone product (**350**). A less basic system utilising 0.5M lithium hydroxide in THF/water (50:50) at 0°C was successful in the formation of the desired carboxylic acid (349) in 79% isolated yield. The common silyl deprotecting agents such as TBAF resulted in the unwanted cyclized lactone product. TBDMS deprotection was accomplished using the mild acid, camphorsulphonic acid (CSA) to provide the carboxylic acid standard in quantitative yield (Scheme 56).

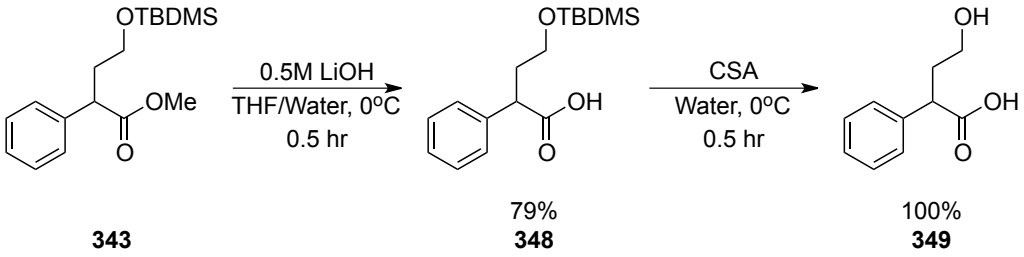

Scheme 56 Synthesis of carboxylic acid standard.

3.4.2 Enzymatic oxidation of lactol substrate.

Interestingly when lactol **346** was subjected to oxidation by PaoABC, no carboxylic acid product was formed. DCPIP indicated oxidation was taken place but not to our expected product. The oxidation product was determined to be the lactone after HPLC analysis (Scheme 57).

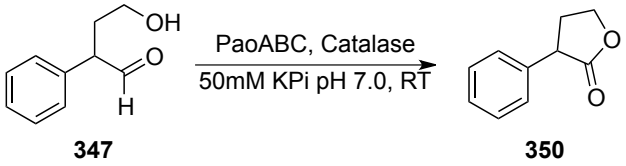

Scheme 57 Lactone formation by PaoABC

Although lactones have been formed from diols using alcohol dehydrogenases such as HLADH via a lactol intermediate[257], the substrate for these oxidations is not the aldehyde but the hemiacetal. Aldehyde oxidases on the other hand are known to not accept hydrates due to the presence of nucleophilic Mo-OH and so the resulting product should be the acyclic alcohol-acid. However in this case we obtain the lactone product Scheme 57.

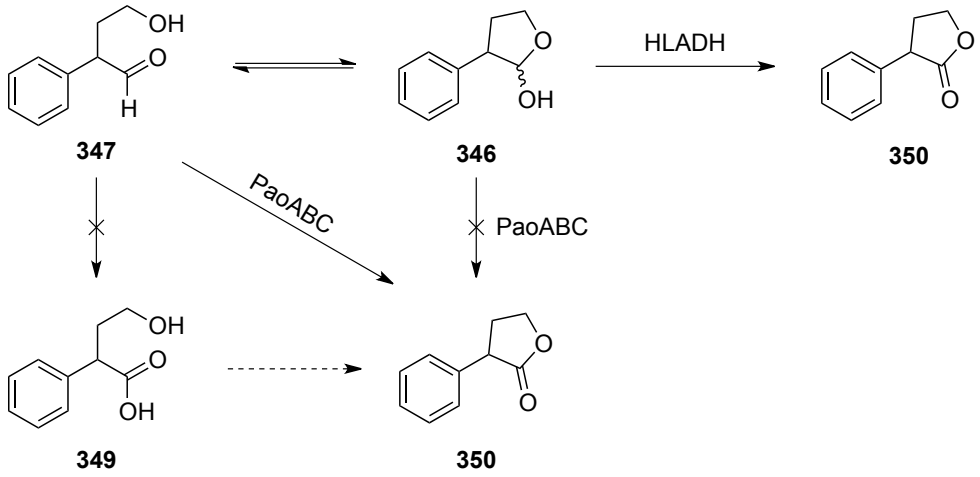

Scheme 58 Different substrates for molybdoenzymes and alcohol dehydrogenase

In molybdoenzyme oxidations of aldehydes, the incorporated oxygen is derived from water[208,216]. We therefore believe that in the presence of tethered intramolecular nucleophiles such as the hydroxyl group present in our substrate, the rate of cleavage of the molybdoester

intermediate by water may be lower than cyclisation by the tethered hydroxyl group. (Figure 23). To eliminate the possibility that the hydroxyl acid is spontaneously cyclizing we incubated the hydroxy-acid with paoABC. No cyclisation was evident after HPLC analysis and so we believe the postulated mechanism is plausible.

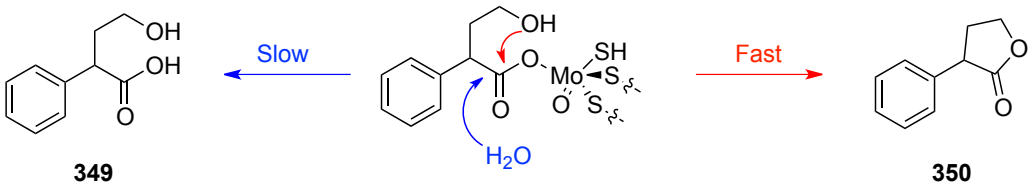

Figure 23 Postulated mechanism for the formation of lactone products.

Despite the interesting reactivity displayed by PaoABC on substrate **346** no enantiodiscrimination was observed and the lactone (**350**) was racemic at 50% conversion.

3.5 Conclusion:

The E values for the oxidation of a range of racemic aldehyde substrates by PaoABC have been determined. The enantioselectivity of PaoABC for aldehyde substrates is generally low and this correlates with unpublished findings that the active site of PaoABC is open and large. There is a steric influence associated with PaoABC's enantioselectivity as sterically bulky carbons close to the reaction centre display slightly improved E values (14). To further test this steric effect, future studies could include substrates with a more sterically demanding R group such as trityl or t-butyl group. Additionally, medium engineering techniques such as the addition of water-miscible organic co-solvents to the reaction mixture[258] or the use of ionic liquids could improve the enantioselectivity[259]. Directed evolution stratagies could also increase the enantioselectivity of PaoABC

Kinetic resolutions are largely unsustainable in organic synthesis due to a theoretical 50% maximum yield of enantiopure product. Therefore, if successful kinetic resolutions using PaoABC could be identified these could be adapted as dynamic kinetic resolutions by

manipulation of reaction conditions such as temperature or pH to facilitate *in situ* racemisation of the. However, at present wild type PaoABC is unsuitable to realise this task. Directed evolution strategies would be necessary to develop a more enantioselective catalyst. Further studies will then be needed to identify whether successful dynamic kinetic resolutions could be combined with the alcohol to aldehyde biotransformation catalysed by GOase$M_{3\text{-}5}$ or additional mutants in a one pot racemic alcohol to chiral carboxylic acid catalytic *in vivo* enzymatic cascade.

Despite the lack of enantioselectivity associated with PaoABC, the biocatalyst did display unusual reactivity with lactols. The expected alcohol acid was not formed, rather the unexpected lactone was provided in a oxidative cyclisation transformation. This reaction has not been previously reported using molybdoenzymes.

Chapter 4

4.0 Oxidative cyclisation of amino alcohols.

4.1 Introduction

Amide bond formation is a fundamental reaction in chemical synthesis[260,261]. The importance of amides in chemistry is well recognized and has been studied extensively over the past century[262]. Although many methods are known for the synthesis of amides, preparation under neutral conditions without the generation of copious amounts of waste is a challenging goal[263]. For this reason, the ACS GCIPR (American Chemical Society Green Chemistry Institute Pharmaceutical Roundtable) identified amide bond formation as one of the most problematic reaction in the pharmaceutical industry, and labeled it as a high priority research field[264].

Direct coupling between activated carboxylic acids (acid chlorides, anhydrides) is a common approach for amide bond formation. These methods suffer from several limitations such as the production of large amounts of waste (as a result of the use of stoichiometric coupling reagents), tedious work-up and difficulties in avoiding racemisation/epimerisation[260,265]. With the demand for environmentally benign methods for amide formation a number of transition metal-catalysed procedures[266] starting from alcohols[267-269], aldehydes[270], nitriles[271], aryl halides[272], aldoximes[273], alkenes and alkenes[274] have been developed. In particular, metal-catalysed reactions between an alcohol and amine in which only hydrogen is produced as a by-product are the most atom economical and environmentally friendly procedures for mild amide bond formation to date[275,276].

Biomimetic aerobic oxidation of amino alcohols to lactams have recently been reported by Bäckvall[275]. Oxidation was performed using a ruthenium catalyst which oxidised the protected amino alcohol to an aldehyde intermediate which spontaneously cyclised into the corresponding hemiaminal. The intermediate is subsequently transformed to the lactam product (Scheme 59).

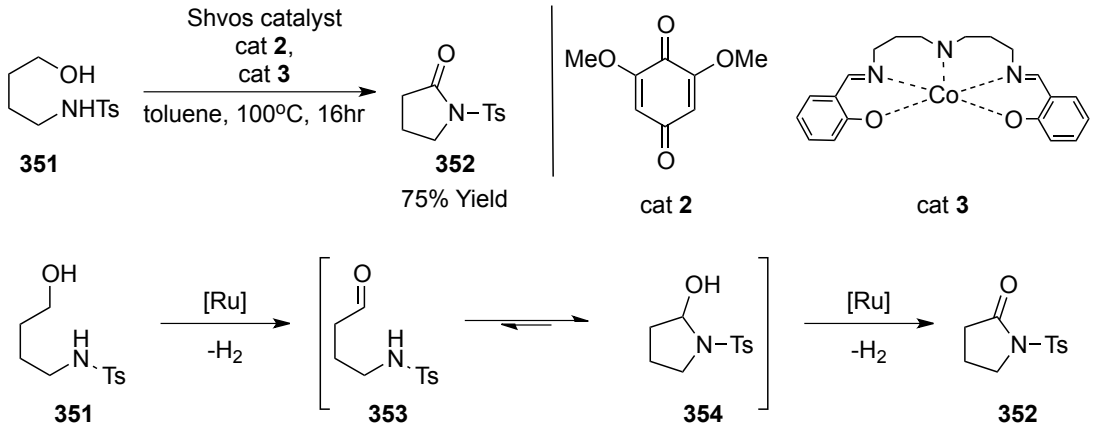

Scheme 59 Aerobic lactamisation of amino alcohols

This oxidative cyclisation approach has been demonstrated to provide five-, six-, and seven-membered benzo fused lactams[276] and also a range of lactones[277]. As only catalytic amounts of transition metals are required, these reactions hold good green credentials as atom economy is very high. Unfortunately they suffer from high temperatures and the use of environmentally damaging solvents. Solvents account for 80-90% of mass utilisation in a typical pharmaceutical/fine chemical process and contribute significantly to waste generation[278]. If the aforementioned transformation could be performed at ambient temperature in water with a biodegradable catalyst, it would possess superior green credentials and provide a possible solution to the lactam bond formation problem. Unfortunately this goal has not been achieved.

We believe this transformation could be accomplished by employing our recently developed enzymatic cascade based on GOase$M_{3\text{-}5}$ and molybdenum hydroxylases. The double oxidation process could provide lactams from amino alcohols *via* an *in situ* generated imine. This transformation would afford a green amide bond forming reaction as molecular oxygen (air) is used as the oxident with the only side product being H_2O_2.

4.2 Activated amino alcohol cyclisation

We have previously demonstrated in the group that 3,4-dihydrisoquinoline (DHIQ)(**356)** is an excellent substrate for *E.coli* XDH when used in a cascade with monoamine oxidase (MAO-N) which catalayses the oxidation of tetrahydroisoquinolines (THIQ) (**355**). (Scheme 60)

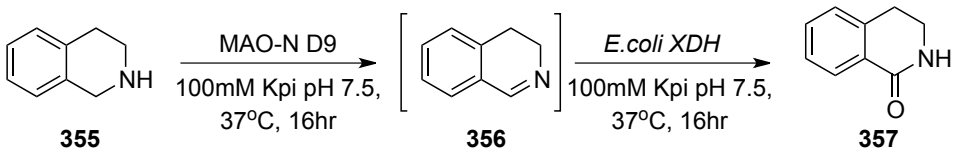

Scheme 60 MAO-N D9/E.coli XDH oxidation of THIQ

Hence, we were intrigued to test if the oxidised lactam product could be obtained from the oxidative cyclisation of the precursor amino alcohol (Scheme 61).

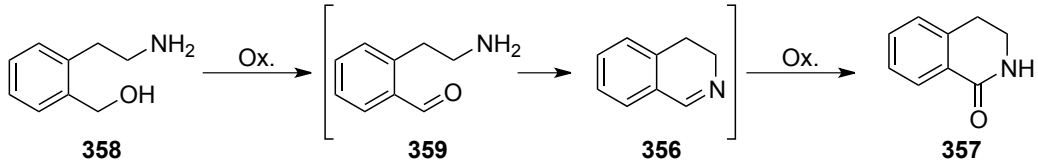

Scheme 61 Proposed oxidative cyclisation biosynthetic route

Amino alcohol **358** was prepared by reduction of the commercially available cyanoester **360** with $LiAlH_4/AlCl_3$ albeit in low yield of 25%. Other reductants such as DIBAL-H, Superhydride and $LiAlH_4$ gave lower conversions to the desired amino alcohol (Scheme 62)

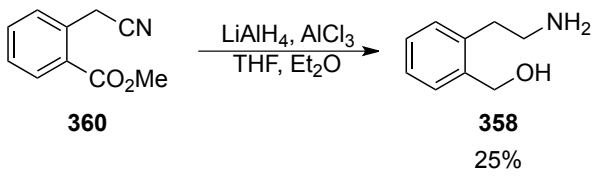

Scheme 62 Synthesis of amino acid starting material

The oxidation of amino alcohol **358** with $GOaseM_{3-5}$ was remarkably pH sensitive within the range of pH 7.0-8.5 with a pH of 7.0 required to achieve full conversion to DHIQ (Table 15, entry 1). Formation of DHIQ is presumed to occur by cyclisation of the initially formed amino aldehyde.

To identify which of our available molybdoenzymes was best suited for the transformation to the amide we performed the reaction with both PaoABC and *E.coli* XDH at different pHs to determine if optimimum mutual conditions with $GOaseM_{3-5}$ could be obtained (Table 16). *E. coli* XDH performed extremely well at every pH, oxidising DHIQ to the corresponding lactam in 100% conversion.

Table 15 Conversion of (2-(2-aminoethyl)phenyl)methanol (**358**) in $GOaseM_{3-5}$ catalysed reactions with different pH-values of the reaction system[a].

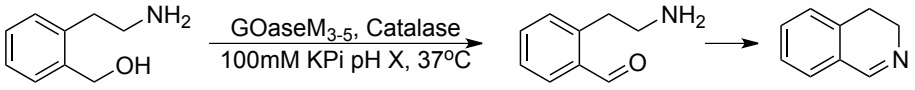

358 **359** **356**

Entry	Molarity (mM)	pH value	Conversion [%][b]
1	10	7.0	100
2	"	7.5	39.7
3	"	8.0	47.6
4	"	8.5	11

[a]Reaction conditions: 103 µL $GOaseM_{3-5}$ (3.0 mg/mL), 33 µL catalase (3.3 mg/mL), 3 µL substrate (1 M in MeCN 10 mM final concentration) in 100 mM pH X potassium phosphate buffer final volume 300 µL, 16hr. [b]Conversions adjusted by comparing the NMR of a 1:1 mix of amino alcohol **358** and DHIQ **356** with HPLC trace. HPLC-conditions: Chiracel OD-H column, 1.0 mL/min, 90% hexane (0.1% ethanolamine) : 10% IPA.

Unfortunately, PaoABC was less efficient at oxidising the imine affording only 65% conversion (Table 16, entry 1). However, with the increase of pH an increase in conversion was obtained (Table 16, entry 4). This result is noteworthy as this is the first time PaoABC has been reported to act on an imine substrate. The poor performance of PaoABC compared to *E.coli* XDH's is not surprising as the natural substrate of *E.coli* XDH is xanthine which contains a

similar activated imine bond[217]. To this end, *E.coli* XDH was chosen as the second enzyme in the cascade as it showed satisfactory performance under the reaction conditions identical to the GOaseM$_{3\text{-}5}$ catalysed step (Table 16, entry 5)

To our delight, combining GOaseM$_{3\text{-}5}$ and *E.coli* XDH in a one-pot reaction for the direct synthesis of lactam **357** with an overall conversion of 69% (Figure 24). HPLC analysis showed that DHIQ was only present in trace amounts under cascade conditions and was consumed immediately by XDH upon formation. GOaseM$_{3\text{-}5}$ however oxidises amino alcohol **358** at a much slower rate and this step is the limiting factor in the reaction. This observation is contradictory to the earlier result (Table 15, entry 1) in which quantitative conversion of DHIQ was obtained after 16hr. To this end we postulate that GOaseM$_{3\text{-}5}$ may be inhibited by the lactam product which would result in decreased conversion of the lactam product.

Table 16. Conversion of 3,4-dihydroisoquinoline (**356**) in PaoABC or *E. coli* XDH catalysed reactions with different pH-values of the reaction system[a].

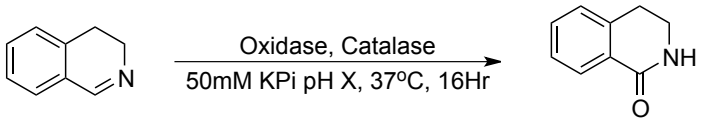

356 **357**

Entry	Molarity (mM)	Aldehyde oxidase	pH-value	Conversion[%][b]
1	10	*E. coli* PaoABC	7.0	65
2	‘	*E. coli* PaoABC	7.5	77
3	‘	*E. coli* PaoABC	8.0	88
4	‘	*E. coli* PaoABC	8.5	85
5	‘	*E. coli* XDH	7.0	>99
6	‘	*E. coli* XDH	7.5	>99
7	‘	*E. coli* XDH	8.0	>99
8	‘	*E. coli* XDH	8.5	>99

[a]Reaction conditions: 5 µL PaoABC (13.2 mg/mL) or 50 µL *E.coli* XDH (1.1 mg/mL) 33 µL catalase (3.3 mg/mL), 3 µL substrate (1 M in MeCN 10mM Final concentration) in 50 mM pH X potassium phosphate buffer final volume 300 µL, 16hr [b]Conversions adjusted by comparing a 1:1 mix of DHIQ (**356**) and lactam (**357**) Conditions: Chiracel OD-H column, 1.0 mL/min, 90% hexane (0.1% ethanolamine) : 10% IPA.

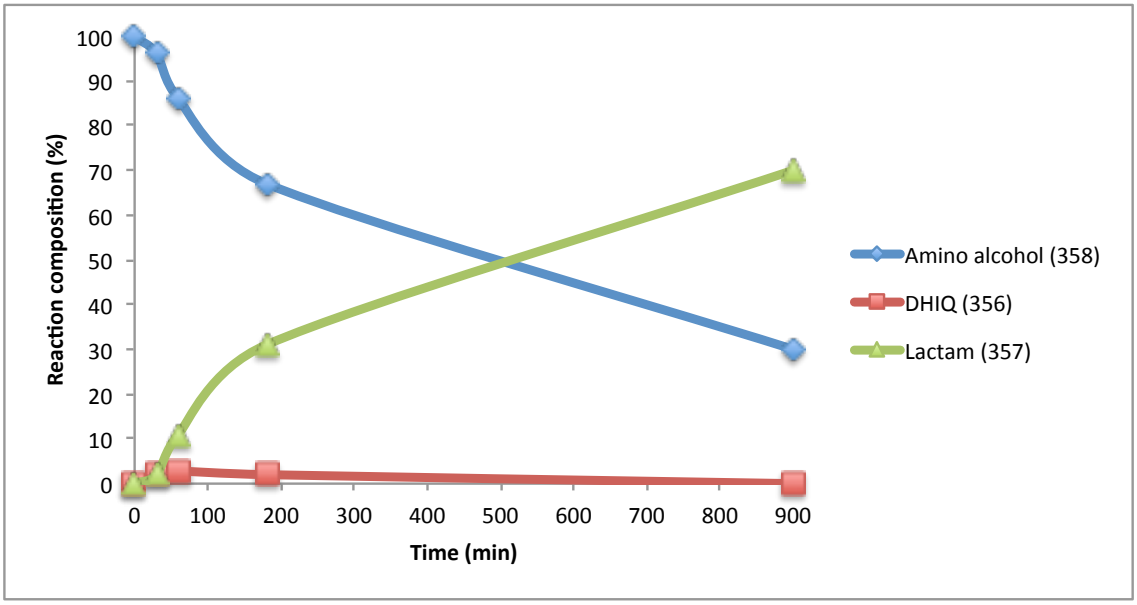

Figure 24 GOase$M_{3\text{-}5}$- XDH cascade timecourse for the conversion of aminoalcohol **358** to lactam **357** *via* the in-situ generated DHIQ (**356**).

4.3 Determination of the true substrate for imine oxidation catalysed by molybdoenzymes PaoABC and XDH

In the literature there are conflicting reports on the nature of the true substrate in imine oxidations catalysed by molybdoenzymes. Some reports indicate that molybdoenzymes act on the hemiaminal[279] intermediate which could form in aqueous media while others indicate that the imine is the true substrate[216]. NMR analysis of DHIQ (**356**) in deuterated potassium phosphate buffer at pH 6.0-8.0 indicated that no amine aldehyde or DHIQ hemi-aminol was present (Figure 25). Only DHIQ signals were observed which suggests DHIQ is the true substrate for XDH rather than the amino aldehyde (Scheme 63). It is however possible that the hemi-aminal could be formed by enzyme catalysis.

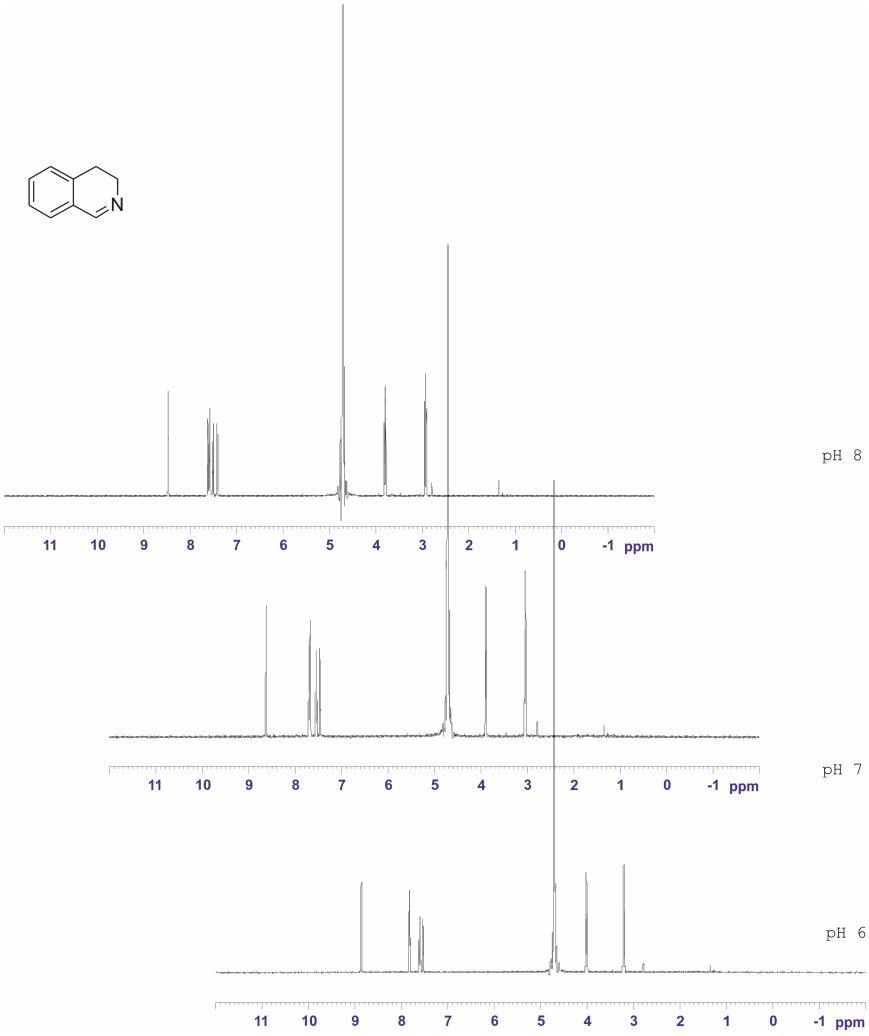

Figure 25 NMR analysis of DHIQ (**356**) in pH 6-8 buffer indicates no aldehyde or hemi-aminal present in reaction conditions. Only DHIQ peaks are observed which suggestes that DHIQ is the substrate for XDH

It is well documented that in the oxidation of aldehydes by xanthine oxidase the substrate is the aldehyde itself and not the hydrated aldehyde[208,216]. Since the hydrated aldehyde is formally analogous to the hemiaminal this fact provides additional support that the imine as the true substrate.

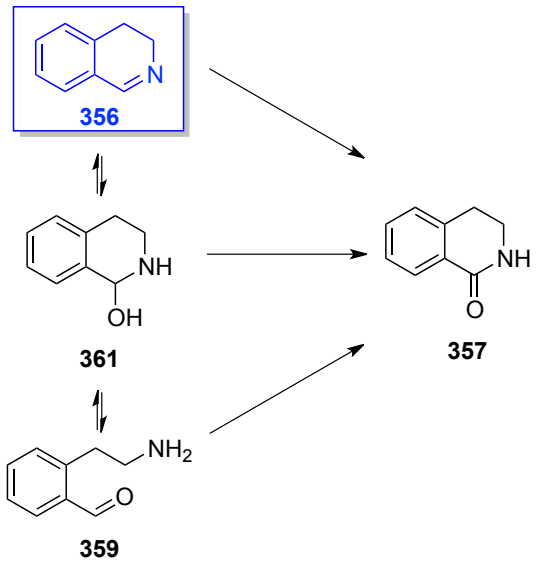

Scheme 63 Potential substrates for XDH imine oxidation.

4.4 Oxidative cyclisation of unactivated amino alcohols

We next turned our attention to a series of more challenging substrates for cascade oxidative cyclisation reactions- aliphatic amino alcohols (**362-364**) (Table 17). Both $GOaseM_{3-5}$ and F_2 and three different xanthine oxidoreductase enzymes were tested: *E.coli* XDH, bovine xanthine oxidase (XO) and *E. coli* PaoABC. Neither the bovine (XO) or *E.coli* XDH gave any lactam products at pH 7.0-8.5 (Table 17, entries 6,7,13,14). To our surprise, in this case the combination of $GOaseM_{3-5}$ and PaoABC performed much better, which was the opposite of what we observed in the DHIQ oxidation. Substrate with n=2 yielded a trace of valerolactam at pH 7.0 (Table 17, entry 8) but at pH 8.5 the conversion increased to 26% (Table 17, entry 11). With the shorter chain homologue (n=1) the same pH effect was evident, however in this case the conversion to 2-pyrrolidone (**365**) reached 85% at pH 8.5. The longer chain substrate n=3 gave no conversion to caprolactam (**367**) when either alcohol oxidases were employed (Table 17, entry 15 & 16).

The higher conversion to 2-pyrrolidone (**365**) compared with valerolactam (**366**) presumably reflects the more rapid formation of the 5 membered rather than 6-membered ring imine. It is unclear if any carboxylic acid is present in the reaction mixture as only the lactam products possess a suitable chromophore (amide bond) for detection by our HPLC. This

alternate product could account for the poor yield of the lactams as the longer chain aldehydes would be rapidly oxidised to the corresponding acids before cyclisation. Unfortunately another limitation is that the formation of imines or aldehydes cannot be monitored (no detectable chromophore) and so we cannot determine to what extent the galactose oxidase mutants are accepting the amino alcohols as substrates.

Table 17 Conversion of aliphatic amino alcohols in GOaseM_{3-5}/F_2-XOR catalysed reactions at different pH values.

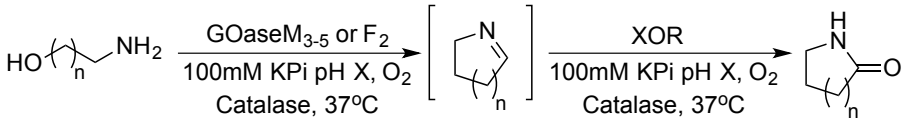

n= 1 (**362**)
n= 2 (**363**)
n= 3 (**364**)

n= 1 (**365**)
n= 2 (**366**)
n= 3 (**367**)

Entry	Substrate (n = X)	GOase	XOR Enzyme	pH	Yield [%][a]
1	1	M_{3-5}	*E. coli* PaoABC	7.0	9.6
2	1	M_{3-5}	*E. coli* PaoABC	7.5	41
3	1	M_{3-5}	*E. coli* PaoABC	8.0	56
4	1	M_{3-5}	*E. coli* PaoABC	8.5	85
5	1	F_2	*E. coli* PaoABC	8.5	22
6	2	M_{3-5}	*Bovine* XO	7.0	0
7	2	M_{3-5}	*E. coli* XDH	7.0	0
8	2	M_{3-5}	*E. coli* PaoABC	7.0	Trace
9	2	M_{3-5}	*E. coli* PaoABC	7.5	3.4
10	2	M_{3-5}	*E. coli* PaoABC	8.0	20
11	2	M_{3-5}	*E. coli* PaoABC	8.5	26
12	2	F_2	*E. coli* PaoABC	8.5	7.5
13	2	M_{3-5}	*Bovine* XO	8.5	0
14	2	M_{3-5}	*E. coli* XDH	8.5	0
15	3	M_{3-5}	*E. coli* PaoABC	8.5	0
16	3	F_2	*E. coli* PaoABC	8.5	0

[a]Reaction Conditions: 2.4 µL substrate (1M in MeCN), 103 µL GOase M_{3-5} or F_2 (103 uL of 3.7 mg/mL), 33 µL catalase (3.3mg/mL), XOR enzyme in 100mM KPi buffer (300 uL final volume). [b]Yields calculated by calibration curves of 2-pyrrolidone, valerolactam and caprolactone.

It is evident that increasing pH has remarkable effect on conversion. A possible explanation for this is that the increased pH facilitates cyclisation of the assumed amino-aldehyde intermediate giving a higher concentration of the imine for the PaoABC. Unfortunately at high pH, $GOaseM_{3-5}$ is operating above its pH optimum whereas PaoABC is known to work over a broad pH range. In order to improve conversion, additional $GOaseM_{3-5}$ and XOR mutants must be created and improved analytical methods need to be developed to analyse not only product formation but also the intermediate imine and possible non-UV active side products.

4.4 Steps towards β-Lactam forming reactions.

It is well documented that for XOR-catalysed aldehyde oxidations, the aldehyde is the enzymatically active substrate and not the hydrate[217]. Previously we have demonstrated an oxidative cyclisation of hydroxyaldehydes to provide lactones. This may proceed by two pathways, 1) intramolecular nucleophilic displacement of the molbydoester *via* the free alcohol and 2) enzymatic oxidation of the lactol intermediate (Scheme 64). Although as already mentioned the former is more likely as aldehydes are the known substrates for XOR and not lactols.

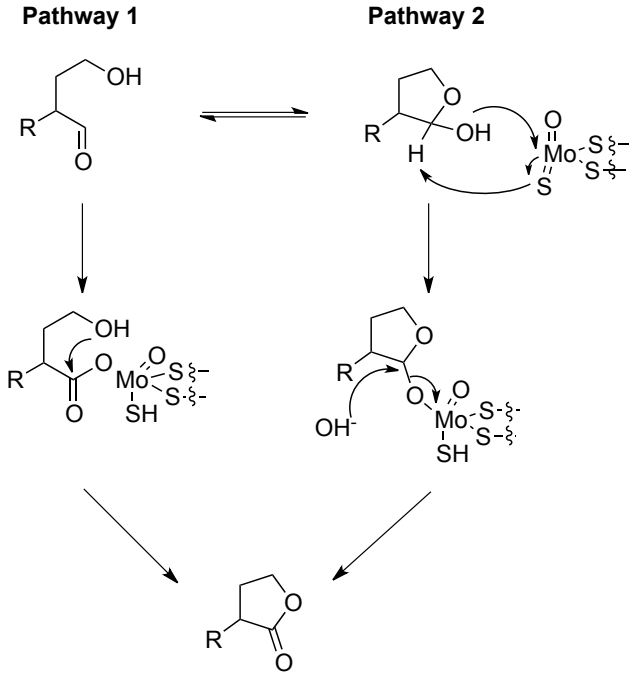

Scheme 64 Oxidative Lactone formation from hemiacetals

If the Mo-ester mechanism is a reality, it is possible more nucleophilic tethered amines could also displace the molybdo esters leading to lactam products but imine formation from oxidised amino alcohols would undergo further oxidation as already shown. However, short chain amino alcohols, which would form highly strained imines, would be excellent substates to test this hypothesis as imine formation would not occur.

β-Lactams contain a highly strained four membered lactam bond which is of vital importance in antibiotic drugs[280]. Four membered imines are extremely strained and their formation under the oxidative cyclisation conditions previously employed with amino alcohols and our enzymes would be highly unlikely.

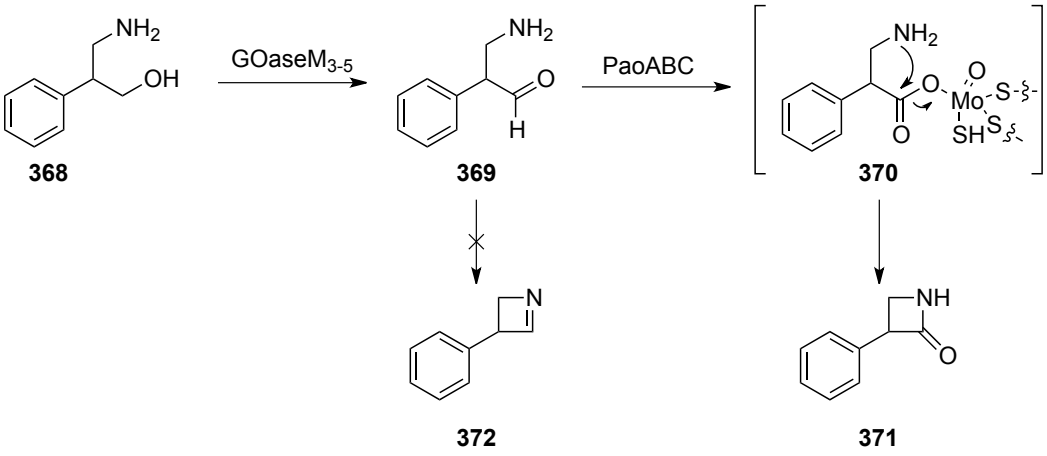

Scheme 65 Possible β-Lactam formation *via* a molybdoester intermediate

Therefore the oxidation of amino alcohol would only produce amino aldehydes and these may cyclise via the proposed molybdoester intermediate (Scheme 65).

In order to test this hypothesis we synthesized the amino alcohol **368**. Amino alcohol **368** would not form the imine intermediate **372** and can also be detected via RP-HPLC. Upon analysis of the reaction mixture by LC-MS, we established that a mass peak corresponding to the β-lactam was present indicating that oxidative cyclisation may have taken place (Figure 26).

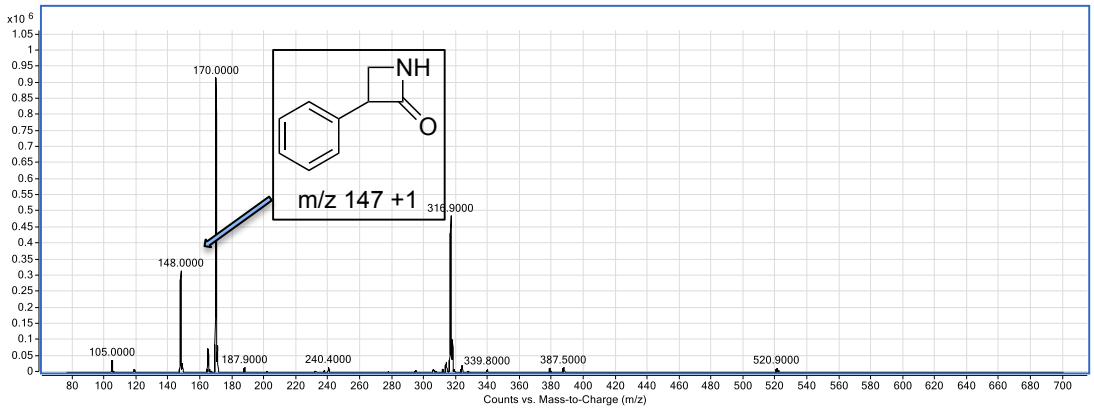

Figure 26 LC-MS of reaction mixture of the GOase$M_{3\text{-}5}$-PaoABC cascade indicating a mass peak corresponding to the desired lactam.

In addition, when the reaction was subject to HPLC analysis all the starting material had been consumed and no peak corresponding to the amino acid was present further indicating the presence of the cyclized product. Further work including the synthesis of a genuine standard of the β-Lactam and preparative scale biotransformation is ongoing.

4.5 Conclusion

We have demonstrated that the oxidative cyclisation of amino alcohols to lactams is possible using two oxygen-dependent oxidases. The reaction holds very good green credentials as oxygen is the terminal oxidant and the atom economy is high and compares very well against other state of the art oxidative cyclisations[275,276,281]. The major limitation of this methodology is that the substrate scope is rather limited due the enzymes' specificity. The Nylon-6 monomer caprolactam could not be synthesised using our oxidative cyclisation methodology and so additional mutants are required to extend the enzymes specificity. However the smaller pyrrolidone was formed in high conversion (85%). Moreover a refractive index detector (which the group has now) would be would be required to fully monitor the formation of intermediates without a chromophore.

In addition, we have briefly explored the application of oxidative cyclisation to form β-lactams with promising initial results. We believe that this process has a potential to provide a

green alternative to classical β-lactam forming reactions which often employ very harsh conditions or transition metals and use relatively inaccessible from difficult starting materials[282-284]. However, this area must be explored in more detail.

Although the current work is limited to cyclic substrates, the approach could potentially be transferred to acyclic substrates. The major issue of utilising acyclic imines in buffered solutions is the relative stability. Acyclic imines are prone to hydrolysis in aqueous media to provide amines and aldehydes which are very good substrates for XOR. If the rate of oxidation of the imine is faster than that of the rate of hydrolysis then potentially any imine could be transformed into an amide product. However in aqueous media this may not be possible. If the substrate specificity of PaoABC could be switched to imine substrates, then perhaps the removal of imine substrate would shift the equilibrium towards imine formation. Additionally if the reactions could be conducted in organic solvents with minimum water, the rate of hydrolysis would probably be lower than the rate of oxidation. However, there are only few examples of oxidations by molybdoenzymes in organic solvents[285].

The use of organic solvents for XOR-catalysed oxidations is indeed highly interesting. In a standard XOR catalysed oxidation the incorporated oxygen is derived from water. We have suggested that intramolecular displacement of the molybdo ester is possible using hydroxyaldehydes and potentially the amines. If reactions are conducted at very low concentrations of water in the presence of additional nucleophiles then perhaps esters and amides could potentially be synthesised from aldehydes.

Chapter 5

5.0 Enzymatic synthesis of biomass derived furan-2,5 dicarboxylic acid (FDCA)

5.1 Introduction

With the rapid growth of the world population and continuing depletion of petroleum reserves, green approaches using renewable resources for the production of chemicals will be required[45]. Lignocellulosic biomass is an abundant, inexpensive and sustainable resource from which platform chemicals can be derived. 5-Hydroxymethylfurfural (HMF, **373**) is derived from cellulose *via* dehydration of glucose and fructose. Due to the instability of HMF, its oxidized and more stable form furan-2,5-dicarboxylic acid (FDCA, **377**) is listed as one of twelve sugar based platform chemicals of interest by the American DOE[286,287].

Polyethylene terephthalate (PET) makes up 5.9% of the global plastics industry with approximately 15 million tons per year being manufactured. It is considered that bio-based furan-2,5-dicarboxylic acid (FDCA, **377**) could replace PET in this and related co-polymers which would be a substantial step towards sustainable plastics manufacture[288]. In addition, FDCA is a building block[287] and can be used to synthesise other polyesters[289], polyamides[290] and valuable furanic chemicals[291]. Obtaining FDCA from biomass at low cost will be essential to allow a paradigm shift in green manufacturing although this target is yet to be realized.

HMF consists of a furan ring with 2,5-disposed aldehyde and hydroxylmethyl functional groups. It can be synthesized from glucose/fructose by dehydration[292] in high yield although currently only with continuous removal of water or extraction into non aqueous solvents or ionic liquids due to instability at high temperatures[293]. Numerous metal catalysts and nano particles have been employed such as Au-TiO_2[294], Au-C modified with Pd[295], Au-hydrotalicite[296], Pt-C[297], Au/TiO_2[298], Pt/ZrO_2[235], however, these reactions require high pressure/temperature and additional additives which decreases the sustainability for manufacturing. Thus, there remains a number of challenges for the steps from cellulose to FDCA and their integration.

A catalytic system that uses O_2 from air and produces water as the only by-product would contribute to establishing a green and sustainable process for conversion of HMF (**373**) to FDCA (**377**)[299]. To this end, aerobic Pt nanoparticles[300] and gold systems[301] have been developed but usually require high pH which can partially decompose the unstable HMF.

Biocatalytic reactions offer many benefits in the context of green chemistry since they can be performed under mild conditions using a biodegradable catalysts[302]. Synthesis of FDCA from HMF has been demonstrated using whole cells, however the need for a continuous carbon source feed and low product recovery of the polar FDCA from cell biomass limited its potential[303]. Bioconversions using isolated enzymes can proceed at a significantly higher substrate concentration and combine higher productivity with lower water usage. Recently an FAD-dependent HMF oxidase was reported to fully oxidise HMF to FDCA using molecular oxygen albeit at low substrate concentrations[304]. In another approach, aryl alcohol oxidase (AAO) was used to convert HMF to 5-formylfuran-2-carboxylic acid (FFCA) which was then converted to FDCA by an unspecific peroxygenase (UPO) in a second much slower step.

We believed that our previously developed GOaseM_{3-5}- XDH/PaoABC system could be adopted for the synthesis of FDCA from HMF (Scheme 66).

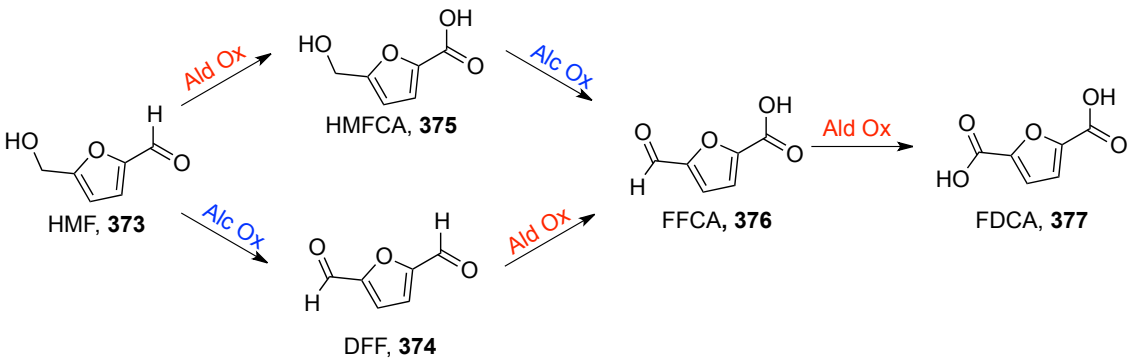

Scheme 66 Possible intermediates en route from HMF to FDCA.

5.1 Oxidation of HMF to FDCA

5.1.1 Initial aldehyde oxidase screening

Initial studies revealed that HMF was indeed a substrate for GOaseM_{3-5} yielding the dialdehyde DFF (**374**), however HMFCA (**375**) was not available to test. Four molybdenum dependent xanthine oxidoreducatases were chosen to screen for activity against all available aldehyde substrates DFF (**374**), HMF (**373**) and FFCA (**376**) (Table 18).

Table 18 Screening of xanthine oxidoreductases for oxidation of HMF, DFF, FFCA

Entry[a]	Enzyme	HMF (**373**)	DFF (**374**)	FFCA (**375**)	Oxidant
1	*E.coli* XDH[b]	Active	Not active	Not active	O_2
2	XDH E232V[c]	Active	Active	Active	DCPIP
3	XDH E232V/R310[d]	Active	Active	Active	DCPIP
4	PaoABC[e]	Active	Active	Active	O_2

[a]Reaction conditions: Potassium phosphate buffer (50mM, pH 7.6), 3 µL 0.1 M substrate), 30 µL 0.01 M DCPIP(aq.) final volume 300 µL, 36°C. Activity was determined by the colour change from blue to colourless.[b] *E.coli* XDH (1.1 mg/mL), [c]XDH E232V (25.4 mg/mL), [d]XDH E232V/R310M (23 mg/mL), [e]PaoABC(13.3 mg/mL)

The commercially available *E. coli* XDH, which we had previously shown to oxidise benzylic aldehydes was only active on HMF (Table 18, entry 1). The *Rhodococcus capsulatus* xanthine dehydrogenase (XDH) single variant E232V and double mutant XDH E232V/R310M showed activity against all three substrates. These variants possess very low reactivity using oxygen from air and require an exogenous electron acceptor such as DCPIP for high conversions as electron transport to oxygen is poor. PaoABC, however was able to oxidise all three substrates using molecular oxygen as its terminal electron acceptor and so was chosen for its green chemistry attributes.

5.1.2 Enzymatic oxidation of 50mM HMF by GOaseM_{3-5} and PaoABC

A test cascade reaction was performed using HMF with both GOaseM_{3-5} and PaoABC present to identify if FDCA could be produced. Gratifyingly at 10 mM HMF concentration, almost full conversion to FDCA was observed (97%) after 1hr, with the key intermediates being DFF and FFCA (Figure 27).

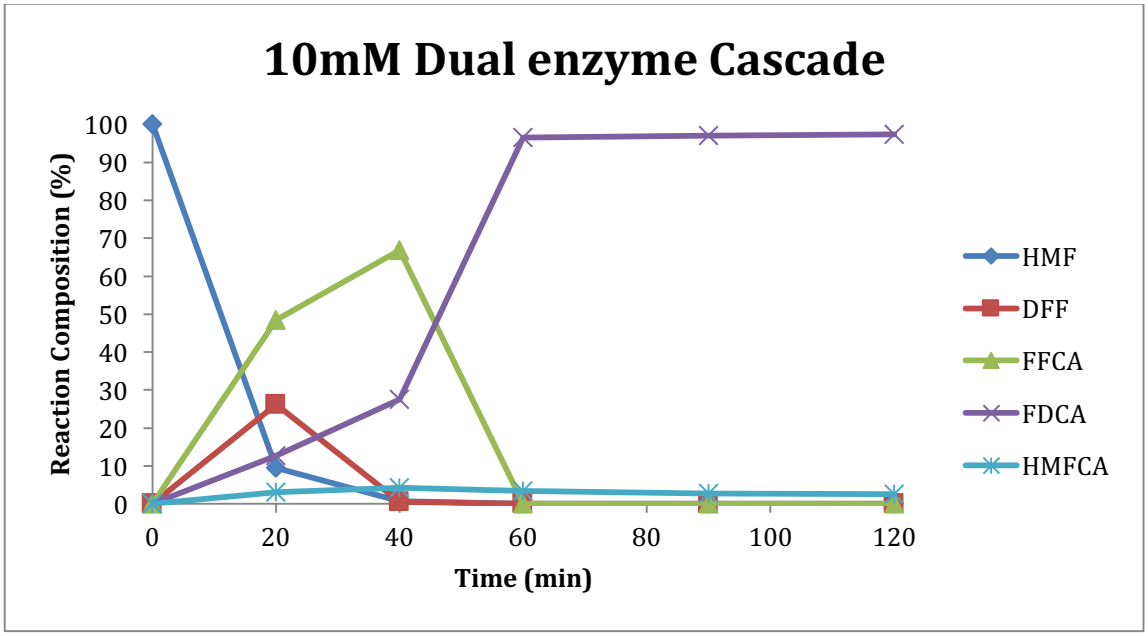

Figure 27 Enzyme cascade for conversion of HMF with dual combined enzymes (GOaseM_{3-5} + PaoABC) [HMF] = 10 mM

We then investigated the effect of increasing the concentration of HMF (Table 19). At 20 mM HMF, after 1 hr, FDCA (44%) was formed along with HMFCA (50%), then after a further 1 hr, a small amount of HMFCA was converted to give a final conversion of 55% FDCA (Figure 28). This time course indicates that the formation of FDCA occurs mainly *via* DFF and FFCA and that HMFCA is a poor substrate for GOaseM_{3-5}. It is also clear that PaoABC is responsible for the formation of HMFCA at this substrate concentration.

Production of HMFCA could be avoided by using a sequential, stepwise process in which the GOaseM_{3-5} conversion of HMF to DFF was allowed to run to completion prior to addition of the PaoABC enzyme. This stepwise reaction furnished the desired FDCA as the only

oxidation product cleanly and with 100% conversion (Table 19, entry 3). On increasing the starting concentration of HMF further, we found that sufficient buffer capacity to control pH was important to enable the reaction to reach completion (Table 19, entry 6).

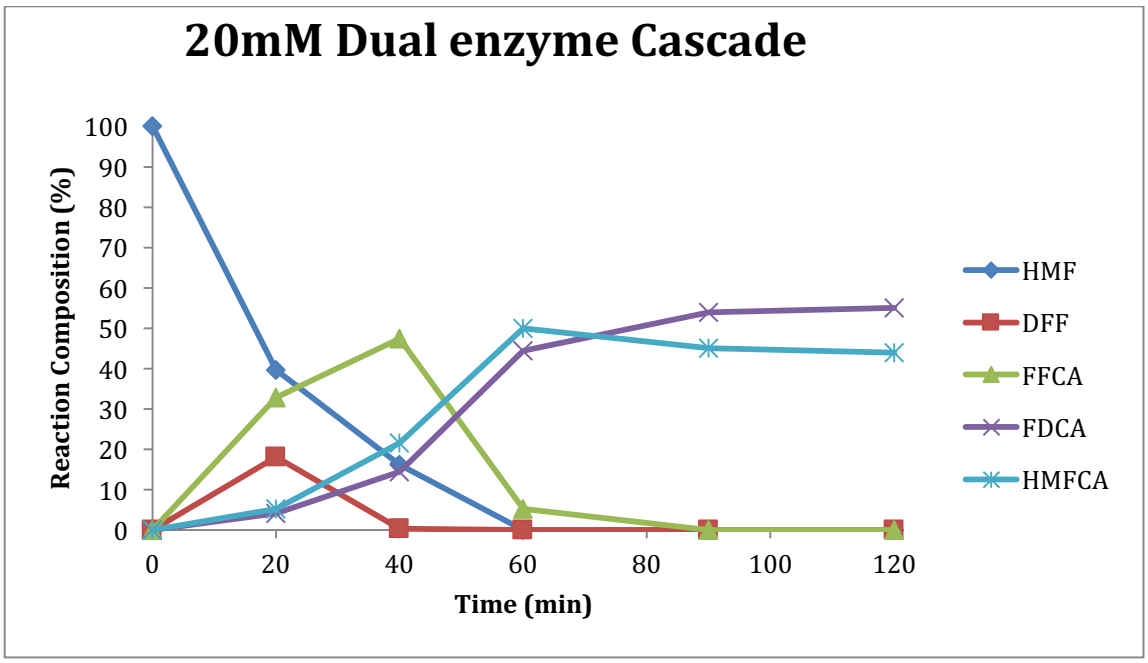

Figure 28 Enzyme cascade for conversion of HMF with dual combined enzymes (GOase$M_{3\text{-}5}$ + PaoABC) [HMF] = 20 mM

This has previously been reported in whole cell biotransformation of HMF to FDCA[303]. To increase the reaction concentration further, we decided that it was necessary to identify the reason for PaoABCs low activity at low pH.

5.1.3 Optimisation of DFF conversion by PaoABC to 100mM substrate conc.

We first implemented the 50 mM DFF transformation at a variety of pHs to identify the optimum pH (Table 20). At pH 6 no conversion to FDCA was observed however DFF was successfully converted to FFCA (Table 20, entry 1). Additionally pH 9 proved catastrophic to PaoABC reactivity as only 18% FFCA was obtained (Table 20, entry 4). The optimum pH for

the biotransformation was pH 7-8 in which quantitative conversion was observed after 2 hours (Table 20, entries 3-4).

Table 19 Optimisation of the the HMF- 2-step oxidation cascade[a]

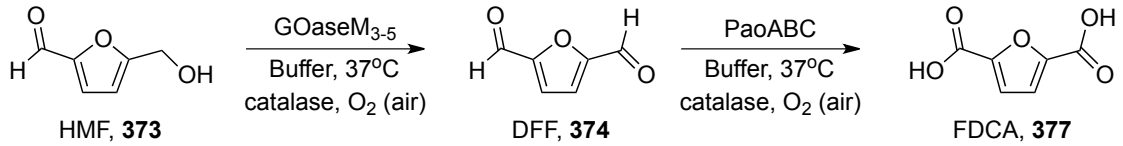

HMF, **373** DFF, **374** FDCA, **377**

Entry	[HMF] (mM)	pH	Buffer (mM)	DFF[b]	FDCA[c]
1	10	7.5	50	-	97
2	20	"	"	-	55
3	20	"	"	>99	>99
4	30	"	"	>99	>99
5	50	"	"	>99	0
6	50	"	100	>99	>99

[a]Reaction conditions: Entries 1&2 are one-pot with all enzymes present; entries 3-6 are sequential with PaoABC added after complete conversion to DFF. $GOaseM_{3-5}$ (3.3 mg/mL) 103 µL, catalase (3.3mg/mL) 33 µL, 3 µL of x M HMF (in MeCN), potassium phosphate buffer (xmM) pH 7.6, final volume 300 µL, then after full conversion to DFF, PaoABC (13.3 mg/mL) 5 µL. [b]Formation of DFF was monitored via RP-HPLC using a Thermofisher Hypurity C18 column with flow rate 0.6 mL/min using 85% water + 0.1% acetic acid and 15% MeCN. [c]Formation of FDCA was monitored via RP-HPLC using a Thermofisher Hypurity C18 column with flow rate 1 mL/min using a 98% 10 mM phosphate buffer (pH 6.5) and 2% MeCN mobile phase

Increasing the concentration further to 80 mM DFF met with increased reaction times with quantitative conversion of DFF to FDCA at pH 7 in 4 hours. The reaction conducted at pH 8 suffered from lower conversions to the desired carboxylic acid. Finally increasing the concentration further to 100 mM met with a major drop in pH (pH <5)(Figure 29) which was below optimum pH (6-8) for PaoABC, determined in a previous chapter (chapter 3).

Table 20 PaoABC catalysed oxidation of DFF

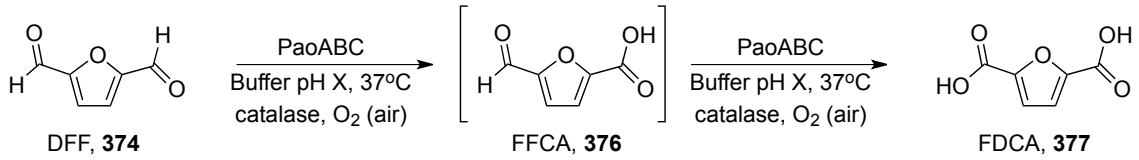

DFF, **374** FFCA, **376** FDCA, **377**

Entry	DFF (mM)	pH[c]	Buffer (mM)	PaoABC (µL)	Time (h)	FFCA[b] (%)	FDCA[b] (%)
1	50	6	200	5	2	100	0
2	"	7	200	"	"	0	>99
3	"	8	200	"	"	0	>99
4	"	9	200	"	"	18	0
5	80	7	200	"	4	0	>99
6	"	8	200	"	"	44	66
7[a]	100	7	200	"	16	40	60
8	"	7	400	"	6	0	>99

PaoABC (13.3mg/mL) [a]pH after 16 h = 4.5. [b]Conversion adjusted by using a 1:1 standard of the aldehyde:acid by NMR and comparing the HPLC trace of the same sample and adjusting the absorbance accordingly. [c]Initial pH

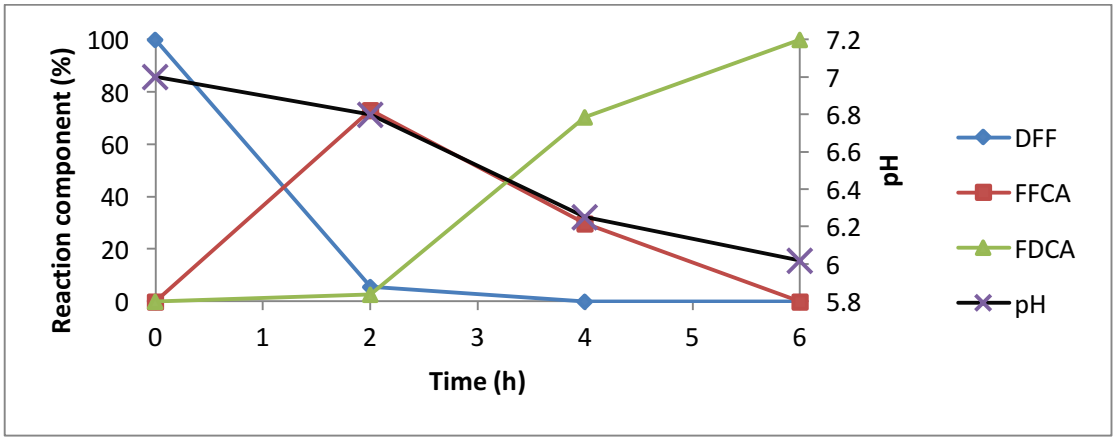

Figure 29 Time course of FDCA production showing decrease in pH over time for entry 8.

The formation of hydrated aldehydes is heavily reliant on the pH of the system. In addition, the formation or lack of formation of hydrated aldehydes can have a significant impact on rates of oxidation by oxidases such as the recently reported FAD dependent HMFO oxidase by Fraaije. DFF readily forms its hydrate at pH 5-8 (Figure 30) however, FFCA does not (Figure 31). This

is a major issue for hydrate dependent oxidases such as HMFO[304] and AAO[305] as the final oxidation step is problematic. However, molybdo-dependent oxidases such as PaoABC require the aldehyde substrate which is present at all pHs and so the final oxidation of FFCA is not a problem. Therefore we believe that the drop in pH is responsible for reduced conversion as PaoABC working outside its optimum pH and not the inability of FFCA to form a hydrate. Increasing the substrate concentration further to 100 mM DFF, it was necessary to maintain the pH within the optimum of pH 7 by increasing the buffer capacity to 400 mM to allow sufficient conversion to the desired dicarboxylic acid (Table 20, entry 8). Thus it appears that the final oxidation of FFCA to FDCA is more pH sensitive than the HMF to DFF conversion.

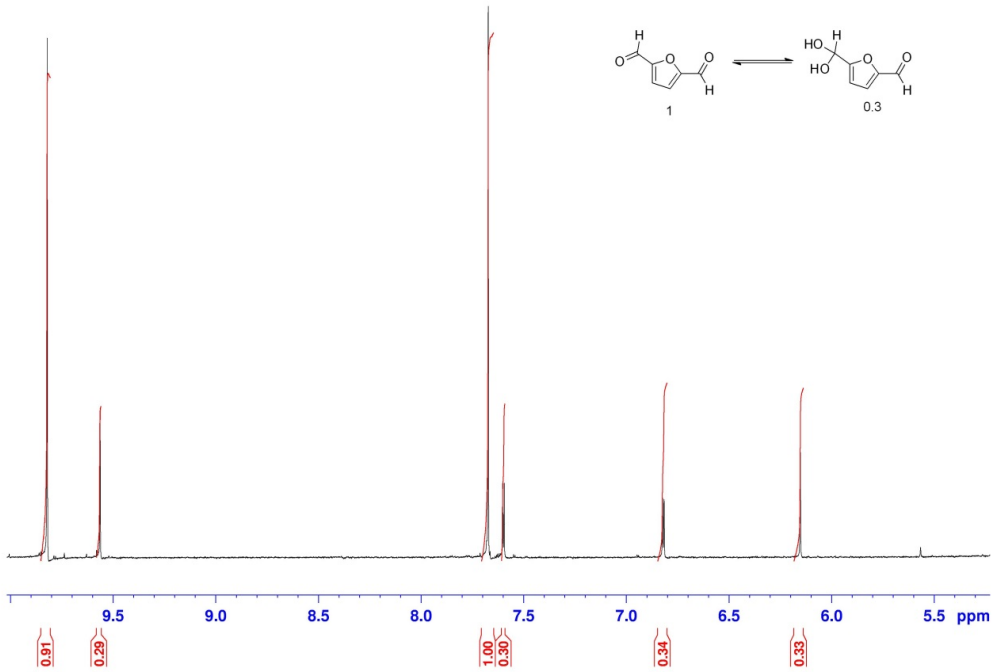

Figure 30 NMR analysis of DFF (**374**) clearly showing hydrate formation, peaks at 9.58, 7.59, 6.82 and 6.15ppm. Ratio of hydrate: aldehyde was identical for each pH.

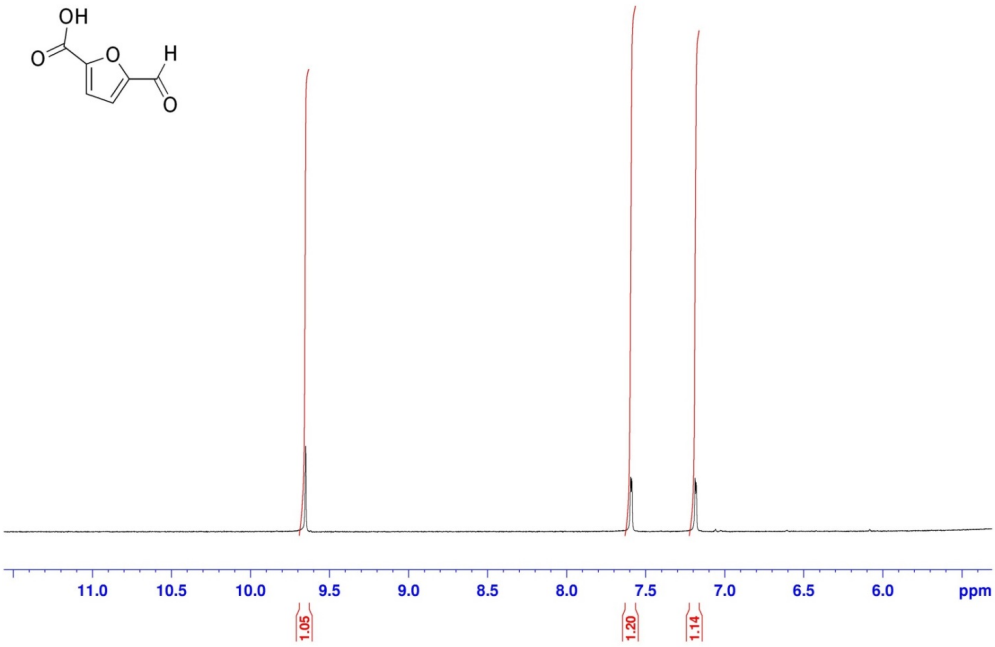

Figure 31 NMR analysis of FFCA (**376**) showing no hydrate formation

5.1.4 100 mM HMF to FDCA bio-bio *in vivo* cascade using GOaseM$_{3\text{-}5}$ and PaoABC.

With the optimized conditions for the DFF conversion in hand it was clear that high buffer capacity is essential for efficient catalysis (Table 20, entry 2). HMF at 70 mM concentration was cleanly converted to FDCA (Table 21, entry 1). At 100 mM an additional portion of catalase was required with the addition of PaoABC (Table 21, entries 2-3), possibly due to the extensive reaction time for the first oxidation (>16 hr), during which catalase may be deactivated. With our optimized conditions in hand for the conversion of 100 mM HMF to FDCA, the preparative scale oxidation of HMF was then realized. Isolation of FDCA by crystallisation has been successful after whole cell biotransformations[303] however, the removal of biomass and numerous extractions into organic solvents reduce sustainability. Therefore, we were pleased to find that in our case heat treatment of the solution to precipitate the protein,

centrifugation, acidification and filtration is all that was required to obtain pure FDCA in 74% isolated yield (Table 21, entry 4)

Table 21 Optimisation of the HMF- 2-step oxidation cascade[a]

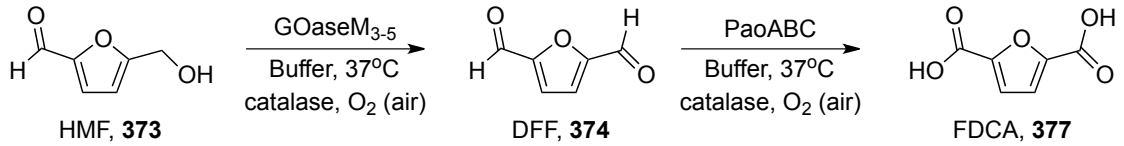

HMF, **373** DFF, **374** FDCA, **377**

Entry	HMF	pH	Buffer	DFF[b]	FDCA[c]
1	70	7	300	>99	>99 (80)[f]
2	100	"	400	>99	0
3[d]	100	"	"	>99	>99
4[d,e]	100	"	"	>99	>99 (74)[f]

[a]Reaction conditions:. $GOaseM_{3-5}$ (3.3 mg/mL) 103 µL, catalase (3.3 mg/mL) 33 µL, 3 µl of xM HMF (in MeCN), potassium phosphate buffer (x mM) pH 7.6, final volume 300 µL, then after full conversion to DFF, PaoABC (13.3 mg/mL) 5 µL. [b] Formation of DFF was monitored via RP-HPLCusing a Thermofisher Hypurity C18 column with flow rate 0.6mL/min using 85% water + 0.1% Acetic acid and 15% MeCN.[c]Formation FDCA was monitored via RP-HPLC using a Thermofisher Hypurity C18 column with flow rate 1mL/min using a 98% 10mM phosphate buffer (pH 6.5) and 2% MeCN mobile phase.[d] Additional portion of catalase was added with PaoABC. [e] Reaction performed on preparative scale. [f] Isolated yield

5.1.5 Time course of HMF to FDCA bio-bio *in vivo* cascade using $GOaseM_{3-5}$ and PaoABC

For the 50 mM sequential reaction the initial oxidation of HMF was found to be the slower step (Figure 25). On addition of PaoABC there is a rapid oxidation of DFF to FFCA. It is noteworthy that FDCA is not produced rapidly until almost all of DFF is converted to FFCA. This suggests that the dialdehyde is a better substrate for PaoABC. DFF forms the hydrate rapidly in buffer but not the FFCA indicating that DFF is more activated to nucleophilic attack by water. Therefore we believe DFF is a better substrate because it is more prone to nucleophilic attack by the Mo-OH.

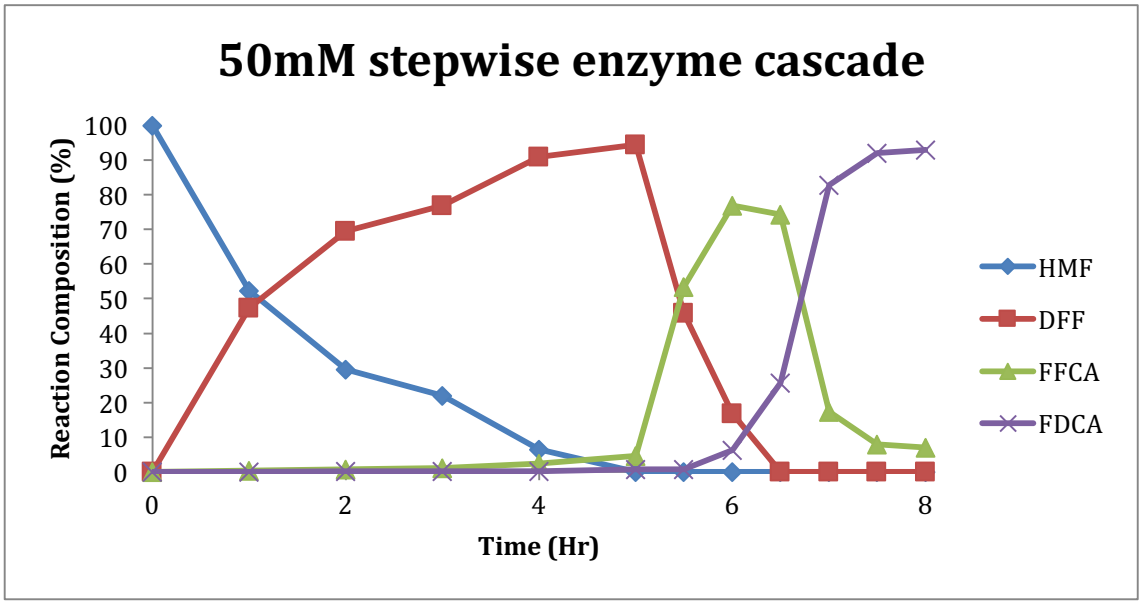

Figure 25 2-Step oxidation showing high conversion to DFF after 5 h and subsequent rapid oxidation of DFF to FFCA and FDCA

Interestingly a small fraction of FFCA is produced prior to the addition of PaoABC which could be a result of residual H_2O_2 in the reaction however we cannot completely exclude the possibility of $GOaseM_{3-5}$ carrying out the oxidation of the hydrate. If the latter is the case, then this would represent the first reported oxidation of an aldehyde by $GOaseM_{3-5}$

Turning our attention back to the dual enzyme one pot *in vivo* cascade, we postulated that a pH drop might be the limiting factor in our previous attempt at simultaneous catalysis. However, oxidation at 50 mM HMF with $GOaseM_{3-5}$ and PaoABC combined at high buffer concentration resulted in predominatly HMFCA after 3 hr which was only slowly converted to FFCA (Figure 25). The latter was then rapidly oxidized to FDCA and after 20 hr, 56% of FDCA was present

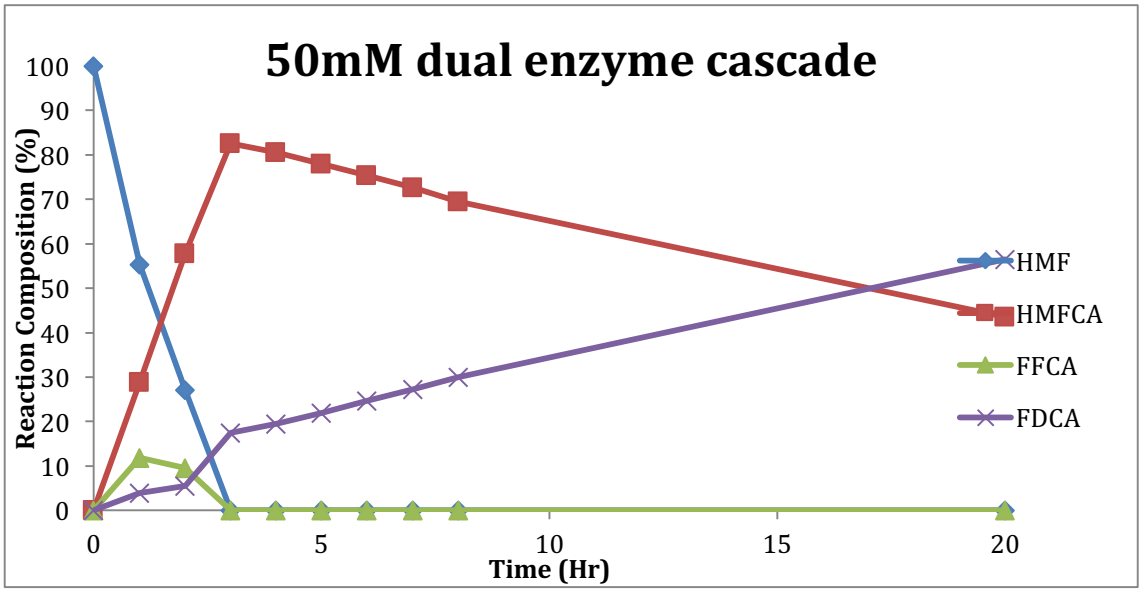

Figure 26 Combined dual enzyme oxidation showing high conversion of HMF to HMFCA after 3hr and slow oxidation to FDCA over 20 hr

5.2 Conclusion:

In summary we have developed a promising tandem cascade reaction using two oxygen-dependent enzymes, galactose oxidase M_{3-5} and periplasmic aldehyde oxidase PaoABC, that results in high conversion of HMF to FDCA at ambient temperature, near neutral pH and using oxygen as the terminal oxidant. The substrate concentration of HMF (100mM) is the highest reported for an enzyme-based process and uses enzymes that do not require the addition of co-factors. PaoABC has performed extremely well compared to other aldehyde oxidases and is not limited by FFCAs inability to form its hydrate, which is the case with other reported procedures[304].

The major limitation of this methodology is the sequential addition of enzymes. GOaseM_{3-5} represents a major limitation inflicted by many biocatalysts in which substrate specificity is an issue. Additional mutants of GOase or an alternative enzyme for the alcohol oxidation would lead to a more attractive process as continuous catalysis could take place.

The upstream reaction to produce HMF from cellulose would likely contain many dehydrated sugars and other impurities[292]. If our established oxidation procedure could be

applied to efficient oxidation of crude HMF, it would provide an extremely green and economic route to highly pure FDCA. To realise this further developments of the enzymes such as enzyme immobilization or additional genetic modifications to deal with high substrate concentrations or tolerate organic solvents would be necessary to create a viable industrial synthesis of FDCA.

Conclusion

In conclusion, we have exploited two molybdenum-dependent oxidoreductases, *E. coli* XDH and PaoABC in preparative enzymatic cascades. E. coli XDH has been shown to accept a range of benzylic aldehydes and also activated imines such as xanthine and DHIQ. However, more challenging substrates such as unactivated and bulky aldehydes are not tolerated. PaoABC however tolerates a much wider spectrum of aldehydes and to this date all aldehydes tested have been accepted. PaoABC activity with imine substrates is much less than that of E. coli XDH, however unactivated imines are oxidised to a small degree.

We have demonstrated a one-pot, single stage tandem cascade for the quantitative conversion of 26 alcohols directly to their corresponding carboxylic acids, including aliphatic examples employing three oxygen-dependent enzymes, GOaseM_{3-5}, PaoABC and *E. coli* XDH. The major limitation with these cascades is the low substrate concentration that the enzymes tolerate. For the aryl alcohols, *E. coli* XDH can tolerate concentrations of >50 mM, however this may be alleviated by the use of PaoABC which can tolerate much higher substrate concentrations. Unfortunately, for aliphatic substrates GOaseM_{3-5} can only accept concentrations <30 mM. Creation of additional mutants will facilitate scale up of these cascade processes. In addition, we have observed a novel potentiation effect by combining GOaseM_{3-5} and PaoABC and have therefore expanded the substrate scope of GOaseM_{3-5} by combining the alcohol oxidase with PaoABC. Alcohols previously believed thought to be non-substrates for GOaseM_{3-5} furnished carboxylic acids in cascade conditions with PaoABC.

Possible enantiodiscrimination by PaoABC was also explored as a result of previous cascades in which we obtained 50% conversion, suggesting that a kinetic resolution may have occurred. In turn, a series of -substituted aldehydes were synthesised which may be resolved or subject to DKR for synthesis of profen drugs. Unfortunately, the highest E-value obtained was 14. Despite the poor enantioselectivity of PaoABC, an interesting oxidative cyclisation mechanism was noted which could be applied to the synthesis of lactams or lactones.

With this oxidative cyclisation in hand, we demonstrated that amino alcohols could be cyclized to lactams via an in situ generated imine using both GOaseM_{3-5} and E. coli XDH or PaoABC. The reaction holds good green credentials as oxygen is the terminal oxidant and atom economy is very high. The major drawback to this cascade is the narrow substrate scope. Activated imines such as DHIQ could be successfully oxidized in high conversion, however 6 and 7 membered ring lactams could not be formed in any appreciable conversion. In addition, a -lactam product may have been formed (indicated by mass spec) via internal displacement of the postulated molybdo ester which would highlight novel reactivity of these molybdo enzymes. With the established biocatalytic cascade utilising PaoABC and GOaseM_{3-5} we demonstrated that FDCA can be obtained starting from 100 mM HMF concentration. This represents the highest concentration reported for an enzyme-based process and uses enzymes that do not require the addition of co-factors. PaoABC performed extremely well when compared to other aldehyde oxidases and is not limited by FFCAs inability to form its hydrate. The major limitation of this procedure is the sequential addition of the biocatalyst to avoid substrate specificity issues in which HMFCA is a poor substrate for GOaseM_{3-5}. Further directed evolution of GOaseM_{3-5} or immobilization may expand its substrate scope and thus allow a continuous process.

Experimental

Chapter 6

6.0 Experimental

6.1 General Experimental

Analytical thin layer chromatography (TLC) was performed on Whatman F254 precoated silica gel plates (250 μm thickness). Visualization was accomplished with a UV light and/or a $KMnO_4$ solution. Flash column chromatography (FCC) was performed using Whatman Silica Gel Purasil® 60Å (230-400 mesh). Solvents for extraction and FCC were technical grade. Reported solvents mixtures for both TLC and FCC were volume/volume mixtures. Solvents were of analytical or HPLC grade and were purchased dried over molecular sieves where necessary. Normal and reverse phase HPLC was performed on an Agilent system (Santa Clara, CA, USA) equipped with a G1379A degasser, G1312A binary pump, a G1329 well plate autosampler unit, a G1315B diode array detector and a G1316A temperature controlled column compartment. GC analysis was performed on Agilent 6850 GCs equipped with a Gerstel Multipurposesampler MPS2L using an Alltech SE-30, 30.0 m x 320 μm x 0.25 μm GC capillary column. Elemental analysis and mass spectrometry was provided by the University of Liverpool. ^{1}H NMR and ^{13}C NMR were recorded on Bruker AV 500 MHz & Bruker DPX 400 MHz NMR spectrometers in the indicated deuterated solvents. For ^{1}H NMR $CDCl_3$ was set to 7.26 ppm ($CDCl_3$ singlet) and for ^{13}C NMR to 77.66 ppm ($CDCl_3$ centre of triplet). All values for ^{1}H NMR and ^{13}C NMR chemical shifts for deuterated solvents were obtained from Cambridge Isotope Labs. Data are reported in the following order: chemical shift in ppm (δ) (multiplicity, which are indicated by br (broadened), s (singlet), d (doublet), t (triplet), q (quartet), m (multiplet)); assignment of 2nd order pattern, if applicable; coupling constants (*J*, Hz); integration. Infrared spectra (IR) were

obtained on a Perkin-Elmer Spectrum 100 series FTIR spectrophotometer. Peaks are reported in cm^{-1} Unless otherwise indicated, all reactions were carried out in flame dried round bottom flasks and under an inert atmosphere of nitrogen or Argon. Syringes and needles were oven-dried (125°C) and cooled in a desiccator. All substrate were purified by column chromatography. All chemicals unless included in the experimental section were commercially available.

6.2 Experimental procedure for Chapter 2

6.2.1 Screening of *E. coli* XDH towards a diverse set of selected aldehyde substrates using DCPIP

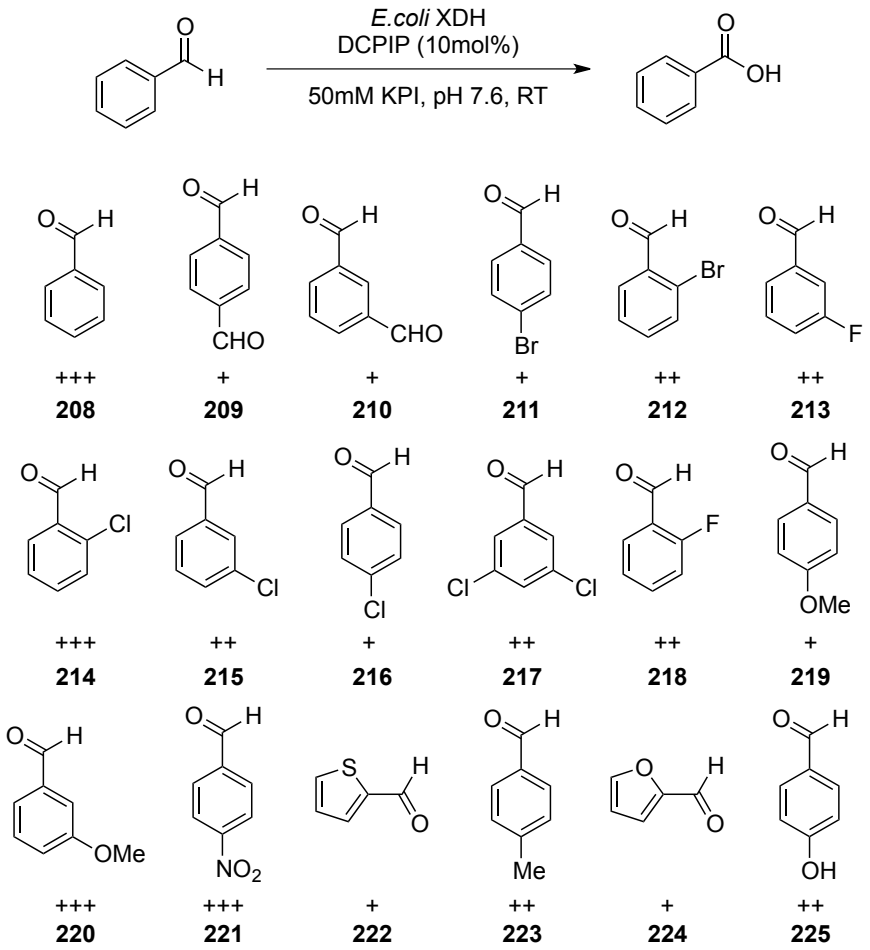

The screening of *E. coli* xanthine dehydrogenase was accomplished using a 96-well, clear, flatbottomed polystyrene microtitre plate in a final volume of 200 µL in potassium phosphate buffer (50 mM, pH 7.6) containing per well: 1 mM of the respective substrate, 0.1 mM DCPIP, 20 µL XDH solution (1.1 mg/mL stock solution). The activity of *E. coli* XDH towards the compounds tested was assessed by eye based on the loss of blue colour.

6.2.2 Time course analysis for the oxidation of benzaldehyde derivatives (1mM) by *E. coli* XDH

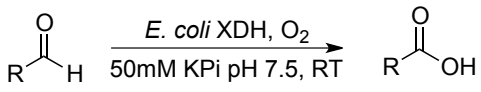

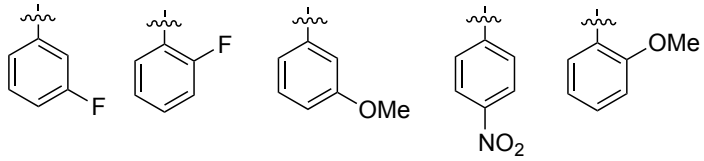

213 **218** **220** **221** **240**

To a 1mL-Eppendorf was added 50 mM potassium phosphate buffer pH 7.5 (50 mM), 3 µL substrate (0.1M in MeCN), 50 µL of *E. coli* XDH (1.1 mg/mL), final volume 300 µL. After the indicated times 30 µL of the reaction was removed, acidified with 10 µL, centrifuged and analysed by RP-HPLC. For HPLC conditions see Section 6.2.4.

6.2.3 Oxidation of *p*-nitrobenzaldehyde (1mM) by incremental addition of substrate

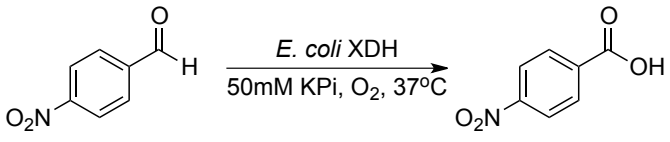

To a 1 mL Eppendorf was added 50 mM potassium phosphate buffer pH 7.5 (50 mM), 3 µL *p*-nitrobenzaldehyde (**221**) (0.1M in MeCN), 50 µL of *E. coli* XDH (1.1 mg/mL), final volume

300 µL. The reaction was then vigourously shaken and the reaction left in a shaking incubator at 37°C. After 2.5 hours, 30 µL of the reaction was removed, acidified with 10 µL of 1M HCl and analysed by RP-HPLC. Another 3 µL of *p*-nitrobenzaldehyde (**221**) was added and the reaction left for a further 2.5 hours before an aliquot was taken as previously described. A final 3µL of *p*-nitrobenzaldehyde (**221**) was added and the recaction left overnight. A final aliquot was taken and analysed by RP-HPLC. For HPLC condition see Section 6.2.4

6.2.4 General method for bio-bio-catalytic cascade reaction for synthesis of benzoic acids from benzyl alcohols in a one-pot one-step approach

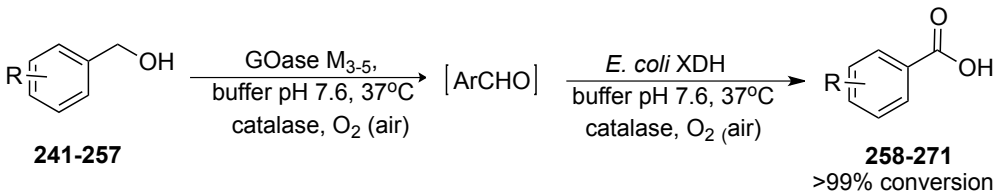

R = 4-NO_2-Ph, 4-Br-Ph, H, 4-Cl-Ph, 4-MeO-Ph, 2-MeO-Ph, 3-Cl-Ph, 3-Br-Ph, 4-Me-Ph, 2-F-Ph, 3-F-Ph, 2-Br-Ph, 3-MeO-Ph, 2,6-Cl_2-Ph, Ar = 2-thiophenyl, Ar = 2-furanyl

To a 1 mL-Eppendorf tube was added 69 µL of 50mM potassium phosphate buffer pH 7.6, 75 µL catalase (1mg/mL), 3 µL of substrate (100 mM stock in MeCN), 50 µL of *E.coli* XDH (1.1 mg/mL) and 103 µL of $GOaseM_{3-5}$ (3.7 mg/mL). The reaction was then vigourously shaken and left in an incubator at 37°C overnight with periodic shaking. Analysis was done by RP-HPLC, see Table 22

Table 22 Galactose oxidase $M_{3\text{-}5}$-*E.coli* xanthine dehydrogenase cascade reactions for formation of acids from alcohols in a one-pot one-step approach. Substrates, HPLC-retention times of alcohols, aldehydes and acid and percentage of conversions after 16 hr based on HPLC peak areas (λ = 254 nm).

Entry	Substrate	Alcohol Retention Time (Min)	Aldehyde Retention Time (Min)	Acid Retention Time (Min)	10mM Conversion Alc:Ald:Acd	HPLC Condtions
1	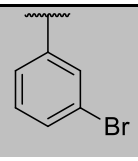	6.4	14.0	10.06	0:0:100	A
2	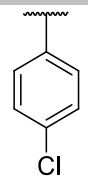	5.4	10.94	8.9	0:0:100	A
3	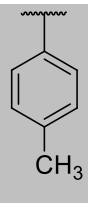	3.05	5.98	4.08	0:0:100	B
4	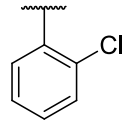	4.7	4.4	2.1	0:100:0	A
5	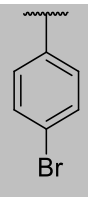	4.4	9.02	6.5	0:0:100	B
6	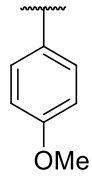	2.5	5.2	3.4	0:0:100	A
7	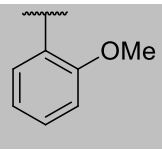	2.9	5.7	2.77	0:0:100	A
8	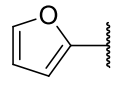	5.1	5.9	8.1	0:0:100	C

9	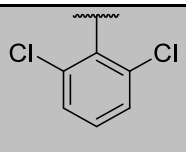	2.73	5.4	2.37	100:0:0	E
10	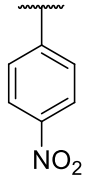	3.1	5.3	4.6	0:0:100	A
11	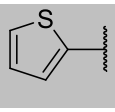	3.1	4.5	4.9	0:0:100	D
12	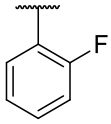	2.82	5.4	4.5	0:0:100	A
13	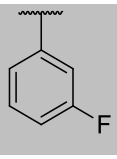	3.1	6.0	4.6	0:0:100	A
14	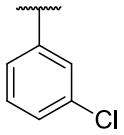	3.8	7.7	5.1	0:0:100	B
15	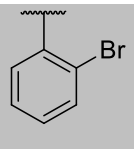	4.0	8.9	3.5	0:0:100	B
16	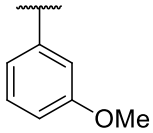	4.0	8.9	3.5	0:0:100	A

HPLC conditions: RP-phase column, ThermoFishserHypurity C-18 column, flow rate 1.0 mL/min, UV 254 nm, Method A: 25% MeCN: 75% water + 0.1% TFA; Method B: 25% MeCN: 75% water + 0.1% TFA; Method C: 1% MeCN : 99% water + 0.1% TFA;Method D: 15% MeCN : 85% water + 0.1% TFA;Method E: 40% MeCN: 60% water + 0.1% TFA.

6.2.5 Optimisation of the bio-biocatalytic cascade for synthesis of 3-methoxybenzoic acid from 3-methoxybenzyl alcohol in a one-pot one-step approach

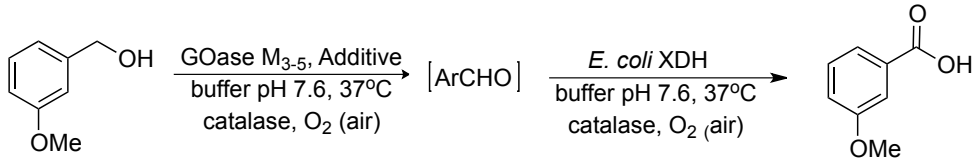

241 **220** **258**

To a 1 mL-Eppendorf was added 50 mM NaPi buffer pH 7.6, X µL catalase (stock 1 mg/mL), 3- methoxybenzyl alcohol (10-100 mM), 50 µL of *E. coli* XDH (1.1 mg/mL) and 103 µL of GOase M_{3-5} (3.7 mg/mL). The reaction was left in a shaking incubator at 36 °C. The reaction was opened to air every hour, closed and shaken to oxygenate the buffer placed back into the incubator. After the indicated time 50 µL of the reaction mixture was acidified with 20 µL of 2 M HCl, centrifuged and analysed by RP-HPLC. Conversions reported are based on relative response factors determined via NMR-HPLC correlations. (see table 22)

6.2.6 Time course analysis of the bio-biocatalytic cascadefor synthesis of 3-methoxybenzoic acid from 3-methoxybenzyl alcohol in a one-pot one-step approach

In a 1-mL-Eppendorf was added 50 mM potassium phosphate buffer pH 7.6, 33 µL catalase (stock 3.3mg/mL), 3-methoxybenzyl alcohol (50 mM), 50 µL of E. coli XDH (1.1 mg/mL) and 103 µL of GOase M_{3-5} (3.7 mg/mL), final volume 300 µL. The reaction was left in a shaking incubator at 36 °C. The reaction was periodically opened to air, closed and shaken to oxygenate the buffer and put back into the incubator. After the indicated times 5 µL of the reaction was extracted, acidified with 10 µL 1M HCl and diluted with 85 µL distilled water. The aliquots were analysed by RP-HPLC and conversions corrected by response factors determined *via* NMR-HPLC correlations.

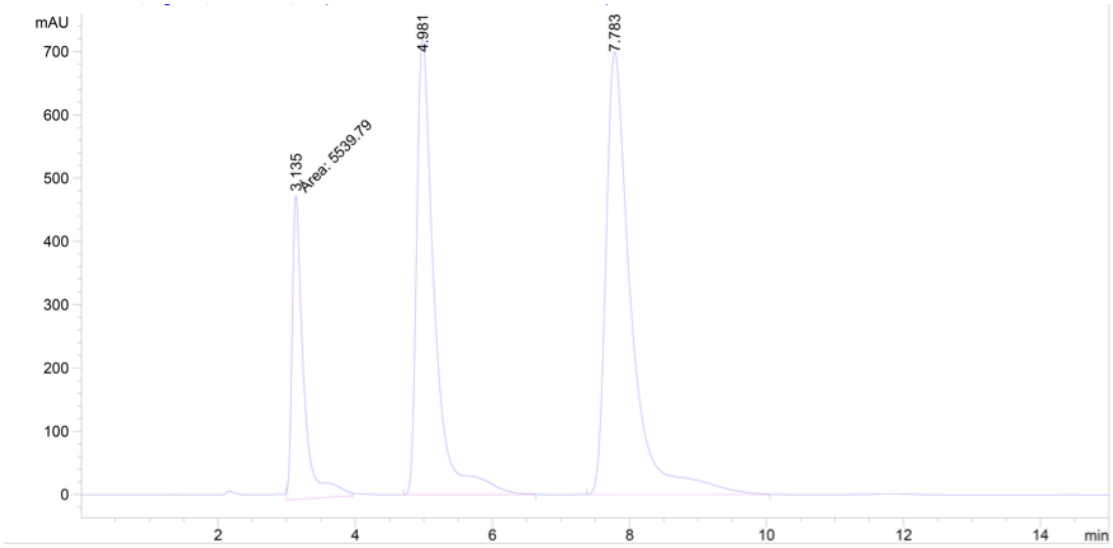

Figure 27 HPLC trace of a 1:1:1 mixture of 3-methoxybenzyl alcohol (**241**) (3.14 min), 3-methoxybenzoic acid (**258**)(4.98 min) and 3-methoxybenzaldehyde (**220**) (7.78 min). HPLC conditions ThermoFisherHypurity C-18 column, flow rate 1.0 mL/min, UV 254 nm, 25% MeCN: 75% water + 0.1% TFA.

.

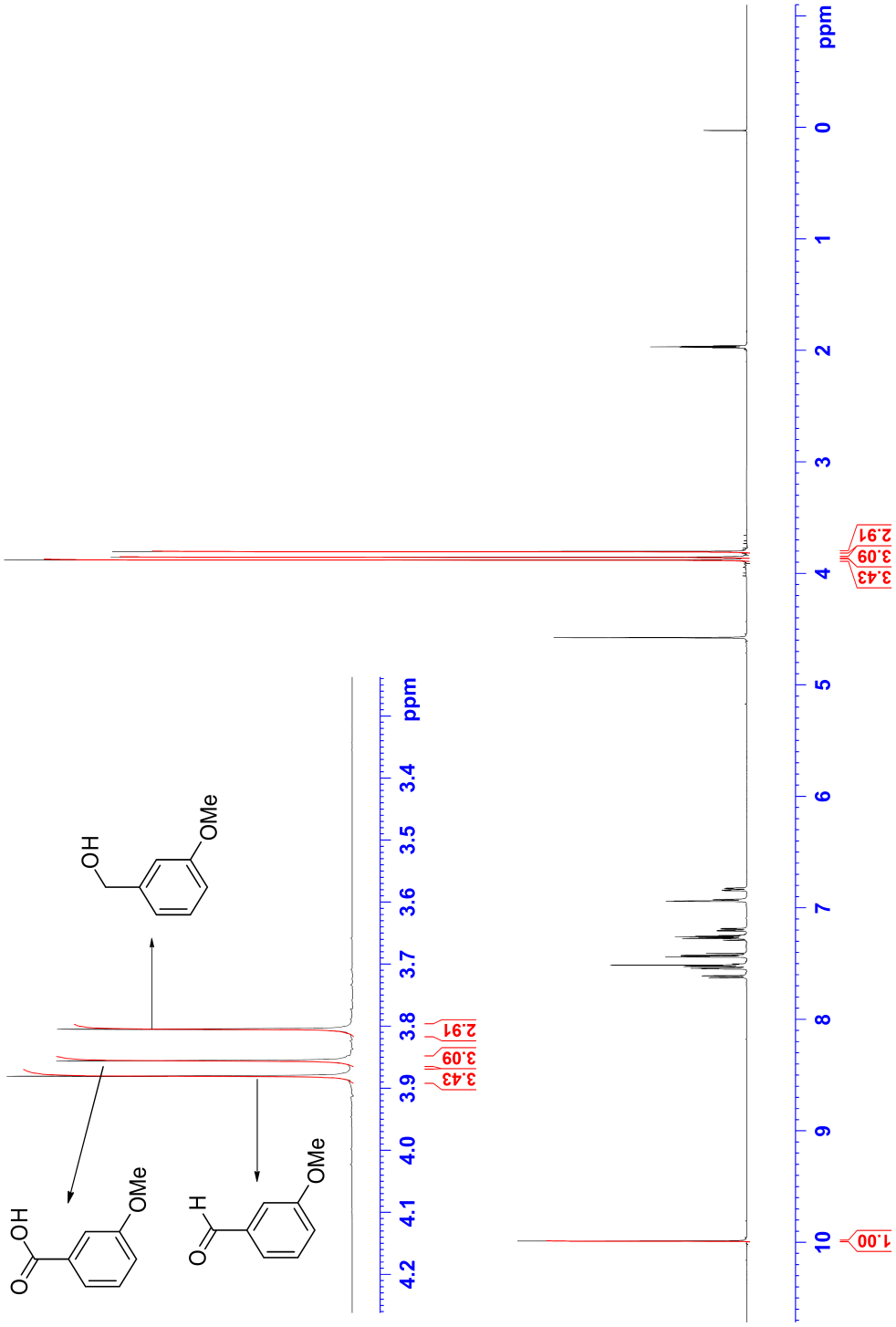

Figure 28 ^{1}H NMR spectrum (500 MHz) of a 1:1:1 mixture of 3-methoxybenzyl alcohol (**241**) (3.8 ppm), 3- methoxybenzoic acid (**258**) (3.86 ppm) and 3-methoxybenzaldehyde (**220**) (3.89 ppm).

6.2.7 pH-Profile for oxidation of *m*-anisaldehyde with PaoABC

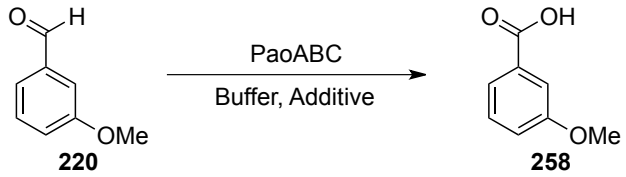

3 µL of a 1 M solution of *m*-anisaldehyde (**220**) was added to 33 µL catalase (3.3 mg/ml) in 262 µL of various pH phosphate buffer (50 mM). 1 µL of PaoABC (13.3mg/mL) was then added and the reaction was shaken vigorously. Aliquots of the reaction mixture were removed, acidified with 2 M HCl, centrifuged and analysed by RP HPLC (For HPLC conditions see 6.2.5)

Table 22 PaoABC catalysed oxidation of m-anisaldehyde (**220**) at different pH.

		Conversion (%)[a]				
Entry	**pH**	**20min**	**40min**	**60min**	**90min**	**120min**
1	5	5.68	11.27	14.03	31.48	46.2
2	5.5	9.32	14.2	23.15	38.9	54.6
3	6	12.3	30.6	39.2	63.5	82.2
4	6.5	11.8	20.2	41.2	62.2	89.2
5	7	16.2	34.7	50.2	72.2	90.2
6	7.5	11.2	28.2	34.2	65.2	83.2
7	8	12.2	26.2	-	72.2	91.2

[a]Conversion adjusted by analysing a 1:1 standard of the aldehyde:acid by NMR and comparing the HPLC trace of the same sample and adjusting the absorbance accordingly (Section 6.2.6)

6.2.8 Screening of PaoABC towards a diverse set of selected aldehyde substrates using DCPIP

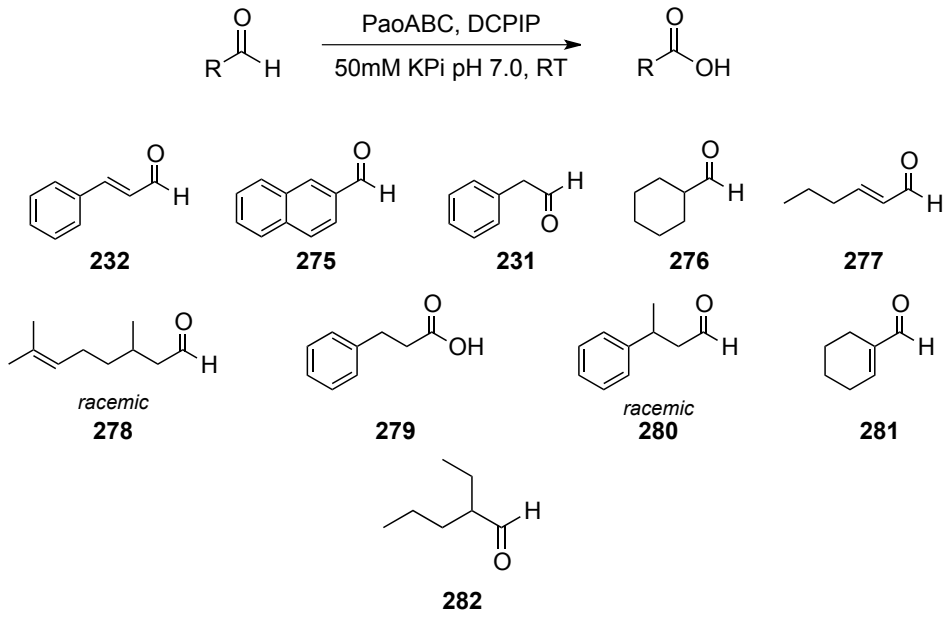

The screening of *E. coli* xanthine dehydrogenase was accomplished using a 96-well, clear, flatbottomed polystyrene microtitre plate in a final volume of 200 µL in potassium phosphate buffer (50 mM, pH 7.6) containing per well: 1 mM of the respective substrate, 0.1mM DCPIP, 5 µL PaoABC solution (13.3 mg/mL stock solution). The activity of *E. coli* XDH towards the compounds tested was assessed by eye based on the loss of colour.

6.2.9 General method for bio-bio-catalytic cascade reaction for synthesis of carboxylic acids from alcohols in a one-pot one-step approach

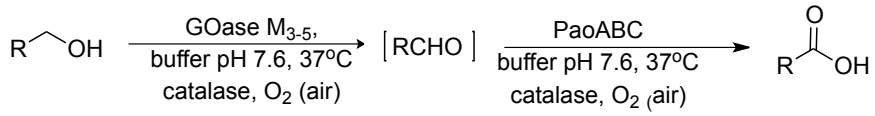

Product	Conversion	Product	Conversion
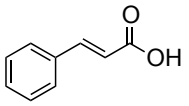 **294**	>99%	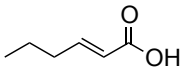 **298**	>99%
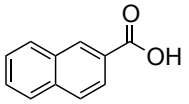 **295**	>99%	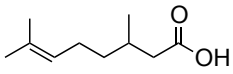 **299**	>99%
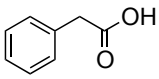 **296**	>99%	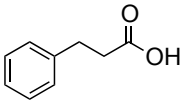 **300**	>99%
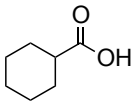 **297**	>99%	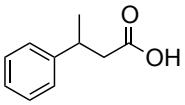 **301**	>99%
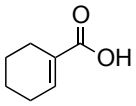 **302**	81%	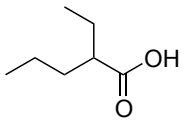 **303**	50%

To 50 mM pH 7.6 potassium phosphate buffer (159 µL) and 33 µL catalase (3.3 mg/mL) was added 3µL of substrate alcohol (1 M in MeCN, 10 mM final concentration). 103 µL of GOase $M_{3\text{-}5}$ (1.3 mg/mL) and 5µL PaoABC (13.2 mg/mL) was then added. The reaction was incubated at 37°C in a shaking incubator and left shake overnight. The reaction was quenched by the addition of 50µL 1 M HCl and extracted into 200 µL DCM. The DCM was then analysed by GC

Table 23 Galactose oxidase M_{3-5} PaoABC cascade reactions for formation of acids from alcohols in a one-pot one-step approach. Substrates, GC-retention times of alcohols, aldehydes and acid and percentage of conversions after 16hr based on GC peak areas

R=	**-CH_2OH**	**-CHO**	**-CO_2H**	Conversion (%)
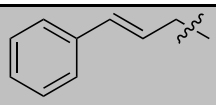	11.87	11.28	13.98	100
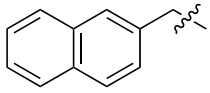	14.91	14.52	16.92	100
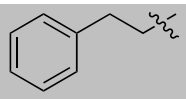	8.9	7.57	11.48	100
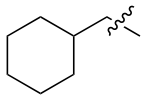	7.18	N/A	9.584	100
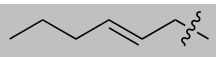	4.71	N/A	8.449	100
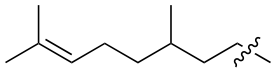	10.91	9.68	12.78	100
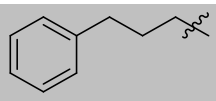	10.92	9.6	13.0	100
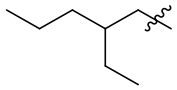	7.8	6.2	10.1	50
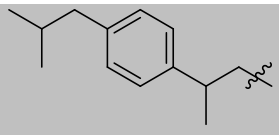	14.7	13.8	16.38	0
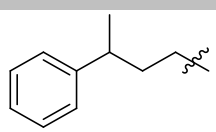	11.49	10.4	13.6	100

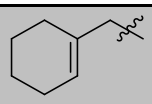	7.60	7.07	10.718	81

GC Conditions: All samples were analysed using an Alltech SE-30, 30.0 m x 320 µm x 0.25 µm GC capillary column (40°C for 5 min, 50°C/min to 140°C and held for 5 min, 10°C/min to 300°C).

6.2.10 Timecourse analysis of 10 mM cascade for oxidation of phenylethanol (10mM)

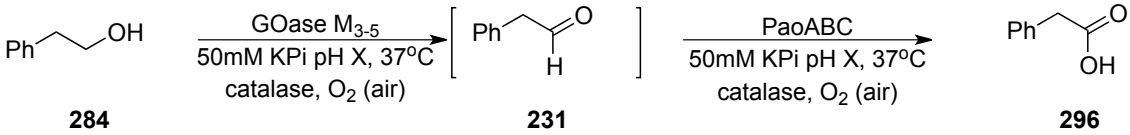

284 **231** **296**

To a solution of 200 mM pH 7.6 potassium phosphate buffer (159 µL) and 33 µL catalase (3.3 mg/mL) was added 3 µL of phenylethanol (**284**) (1M in MeCN, 10mM final concentration). 103 µL of GOase M3-5 (3 mg/mL) and 5 µL PaoABC (13.2 mg/mL) was then added and the reaction incubated at 36°C in a shaking incubator and left to shake. 30 µL aliquots of reaction mixture were taken out, acidified by addition of 20 µL of 1M HCl, centrifuged and analysed by RP-HPLC. HPLC conditions: ODS-Hypersil C18 column, 1 mL/min, 82% water (0.1% TFA) 18% MeCN.

6.2.11 GOaseM_{3-5} PaoABC 30mM scale conversion of 3-phenylbutanol

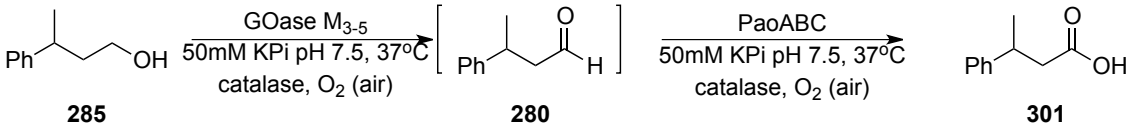

285 **280** **301**

To a solution of pH 7.6 50 mM phosphate buffer was added 15 µL of 3-phenylbutanol (**285**) (2M in MeCN). GOase M_{3-5} (1.3 mg/mL) and PaoABC (13.3 mg/mL) was then added to final volume 1 mL. The reaction was then placed in a shaking incubator for 16 hr. The reaction was then acidified to pH 1 using 1M HCl and extracted into $CDCl_3$ and analysed by H^1 NMR

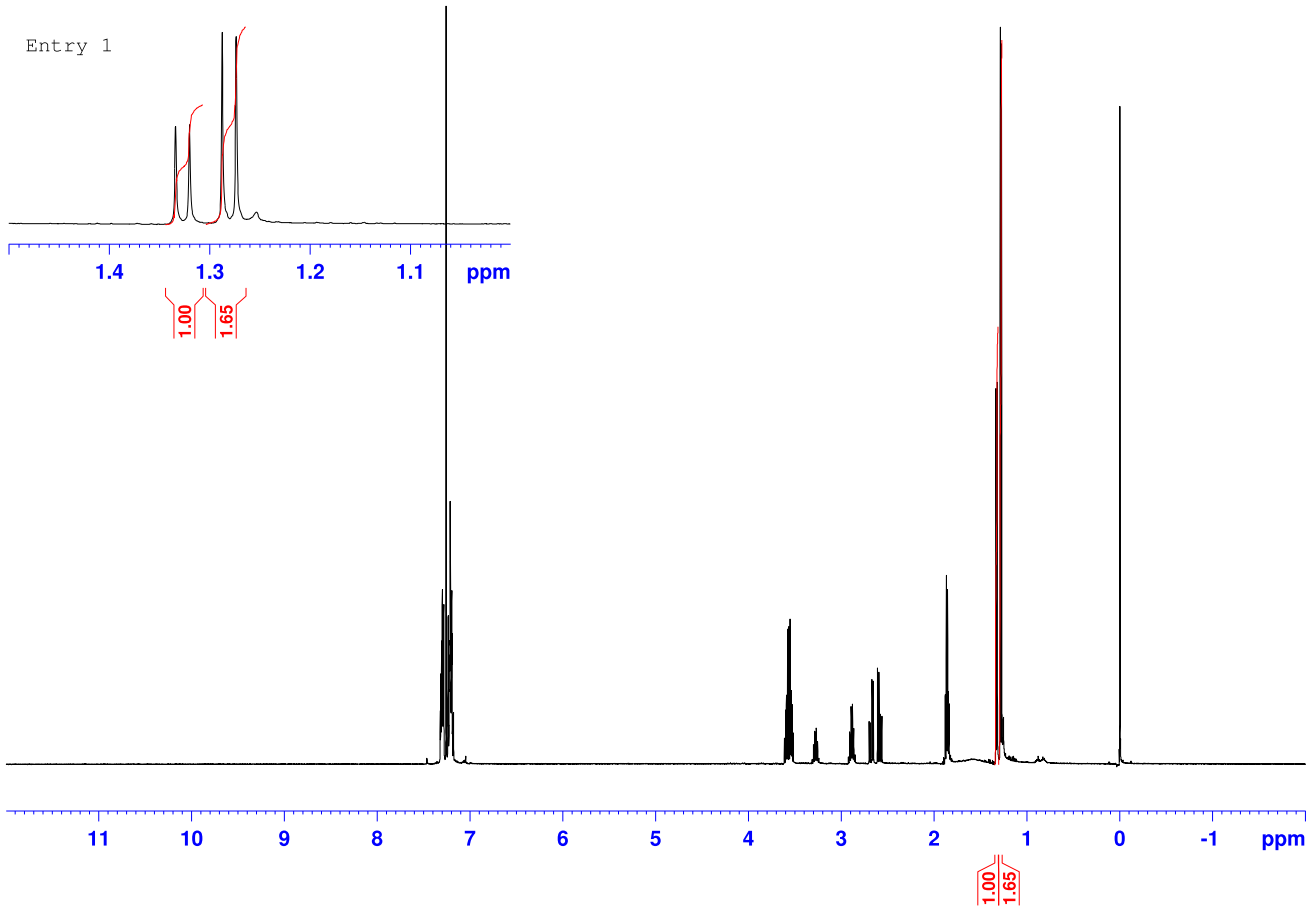

Figure 29 ^{1}H NMR spectrum (500 MHz) of the crude reaction mixture (Table 7, entry 1), Signals at 1.35 correspond to the CH_3 of acid product, Signals at 1.29 correspond to alcohol product.

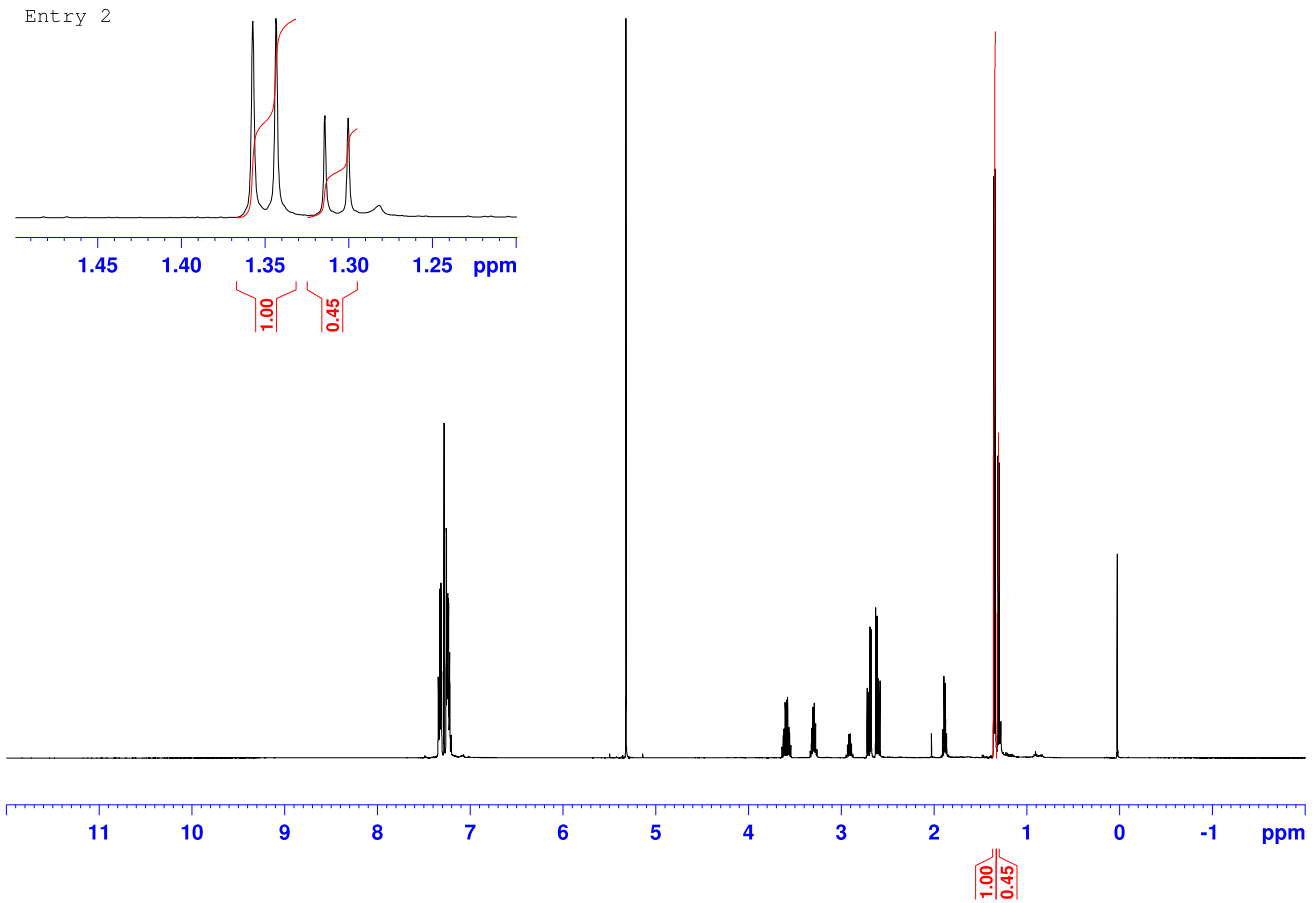

Figure 30 ^{1}H NMR spectrum (500 MHz) of the crude reaction mixture (Table 7, entry 2), Signals at 1.35 correspond to the CH_3 of acid product, Signals at 1.29 correspond to alcohol product.

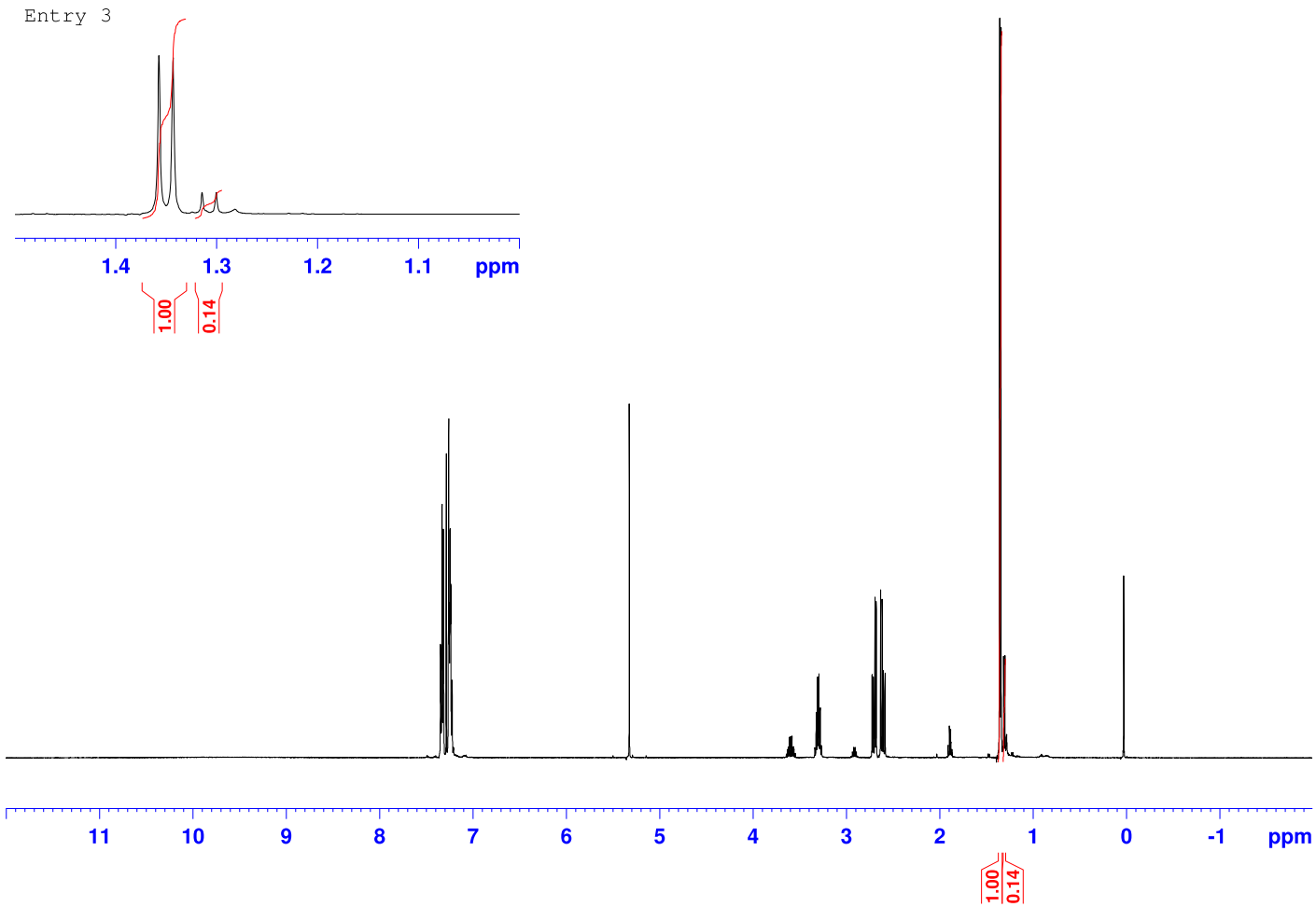

Figure 31 ^{1}H NMR spectrum (500 MHz) of the crude reaction mixture (Table 7, entry 3), Signals at 1.35 correspond to the CH_3 of acid product, Signals at 1.29 correspond to alcohol product.

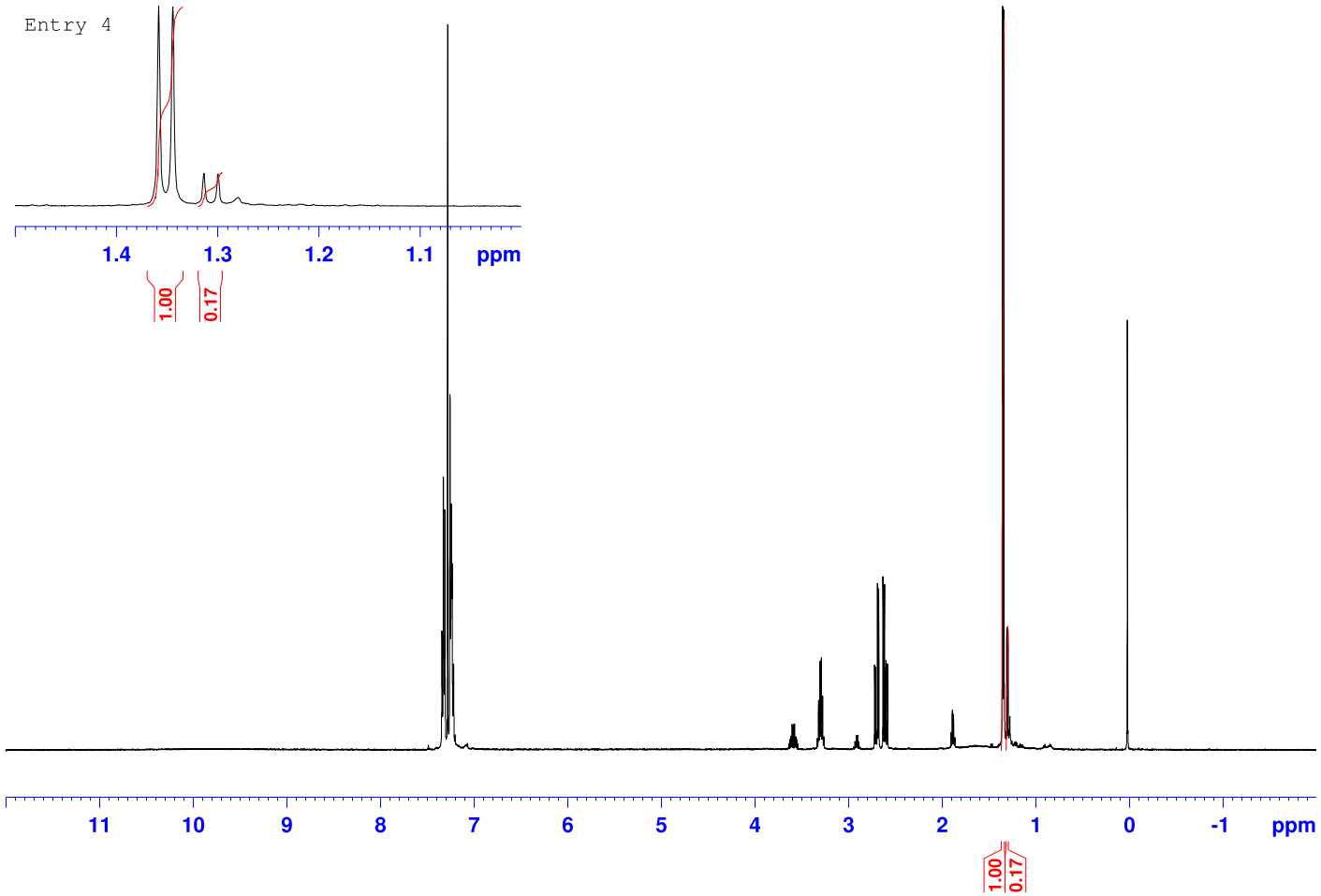

Figure 32 ^{1}H NMR spectrum (500 MHz) of the crude reaction mixture (Table 7, entry 4), Signals at 1.35 correspond to the CH_3 of acid product, Signals at 1.29 correspond to alcohol product.

6.2.12 GOaseM_{3-5} inhibition studies

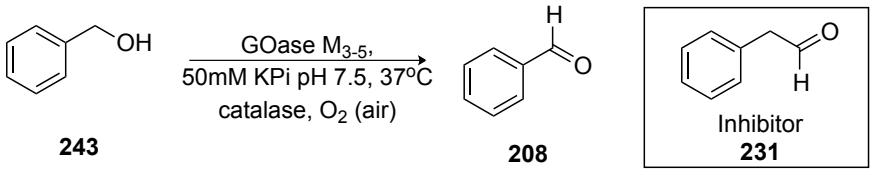

243 **208** **231**

To 50mM phosphate buffer pH 7.5 was added 3 μL benzaldehyde and a specific concentration of phenylacetaldehyde as indicated in Table 8. 103 μL of GOaseM_{3-5} (3mg/mL) was then added and the reaction (final volume 300 μL) placed in a shaking incubator at 37°C. After 1 hour the reaction was quenched with 1M HCl and analysed by RP-HPLC. HPLC conditionns: ODS-Hypersil C18 column, 1 mL/min, 82% water (0.1% TFA) 18% MeCN.

6.3 Experimental procedures for Chapter 3

6.3.1 General procedure for the alkylation of methyl phenylacetate.

Under a nitrogen atmosphere, to a stirred colourless solution of di*iso*propylamine (2.05 mL, 14.7mmol) in anhydrous tetrahydrofuran (133 mL), was added *n*-butyl lithium (9.16mL of 1.6M solution in *n*-hexane, 14.7mmol) was added dropwise. The resultant pale yellow mixture was then stirred for 15 minutes. The reaction mixture was cooled to -78°C and then methyl phenylacetate (1.88 mL, 13.3mmol) was added dropwsise forming the enolate. The consequent stirred reaction mixture was left for 15 minutes at -78°C. The alkyl halide (14.7mmol) was then added to the reaction mixture dropwsie. The resultant mixture was then left stirring at room temperature until reaction was complete as determined by TLC. The reaction mixture was quenched with saturated ammonium chloride (60 mL) and extracted with diethyl ether (3x30 mL). The combined organic extracts were then dried over anhydrous magnesium sulphate. Filtration and removal of the solvent under reduced pressure gave a crude oil. The crude product was then purified by flash column chromatography furnishing a pure oil.

*methyl 2-phenylbutanoate (**308**)*

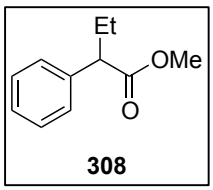

308

The crude product was purified by flash column chromatography (98:2 hexane:diethyl ether) furnishing a pure colourless oil (1.66 g, 70%). **^{1}H NMR (500 MHz, $CDCl_3$)** δ 7.37 – 7.31 (m, 4H), 7.30 – 7.26 (m, 1H), 3.68 (s, 3H), 3.48 (t, *J* = 7.4 Hz, 1H), 2.18 – 2.07 (m, 1H), 1.87 – 1.79 (m, 1H), 0.92 (t, *J* = 7.3 Hz, 3H); **^{13}C NMR (500 MHz, $CDCl_3$)** δ 174.50, 139.11, 128.56, 127.94, 127.17, 53.38, 51.86, 26.75, 12.15; HRMS CI+: $C_{11}H_{14}O_2NH_4^+$ {$[M+NH_4]^+$}, Calc.: 196.1333, Found: 196.1339; **IR:** 3030, 2966, 2876, 1732, 1492, 1454, 1351, 1202, 1161, 732cm^{-1}.

*methyl 2-phenylpentanoate (**309**)*

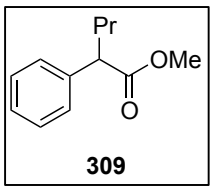

309

The crude product was purified by flash column chromatography (97.5:2.5 hexane:diethyl ether) furnishing a pure colourless oil (1.45 g, 67%). **^{1}H NMR (500 MHz, $CDCl_3$)** δ 7.37 – 7.31 (m, 4H), 7.30 – 7.25 (m, 1H), 3.68 (s, 3H), 3.59 (t, *J* = 7.7 *Hz*, 1H), 2.11 – 2.04 (m, 1H), 1.82 – 1.75 (m, 1H), 1.36 – 1.24 (m, 2H), 0.94 (t, *J* = 7.3 Hz, 3H); **^{13}C NMR (500 MHz, $CDCl_3$)** δ 174.59, 139.28, 128.56, 127.92, 127.14, 51.87, 51.38, 35.67, 20.74, 13.79; **HRMS CI+**: $C_{12}H_{16}O_2NH_4^+$ {$[M+NH_4]^+$}, Calc.: 210.1489, Found: 210.1493; **IR**: 3063, 3030, 2872, 1732, 1454, 1433, 1350, 1231, 1198, 698cm^{-1}

*methyl 2-phenylhexanoate (**310**)*

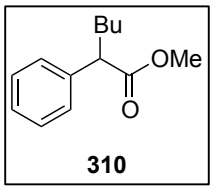

310

The crude product was purified by flash column chromatography (97.5:2.5 hexane:diethyl ether) furnishing a pure colourless oil (1.91 g, 69%). **^{1}H NMR (500 MHz, $CDCl_3$)** δ 7.39 – 7.23 (m, 5H), 3.69 (s, 3H), 3.61-3.50 (m, 1H), 2.12-2.05 (m, 1H), 1.85-1.75 (m, 1H), 1.40-1.15 (m, 4H), 0.87(d, *J* = 7.2 Hz, 3H)**; ^{13}C NMR (500 MHz, $CDCl_3$)** δ 174.6, 139.3, 128.6, 127.9, 127.1, 51.9, 51.6, 33.3, 29.7, 22.5, 13.9**; HRMS CI+**: $C_{16}H_{16}O_2H^+$ {$[M+NH_4]^+$}, Calc.: 224.1652, Found: 224.1645; **IR:** 3086, 306, 2950, 1731, 1495, 1454, 1434, 1350, 1213, 1152, 1030cm^{-1}

*methyl 4-methyl-2-phenylpentanoate (**311**)*

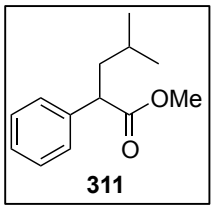

311

The reaction mixture was left overnight to achieve completion. The crude product was purified by flash column chromatography (98:2 hexane:diethyl ether) furnishing a pure colourless oil (1.48 g, 54%). **^{1}H NMR (500 MHz, $CDCl_3$)** δ 7.36 – 7.25 (m, 5H), 3.72 – 3.66 (m, 4H), 1.99 (ddd, *J* = 13.6, 8.0, 7.3 Hz, 1H), 1.71 (ddd, *J* = 13.6, 8.0, 6.7 Hz, 1H), 1.53 – 1.44 (m, 1H), 0.93 (d, *J* = 6.6 Hz, 6H**); ^{13}C NMR (500 MHz, $CDCl_3$)** δ 174.72, 139.34, 128.59, 127.95, 127.15, 51.93, 49.52, 42.51, 25.85, 22.62, 22.22; **HRMS CI+**: $C_{13}H_{18}O_2NH_4^+$ {$[M+NH_4]^+$}, Calc.: 224.1645, Found: 224.1645; **IR**: 3065, 3030, 2955, 1733, 1454, 1434, 1244, 1197, 731cm^{-1}

*methyl 2,3-diphenylpropanoate (**312**)*

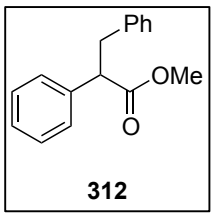

312

The crude product was purified by flash column chromatography (99:1 hexane:diethyl ether) furnishing a pure colourless oil (1.44 g, 63%). **^{1}H NMR (500 MHz, $CDCl_3$)** δ 7.39 – 7.23 (m, 7H), 7.23 – 7.18 (m, 1H), 7.18 – 7.11 (m, 2H), 3.88 (dd, *J* = 8.8, 6.7 Hz, 1H), 3.63 (s, 3H), 3.45 (dd, *J* = 13.7, 8.8 Hz, 1H), 3.05 (dd, *J* = 13.7, 6.7 Hz, 1H); **^{13}C NMR (500 MHz, $CDCl_3$)** δ 173.83, 139.04, 138.63, 128.92, 128.64, 128.33, 127.94, 127.39, 126.37, 53.61, 52.00, 39.82; **HRMS CI+:** $C_{16}H_{16}O_2H^+$ {$[M+H]^+$}, Calc.: 241.1223, Found: 241.1225; **IR**: 3086, 306, 2950, 1731, 1495, 1454, 1434, 1350, 1213, 1152, 1030cm^{-1}

*methyl 3-cyclohexyl-2-phenylpropanoate (**313**)*

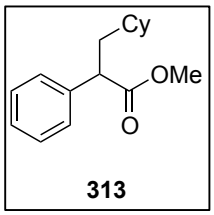

313

The crude product was purified by flash column chromatography (99:1 hexane:diethyl ether) furnishing a pure colourless oil (1.93 g, 59%). **^{1}H NMR (500 MHz, $CDCl_3$)** δ 7.38 – 7.23 (m, 5H), 3.72 (t, *J* = 7.8 Hz, 1H), 3.67 (s, 3H), 2.06 – 1.95 (m, 1H), 1.81 – 1.59 (m, 6H), 1.25 – 1.09 (m, 4H), 0.97 – 0.89 (m, 2H); **^{13}C NMR (500 MHz, $CDCl_3$)** δ 174.80, 139.50, 128.58, 128.49, 127.11, 51.94, 48.77, 41.12, 35.29, 33.29, 32.99, 26.50, 26.12, 26.09; **HRMS CI+:**

$C_{16}H_{22}O_2NH_4^+$ {$[M+NH_4]^+$}, Calc.: 264.1958, Found: 264.1963; **IR**: 2921, 2850, 1734, 1495, 1449, 1307, 1155, 697cm^{-1}.

*methyl 2-phenylpent-4-enoate (**314**)*

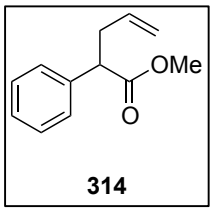

314

The crude product was purified by flash column chromatography (98:2 hexane:diethyl ether) furnishing a pure colourless oil (1.67 g, 66**%**). **^{1}H NMR (500 MHz, $CDCl_3$)** δ 7.37 – 7.31 (m, 4H), 7.30 – 7.26 (m, 1H), 5.75 (ddt, *J* = 17.1, 10.2, 6.8 Hz, 1H), 5.10 (dq, *J* = 17.1, 1.6 Hz, 1H), 5.03 (dq *J* = 10.2, 1.6 Hz, 1H), 3.68 (s, 3H), 3.67 (m, 1H), 2.89 – 2.82 (m, 1H), 2.57 – 2.51 (m, 1H). **^{13}C NMR (500 MHz, $CDCl_3$)** δ 173.87, 138.54, 135.24, 128.63, 127.91, 127.33, 116.97, 76.76, 51.98, 51.41, 37.59; **HRMS CI+**: $C_{12}H_{14}O_2H^+$ {$[M+H]^+$}, Calc.: 191.1067, Found: 191.1066; **IR**: 3078, 3066, 3030, 3004, 2951, 1732, 1620, 1434, 1229, 1160cm^{-1}.

methyl 3-methyl-2-phenylbutanoate (315)

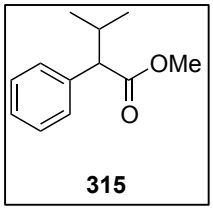

315

Under a nitrogen atmosphere, to a stirred colourless solution of diisipropylamine (2.05 mL, 14.7 mmol) in anhydrous tetrahydrofuran (133 mL), n-Butyl Lithium (9.16 mL of 1.6M solution in n-hexane, 14.7mmol) was added dropwise. The resultant pale yellow mixture was then stirred for 15 minutes. The reaction mixture was then cooled to -78^{o}C and methyl phenylacetate (1.88 mL, 13.3 mmol) was added dropwise forming the enolate. The resultant stirred reaction mixture was left for 15 minutes at -78^{o}C. 2-Bromopropane (1.37 mL, 14.7 mmol) and DMPU (1.61 mL, 13.3 mmol) in anhydrous THF (4 mL) was then added dropwise. The resultant stirred reaction mixture was left overnight at room temperature. Once complete, the reaction mixture was quenched with saturated ammonium chloride (60 mL) and extracted with diethyl ether (3x30 mL). The combined organic extracts were then dried over anhydrous magnesium sulphate. Filtration and removal of the solvent under reduced pressure gave a crude oil. The crude product was then purified by flash column chromatography (98:2 n-hexane:diethyl ether) furnishing a pure colourless oil (1.61 g, 63%). **^{1}H NMR (500 MHz,**

$CDCl_3$) δ 7.37 – 7.31 (m, 4H), 7.30 – 7.25 (m, 1H), 3.67 (s, 3H), 3.18 (d, *J* = 10.5 Hz, 1H), 2.41 – 2.33 (m, 1H), 1.06 (d, *J* = 6.5 Hz, 3H), 0.73 (d, *J* = 6.7 Hz, 3H); **^{13}C NMR (500 MHz, $CDCl_3$)** δ 174.44, 138.34, 128.47, 128.45, 127.22, 60.00, 51.72, 31.92, 22.66, 21.49, 20.20; **HRMS** CI+: $C_{12}H_{16}O_2NH_4^+$ {$[M+NH_4]^+$}, Calc.: 210.1489, Found: 210.1493; **IR**: 3064, 2959, 2872, 1732, 1468, 1454, 1072, 1011, 698cm^{-1}.

methyl 4-((tert-butyldimethylsilyl)oxy)-2-phenylbutanoate (**343**)

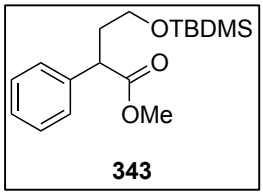

343

Under a nitrogen atmosphere, to a stirred solution of potassium tert-butoxide (4.1 g, 36.6 mmol) in anhydrous DMF (333 mL) was added dropwise methyl phenylacetate (4.69 mL, 33 mmol). The reaction mixture was left stirring for one hour. (2-bromoethoxy)(*tert*-butyl)dimethylsilane (8.76 g, 36 mmol) was added dropwsie. The resultant stirred reaction mixture was left stirring overnight. Once complete, the reaction mixture was quenched with saturated ammonium chloride (100 mL) and extracted with diethyl ether (3x30 mL). The combined organic extracts were then dried over anhydrous magnesium sulphate, filtered and concentrated *in vacuo* to give a crude oil. The crude product was then purified by flash column chromatography (97:3 hexane:diethyl ether) furnishing a pure colourless oil (7.0g, 69%). **^{1}H NMR (500 MHz, $CDCl_3$)** δ 7.36 – 7.25 (m, 5H), 3.84 (t, *J* = 7.6 Hz, 1H), 3.69 – 3.59 (m, 4H), 3.55 – 3.48 (m, 1H), 2.38 – 2.28 (m, 1H), 2.00 – 1.91 (m, 1H), 0.92 (d, *J* = 1.5 Hz, 9H), 0.03 (d, *J* = 5.3 Hz, 6H); **HRMS** CI+: $C_{17}H_{28}O_3SiH^+$ {$[M+H]^+$}, Calc.: 309.188, Found: 309.1892; **^{13}C NMR (500 MHz, $CDCl_3$)** δ 174.46, 138.95, 128.60, 128.07, 127.19, 60.34, 51.93, 47.60, 36.22, 25.9, 18.28, -5.43, -5.48; **IR**: 3031, 2857, 1736, 1455, 1434, 1360, 1255, 1161, 1065, 950cm^{-1}

6.3.2 Synthesis of alcohols from alkylated esters

*2-phenylbutan-1-ol (**316**)*

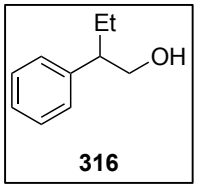

316

Under a nitrogen atmosphere, to a stirred solution of the alkylated ester **308** (1.2004 g, 6,74 mmol), dissolved in 67 mL anhydrous diethyl at 0°C, was added lithium aluminium hydride (0.7668 g, 20.2 mmol). The resultant mixture was stirred at room temperature for 2 hr. The reaction mixture was quenched with saturated sodium sulfate solution (added dropwise) until no effervescence was observed and a white precipitate formed. The mixture was filtered and the solvent of the filtrate was evaporated under reduced pressure furnishing a colourless pure oil (0.7187 g, 71%).**^{1}H NMR (500 MHz, $CDCl_3$)** δ 7.38 – 7.33 (m, 2H), 7.29 – 7.22 (m, 3H), 3.81 – 3.73 (m, 2H), 2.74 – 2.69 (m, 1H), 1.84 – 1.73 (m, 1H), 1.64 – 1.57 (m, 1H), 1.40 (br s, 1H), 0.87 (t, *J* = 7.4 Hz, 3H); **^{13}C NMR (500 MHz, $CDCl_3$)** δ 142.30, 128.62, 128.12, 126.69, 67.33, 50.51, 25.00, 11.98; **HRMS** CI+: $C_{10}H_{14}ONH_4^+$ {$[M+NH_4]^+$}, Calc.: 168.1383, Found: 168.1385; **IR**: 3339, 3028, 2961, 2929, 1494, 1453, 1378, 1034, 698cm^{-1}.

*2-phenylpentan-1-ol (**317**)*

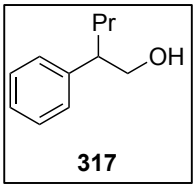

317

Under a nitrogen atmosphere, to a stirred solution of the alkylated ester **309** (1.2006 g, 6.24 mmol), dissolved in 62 mL anhydrous diethyl at 0°C, was added lithium aluminium hydride (0.7109 g, 18.73 mmol). The resultant mixture was stirred at room temperature for 3 hr. The rereaction mixture was quenched with saturated sodium sulfate solution (added dropwsie) until no effervescence was observed and a white precipitate formed. The mixture was filtered and the solvent of the filtrate was evaporated under reduced pressure furnishing a colourless pure oil (0.8334 g, 81%). **^{1}H NMR (500 MHz, $CDCl_3$)** δ 7.35 – 7.30 (m, 2H), 7.25 – 7.19 (m, 3H), 3.77 – 3.69 (m, 2H), 2.82 – 2.76 (m, 1H), 1.71 – 1.62 (m, 1H), 1.60 – 1.51 (m, 1H), 1.23 (sex, *J* = 7.4 Hz, 2H), 0.87 (t, *J* = 7.4 Hz, 3H); **^{13}C NMR (500 MHz, $CDCl_3$)** δ 142.51, 128.62, 128.08, 126.68, 67.61, 48.44, 34.28, 20.49, 14.11; **HRMS** CI+: $C_{11}H_{16}ONH_4^+$ {$[M+NH_4]^+$}, Calc.: 182.1540, Found: 182.1541; **IR**: 3334, 3028, 2929, 1493, 1453, 1379, 1050, 733cm^{-1}

*2-phenylpentan-1-ol (**318**)*

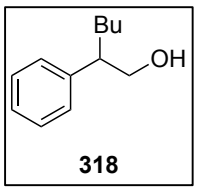

318

Under a nitrogen atmosphere, to a stirred solution of the alkylated ester **310** (1.5009 g, 7.27 mmol), dissolved in 73 mL anhydrous diethyl at 0^{o}C, was added lithium aluminium hydride (0.8284 g, 21.83 mmol). The resultant mixture was stirred at room temperature for 3 hr. The rereaction mixture was quenched with saturated sodium sulfate solution (added dropwsie) until no effervescence was observed and a white precipitate formed. The mixture was filtered and the solvent of the filtrate was evaporated under reduced pressure furnishing a colourless pure oil (1.013g, 85%).**^{1}H NMR (500 MHz, $CDCl_3$)** δ 7.38 – 7.33 (m, 2H), 7.29 – 7.22 (m, 3H), 3.82 – 3.66 (m, 2H), 2.82 – 2.77 (m, 1H), 1.76 – 1.69 (m, 1H), 1.62 – 1.56 (m, 5.4 Hz, 1H), 1.41 – 1.11 (m, 5H), 0.87 (t, *J* = 7.2 Hz, 3H); **^{13}C NMR (500 MHz, $CDCl_3$)** δ 142.57, 128.62, 128.07, 126.67, 67.64, 48.71, 31.78, 29.56, 22.75, 13.96; **HRMS** CI+: $C_{12}H_{18}ONH_4^+$ {$[M+NH_4]^+$}, Calc.: 196.1696, Found: 196.1698; **IR**: 3370, 3084, 2955, 1708, 1452, 1377, 1363, 1051cm^{-1}

*4-methyl-2-phenylpentan-1-ol (**319**)*

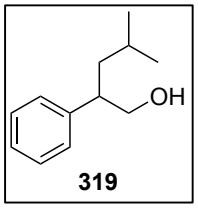

319

Under a nitrogen atmosphere, to a stirred solution of the alkylated ester **311** (1.1011 g, 5.34 mmol), dissolved in 53 mL anhydrous diethyl at 0^{o}C, was added lithium aluminium hydride (0.6077 g, 16.01 mmol). The resultant mixture was stirred at room temperature for 3 hr. The rereaction mixture was quenched with saturated sodium sulfate solution (added dropwsie) until no effervescence was observed and a white precipitate formed. The mixture was filtered and the solvent of the filtrate was evaporated under reduced pressure furnishing a colourless pure oil (1.013g, 85%).**^{1}H NMR (500 MHz, $CDCl_3$)** δ 7.40 – 7.31 (m, 2H), 7.29 – 7.21 (m, 3H), 3.78 – 3.65 (m, 2H), 2.95 – 2.87 (m, 1H), 1.64 – 1.54 (m, 1H), 1.52 – 1.36 (m, 3H), 0.89 (d, *J* = 8.3 Hz, 6H); **^{13}C NMR (500 MHz, $CDCl_3$)** δ 142.50, 128.64, 128.12, 126.68, 68.03, 46.44, 41.18, 25.27, 23.54, 21.84; **HRMS** CI+: $C_{12}H_{18}ONH_4^+$ {$[M+NH_4]^+$}, Calc.: 196.1696, Found: 196.1699; **IR**: 3354, 3044, 2937, 2772, 1488, 1446, 1389, 1088, 673cm^{-1}.

*2,3-diphenylpropan-1-ol (**320**)*

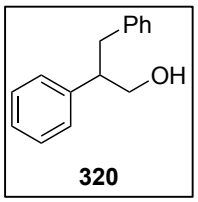

320

Under a nitrogen atmosphere, to a stirred solution of the alkylated ester **312** (1.7016 g, 7.08 mmol), dissolved in 71 mL anhydrous diethyl at 0°C, was added lithium aluminium hydride (0.8062 g, 21.24 mmol). The resultant mixture was stirred at room temperature for 1 hour. The reaction mixture was quenched with saturated sodium sulfate solution (added dropwsie) until no effervescence was observed and a white precipitate formed. The mixture was filtered and the solvent of the filtrate was evaporated under reduced pressure furnishing a colourless pure oil (1.0221 g, 68%).**^{1}H NMR (500 MHz, $CDCl_3$)** δ7.42-7.12 (M, 10H), 3.86 – 3.78 (m, 2H), 3.13 (quin, *J* = 7.4 Hz 1H), 3.06 (dd, *J* = 13.5, 7.4 Hz, 1H), 2.94 (dd, *J* = 13.5, 7.5 Hz, 1H), 1.34 (br s, 1H); **^{13}C NMR (500 MHz, $CDCl_3$)** δ 141.90, 139.91, 129.06, 128.64, 128.25, 128.10, 126.86, 126.03, 66.39, 53.44, 38.72; **HRMS** CI+: $C_{15}H_{16}ONH_4^+$ {$[M+NH_4]^+$}, Calc.: 230.1539, Found: 230.1549; IR: 3369, 3084, 2924, 1494, 1452, 1265, 1060, 1027, 696cm^{-1}.

*3-cyclohexyl-2-phenylpropan-1-ol (**321**)*

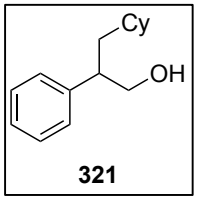

321

Under a nitrogen atmosphere, to a stirred solution of the alkylated ester **313** (1.5012 g, 6.09 mmol), dissolved in 61 mL anhydrous diethyl at 0°C, was added lithium aluminium hydride (0.6938 g, 18.28 mmol). The resultant mixture was stirred at room temperature for 16 hours. The reaction mixture was quenched with saturated sodium sulfate solution (added dropwsie) until no effervescence was observed and a white precipitate formed. The mixture was filtered and the solvent of the filtrate was evaporated under reduced pressure furnishing a colourless pure oil (0.7712g, 58%).**^{1}H NMR (500 MHz, $CDCl_3$)** δ 7.35 (t, *J* = 7.4 Hz, 2H), 7.30 – 7.20 (m, 3H), 3.79 – 3.64 (m, 2H), 2.98 – 2.92 (m, 1H), 1.81 (d, *J* = 13.1 Hz, 1H), 1.72 – 1.43 (m, 7H), 1.30 (br s, 1H), 1.23 – 1.12 (m, 4H), 0.99 – 0.81 (m, 2H); **^{13}C NMR (500 MHz, $CDCl_3$)** δ 142.64, 128.65, 128.10, 126.65, 68.08, 45.56, 39.75, 34.70, 34.18, 32.78, 26.59, 26.22, 26.11; **HRMS** CI+: $C_{15}H_{22}ONH_4^+$ {$[M+NH_4]^+$}, Calc.: 236.2009, Found: 236.2015; **IR**: 3368, 2920, 2849, 1494, 1448, 13360, 1053, 699cm^{-1}

*2-phenylpent-4-en-1-ol (**322**)*

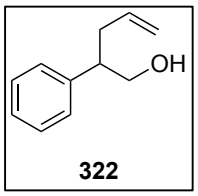

322

Under a nitrogen atmosphere, to a stirred solution of the alkylated ester **314** (1.2018 g, 6.32 mmol), dissolved in 63 mL anhydrous diethyl at 0°C, was added lithium aluminium hydride (0.7192 g, 18.95 mmol). The resultant mixture was stirred at room temperature for 1 hour. The reaction mixture was quenched with saturated sodium sulfate solution (added dropwise) until no effervescence was observed and a white precipitate formed. The mixture was filtered and the solvent of the filtrate was evaporated under reduced pressure furnishing a colourless pure oil (0.6561 g, 64%).**^{1}H NMR (500 MHz, $CDCl_3$)** δ 7.38 – 7.33 (m, 2H), 7.29 – 7.22 (m, 3H), 5.75 (dddd, *J* = 17.1, 10.1, 7.5, 6.5 Hz, 1H), 5.06 (dq, *J* = 17.1, 1.6 Hz, 1H), 4.99 (dq, *J* = 10.1, 1.6 Hz, 1H), 3.87 – 3.72 (m, 2H), 2.91 (quin, *J* = 7.1, 1H), 2.54 - 2.48 (m, 1H), 2.45 – 2.39 (m, 1H), 2.19 (br s, 1H); **^{13}C NMR (500 MHz, $CDCl_3$)** δ 141.92, 136.35, 128.63, 128.04, 126.80, 116.38, 66.92, 48.18, 36.63; **HRMS** CI+: $C_{11}H_{14}ONH_4^+$ {$[M+NH_4]^+$}, Calc.: 180.1383, Found: 180.1385; **IR**: 3362, 3077, 3063, 3028, 2917, 1601, 1493, 1442, 1053cm^{-1}

*3-methyl-2-phenylbutan-1-ol (**323**)*

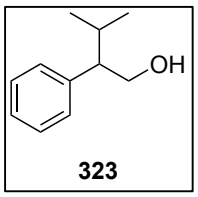

323

Under a nitrogen atmosphere, to a stirred solution of the alkylated ester **315** (1.2010 g, 6.25 mmol), dissolved in 63 mL anhydrous diethyl at 0°C, was added lithium aluminium hydride (0.7112 g, 18.74 mmol). The resultant mixture was stirred at room temperature for 2 hour. The reaction mixture was quenched with saturated sodium sulfate solution (added dropwise) until no effervescence was observed and a white precipitate formed. The mixture was filtered and the solvent of the filtrate was evaporated under reduced pressure furnishing a colourless pure oil (0.9958g, 97%).**^{1}H NMR (500 MHz, $CDCl_3$) δ** 7.38 – 7.32 (m, 2H), 7.30 – 7.20 (m, 3H), 3.96 (dd, *J* = 11.1, 4.7 Hz, 1H), 3.88 – 3.81 (m, 1H), 2.55 – 2.51 (m, 1H), 2.02 – 1.89 (m, 1H), 1.25 (br s, 1H), 1.03 (d, *J* = 6.7 Hz, 3H), 0.76 (d, *J* = 6.8 Hz, 3H); **^{13}C NMR (500 MHz, $CDCl_3$)** δ 141.68, 128.73, 128.53, 126.70, 65.23, 55.82, 30.08, 21.02, 21.00; **HRMS** CI+: $C_{11}H_{16}ONH_4^+$

{[M+NH_4]$^+$}, Calc.: 182.1539, Found: 182.1541; **IR**: 3360, 3061, 2957, 2872, 1494, 1453, 1385, 1078, 699cm^{-1}.

*4-((tert-butyldimethylsilyl)oxy)-2-phenylbutan-1-ol (**344**)*

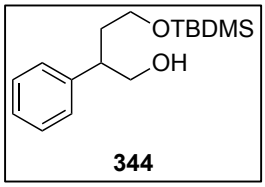

344

Compound **343** (3.4 g, 11.3 mmol) was dissolved in THF (30 mL) in 250 mL round-bottomed flask at 0°C. $NaBH_4$ (0.86 g, 22.6 mmol), LiCl (0.96 g, 22.6 mmol) and ethanol (20 mL) was then added. The reaction mixture was stirred for 23 hours at room temperature. The solvent mixture was evaporated in vacuo and the product was extracted with CH_2Cl_2 and water. Organic layer was dried with $MgSO_4$ and evaporated *in vacuo*. The crude product was purified by flash column chromatography (70:30 hexane: diethyl ether) to provide a colourless oil (2.5 g, 80%).**^{1}H NMR (500 MHz, $CDCl_3$) δ** 7.34 – 7.29 (m, 2H), 7.27 – 7.19 (m, 3H), 3.80 – 3.71 (m, 2H), 3.70 – 3.64 (m, 1H), 3.58 – 3.51 (m, 1H), 2.96 (quin, *J* = 6.9 Hz, 1H), 2.35 (s, 1H), 2.02 – 1.91 (m, 1H), 1.90 – 1.80 (m, 1H), 0.89 (s, 9H), 0.03 (d, *J* = 3.8 Hz, 6H); **^{13}C NMR (500 MHz, $CDCl_3$)** δ 142.72, 128.62, 127.89, 126.67, 68.15, 61.48, 47.26, 38.32, 25.92, 18.28, -5.71, -5.43; **HRMS** CI+: $C_{16}H_{28}O_2SiNH_4^+$ {[M+NH_4]$^+$}, Calc.: 298.2197, Found: 298.2199; **IR**: 3384, 3029, 2857, 1471, 1253, 1081, 1043, 832cm^{-1}.

6.3.3 Synthesis of aldehydes from alcohols.

*2-phenylbutanal (**324**)*

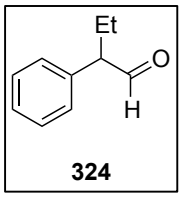

324

Under a nitrogen atmosphere, oxalyl chloride (0.21 mL, 2.54mmol) in dichloromethane 21m at -78^{o}C, was added dropwise DMSO (0.36 mL, 5.08mmol) dissolved in a little dichloromethane. The resultant mixture was left for 15 minutes at -78^{o}C. Subsequently the alcohol **316** (0.3184 g, 2.11 mmol) dissolved in a little dichloromethane was added dropwise to the reaction mixture and left sit for 45 minutes at -78^{o}C. Triethylamine (1.48 mL, 10.6mmol) was then added and the reaction brought to room temperature and left for 4 hours. The reaction mixture was quenched with

saturated ammonium chloride solution. The mixture was then extracted with dichloromethane three times. The combined organic extracts were washed with water three times and once with brine. The organic layer was then dried with anhydrous magnesium sulphate, filtered and concentrated in vacuo to provide the crude product. After flash chromatography (95:5 hexane: diethyl ether), the product was isolated as a colourless oil (0.1845 g, 59%) **^{1}H NMR (500 MHz, $CDCl_3$)** δ 9.71 (d, *J* = 2.1 Hz, 1H), 7.40 (t, *J* = 7.3Hz, 2H), 7.35 – 7.30 (m, 1H), 7.24 – 7.20 (m, 2H), 3.43 (ddd, *J* = 8.4, 6.6, 2.1 Hz, 1H), 2.14 (ddd, *J* = 14.1, 7.4, 6.6 Hz, 1H), 1.79 (ddd, *J* = 14.1, 7.4, 6.6 Hz, 1H), 0.93 (t, *J* = 7.4 Hz, 3H); **^{13}C NMR (500 MHz, $CDCl_3$)** δ 201.03, 136.30, 129.01, 128.83, 127.53, 60.88, 22.95, 11.72; **HRMS** CI+: $C_{10}H_{12}OH^+$ {$[M+H]^+$}, Calc.: 149.0961, Found: 149.0961; IR: 3084, 2965, 2815, 2714, 1720, 1492, 1453, 756cm^{-1}.

*2-phenylpentanal (**325**)*

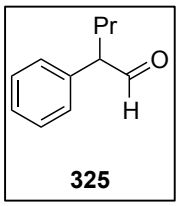

325

Under a nitrogen atmosphere, oxalyl chloride (0.25 mL, 2.93mmol) in dichloromethane 29 mL at -78^{o}C, was added dropwise DMSO (0.42 ml, 5.88mmol) dissolved in a little dichloromethane. The resultant mixture was left for 15 minutes at -78^{o}C. Subsequently the alcohol **317** (0.4014 g, 2.44 mmol) dissolved in a little dichloromethane was added dropwise to the reaction mixture and left sit for 45 minutes at -78^{o}C. Triethylamine (1.71 mL, 12.22 mmol) was then added and the reaction brought to room temperature and left for 3 hours. The reaction mixture was quenched with saturated ammonium chloride solution. The mixture was then extracted with dichloromethane three times. The combined organic extracts were washed with water three times and once with brine. The organic layer was then dried with anhydrous magnesium sulphate, filtered and concentrated in vacuo to provide the crude product. After flash chromatography (95:5 hexane: diethyl ether), the product was isolated as a colourless oil (0.2691g, 68%) **^{1}H NMR (500 MHz, $CDCl_3$)** δ 9.70 (d, *J* = 2.1 Hz, 1H), 7.44 – 7.36 (m, 2H), 7.35 – 7.29 (m, 1H), 7.25 – 7.19 (m, 2H), 3.53 (ddd, *J* = 8.4, 6.5, 2.1 Hz, 1H), 2.12 – 2.02 (m, 1H), 1.81 – 1.70 (m, 1H), 1.32 (sex, *J* = 7.4 Hz, 2H), 0.94 (t, *J* = 7.4 Hz, 3H); **^{13}C NMR (500**

MHz, $CDCl_3$) δ 201.06, 136.50, 129.01, 128.79, 127.50, 58.96, 31.79, 20.27, 13.91; **HRMS** CI+: $C_{11}H_{14}OH^+$ {$[M+H]^+$}, Calc.: 163.1117, Found: 163.1122; **IR**: 3063, 2958, 2814, 2714, 1721, 1493, 1454, 1380, 1082cm^{-1}.

*2-phenylhexanal (**326**)*

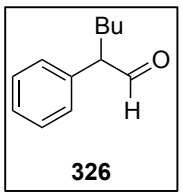

326

Under a nitrogen atmosphere, oxalyl chloride (0.40 mL, 4.71mmol) in dichloromethane 39 mL at -78°C, was added dropwise DMSO (0.67 ml, 9.43 mmol) dissolved in a little dichloromethane. The resultant mixture was left for 15 minutes at -78°C. Subsequently the alcohol **318** (0.7002 g, 3.93mmol) dissolved in a little dichloromethane was added dropwise to the reaction mixture and left sit for 45 minutes at -78°C. Triethylamine (2.74g, 19.64 mmol) was then added and the reaction brought to room temperature and left for 3 hours. The reaction mixture was quenched with saturated ammonium chloride solution. The mixture was then extracted with dichloromethane three times. The combined organic extracts were washed with water three times and once with brine. The organic layer was then dried with anhydrous magnesium sulphate, filtered and concentrated in vacuo to provide the crude product. After flash chromatography (96:4 hexane:diethyl ether), the product was isolated as a colourless oil (0.4291 g, 62%) **^{1}H NMR (500 MHz, $CDCl_3$)** δ 9.70 (s, 1H), 7.40 (t, *J* = 7.5 Hz, 2H), 7.33 (t, *J* = 7.5 Hz, 1H), 7.22 (d, *J* = 7.5 Hz, 2H), 3.51 (t, *J* = 7.5 Hz, 1H), 2.14 – 2.06 (m, 1H), 1.82 – 1.70 (m, 1H), 1.40 – 1.23 (m, 4H), 0.90 (t, *J* = 7.1 Hz, 4H); **^{13}C NMR (500 MHz, $CDCl_3$)** δ 201.05, 136.54, 129.01, 128.78, 127.49, 59.21, 29.41, 29.25, 22.55, 13.86; **HRMS** CI+: $C_{12}H_{16}ONH_4^+$ {$[M+NH_4]^+$}, Calc.: 194.1539, Found: 194.1543; **IR**: 3062, 2930, 2813, 2712, 1721, 1492, 1453, 1379, 1075cm^{-1}.

*4-methyl-2-phenylpentanal (**327**)*

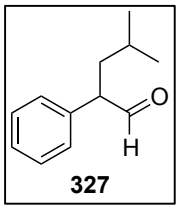

327

Under a nitrogen atmosphere, oxalyl chloride (0.18 mL, 2.09mmol) in dichloromethane 21 mL at -78°C, was added dropwise DMSO (0.3 mL, 4.17 mmol) dissolved in a little dichloromethane. The resultant mixture was left for 15 minutes at -78°C. Subsequently the alcohol **319** (0.3100 g, 1.74 mmol) dissolved in a little dichloromethane was added dropwise to the reaction mixture and left sit for 45 minutes at -78°C. Triethylamine (1.21 mL, 8.70 mmol) was then added and the reaction brought to room temperature and left for 4 hours. The reaction mixture was quenched with saturated ammonium chloride solution. The mixture was then extracted with dichloromethane three times. The combined organic extracts were washed with water three times and once with brine. The organic layer was then dried with anhydrous magnesium sulphate, filtered and concentrated in vacuo to provide the crude product. After flash chromatography (96:4 hexane:diethyl ether), the product was isolated as a colourless oil (0.2024 g, 66%) **^{1}H NMR (500 MHz, $CDCl_3$)** δ 9.69 (s, 1H), 7.40 (t, *J* = 7.8 Hz, 2H), 7.34-7.29 (m, 1H), 7.23 (d, *J* = 7.8 Hz, 2H), 3.63 (t, *J* = 7.5 Hz, 1H), 1.97 – 1.90 (m, 1H), 1.77-1.65 (m, 1H), 1.51 (sept, *J* = 6.9 Hz, 1H), 0.96 – 0.91 (m, 6H); **^{13}C NMR (500 MHz, $CDCl_3$)** δ 201.08, 136.52, 129.04, 128.80, 127.51, 57.25, 38.53, 25.33, 23.02, 21.96; **HRMS** CI+: $C_{13}H_{16}ONH_4^+$ {$[M+NH_4]^+$}, Calc.: 194.1539, Found: 194.1543; **IR**: 3063, 2956, 2812, 2713, 1721, 1492, 1467, 1367, 1074, 756cm^{-1}.

2,3-diphenylpropanal (**328**)

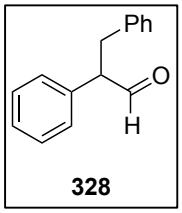

328

Under a nitrogen atmosphere, oxalyl chloride (0.29 mL, 3.4mmol) in dichloromethane 34 mL at -78°C, was added dropwise DMSO (0.31 mL, 4.41mmol) dissolved in a little dichloromethane. The resultant mixture was left for 15 minutes at -78°C. Subsequently the alcohol **320** (0.6012 g, 2.83 mmol) dissolved in a little dichloromethane was added dropwise to the reaction mixture and left sit for 45 minutes at -78°C. Triethylamine (0.31 mL, 3.4 mmol) was then added and the reaction brought to room temperature and left for 4 hours. The reaction mixture was quenched

with saturated ammonium chloride solution. The mixture was then extracted with dichloromethane three times. The combined organic extracts were washed with water three times and once with brine. The organic layer was then dried with anhydrous magnesium sulphate, filtered and concentrated in vacuo to provide the crude product. After flash chromatography (96:4 hexane:diethyl ether), the product was isolated as a colourless oil (0.2569g, 54%) **^{1}H NMR (500 MHz, $CDCl_3$) δ** 9.78 (s, 1H), 7.40 – 7.34 (m, 2H), 7.34 – 7.29 (m, 1H), 7.25 – 7.22 (m, 2H), 7.21 – 7.14 (m, 3H), 7.10 – 7.06 (m, 2H), 3.86 (t, *J* = 7.4 Hz, 1H), 3.50 (dd, *J* = 14.0, 7.4 Hz, 1H), 3.00 (dd, *J* = 14.0, 7.4 Hz, 1H); **^{13}C NMR (500 MHz, $CDCl_3$)** δ 199.93, 138.81, 135.73, 129.05, 128.36, 128.31, 128.15, 127.71, 126.33, 60.97, 36.18; **HRMS** CI+: $C_{15}H_{14}ONH_4^+$ {$[M+NH_4]^+$}, Calc.: 228.1383, Found: 228.1391; **IR**: 3085, 2817, 2716, 1719, 1493, 1452, 1029cm^{-1}.

*3-cyclohexyl-2-phenylpropanal (**329**)*

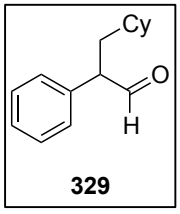

329

Under a nitrogen atmosphere, oxalyl chloride (0.19 mL, 2.2 mmol) in dichloromethane 18.4 mL at -78^{o}C, was added dropwise DMSO (0.31ml, 4.41mmol) dissolved in a little dichloromethane. The resultant mixture was left for 15 minutes at -78^{o}C. Subsequently the alcohol **321** (0.4016 g, 1.84 mmol) dissolved in a little dichloromethane was added dropwise to the reaction mixture and left sit for 45 minutes at -78^{o}C. Triethylamine (1.28 mL, 9.20 mmol) was then added and the reaction brought to room temperature and left for 4 hours. The reaction mixture was quenched with saturated ammonium chloride solution. The mixture was then extracted with dichloromethane three times. The combined organic extracts were washed with water three times and once with brine. The organic layer was then dried with anhydrous magnesium sulphate, filtered and concentrated in vacuo to provide the crude product. After flash chromatography (96:4 hexane:diethyl ether), the product was isolated as a colourless oil (0.2569g, 54%) **^{1}H NMR (500 MHz, $CDCl_3$)** δ 9.68 (s, 1H), 7.40 (t, *J* = 7.4 Hz, 2H), 7.32 (d, *J* = 7.4 Hz, 1H), 7.22 (d, *J* = 7.4 Hz, 2H), 3.66 (t, *J* = 7.1 Hz, 1H), 1.96 (p, *J* = 7.1 Hz, 1H), 1.79 (d, *J* = 13.0 Hz, 1H), 1.74 – 1.60 (m, 6H), 1.24 – 1.14 (m, 4H), 1.01 – 0.87 (m, 2H); **^{13}C**

NMR (500 MHz, $CDCl_3$) δ 201.20, 136.66, 129.04, 128.78, 127.47, 56.48, 37.14, 34.71, 33.69, 32.81, 26.46, 26.12, 26.05; **HRMS** CI+: $C_{15}H_{20}ONH_4^+$ {$[M+NH_4]^+$}, Calc.: 234.1853, Found: 234.1862; **IR**: 3061, 2920, 2709, 1721, 1492, 1448, 1074, 891cm^{-1}.

*2-phenylpent-4-enal (**330**)*

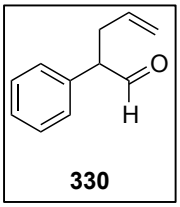

330

Under a nitrogen atmosphere, oxalyl chloride (0.4001g, 2.47mmol) in dichloromethane 30 mL at -78°C, was added dropwise DMSO (0.42 mL, 5.92mmol) dissolved in a little dichloromethane. The resultant mixture was left for 15 minutes at -78°C. Subsequently the alcohol **322** (0.4001g, 2.47 mmol) dissolved in a little dichloromethane was added dropwise to the reaction mixture and left sit for 45 minutes at -78°C. Triethylamine (1.72 ml, 12.33 mmol) was then added and the reaction brought to room temperature and left for 4 hours. The reaction mixture was quenched with saturated ammonium chloride solution. The mixture was then extracted with dichloromethane three times. The combined organic extracts were washed with water three times and once with brine. The organic layer was then dried with anhydrous magnesium sulphate, filtered and concentrated in vacuo to provide the crude product. After flash chromatography (95:5 hexane:diethyl ether), the product was isolated as a colourless oil (0.2451 g, 62%) **^{1}H NMR (500 MHz, $CDCl_3$)** δ 9.72 (d, *J* = 1.8 Hz, 1H), 7.43 – 7.38 (m, 2H), 7.35 – 7.31 (m, 1H), 7.24 – 7.20 (m, 2H), 5.74 (ddt, *J* = 17.1, 10.1, 6.9 Hz, 1H), 5.08 (dq, *J* = 17.1, 1.5 Hz, 1H), 5.03 (dq, *J* = 10.1, 1.5 Hz, 1H), 3.64 (ddd, *J* = 8.2, 7.0, 1.8 Hz, 1H), 2.92 – 2.83 (m, 1H), 2.53 (m, 1H); **^{13}C NMR (500 MHz, $CDCl_3$)** δ 200.14, 135.71, 134.87, 129.07, 128.88, 127.68, 117.18, 58.76, 33.97; **HRMS** CI+: $C_{10}H_{12}ONH_4^+$ {$[M+NH_4]^+$}, Calc.: 178.1226, Found: 178.1226; **IR**: 3079, 2979, 2817, 2717, 1721, 1492, 915cm^{-1}

*3-methyl-2-phenylbutanal (**331**)*

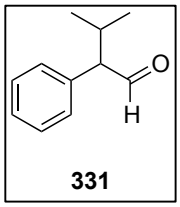

331

Under a nitrogen atmosphere, oxalyl chloride (0.19 mL, 2.19 mmol) in dichloromethane 13 mL at -78°C, was added dropwise DMSO (0.31 mL, 4.39 mmol) dissolved in a little dichloromethane. The resultant mixture was left for 15 minutes at -78°C. Subsequently the alcohol **323** (0.3000 g, 1.33 mmol) dissolved in a little dichloromethane was added dropwise to the reaction mixture and left sit for 45 minutes at -78°C. Triethylamine (1.28 mL, 9.14 mmol) was then added and the reaction brought to room temperature and left for 4 hours. The reaction mixture was quenched with saturated ammonium chloride solution. The mixture was then extracted with dichloromethane three times. The combined organic extracts were washed with water three times and once with brine. The organic layer was then dried with anhydrous magnesium sulphate, filtered and concentrated in vacuo to provide the crude product. After flash chromatography (96:4 hexane:diethyl ether), the product was isolated as a colourless oil (0.1597 g, 74%) **^{1}H NMR (500 MHz, $CDCl_3$)** δ 9.73 (s, 1H), 7.39 (t, *J* = 7.358 Hz, 2H), 7.32 (t, *J* = 7.35 Hz, 1H), 7.21 (d, *J* = 7.35 Hz, 2H), 3.21 (d, *J* = 9.7 Hz, 1H), 2.48 – 2.41 (m, 1H), 1.07 (d, *J* = 6.7, 3H), 0.80 (d, *J* = 6.9, 3H); **^{13}C NMR (500 MHz, $CDCl_3$)** δ 201.13, 135.50, 129.32, 128.90, 127.47, 66.86, 28.80, 21.19, 20.05; **HRMS** CI+: $C_{11}H_{14}ONH_4^+$ {$[M+NH_4]^+$}, Calc.: 180.1383, Found: 180.1385; **IR**: 3082, 2960, 2711, 1721, 1491, 1466, 1388, 1046cm^{-1}.

*4-((tert-butyldimethylsilyl)oxy)-2-phenylbutanal (**345**)*

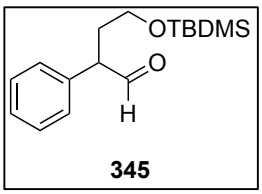

345

Under a nitrogen atmosphere, oxalyl chloride (0.7 mL, 8.16 mmol) in dichloromethane 60 mL at -78°C, was added dropwise DMSO (1.08 mL, 15.3 mmol) dissolved in a little dichloromethane. The resultant mixture was left for 15 minutes at -78°C. Subsequently the alcohol **344** (1.42 g, 5.1 mmol) dissolved in a little dichloromethane was added dropwise to the reaction mixture and left sit for 45 minutes at -78°C. Triethylamine (12.8 mL, 51 mmol) was then added and the reaction

brought to room temperature and left for 4 hours. The reaction mixture was quenched with saturated ammonium chloride solution. The mixture was then extracted with dichloromethane three times. The combined organic extracts were washed with water three times and once with brine. The organic layer was then dried with anhydrous magnesium sulphate, filtered and concentrated in vacuo to provide the crude product. After flash chromatography (96:4 hexane:diethyl ether), the product was isolated as a colourless oil (0.7091 g, 50%) **^{1}H NMR (500 MHz, $CDCl_3$)** δ 9.71 (s, 1H), 7.39 – 7.34 (m, 2H), 7.32 – 7.27 (m, 1H), 7.22 – 7.18 (m, 2H), 3.81 – 3.75 (m, 1H), 3.69 – 3.63 (m, 1H), 3.54 – 3.47 (m, 1H), 2.40 – 2.31 (m, 1H), 1.92 – 1.84 (m, 1H), 0.89 (s, 9H), 0.03 (d, *J* = 3.8 Hz, 6H); **^{13}C NMR (500 MHz, $CDCl_3$)** δ 200.78, 136.12, 129.01, 127.54, 60.06, 55.63, 32.90, 25.90, 18.25, -5.44, -5.45; **HRMS** CI+: $C_{16}H_{26}O_2SiNH_4^+$ {$[M+NH_4]^+$}, Calc.: 296.2041, Found: 2096.2044; **IR**: 2924, 2855, 1731, 1462, 1388, 1287, 1118, 1073cm^{-1}.

6.3.4 Synthesis of Carboxylic acids

*2-phenylbutanoic acid (**332**)*

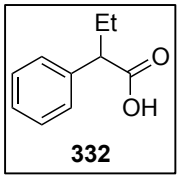

332

To a stirred solution of the alkylated ester **308** (200.7 mg, 1.13 mmol) dissolved in THF (4 mL), was added 2 M aqueous sodium hydroxide (4 mL, 8 mmol). The resultant reaction mixture was heated under reflux at 80^{o}C overnight. Diethyl ether was added and the aqueous layer removed. The aqueous layer was acidified with 2 M hydrochloric acid until a cloudy solution formed. The reaction mixture was then extracted with diethyl ether (3x10 mL). The organic extracts were then dried over magnesium sulphate, filtered and concentrated *in vacuo* to furnish a white crystalline solid (128.9 mg, 64%).). **^{1}H NMR (500 MHz, $CDCl_3$)** δ 11.55 (br s, 1H), 7.38 – 7.27 (m, 5H), 3.49 (t, *J* = 7.7 Hz, 1H), 2.16 – 2.09 (m, 1H), 1.89 – 1.81 (m, 1H), 0.94 (t, *J* = 7.3 Hz, 3H); **^{13}C NMR (500 MHz, $CDCl_3$)** δ 180.05, 138.37, 128.63, 128.09, 127.43, 53.30, 26.30, 12.10; **HRMS** CI+: $C_{10}H_{12}O_2NH_4^+$ {$[M+NH_4]^+$}, Calc.: 182.1176, Found: 182.1181; **IR**: 3058, 2964, 2608, 1714, 1454, 1415, 1308, 1283, 1220, 937cm^{-1}.

*2-phenylpentanoic acid (**333**)*

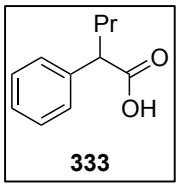

333

To a stirred solution of the alkylated ester **309** (211.1 mg, 1.10 mmol) dissolved in THF (4 mL), was added 2 M aqueous sodium hydroxide (4 mL, 8 mmol). The resultant reaction mixture was heated under reflux at 80°C overnight. Diethyl ether was added and the aqueous layer removed. The aqueous layer was acidified with 2M hydrochloric acid until a cloudy solution formed. The reaction mixture was then extracted with diethyl ether (3x10mL). The organic extracts were then dried over magnesium sulphate, filtered and concentrated *in vacuo* to furnish a white crystalline solid (128.9 mg, 64%). **^{1}H NMR (500 MHz, $CDCl_3$)** δ 11.45 (br s, 1H), 7.39 – 7.29 (m, 5H), 3.60 (t, *J* = 7.7 Hz, 1H), 2.13 – 2.05 (m, 1H), 1.86 – 1.75 (m, 1H), 1.41 – 1.23 (m, 2H), 0.95 (t, *J* = 7.3 Hz, 3H); **^{13}C NMR (500 MHz, $CDCl_3$)** δ 180.49, 138.54, 128.63, 128.08, 127.41, 51.35, 35.17, 20.67, 13.79; **HRMS** CI+: $C_{11}H_{14}O_2NH_4^+$ {$[M+NH_4]^+$}, Calc.: 196.1333, Found: 196.1332; **IR**: 3086, 2957, 2619, 1692, 1449, 1411, 1292, 1213, 948cm^{-1}.

*2-phenylhexanoic acid (**334**)*

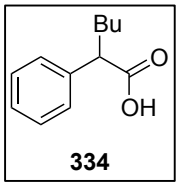

334

To a stirred solution of the alkylated ester **310** (202.3mg, 0.981 mmol) dissolved in THF (4 mL), was added 2 M aqueous sodium hydroxide (4 mL, 8 mmol). The resultant reaction mixture was heated under reflux at 80°C overnight. Diethyl ether was added and the aqueous layer removed. The aqueous layer was acidified with 2 M hydrochloric acid until a cloudy solution formed. The reaction mixture was then extracted with diethyl ether (3x10 mL). The organic extracts were then dried over magnesium sulphate, filtered and concentrated *in vacuo* to furnish a white crystalline solid (113.2g, 60%). **^{1}H NMR (500 MHz, $CDCl_3$)** δ 7.39 – 7.24 (m, 6H), 3.55 (t, *J* = 7.7 Hz, 1H), 2.06 – 2.13 (m, 1H), 1.77 – 1.84 (m, 1H), 1.42 – 1.18 (m, 4H), 0.89 (t, *J* = 7.0 Hz, 3H); **^{13}C NMR (500 MHz, $CDCl_3$)** δ 180.08, 138.64, 128.62, 128.05, 127.38, 51.60, 32.82, 29.63, 22.43, 13.85; **HRMS** CI+: $C_{12}H_{16}O_2NH_4^+$ {$[M+NH_4]^+$}, Calc.: 210.1489, Found: 210.1493; IR: 3030, 2860, 1701, 1455, 1413, 1380, 1239, 725cm^{-1}.

*4-methyl-2-phenylpentanoic acid (**335**)*

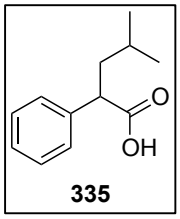

335

To a stirred solution of the alkylated ester **311** (201.9 mg, 0.979 mmol) dissolved in THF (4 mL), was added 2 M aqueous sodium hydroxide (4 mL, 8mmol). The resultant reaction mixture was heated under reflux at 80°C overnight. Diethyl ether was added and the aqueous layer removed. The aqueous layer was acidified with 2 M hydrochloric acid until a cloudy solution formed. The reaction mixture was then extracted with diethyl ether (3x10 mL). The organic extracts were then dried over magnesium sulphate, filtered and concentrated *in vacuo* to furnish a white crystalline solid (133.6 g, 71%). **^{1}H NMR (500 MHz, $CDCl_3$)** δ 7.41 – 7.26 (m, 7H), 3.71 – 3.67 (m, 1H), 1.99 (dd, *J* = 13.6, 6.6 Hz, 1H), 1.72 (dd, *J* = 13.6, 6.8 Hz, 1H), 1.59 – 1.46 (m, 1H), 0.94 (d, *J* = 6.6 Hz, 6H); **^{13}C NMR (500 MHz, $CDCl_3$)** δ 180.61, 138.60, 129.40, 128.66, 128.11, 127.42, 49.53, 42.01, 41.12, 25.77, 22.60, 22.21; **HRMS** CI+: $C_{12}H_{16}O_2NH_4^+$ {$[M+NH_4]^+$}, Calc.: 210.1489, Found: 210.1493; **IR**: 3063, 2930, 2653, 1690, 1453, 1406, 1283, 1237, 1211, 1185, 932cm^{-1}.

*2,3-diphenylpropanoic acid (**336**)*

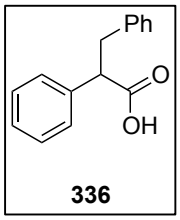

336

To a stirred solution of the alkylated ester **312** (212.0 mg, 0.882 mmol) dissolved in THF (4 mL), was added 2 M aqueous sodium hydroxide (4 mL, 8mmol). The resultant reaction mixture was heated under reflux at 80°C overnight. Diethyl ether was added and the aqueous layer removed. The aqueous layer was acidified with 2 M hydrochloric acid until a cloudy solution formed. The reaction mixture was then extracted with diethyl ether (3x10 mL). The organic extracts were then dried over magnesium sulphate, filtered and concentrated *in vacuo* to furnish a white crystalline solid (145.7mg, 73%). **^{1}H NMR (500 MHz, $CDCl_3$)** δ 7.40 – 7.27 (m, 6H), 7.27 – 7.17 (m, 3H), 7.30 – 7.10 (m, 2H), 3.89 (dd, *J* = 8.4, 7.0 Hz, 1H), 3.43 (dd, *J* = 13.9, 8.4 Hz, 1H), 3.06 (dd, *J* = 13.9, 7.0 Hz, 1H), 1.28 (s, 1H); **^{13}C NMR (500 MHz, $CDCl_3$)** δ 178.18, 138.69, 137.96, 128.91, 128.70, 128.37, 128.08, 127.61, 126.45, 53.34, 39.30; **HRMS** CI+:

$C_{15}H_{14}O_2NH_4^+$ {$[M+NH_4]^+$}, Calc.: 244.1332, Found: 244.1337; **IR**: 3162, 3029, 2926, 1720, 1493, 1451, 1399, 1251cm^{-1}.

*3-cyclohexyl-2-phenylpropanoic acid (**337**)*

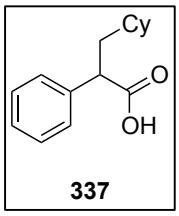

337

To a stirred solution of the alkylated ester **313** (200.6 mg, 0.818 mmol) dissolved in THF (4 mL), was added 2M aqueous sodium hydroxide (4 mL, 8mmol). The resultant reaction mixture was heated under reflux at 80^{o}C overnight. Diethyl ether was added and the aqueous layer removed. The aqueous layer was acidified with 2 M hydrochloric acid until a cloudy solution formed. The reaction mixture was then extracted with diethyl ether (3x10 mL). The organic extracts were then dried over magnesium sulphate, filtered and concentrated *in vacuo* to furnish a white crystalline solid (96.9mg, 51%). **^{1}H NMR (500 MHz, $CDCl_3$)** δ 7.37 – 7.26 (m, 5H), 3.72 (t, *J* = 7.7 Hz, 1H), 2.02 – 1.97 (m, 1H), 1.81 – 1.59 (m, 6H), 1.23 – 1.12 (m, 4H), 0.99 – 0.87 (m, 2H); **^{13}C NMR (500 MHz, $CDCl_3$)** δ 180.16, 138.78, 128.64, 128.08, 127.36, 48.67, 40.62, 35.12, 33.28, 32.93, 26.47, 26.07, 26.03; **HRMS** CI+: $C_{15}H_{20}O_2NH_4^+$ {$[M+NH_4]^+$}, Calc.: 250.1802, Found: 250.1802; **IR**: 3058, 2922, 1695, 1449, 1410, 1329, 1233, 956cm^{-1}

*2-phenylpent-4-enoic acid (**338**)*

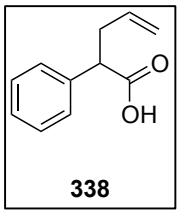

338

To a stirred solution of the alkylated ester **314** (200.3 mg, 1.05 mmol) dissolved in THF (4 mL), was added 2 M aqueous sodium hydroxide (4 mL, 8mmol). The resultant reaction mixture was heated under reflux at 80^{o}C overnight. Diethyl ether was added and the aqueous layer removed. The aqueous layer was acidified with 2 M hydrochloric acid until a cloudy solution formed. The reaction mixture was then extracted with diethyl ether (3x10 mL). The organic extracts were then dried over magnesium sulphate, filtered and concentrated *in vacuo* to furnish a white crystalline solid (131.5 mg, 71%). **^{1}H NMR (500 MHz, $CDCl_3$)** δ 10.30 (br s, 1H), 7.38 – 7.29 (m, 5H), 5.75 (ddt, *J* = 17.1, 10.2, 6.8 Hz, 1H), 5.14 – 5.00 (m, 2H), 3.68 (dd, *J* = 8.4,

7.1 Hz, 1H), 2.85 (dddt, *J* = 14.4, 8.4, 6.8, 1.2 Hz, 1H), 2.60 – 2.50 (dddt, *J* = 14.4, 7.1, 6,8, 1.2 Hz, 1H); **^{13}C NMR (500 MHz, $CDCl_3$)** δ 178.60, 137.84, 134.88, 128.71, 128.05, 127.59, 117.27, 51.21, 37.09; **HRMS** CI+: $C_{11}H_{12}O_2H^+$ {$[M+H]^+$}, Calc.: 177.091, Found: 177.0908; **IR**: 3058, 2895, 2648, 1702, 1453, 1439, 1414, 1244, 978cm^{-1}.

*3-methyl-2-phenylbutanoic acid (**339**)*

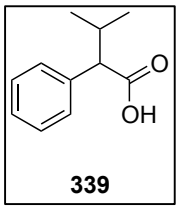

339

To a stirred solution of the alkylated ester **315** (203.1 mg, 1.06 mmol) dissolved in THF (4 mL), was added 2 M aqueous sodium hydroxide (4 mL, 8mmol). The resultant reaction mixture was heated under reflux at 80^{o}C overnight. Diethyl ether was added and the aqueous layer removed. The aqueous layer was acidified with 2 M hydrochloric acid until a cloudy solution formed. The reaction mixture was then extracted with diethyl ether (3x10 mL). The organic extracts were then dried over magnesium sulphate, filtered and concentrated *in vacuo* to furnish a white crystalline solid (187.0 mg, 99%). **^{1}H NMR (500 MHz, $CDCl_3$)** δ 10.87 (br s, 1H), 7.39 – 7.25 (m, 5H), 3.16 (d, *J* = 10.6 Hz, 1H), 2.39 – 2.32 (m,1H), 1.10 (d, *J* = 6.5 Hz, 3H), 0.73 (d, *J* = 6.7 Hz, 3H); **^{13}C NMR (500 MHz, $CDCl_3$)** δ 180.16, 137.75, 128.60, 128.53, 127.45, 60.04, 31.56, 21.46, 20.11; **HRMS** CI+: $C_{11}H_{14}O_2NH_4^+$ {$[M+NH_4]^+$}, Calc.: 196.1332, Found: 196.1339; **IR**: 3065, 2966, 2868, 1698, 1454, 1407, 1385, 1288, 1185, 965cm^{-1}.

*4-((tert-butyldimethylsilyl)oxy)-2-phenylbutanoic acid (**348**)*

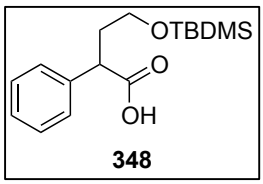

348

To a stirred solution of the alkylated ester **343** (210.6 mg, 0.68 mmol) dissolved in THF (2.4 mL), was added 0.5M aqueous lithium hydroxide (2.4 mL, 1.19 mmol) at 0^{o}C. Once the reaction was complete, diethyl ether (8 mL) was added forming a biphasic reaction mixture. The aqueous layer was then isolated and acidified with dropwsie addition of 1 M hydrochloric acid until pH 3 using a pH meter. The reaction mixture was then extracted with diethyl ether (3x10 ml). The organic extracts were then dried over magnesium sulphate filtered and concentrated *in vacuo* to furnished a pure white crystalline solid (131.9 g, 66%). **^{1}H NMR (500 MHz,**

$CDCl_3$) δ 7.37 – 7.27 (m, 5H), 3.84 (t, *J* = 7.4 Hz, 1H), 3.68 – 3.61 (m, 1H), 3.56 – 3.50 (m, 1H), 2.40 – 2.31 (m, 1H), 2.00 – 1.91 (m, 1H), 0.90 (s, 9H), 0.02 (d, *J* = 5.8 Hz, 6H); **^{13}C NMR (500 MHz, $CDCl_3$)** δ 179.42, 138.30, 128.66, 128.20, 127.42, 60.37, 47.82, 35.72, 25.91, 25.87, 18.24, -5.49, -5.51; **HRMS** CI+: $C_{16}H_{26}O_3SiNH_4^+$ {$[M+NH_4]^+$}, Calc.: 312.1990, Found: 312.1992; **IR**: 3067, 2929, 2645, 1704, 1250, 1086, 962cm^{-1}.

6.3.5 Synthesis of lactones

*3-phenyldihydrofuran-2(3H)-one (**350**)*

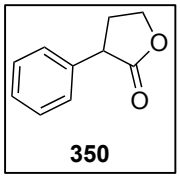
350

To a stirred solution of the alkylated ester **343** (200.9 mg, 0.68 mmol) dissolved in THF (4 mL), was added 2M aqueous sodium hydroxide (4 mL, 8mmol). The resultant reaction mixture was heated under reflux at 100^{o}C overnight. To this was added diethyl ether (8 mL) forming a biphasic reaction mixture. The aqueous layer was then isolated and acidified with 2 M hydrochloric acid until a cloudy solution formed. The reaction mixture was then extracted with diethyl ether (3x10 mL). The organic extracts were then dried over magnesium sulphate filtered and concentrated *in vacuo* to furnished a viscous brown oil (77.1 mg, 73%). **^{1}H NMR (500 MHz, $CDCl_3$)** δ 7.39 – 7.25 (m, 5H), 7.39 – 7.25 (m, 5H), 4.48 – 4.42 (m,1H), 4.36 – 4.32 (m,1H), 2.25 – 2.18 (m,1H), 2.66 – 2.58 (m,1H), 2.46 – 2.40 (m, 1H); **^{13}C NMR (500 MHz, $CDCl_3$)** δ 177.52, 136.65, 128.95, 128.11, 127.67, 66.56, 45.52, 31.58; **HRMS** CI+: $C_{10}H_{10}O_2NH_4^+$ {$[M+NH_4]^+$}, Calc.: 180.1020, Found: 180.1023; **IR**: 3031, 2920, 1743, 1485, 1444, 1426, 1234, 1175, 1155cm^{-1}.

6.3.6 Deprotection of TBDMS protected alcohols.

*4-hydroxy-2-phenylbutanoic acid (**349**)*

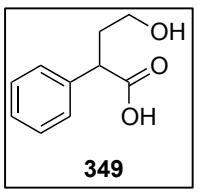
349

To a solution of acid **348** (0.1g, 0.4 mmol) dissolved in 3 mL DCM and 3 mL MeOH was added CSA (0.082g, 0.35 mmol) at -10°C and left stir for 1 hour. Saturated $NaHCO_3$ was added and the reaction extracted into DCM. The organic layer was dried with MgSO4, filtered and concentrated *in vacuo* to give a white

crystalline solid in quantitative yield. **^{1}H NMR (500 MHz, $CDCl_3$)** δ 7.37 – 7.27 (m, 5H), 3.84 (t, *J* = 7.*6Hz*), 3.7-3.65 (m,1H), 3.63-3.57 (m, 1H), 2.38(dddd, *J* = 13.89, 7.89, 7.03, 5.32*Hz)*, 2.07-1.99 (m, 1H)**. HRMS** CI+: $C_{10}H_{12}O_3NH_4^+$ {$[M+NH_4]^+$}, Calc.: 196.1030, Found: 196.1023; **IR**: 3031, 2920, 1760, 1485, 1444, 1426, 1234, 1175, 1155cm^{-1}.

*3-phenyltetrahydrofuran-2-ol (**346**)*

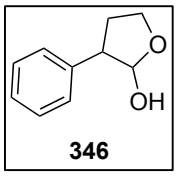

346

To a solution of **345** (0.4g, 1.4 mmol) in 10 mL THF was added 2.8 mL TBAF (1 M, 2.8 mmol) at -40°C. The reaction was left stir for 30mins. After this time the reaction was quenched with saturated solution of ammonia chloride and the reaction brought to room temperature. The reaction was extracted three times DCM and the organic layer dried with $MgSO_4$, filtered and concentrated *in vacuo* to yield a white solid (0.17 g, 75%).

^{1}H NMR (500 MHz, $CDCl_3$) δ 7.38 – 7.24 (m, 7H), 5.53 (t, J=3.8Hz, 0.3H), 5.46 (t, J = 2.64*Hz*, 1H), 4.31(td, J = 8.75, 2.48 Hz, 0.3H), 4.27-4.19 (m, 1H), 4.15 (td, J = 8.1, 5.0 Hz, 1H), 4.02 (dq, J = 8.0, 1.0 Hz, 0.3H), 3.39 (dd, J = 7.7, 4.5 Hz, 0.3H), 3.36 (td, J = 8.23, 2.32 Hz, 1H), 2.76(bs, 1H), 2.58-2.44 (m, 1.3H), 2.32-2.24 (m, 0.3H), 2.07 (m, 1H) **^{13}C NMR (500 MHz, $CDCl_3$)** δ 141.8, 128.8, 128.6, 128.4, 127.25, 127.04, 126.69. 104.0, 98.5, 67.5, 52.2, 32.8. **HRMS** CI^+: $C_{10}H_{12}O_2NH4^+$$\{[M+NH4^+]\}$, Calc: 180.2104, Found: 180.2101

Initial PaoABC catalysed oxidation of α-substituted aldehydes

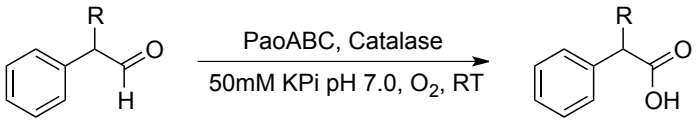

324-331 **323-339**

3μL of of a 1M stock solution of compound **324-331** and 33 μL catalase (3.3 mg/mL) was added to 50mM KPi-buffer pH 7.5. 2 μL of PaoABC(13.2mg/mL) was then added. Final concentration 300 μL. The reaction was then placed in a shaking incubator and incubated at room temperature for 2 hours. 50 μL of 1M NaOH was then added with 300 μL of DCM. The organic layer was extracted and concentrated in vacuo. The solid was then re-suspended in 300μL of a 10% IPA : 90% hexane solution and analysed by normal phase HPLC. HPLC conditions: chiracell AD-H column 95:5 hex:IPA, flowrate = 1mL/min. Conversions adjusted by the comparison of a 1:1 NMR authenticated standard of aldehyde and acid.

E value of α-substituted aldehydes and time course analysis

3 μL of of a 1 M stock solution of compound **324-331** and 33 μL catalase (3.3 mg/mL) was added to 50 mM KPi-buffer pH 7.5. 2 μL of PaoABC(13.2mg/mL) was then added. Final concentration 300 μL. The reaction was then placed in a shaking incubator and incubated at room temperature. The reaction was then closely monitored by normal HPLC. For each alqiquot, 20μL of the reaction was extracted. 20 μL of 1 M NaOH and 300 μL DCM was then added. The organic layer was extracted and concentrated *in vacuo*. The solid was then re-suspended in 100 μL of a 10% IPA : 90% hexane solution and analysed by normal phase HPLC. HPLC conditions: chiracell AD-H column 95:5 hex:IPA, flowrate = 1mL/min. Conversions adjusted by the comparison of a 1:1 NMR authenticated standard of aldehyde and acid. E value then calculated via equation 1.

pH affect on the E value associated with the oxidation of 331 with PaoABC

3 µL of of a 1M stock solution of compound **331** and 33 µL catalase (3.3 mg/mL) was added to added to buffers listed in Table 12 (50 mM). 2 µL of PaoABC (13.2 mg/mL) was then added. Final concentration 300 µL. The reaction was then placed in a shaking incubator and incubated at room temperature. The reaction was closely monitored by normal HPLC. For each alqiquot, 20 µL of the reaction was extracted. 20 µL of 1 M NaOH and 300 µL DCM was then added. The organic layer was extracted and concentrated *in vacuo*. The solid was then re-suspended in 100 µL of a 10% IPA : 90% hexane solution and analysed by normal phase HPLC. HPLC conditions: chiracell AD-H column 95:5 hex:IPA, flowrate = 1mL/min. Conversions adjusted by the comparison of a 1:1 NMR authenticated standard of aldehyde and acid. E value then calculated via equation 1.

6.4 Experimental procedures for Chapter 4

6.4.1 Synthesis of amino alcohol substrates.

*Synthesis of (2-(2-aminoethyl)phenyl)methanol (**358**)*

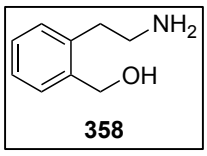

358

Methyl 2-(cyanomethyl)benzoate (**360**) (3 g, 17.1 mmol) in Et_2O (30 mL) was added dropwise to a stirred solution of $AlCl_3$ / $LiAlH_4$ [$AlCl_3$ (5 g, 37.6 mmol, 2.2 eq) in THF (60 mL) was added to a suspension of $LiAlH_4$ (1.4 g, 37.6 mmol, 2.2 equiv) in THF (36 mL)]. This combined suspension was then left to stir overnight at room temperature and quenched with a mixture of water (26 mL) and H_2SO_4 (52 mL, 3 M). The resulting solution was extracted with Et_2O (3 x 80 mL), the aqueous phase was then basified to pH ~12 by addition of solid KOH. After further dilution with H_2O (120 mL) the aqueous phase was further extracted with EtOAc (5 x 120 mL). The 5 new extracts were combined and dried over Na_2SO_4 before evaporating to yield the crude product as a dark brown oil. Purification via FCC on deactivated silica (1% Et_3N) (10 % MeOH/DCM) to yield a pale solid (1.6 g, 62 %). NMR ^1H (400 MHz, $CDCl_3$) δ 7.33-7.19 (m, 4H) 4.59 (s, 2H), 3.05 (br s, 2H), 2.99 (t, J = 4.6 *Hz*, 2H), 2.85 (t, J = 6.1*Hz*, 2H). ^{13}C NMR (100 MHz, $CDCl_3$) δ

140.43, 138.87, 130.04, 129.84, 128.39, 126.64, 62.87, 53.45, 34.85, HRMS CI+: $C_9H_{13}ON$ H^+ {$[M+H]^+$} Calc. 152.107, Found. 152.1072.

*3-amino-2-phenylpropan-1-ol (**368**)*

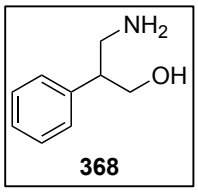

368

Ethyl 2-cyano-2-phenylacetate (1 g, 5.2 mmol) in Et_2O (10 mL) was added dropwise to a stirred solution of $AlCl_3$ / $LiAlH_4$ [$AlCl_3$ (1.6g, 12.5 mmol, 2.2 eq) in THF (20 mL) was added to a suspension of $LiAlH_4$ (0.46g, 12.5 mmol, 2.2 equiv) in THF (12 mL)]. This combined suspension was then left to stir overnight at room temperature and quenched with a mixture of water (26 mL) and H_2SO_4 (52 mL, 3 M). The resulting solution was extracted with Et_2O (3 x 80 mL), the aqueous phase was then basified to pH ~12 by addition of solid KOH. After further dilution with H_2O (120 mL) the aqueous phase was further extracted with EtOAc (5 x 120 mL). The 5 new extracts were combined and dried over Na_2SO_4 before evaporating to yield the crude product as a dark brown oil. Purification via FCC on deactivated silica (1% Et_3N) (10 % MeOH/DCM) to yield a yellow oil (0.1g, 18%). NMR ^1H (500 MHz, DMSO-d_6) δ 7.32-7.26 (m, 2H), 7.23-7.17 (m, 2H), 3.68-3.62 (m, 1H). 3.61-3.55(m, 1H), 2.94(dd, J = 11.8 *Hz*, 6.42, 1H), 2.81-2.75 (m, 1H), 2.74-2.67(m, 1H), ^{13}C NMR (100 MHz, DMSO-d_6) δ 143.2, 128.6, 128.5, 126.6, 64.9, 51.3, 45.2. HRMS CI+: $C_9H_{13}ON$ H^+ {$[M+H]^+$} Calc. 152.1004, Found.152.1062

6.4.2 Determination of response factors for 3,4-dihydroisoquinoline, 3,4-dihydroisoquinolin-1(2H)-one and (2-(2-aminoethyl)phenyl)methanol

A 1:1:1 standard mixture of DHIQ (**356**):lactam (**357**):amino alcohol (**358**) was prepared and analysed by 1H NMR. The HPLC trace of this standard was recorded to obtain a calibrated standard to take account of response factors when calculating actual conversion for lactam production. HPLC conditions: Chiracel OD-H column, 1.0 mL/min, 90% Hexane (0.1% ethanolamine):10% IPA.

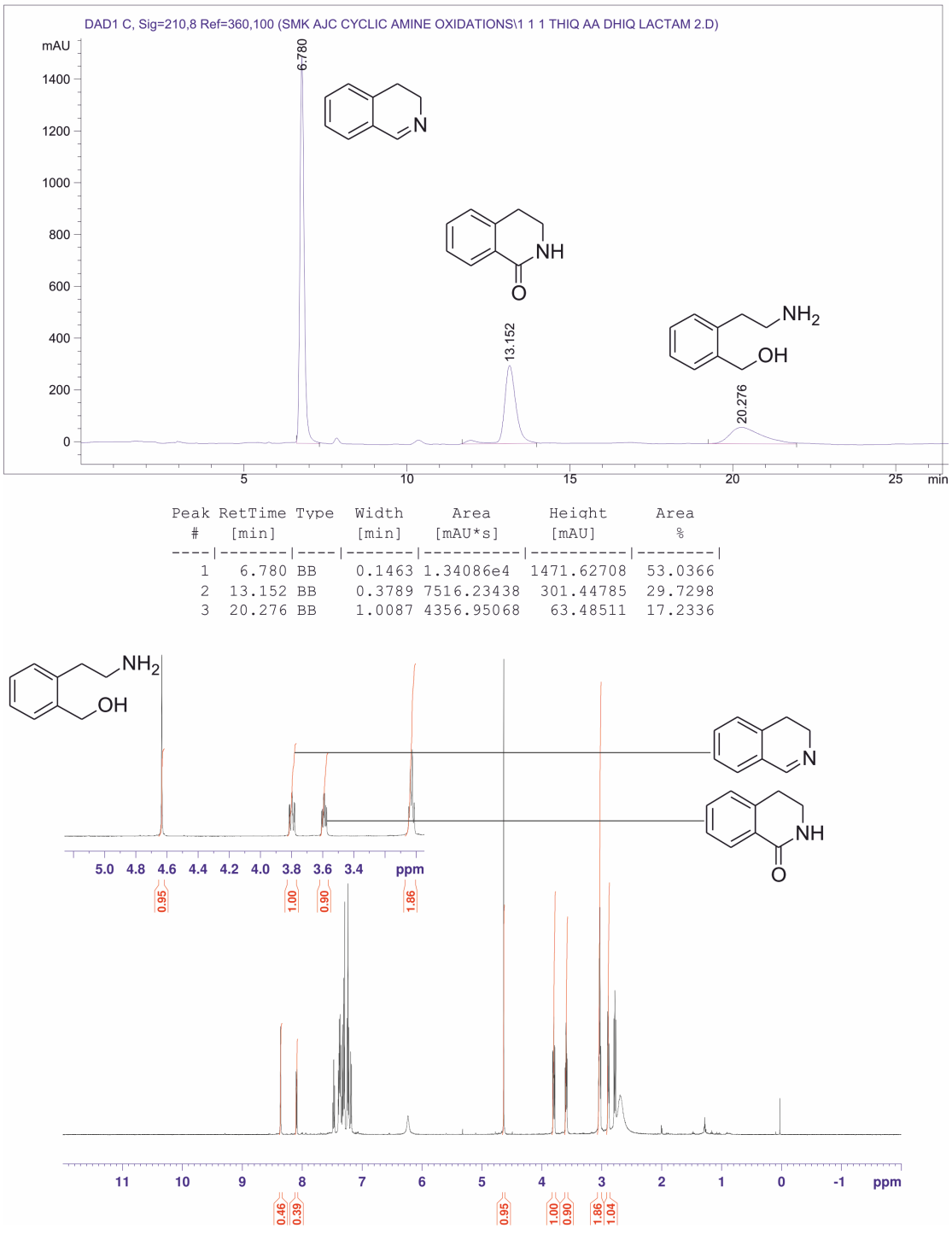

Figure 33 HPLC and ^{1}H NMR analysis of a 1:1:1 mixture of standards of DHIQ (**356**) lactam (**357**) amino alcohol (**358**).

6.4.3 Procedure and pH-screen for the GOase catalysed oxidation of (2-(2-aminoethyl)phenyl)methanol (358)

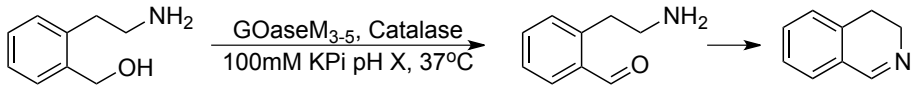

358 **359** **356**

3 µL of (2-(2-aminoethyl)phenyl)methanol (**358**) (1M in DMF) and 33 µL catalase (3.3 mg/mL) was added to 200 mM KPi-buffer. 103 µL of GOase M3-5 (3.7 mg/mL) was added to give a final volume of 300 µL. The reaction was then placed in a shaking incubator and incubated at 37°C and 250 rpm for 16h. 50 uL of 1 M NaOH was then added with 300 µL of DCM. The organic layer was extracted and concentrated in vacuo. The solid was then re-suspended in 300 µL of a 10% IPA : 90% hexane solution and analysed by normal phase HPLC. For HPLC conditions see 6.4.2. Conversion reported are based on relative response factors determined via NMR-HPLC correlations (Figure 33)

6.4.4 Procedure and pH-screen for the XDH/aldehyde oxidase catalysed oxidation of 3,4-dihydroisoquinoline (357)

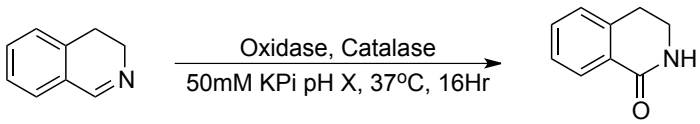

356 **357**

3 µL of a DHIQ **356** (1M in DMF) and 33 µL catalase (3.3mg/mL) was added to 200mM potassium phosphate buffer. 5 µl of *E.coli* PaoABC (13.3mg/mL) or 50 µL of *E.coli* XDH (1.1mg/mL) was added to a final volume of 300 µL. The reaction was then placed in a shaking incubator and left for 16h. 300 µL of DCM was then added and the organic layer extracted and concentrated in vacuo. The solid was then re-suspended in 300 µL of a 10% IPA:90% hexane solution and analysed by normal phase HPLC. For HPLC conditions see 6.4.2. . Conversion reported are based on relative response factors determined via NMR-HPLC correlations (Figure 33)

6.4.5 Procedure for GOase-XDH cascade reactions for the synthesis of 3,4-dihydroisoquinolin-1(2H)-one (357).

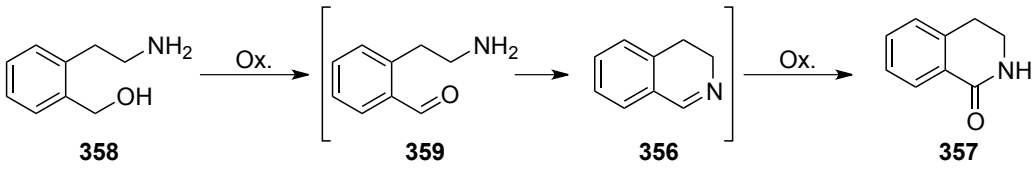

358 **359** **356** **357**

3 µL of (2-(2-aminoethyl)phenyl)methanol **358** (1M in DMF) and 33 µL catalase (3.3 mg/mL) was added to 200 mM KPi-buffer (pH 7.0) with 103 µL of GOase $M_{3\text{-}5}$ (3mg/mL) and 50 µL XDH (1.1 mg/mL) to a final volume of 300 µL. The reaction was then placed in a shaking incubator and incubated at 37°C and 250 rpm for 16h. 50 µL of 1M NaOH was then added and the mixture extracted with 300 uL of DCM. The organic layer was separated and concentrated in *vacuo*. The solid was then re-suspended in 300 µL of a 10% IPA : 90% hexane solution and analysed by normal phase HPLC. The conversion to the lactam was 69%. Conversion reported are based on relative response factors determined via NMR-HPLC correlations (Figure 33).

6.4.6 Calibration curves of 2-pyrrolidone and valerolactam

6.4.6.1 2-pyrrolidone (**365**)

Solutions of 2-pyrrolidone (**365**) were prepared in triplicate and analysed by RP-HPLC. A calibration curve was then produced using the average of each molarity. HPLC conditions: Thermofisher ODS Hypersil C-18 column, flow-rate 1.0 mL/min, 15% MeCN : 85% H_2O (0.1% TFA).

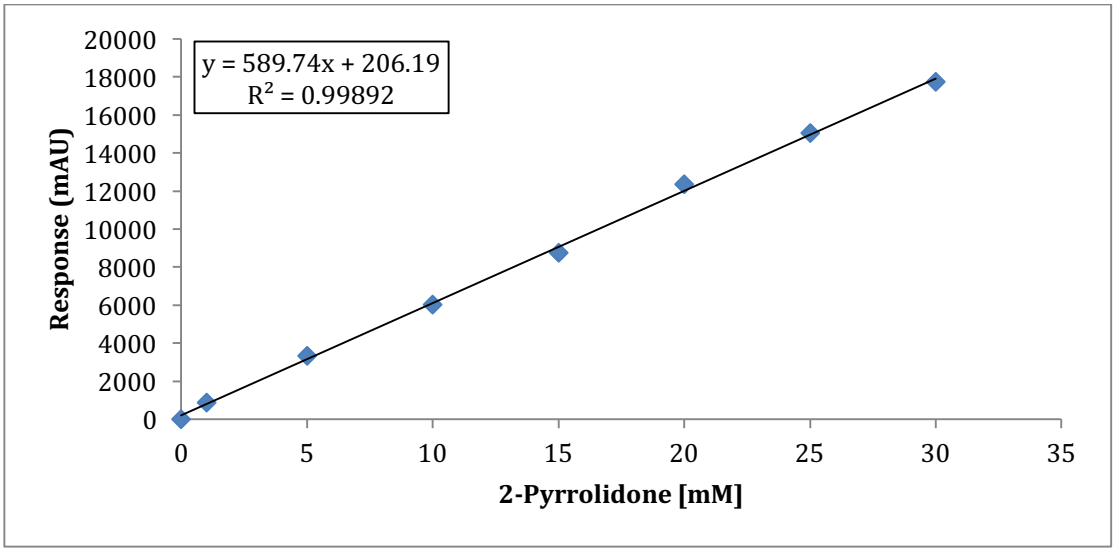

Figure 34 Calibration curve for 2-pyrrolidone (**365**) used for the determination of product concentrations in reactions with **362**.

6.4.6.2 Valerolactam (**366**)

Solutions of valerolactam (**366**) were prepared in triplicate and analysed by RP-HPLC. A calibration curve was then produced using the average of each molarity. HPLC conditions: Thermofisher ODS Hypersil C-18 column, flow-rate 1.0 mL/min, 10% MeOH : 90% H_2O (0.1% TFA)

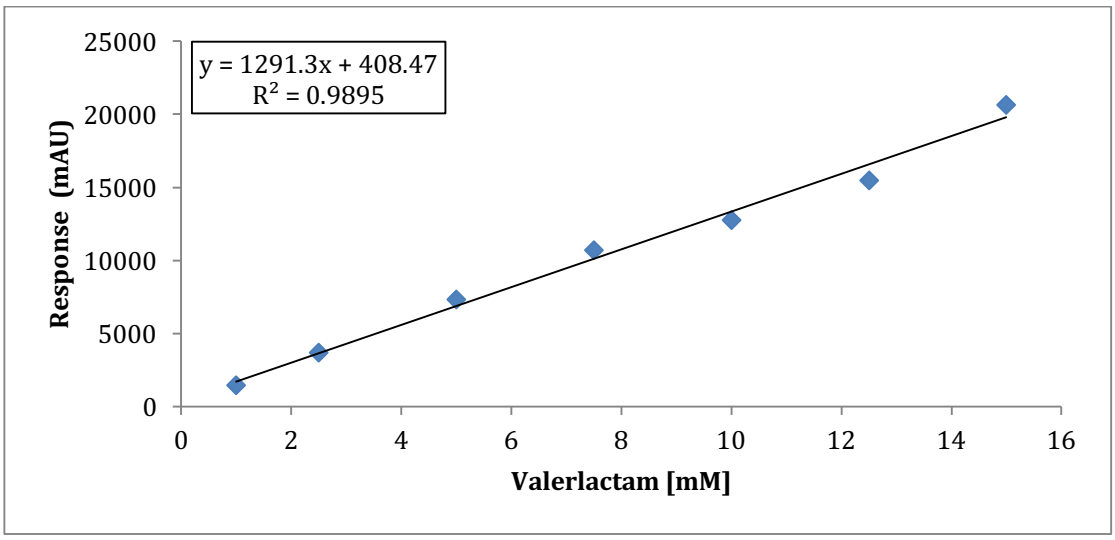

Figure 35 Calibration curve for valerolactam (**366**) used for the determination of product concentrations in reactions with **363**.

6.4.7 Procedure for GOase-XDH cascade reactions for the synthesis of lactams by oxidative cyclisation

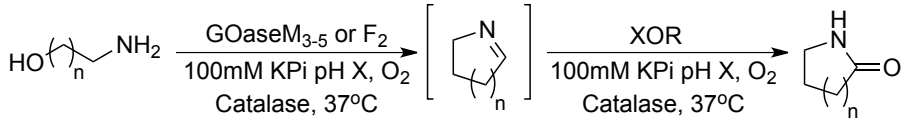

n= 3 (**362**)
n= 4 (**363**)
n= 5 (**364**)

n= 3 (**365**)
n= 4 (**366**)
n= 5 (**367**)

2.1 µL of aliphatic amino alcohol **262-264** (1 M in water) and 33 µL catalase (3.3 mg/mL) was added to 200 mM KPi-buffer. 103 µL of GOase M_{3-5} or F_2 (3.7 mg/mL) and 5 µL of E. coli PaoABC (13.3 mg/mL) or 50 µL of E. coli XDH (1.1 mg/mL) was added to give a final volume of 300 µL. The reaction was then placed in a shaking incubator and incubated at 37°C and 250 rpm for 16h. The reaction was then centrifuged at 13,000 rpm for 2 minutes and then analysed by RP-HPLC. Yields calculated by calibration curves of 2-pyrrolidone (**365**) and valerolactam (**366**) (Section 6.4.6).

6.4.8 Procedure for GOase-PaoABC cascade reactions for the synthesis of 3-phenylazetidin-2-one (371)

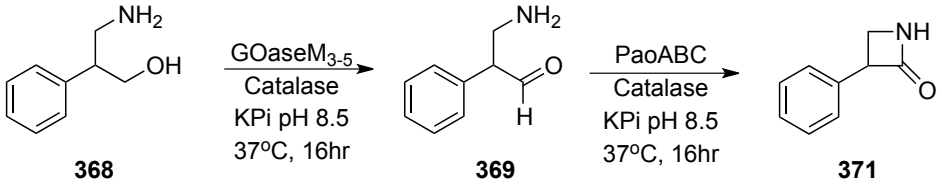

368 **369** **371**

3 µL of 3-amino-2-phenylpropan-1-ol (**368**) (1M in DMF) and 33 µL catalase (3.3 mg/mL) was added to 200 mM KPi-buffer (pH 7.0) with 103 µL of GOase M_{3-5} (3.7 mg/mL) and 50 µL XDH (1.1 mg/mL) to a final volume of 300 µL. The reaction was then placed in a shaking incubator and incubated at 37°C and 250 rpm for 16h. 50 µL of 1M NaOH was then added and the reaction analysed by LC-MS. **HPLC Conditions** = ODS hypurity C-18, Hold 1 min (95% H_2O + 0.1% ammonia formate : 5% MeCN)), 2.5 min (30% H_2O + 0.1% ammonia formate : 70% MeCN), 6 min (30% H_2O + 0.1% ammonia formate : 70% MeCN), 7 min (95% H_2O + 0.1% ammonia formate : 5% MeCN), flow rate 1 mL/min.

6.5 Experimental procedure for chapter 5.

6.5.1 Screening of XOR for the oxidation of HMF (373), DFF (374) and FFCA (377)

The screening of suitable XOR was accomplished using a 96-well, clear, flatbottomed polystyrene microtitre plate in a final volume of 200 µL in potassium phosphate buffer (50 mM, pH 7.6) containing per well: 1 mM of the respective substrate (HMF, DFF or FFCA) 0.1mM DCPIP. 20 µL *E.coli* XDH solution (1.1 mg/mL stock solution), 20 µL XDH E232V (25.4 mg/mL), 20 µL XDH E232V/R310M (23 mg/mL) or 5 µL PaoABC (13.3 mg/mL) was added to each well and the activity was assessed by eye based on the loss of blue colour.

6.5.2 10 mM and 20 mM combined dual enzyme (GOase M_{3-5} +PaoABC) time course oxidation of HMF (373) to FDCA (377).

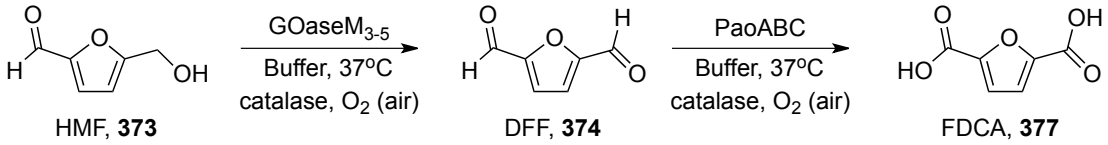

HMF, **373** DFF, **374** FDCA, **377**

To a solution of 200 mM potassium phosphate buffer (pH 7) (156 µL) and catalase 33 µL (3.3 mg/mL) was added 3 µL or 6 µL HMF (**373**) (1M in MeCN). 103 µL GOase M_{3-5} (3.3 mg/mL solution) and 5 µL PaoABC (13.3 mg/mL) was then added and the reaction incubated at 37°C in a shaking incubator. Aliquots (10 µL) of the reaction were then diluted with 50 µL distilled water and 10 µL 1 M HCl. The aliquot was then centrifuged and analysed by RP-HPLC. HPLC conditions: Bio-Rad Aminex HPX-87H, 300 mm × 7.8 mm pre-packed column with 100% 0.005 M H_2SO_4 at 60°C with flow rate 0.6mL/min.

6.5.3 Optimisation of DFF (374) oxidation using PaoABC

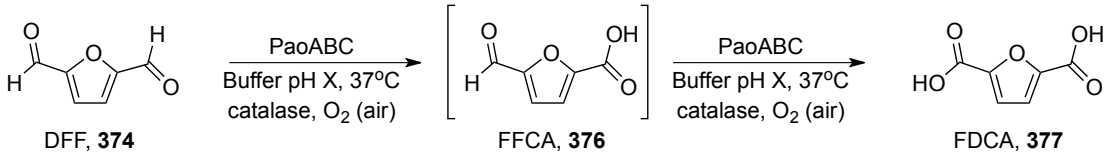

DFF, **374** FFCA, **376** FDCA, **377**

To a solution of potassium phosphate buffer was added DFF (**374**) (2M in MeCN), 33 µL catalase (3.3 mg/mL) and PaoABC (13.3 mg/mL), final volume 300 µL. The reaction was vigorously shaken and placed in a shaking incubator at 37°C. Aliquots of the reaction mixture were taken out, acidified with 2 M HCl and analysed by RP HPLC. HPLC Conditions: Thermo Fisher Hypurity C18, 98% 10 mM phosphate buffer pH 6.5, 2% MeCN with a flow rate of 1 mL/min.

6.5.4 Preparative scale oxidation of DFF (374) with PaoABC

To a solution of 400 mM pH 7 phosphate buffer was added DFF (**374**) (37 mg, 0.29 mmol), 330 µL catalase (3.3 mg/mL), 150 µL MeCN and 50 µL PaoABC (13.3 mg/mL), final volume 3 mL. The reaction was vigorously shaken and placed in a shaking incubator at 37°C. The pH was maintained at pH 7 by the careful addition of 1 M NaOH. After this time the reaction was heated to 80°C for 5 minutes and left cool. The solution containing denatured protein was centrifuged and the supernatant removed. The supernatant was then cooled to 0°C and concentrated HCl was added until a precipitate formed. The solution was then centrifuged and the supernatant removed and the pellet washed with 1 M HCl. The pellet was dissolved in acetone and then concentrated in vacuo three times yielding FDCA (**377**) as a slight yellow solid (41 mg, 0.26 mmol, 90%). **^{1}H-NMR (500 MHz, DMSO-d6)** δ ppm: 13.63 (bs, 2H), 7.29 (s, 2H) **^{13}C (500 MHz, DMSO-d6)** δ ppm: 159.4, 147.5, 118.86

6.5.5 50 mM 2 step time course oxidation of HMF (373) using GOase M_{3-5} and PaoABC

To a solution of 400 mM potassium phosphate buffer (pH 7) (156 µL) and catalase 33 µL (3.3 mg/mL) was added 7.5 µL 1 (2 M in MeCN). 103 µL GOase M_{3-5} (3.3 mg/mL solution) was then added and incubated at 37°C in a shaking incubator. Aliquots (10 µL) of the reaction

were then diluted with 90 µL distilled water and 10 µL 1 M HCl. The aliquot was then centrifuged and analysed by RP-HPLC. After all **373** was oxidised, as determined by HPLC, 5 µL PaoABC (13.3 mg/mL) was added and the reaction placed back into the shaking incubator and aliquots taken as previously. HPLC conditions: Bio-Rad Aminex HPX-87H, 300 mm × 7.8 mm pre-packed column with 100% 0.005 M H_2SO_4 at 60°C with flow rate 0.6 mL/min.

6.5.6 Preparative scale 0.1 M HMF 3 mL oxidation procedure

To a solution of 400 mM pH 7 potassium phosphate buffer (1.09 mL), MeCN (0.03mL) and catalase (0.33 mL of a 3.3 mg/mL solution) was added **373** (38 mg, 0.3 mmol) (final concentration = 100mM). GOase $M_{3\text{-}5}$ (1.5 mL of a 3.3 mg/mL solution) was then added and the reaction shaken at 37°C in an incubated shaker for 10 h. After this time, another portion of catalase (0.33 mL of a 3.3 mg/mL solution) was added along with PaoABC (0.05 mL of a 13.2 mg/mL solution) and left for another 5 h in the shaking incubator. The pH was carefully monitored and adjusted to pH 7 with 1 M NaOH. After this time the reaction was heated to 80°C for 5 minutes and left to cool. The solution containing denatured protein was centrifuged and the supernatant removed. The supernatant was then cooled to 0°C and concentrated HCl was added until a precipitate formed. The solution was then centrifuged and the supernatant removed and the pellet washed with 1M HCl. The pellet was dissolved in acetone and then concentrated in vacuo three times yielding 2 as a slight yellow solid (35 mg, 0.22 mmol, 74% yield). **1H-NMR (500 MHz, DMSO-d6)** δ ppm: 13.63 (bs, 2H), 7.29 (s, 2H) **^{13}C (500 MHz, DMSO-d_6)** δ ppm: 159.4, 147.5, 118.86

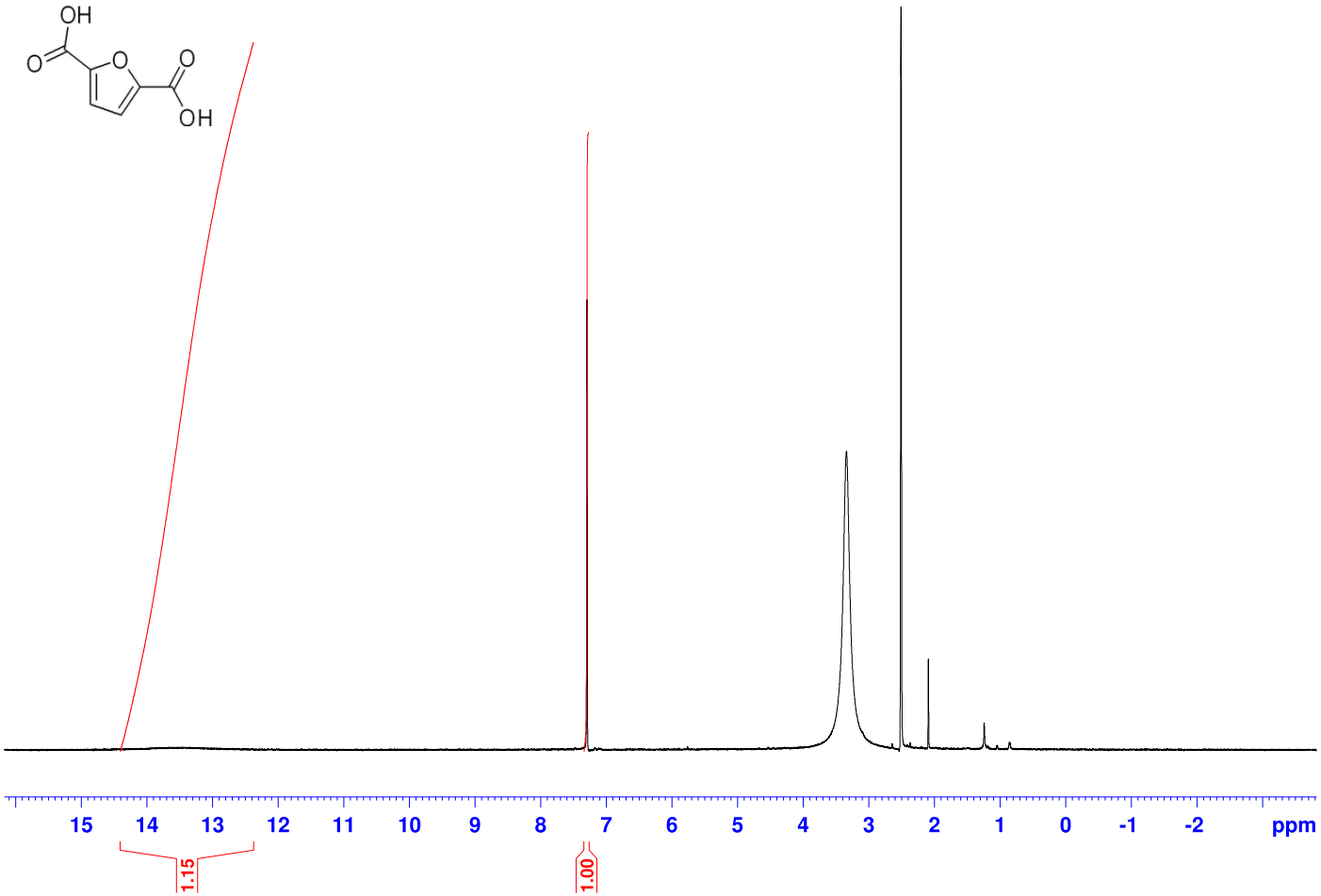

Figure 36 H NMR spectrum (500 MHz) of isolated FDCA (**377**) (Signal at 7.40ppm correspond to aromatic CH of acid product, broad signal from 13.63ppm correspond to carboxylic acid peak.

6.5.6 1:1:1:1 standard of HMF (373), DFF (374), HMFCA (375), FFCA (376) and FDCA (377) used to adjust absorbance in Chapter 6.5

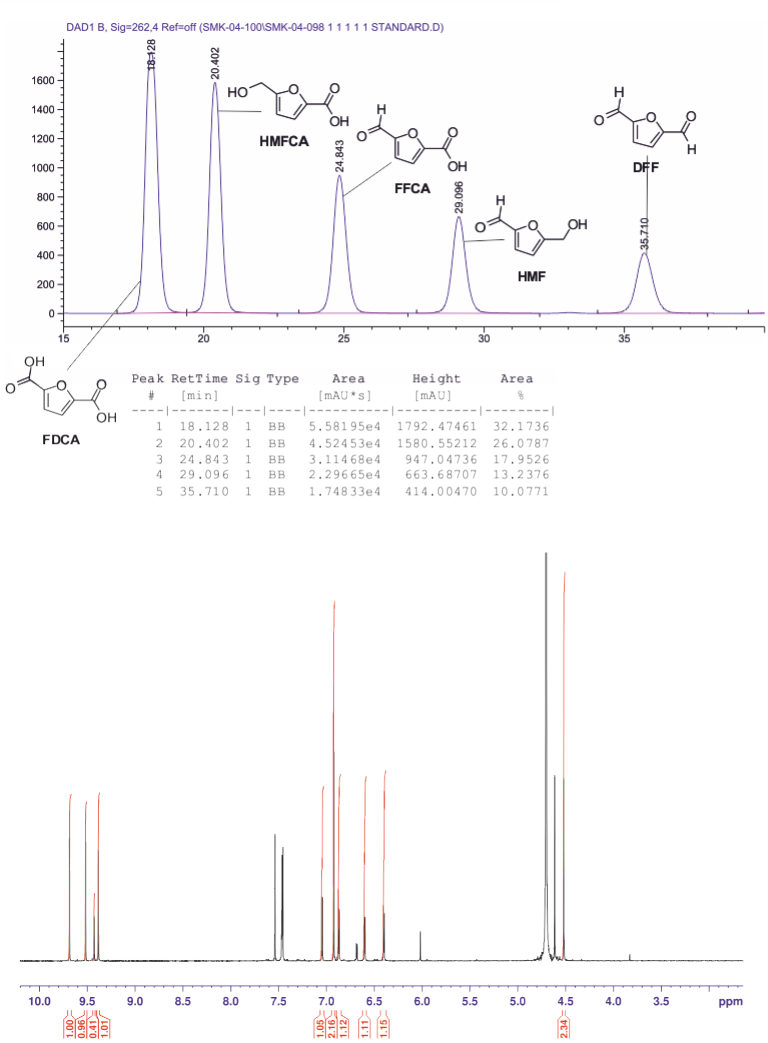

Figure 37 1:1:1:1 standard of HMF (**373**), DFF (**374**), HMFCA (**375**), FFCA (**376**) and FDCA (**377**) used to adjust absorbance in section 7.0. Peaks used in NMR are FFCA = 9.67, DFF = 9.51, DFF Hydrate = 9.421, HMF = 9.38, FDCA = 6.92 and HMFCA = 4.4. HPLC Conditions: Bio-Rad Aminex HPX-87H, 300 mm × 7.8 mm pre-packed column with 100% 0.005 M H_2SO_4 at 60°C with flow rate 0.6 mL/min.

References

1 A. Liese, K. Seelbach and C. Wandrey, Industrial Biotransformations, Wiley, New York, 2nd edn, 2006.
2 K. Drauz,H. Waldmann, O. May, Enzyme catalysis in Organic Synthesis, Wiley, New York, 3rd edn, 2012.
3 K. Faber, Biotransformations in Organic Synthesis, Springer, 2011, 1–454.
4 I. Kozhevnikov, Catalysts for fine chemical synthesis, Wiley, vol 2, 2004.
5 G. Torrelo, U. Hanefeld and F. Hollmann, *Catal Lett*, 2014, **145**, 309–345.
6 N. J. Turner, *Chem. Rev.*, 2011, **111**, 4073–4087.
7 J. H. Schrittwieser, J. Sattler, V. Resch, F. G. Mutti and W. Kroutil, *Current Opinion in Chemical Biology*, 2011, **15**, 249–256.
8 M. Brovetto, D. Gamenara, P. S. Méndez and G. A. Seoane, *Chem. Rev.*, 2011, **111**, 4346–4403.
9 J. S. Carey, D. Laffan, C. Thomson and M. T. Williams, *Org. Biomol. Chem.*, 2006, **4**, 2337.
10 M. T. Reetz, *J. Am. Chem. Soc.*, 2013, **135**, 12480–12496.
11 Junhua, L. Zhao and N. Ran, *Org. Process Res. Dev.*, 2007, **11**, 259–267.
12 A. J. J. Straathof, S. Panke and A. Schmid, *Current Opinion in Biotechnology*, 2002, **13**, 548–556.
13 C. A. Martinez, S. Hu, Y. Dumond, J. Tao, P. Kelleher and L. Tully, *Org. Process Res. Dev.*, 2008, **12**, 392–398.
14 E. Busto, V. Gotor-Fernández and V. Gotor, *Chem. Rev.*, 2011, **111**, 3998–4035.
15 U. T. Bornscheuer and R. J. Kazlauskas, Hydrolases in Organic Synthesis, Wilet New York 2nd edn, 2006.
16 P. L. Brower, D. E. Butler, C. F. Deering, T. V. Le, A. Millar, T. N. Nanninga and B. D. Roth, *Tetrahedron Letters*, 1992, **33**, 2279–2282.
17 C. D. Reeve, US Pat., US6001615 1999.
18 G. DeSantis, K. Wong, B. Farwell, K. Chatman, Z. Zhu, G. Tomlinson, H. Huang, X. Tan, L. Bibbs, P. Chen, K. Kretz and M. J. Burk, *J. Am. Chem. Soc.*, 2003, **125**, 11476–11477.
19 H. Yamada and M. Kobayashi, *Bioscience, Biotechnology and Biochemistry*, 2014, **60**, 1391–1400.
20 L. J. Mersinger, E. C. Hann, F. B. Cooling, J. E. Gavagan, A. Ben-Bassat, S. Wu, K. L. Petrillo, M. S. Payne and R. DiCosimo, *Adv. Synth. Catal.*, 2005, **347**, 1125–1131.
21 N. J. Turner and E. O'Reilly, *Nature Publishing Group*, 2013, **9**, 285–288.
22 D. L. Nelson and M. Cox, Principles of Biochemistry, Palgrave Macmillan, 2015.
23 T. Ahern and A. Klibanov, *Science*, 1985, **228**, 1280–1284.
24 V. V. Mozhaev and K. Martinek, *Enzyme and Microbial Technology*, 2002, **6**, 50–59.
25 A. Warshel, P. K. Sharma, M. Kato, Y. Xiang, H. Liu and M. H. M. Olsson, *Chem. Rev.*, 2006, **106**, 3210–3235.
26 E. Fischer, *Ber. Dtsch. Chem. Ges.*, 1894, **27**, 1191–1192.
27 D. E. Koshland Jr, and K. E. Neet, *Annu. Rev. Biochem.*, 1968, **37**, 359–411.
28 A. Cipiciani, F. Fringuelli, V. Mancini, O. Piermatti, A. M. Scappini and R. Ruzziconi, *Tetrahedron*, 2003, **53**, 11853–11858.
29 P. Kielbasinski, P. Goralczyk, M. Mikolajczyk, M. W. Wieczorek and W. R. Majzner, *Tertrahedron Asymmetry*, 1998, **29**, 2641–2650.
30 T. Knaus, F. G. Mutti, L. D. Humphreys, N. J. Turner and N. S. Scrutton, *Org. Biomol. Chem.*, 2015, **13**, 223–233.
31 D. Monti, G. Ottolina, G. Carrea and S. Riva, *Chem. Rev.*, 2011, **111**, 4111–4140.
32 E. Fossati, F. Polentini, G. Carrea and S. Riva, *Biotechnol. Bioeng.*, 2006, **93**, 1216–1220.
33 J.-I. Hirano, K. Miyamoto and H. Ohta, *Tetrahedron Letters*, 2008, **49**, 1217–1219.

34 R. S. Phillips, *Trends in Biotechnology*, **14**, 13–16.
35 A. M. Klibanov, *Acc. Chem. Res.*, 1990, **23**, 114–120.
36 P. Tafelmeyer and K. Johnsson, Directed molecular evolution of proteins, Wiley, 2004.
37 I. Wu and F. H. Arnold, *Biotechnol. Bioeng.*, 2013, **110**, 1874–1883.
38 X.-Q. Peng, *Appl Biochem Biotechnol*, 2012, **169**, 351–358.
39 Q. Wu, P. Soni and M. T. Reetz, *J. Am. Chem. Soc.*, 2013, **135**, 1872–1881.
40 R. Agudo, G.-D. Roiban and M. T. Reetz, *J. Am. Chem. Soc.*, 2013, **135**, 1665–1668.
41 M. Höhne, S. Schätzle, H. Jochens, K. Robins and U. T. Bornscheuer, *Nature Publishing Group*, 2010, 1–7.
42 J. Attieh, S. A. Sparace and H. S. Saini, *Archives of Biochemistry and Biophysics*, 2000, **380**, 257–266.
43 T. Punniyamurthy, S. Velusamy and J. Iqbal, *Chem. Rev.*, 2005, **105**, 2329–2364.
44 I. D. Paul, G. P. Bhole and J. R. Chaudhari, *Procedia Materials Science*, 2014, **6**, 1644–1649.
45 R. A. Sheldon, *Chem. Soc. Rev.*, 2012, **41**, 1437.
46 F. Hollmann, I. W. C. E. Arends, K. Buehler, A. Schallmey and B. Bühler, *Green Chem.*, 2011, **13**, 226.
47 D. Romano, R. Villa and F. Molinari, *ChemCatChem*, 2012, **4**, 739–749.
48 R. A. Sheldon, *Comptes Rendus de l'Académie des Sciences - Series IIC - Chemistry*, 2000, **3**, 541–551.
49 E. Balaraman, E. Khaskin, G. Leitus and D. Milstein, *Nature Chemistry*, 2013, **5**, 122–125.
50 X. Tong, Y. Sun, Y. Yan, X. Luo, J. Liu and Z. Wu, *'Journal of Molecular Catalysis. A, Chemical'*, 2014, **391**, 1–6.
51 W. Kroutil, H. Mang, K. Edegger and K. Faber, *Adv. Synth. Catal.*, 2004, **346**, 125–142.
52 W. Kroutil, H. Mang, K. Edegger and K. Faber, *Current Opinion in Chemical Biology*, 2004, **8**, 120–126.
53 F. Escalettes and N. J. Turner, *ChemBioChem*, 2008, **9**, 857–860.
54 A. Siebum, A. van Wijk, R. Schoevaart and T. Kieboom, *'Journal of Molecular Catalysis. B, Enzymatic'*, 2006, **41**, 141–145.
55 F. Borzeix, F. Monot and J.-P. Vandecasteele, *Enzyme and Microbial Technology*, 1995, **17**, 615–622.
56 G. Dienys, S. Jarmalavičius, S. Budrien, D. Čitavičius and J. Sereikait, *'Journal of Molecular Catalysis. B, Enzymatic'*, 2003, **21**, 47–49.
57 Y. Liu, J. Pan, P. Wei, J. Zhu, L. Huang, J. Cai and Z. Xu, *Biotechnol Bioproc E*, 2012, **17**, 693–702.
58 A. Kunamneni, S. Camarero, C. García-Burgos, F. J. Plou, A. Ballesteros and M. Alcalde, *Microb Cell Fact*, 2008, **7**, 32.
59 R. Gandolfi, K. Cavenago, R. Gualandris, J. V. Sinisterra Gago and F. Molinari, *Process Biochemistry*, 2004, **39**, 749–753.
60 F. Molinari, R. Villa, F. Aragozzini, P. Cabella, M. Barbeni and F. Squarcia, *J. Chem. Technol. Biotechnol.*, 1997, **70**, 294–298.
61 A. Geerlof, J. Stoorvogel, J. A. Jongejan, E. J. T. M. Leenen, T. J. G. M. van Dooren, W. J. J. van den Tweel and J. A. Duine, *Appl Microbiol Biotechnol*, 1994, **42**, 8–15.
62 U. Wandel, S. S. Machado, J. A. Jongejan and J. A. Duine, *Enzyme and Microbial Technology*, 2001, **28**, 233–239.
63 F. Molinari, R. Villa, F. Aragozzini, R. Leon and D. M. F. Prazeres, *Tetrahedron: Asymmetry*, **10**, 3003–3009.
64 F. Molinari, R. Villa, M. Manzoni and F. Aragozzini, *Appl Microbiol Biotechnol*, 1995, **43**, 989–994–6.
65 A. Romano, R. Gandolfi, P. Nitti, M. Rollini and F. Molinari, *'Journal of Molecular Catalysis. B, Enzymatic'*, 2002, **17**, 235–240.
66 E. W. van Hellemond, L. Vermote, W. Koolen, T. Sonke, E. Zandvoort, D. P. H. M.

Heuts, D. B. Janssen and M. W. Fraaije, *Adv. Synth. Catal.*, 2009, **351**, 1523–1530.
67 K. Yamada-Onodera, A. Nakajima and Y. Tani, *Journal of Bioscience and Bioengineering*, 2006, **102**, 545–551.
68 A. J. Irwin and J. B. Jones, *J. Am. Chem. Soc.*, 1977, **99**, 556–561.
69 K. P. Lok, I. J. Jakovac and J. B. Jones, *J. Am. Chem. Soc.*, 1985, **107**, 2521–2526.
70 A. Díaz-Rodríguez, J. Iglesias-Fernández, C. Rovira and V. Gotor-Fernández, *ChemCatChem*, 2013, **6**, 977–980.
71 T. Orbegozo, I. Lavandera, W. M. F. Fabian, B. Mautner, J. G. de Vries and W. Kroutil, *Tetrahedron*, 2009, **65**, 6805–6809.
72 T. Orbegozo, J. G. de Vries and W. Kroutil, *Eur. J. Org. Chem.*, 2010, **2010**, 3445–3448.
73 R. Gandolfi, N. Ferrara and F. Molinari, *Tetrahedron Letters*, 2001, **42**, 513–514.
74 J. Wu, M. H. Li, J. P. Lin and D. Z. Wei, *Curr Microbiol*, 2010, **62**, 1123–1127.
75 A. J. Irwin and J. B. Jones, *J. Am. Chem. Soc.*, 1976, **98**, 8476–8482.
76 D. S. Clark, S. Geresh and R. DiCosimo, *Bioorganic & Medicinal Chemistry Letters*, 2010, **5**, 1383–1388.
77 W. P. Dijkman and M. W. Fraaije, *Appl. Environ. Microbiol.*, 2014, **80**, 1082–1090.
78 W. P. Dijkman, C. Binda, M. W. Fraaije and A. Mattevi, *ACS Catal.*, 2015, **5**, 1833–1839.
79 S. Riva, *Trends in Biotechnology*, 2006, **24**, 219–226.
80 S. A. Tromp, I. Matijošytė, R. A. Sheldon, I. W. C. E. Arends, G. Mul, M. T. Kreutzer, J. A. Moulijn and S. de Vries, *ChemCatChem*, 2010, **2**, 827–833.
81 M. Fabbrini, C. Galli and P. Gentili, *'Journal of Molecular Catalysis. B, Enzymatic'*, 2004, **16**, 231–240.
82 M. Fabbrini, C. Galli, P. Gentili and D. Macchitella, *Tetrahedron Letters*, 2001, **42**, 7551–7553.
83 F. d'Acunzo, P. Baiocco, M. Fabbrini, C. Galli and P. Gentili, *Eur. J. Org. Chem.*, 2002, **2002**, 4195–4201.
84 A. Barilli, F. Belinghieri, D. Passarella, G. Lesma, S. Riva, A. Silvani and B. Danieli, *Tetrahedron: Asymmetry*, 2004, **15**, 2921–2925.
85 C. Zhu, Z. Zhang, W. Ding, J. Xie, Y. Chen, J. Wu, X. Chen and H. Ying, *Green Chem.*, 2014, **16**, 1131–1138.
86 I. W. C. E. Arends, Y.-X. Li and R. A. Sheldon, *Biocatal Biotransformation*, 2006, **24**, 443–448.
87 A. Matsuyama, H. Yamamoto, N. Kawada and Y. Kobayashi, *'Journal of Molecular Catalysis. B, Enzymatic'*, 2001, **11**, 513–521.
88 M. Fogagnolo, P. P. Giovannini, A. Guerrini, A. Medici, P. Pedrini and N. Colombi, *Tetrahedron: Asymmetry*, 1998, **9**, 2317–2327.
89 W. Adam, M. Lazarus, B. Boss, C. R. Saha-Möller, H.-U. Humpf and P. Schreier, *J. Org. Chem.*, 1997, **62**, 7841–7843.
90 W. Stampfer, B. Kosjek, C. Moitzi, W. Kroutil and K. Faber, *Angew. Chem. Int. Ed.*, 2002, **41**, 1014–1017.
91 E. C. A. Stigter, J. P. van der Lugt and W. A. C. Somers, *'Journal of Molecular Catalysis. B, Enzymatic'*, 1997, **2**, 291–297.
92 L. G. Lee and G. M. Whitesides, *J. Org. Chem.*, 1986, **51**, 25–36.
93 K. Edegger, H. Mang, K. Faber, J. Gross and W. Kroutil, *'Journal of Molecular Catalysis. A, Chemical'*, 2006, **251**, 66–70.
94 T. Tanaka, N. Iwai, T. Matsuda and T. Kitazume, *'Journal of Molecular Catalysis. B, Enzymatic'*, 2009, **57**, 317–320.
95 C. V. Voss, C. C. Gruber and W. Kroutil, *Angew. Chem. Int. Ed.*, 2008, **47**, 741–745.
96 C. V. Voss, C. C. Gruber, K. Faber, T. Knaus, P. Macheroux and W. Kroutil, *J. Am. Chem. Soc.*, 2008, **130**, 13969–13972.
97 Y.-L. Li, J.-H. Xu and Y. Xu, *'Journal of Molecular Catalysis. B, Enzymatic'*, 2010, **64**, 48–52.
98 Y.-P. Xue, Y.-G. Zheng, Y.-Q. Zhang, J.-L. Sun, Z.-Q. Liu and Y.-C. Shen, *Chem.*

Commun., 2013, **49**, 10706.
99 K. Nakamura, M. Fujii and Y. Ida, *Tetrahedron: Asymmetry*, 2010, **12**, 3147–3153.
100 T. Utsukihara, O. Misumi, K. Nakajima, M. Koshimura, M. Kuniyoshi, T. Kuroiwa and C. A. Horiuchi, *'Journal of Molecular Catalysis. B, Enzymatic'*, 2008, **51**, 19–23.
101 S. M. Mantovani, C. F. F. Angolini and A. J. Marsaioli, *Tetrahedron: Asymmetry*, 2009, **20**, 2635–2638.
102 T. Janeczko, A. Panek, A. Świzdor, J. Dmochowska-Gładysz and E. Kostrzewa-Susłow, *Curr Microbiol*, 2012, **65**, 189–194.
103 R. Bauer, N. Katsikis, S. Varga and D. Hekmat, *Bioprocess Biosyst Eng*, 2005, **28**, 37–43.
104 B. H. Landis, J. K. McLaughlin, R. Heeren, R. W. Grabner and P. T. Wang, *Org. Process Res. Dev.*, 2002, **6**, 547–552.
105 R. D. Hancock and R. Viola, *Trends in Biotechnology*, 2002, **20**, 299–305.
106 C. De Muynck, C. Pereira, W. Soetaert and E. Vandamme, *Journal of Biotechnology*, 2006, **125**, 408–415.
107 H.-J. Moon, M. Tiwari, M. Jeya and J.-K. Lee, *Appl Microbiol Biotechnol*, 2010, **87**, 205–214.
108 R. D. Woodyer, N. J. Wymer, F. M. Racine, S. N. Khan and B. C. Saha, *Appl. Environ. Microbiol.*, 2008, **74**, 2967–2975.
109 D. W. Edmund W Hafner, *Proceedings of the National Academy of Sciences of the United States of America*, 1971, **68**, 987–5.
110 J. W. Huh, K. Yokoigawa, N. Esaki and K. Soda, *Bioscience, Biotechnology and Biochemistry*, 1992, **56**, 2081–2082.
111 J. W. Huh, K. Yokoigawa, N. Esaki and K. Soda, *Journal of fermentation and bioengineering*, 1992, **74**, 189–190.
112 A. Enright, F.-R. Alexandre, G. Roff, I. G. Fotheringham, M. J. Dawson and N. J. Turner, *Chem. Commun.*, 2003, 2636.
113 G. J. Roff, R. C. Lloyd and N. J. Turner, *J. Am. Chem. Soc.*, 2004, **126**, 4098–4099.
114 P. F. Fitzpatrick, *Archives of Biochemistry and Biophysics*, 2010, **493**, 13–25.
115 D. E. Edmondson, C. Binda and A. Mattevi, *Archives of Biochemistry and Biophysics*, 2007, **464**, 269–276.
116 S. O. Sablin, V. Yankovskaya, S. Bernard, C. N. Cronin and T. P. Singer, *Eur J Biochem*, 1998, **253**, 270–279.
117 R. Carr, M. Alexeeva, A. Enright, T. S. C. Eve, M. J. Dawson and N. J. Turner, *Angew. Chem. Int. Ed.*, 2003, **42**, 4807–4810.
118 R. Carr, M. Alexeeva, M. J. Dawson, V. Gotor-Fernández, C. E. Humphrey and N. J. Turner, *ChemBioChem*, 2005, **6**, 637–639.
119 D. Ghislieri, A. P. Green, M. Pontini, S. C. Willies, I. Rowles, A. Frank, G. Grogan and N. J. Turner, *J. Am. Chem. Soc.*, 2013, **135**, 10863–10869.
120 D. Ghislieri, D. Houghton, A. P. Green, S. C. Willies and N. J. Turner, *ACS Catal.*, 2013, **3**, 2869–2872.
121 J. H. Schrittwieser, B. Groenendaal, S. C. Willies, D. Ghislieri, I. Rowles, V. Resch, J. H. Sattler, E.-M. Fischereder, B. Grischek, W.-D. Lienhart, N. J. Turner and W. Kroutil, *Catal. Sci. Technol.*, 2014, **4**, 3657–3664.
122 J. H. Schrittwieser, B. Groenendaal, V. Resch, D. Ghislieri, S. Wallner, E.-M. Fischereder, E. Fuchs, B. Grischek, J. H. Sattler, P. Macheroux, N. J. Turner and W. Kroutil, *Angew. Chem. Int. Ed.*, 2014, **53**, 3731–3734.
123 E. O'Reilly, C. Iglesias and N. J. Turner, *ChemCatChem*, 2014, **6**, 992–995.
124 V. Köhler, K. R. Bailey, A. Znabet, J. Raftery, M. Helliwell and N. J. Turner, *Angew. Chem. Int. Ed.*, 2010, **49**, 2182–2184.
125 G. J. ten Brink, I. W. C. E. Arends and R. A. Sheldon, *Chem. Rev.*, 2004, **104**, 4105–4124.
126 G. Strukul, *Angew. Chem. Int. Ed.*, 1998, **37**, 1198–1209.
127 R. A. Michelin, P. Sgarbossa, A. Scarso and G. Strukul, *Coordination Chemistry Reviews*, 2010, **254**, 646–660.

128 W. J. H. van Berkel, N. M. Kamerbeek and M. W. Fraaije, *Journal of Biotechnology*, 2006, **124**, 670–689.
129 B. A. Palfey and C. A. McDonald, *Archives of Biochemistry and Biophysics*, 2010, **493**, 26–36.
130 M. D. Mihovilovic, F. Rudroff, W. Kandioller, B. Grötzl, P. Stanetty and H. Spreitzer, *Synlett*, 2003, 1973–1976.
131 C. Rodríguez, G. de Gonzalo, D. E. T. Pazmiño, M. W. Fraaije and V. Gotor, *Tetrahedron: Asymmetry*, 2009, **20**, 1168–1173.
132 C. Rodríguez, G. de Gonzalo, A. Rioz-Martínez, D. E. Torres Pazmiño, M. W. Fraaije and V. Gotor, *Org. Biomol. Chem.*, 2010, **8**, 1121.
133 G. de Gonzalo, M. D. Mihovilovic and M. W. Fraaije, *ChemBioChem*, 2010, **11**, 2208–2231.
134 R. Snajdrova, I. Braun, T. Bach, K. Mereiter and M. D. Mihovilovic, *J. Org. Chem.*, 2007, **72**, 9597–9603.
135 P. ernuchov and M. D. Mihovilovic, *Org. Biomol. Chem.*, 2007, **5**, 1715.
136 G. Ottolina, G. de Gonzalo, G. Carrea and B. Danieli, *Adv. Synth. Catal.*, 2005, **347**, 1035–1040.
137 G. de Gonzalo, G. Ottolina, G. Carrea and M. W. Fraaije, *Chem. Commun.*, 2005, 3724.
138 R. Snajdrova, G. Grogan and M. D. Mihovilovic, *Bioorganic & Medicinal Chemistry Letters*, 2006, **16**, 4813–4817.
139 A. Kirschner and U. T. Bornscheuer, *Angew. Chem. Int. Ed.*, 2006, **45**, 7004–7006.
140 B. D. Summers, M. Omar, T. O. Ronson, J. Cartwright, M. Lloyd and G. Grogan, *Org. Biomol. Chem.*, 2015, **13**, 1897–1903.
141 N. Berezina, V. Alphand and R. Furstoss, *Tetrahedron: Asymmetry*, 2010, **13**, 1953–1955.
142 M.-C. Gutiérrez, R. Furstoss and V. Alphand, *Adv. Synth. Catal.*, 2005, **347**, 1051–1059.
143 A. Rioz-Martínez, A. Cuetos, C. Rodríguez, G. de Gonzalo, I. Lavandera, M. W. Fraaije and V. Gotor, *Angew. Chem. Int. Ed.*, 2011, **50**, 8387–8390.
144 G. M. Coppola and H. F. Schuster, *alpha-Hydroxy Acids in Enantioselective Syntheses*, Wiley-VCH, 1st edn. 1997.
145 F. Zambianchi, M. W. Fraaije, G. Carrea, G. de Gonzalo, C. Rodríguez, V. Gotor and G. Ottolina, *Adv. Synth. Catal.*, 2007, **349**, 1327–1331.
146 N. Kasai, T. Suzuki and Y. Furukawa, *'Journal of Molecular Catalysis. B, Enzymatic'*, 1998, **4**, 237–252.
147 E. J. de Vries and D. B. Janssen, *Current Opinion in Biotechnology*, 2003, **14**, 414–420.
148 T. Katsuki and K. B. Sharpless, *J. Am. Chem. Soc.*, 1980, **102**, 5974–5976.
149 K. B. Sharpless, *Angew. Chem. Int. Ed.*, 2002, **41**, 2024–2032.
150 W. Zhang, J. L. Loebach, S. R. Wilson and E. N. Jacobsen, *J. Am. Chem. Soc.*, 1990, **112**, 2801–2803.
151 Y. Tu, Z.-X. Wang and Y. Shi, *J. Am. Chem. Soc.*, 1996, **118**, 9806–9807.
152 R. N. Austin, K. Luddy, K. Erickson, M. Pender Cudlip, E. Bertrand, D. Deng, R. S. Buzdygon, J. B. van Beilen and J. T. Groves, *Angew. Chem. Int. Ed.*, 2008, **47**, 5232–5234.
153 E. Bertrand, R. Sakai, E.Rozhkovanovosad, L. Moe, B. Fox, J. Groves and R. Austin, *Journal of Inorganic Biochemistry*, 2005, **99**, 1998–2006.
154 A. N. Collins, G. Sheldrake and J. Crosby, 1997, **2**, A146.
155 C. A. G. M. Weijers, C. G. van Ginkel and J. A. M. de Bont, *Enzyme and Microbial Technology*, 2002, **10**, 214–218.
156 K. Furuhashi and M. Takagi, *Appl Microbiol Biotechnol*, 1984, **20**, 6–9–4.
157 K. Furuhashi, A. Taoka, S. Uchida, I. Karube and S. Suzuki, *European J. Appl. Microbiol. Biotechnol.*, 1981, **12**, 39–45–7.
158 M.-J. de Smet, J. Kingma, H. Wynberg and B. Witholt, *Enzyme and Microbial*

Technology, 1983, **5**, 352–360.
159 R. T. Ruettinger and A. J. Fulco, *J. Biol. Chem.*, 1981, **256**, 5728–5734.
160 J. C. Lewis and F. H. Arnold, *CHIMIA*, 2009, **63**, 309–312.
161 J. A. Dietrich, Y. Yoshikuni, K. J. Fisher, F. X. Woolard, D. Ockey, D. J. McPhee, N. S. Renninger, M. C. Y. Chang, D. Baker and J. D. Keasling, *ACS Chem. Biol.*, 2009, **4**, 261–267.
162 S. G. Bell, R. J. Sowden and L.-L. Wong, *Chem. Commun.*, 2001, 635–636.
163 R. J. Sowden, S. Yasmin, N. H. Rees, S. G. Bell and L.-L. Wong, *Org. Biomol. Chem.*, 2005, **3**, 57.
164 J. N. Kolev, J. M. Zaengle, R. Ravikumar and R. Fasan, *ChemBioChem*, 2014, **15**, 1001–1010.
165 E. J. Allain, L. P. Hager, L. Deng and E. N. Jacobsen, *J. Am. Chem. Soc.*, 1993, **115**, 4415–4416.
166 A. F. Dexter, F. J. Lakner, R. A. Campbell and L. P. Hager, *J. Am. Chem. Soc.*, 1995, **117**, 6412–6413.
167 F. J. Lakner, K. P. Cain and L. P. Hager, *J. Am. Chem. Soc.*, 1997, **119**, 443–444.
168 Y. Liu, Y. Wang, Y. Jiang, M. Hu, S. Li and Q. Zhai, *Biotechnol Progress*, 2015, n/a–n/a.
169 F. Hollmann, P.-C. Lin, B. Witholt and A. Schmid, *J. Am. Chem. Soc.*, 2003, **125**, 8209–8217.
170 A. Schmid, K. Hofstetter, H.-J. Feiten, F. Hollmann and B. Witholt, *Adv. Synth. Catal.*, 2001, **343**, 732–737.
171 H. Lin, Y. Liu and Z.-L. Wu, *Tetrahedron: Asymmetry*, 2011, **22**, 134–137.
172 E. Dalcanale and F. Montanari, *J. Org. Chem.*, 1986, **51**, 567–569.
173 R. H. Abeles and H. A. Lee, *J. Biol. Chem.*, 1960, **235**, 1499–1503.
174 R. J. Lamed and J. Zeikus, *Biochem. J*, 1981, **195**, 183–190.
175 P. Heinstra, K. T. Eisses, W. Schoonen, W. Aben, A. De Winter, D. Van der Horst, W. Van Marrewijk, A. T. Beenakkers, W. Scharloo and G. Thörig, *Genetica*, 1983, **60**, 129–137.
176 G. T. M. Henehan and N. J. Oppenheimer, *Biochemistry*, 1993, **32**, 735–738.
177 C. Wuensch, H. Lechner, S. M. Glueck, K. Zangger, M. Hall and K. Faber, *ChemCatChem*, 2013, **5**, 1744–1748.
178 P. Könst, H. Merkens, S. Kara, S. Kochius, A. Vogel, R. Zuhse, D. Holtmann, I. W. C. E. Arends and F. Hollmann, *Angew. Chem. Int. Ed.*, 2012, **51**, 9914–9917.
179 B. P. Branchaud and C. T. Walsh, *J. Am. Chem. Soc.*, 1985, **107**, 2153–2161.
180 N. M. Kamerbeek, A. J. Olsthoorn, M. W. Fraaije and D. B. Janssen, *Appl. Environ. Microbiol.*, 2003, **69**, 419–426.
181 C. Rodríguez, G. de Gonzalo, M. W. Fraaije and V. Gotor, *Tetrahedron: Asymmetry*, 2007, **18**, 1338–1344.
182 S. Bisagni, B. Summers, S. Kara, R. Hatti-Kaul, G. Grogan, G. Mamo and F. Hollmann, *Top Catal*, 2013, **57**, 366–375.
183 V. H. Booth, *Biochem. J.*, 1938, **32**, 494–541.
184 C. Iobbi-Nivol and S. Leimkühler, *BBA - Bioenergetics*, 2013, **1827**, 1086–1101.
185 R. Sigrist, B. Z. da Costa, A. J. Marsaioli and L. G. de Oliveira, *Biotechnology Advances*, 2015, 1–18.
186 R. C. Simon, F. Zepeck and W. Kroutil, *Chem. Eur. J.*, 2013, **19**, 2859–2865.
187 E. Burda, W. Hummel and H. Gröger, *Angew. Chem. Int. Ed.*, 2008, **47**, 9551–9554.
188 A. Boffi, S. Cacchi, P. Ceci, R. Cirilli, G. Fabrizi, A. Prastaro, S. Niembro, A. Shafir and A. Vallribera, *ChemCatChem*, 2010, **3**, 347–353.
189 E. O'Reilly, C. Iglesias, D. Ghislieri, J. Hopwood, J. L. Galman, R. C. Lloyd and N. J. Turner, *Angew. Chem. Int. Ed.*, 2014, **53**, 2447–2450.
190 V. Köhler, Y. M. Wilson, M. Dürrenberger, D. Ghislieri, E. Churakova, T. Quinto, L. Knörr, D. Häussinger, F. Hollmann, N. J. Turner and T. R. Ward, *Nature Chemistry*, 2012, **5**, 93–99.
191 K. Engström, E. V. Johnston, O. Verho, K. P. J. Gustafson, M. Shakeri, C.-W. Tai and

J.-E. Bäckvall, *Angew. Chem. Int. Ed.*, 2013, **52**, 14006–14010.
192 K. B. Otte and B. Hauer, *Current Opinion in Biotechnology*, 2015, **35**, 16–22.
193 S. Schmidt, C. Scherkus, J. Muschiol, U. Menyes, T. Winkler, W. Hummel, H. Gröger, A. Liese, H.-G. Herz and U. T. Bornscheuer, *Angew. Chem. Int. Ed.*, 2015, **54**, 2784–2787.
194 J. H. Sattler, M. Fuchs, F. G. Mutti, B. Grischek, P. Engel, J. Pfeffer, J. M. Woodley and W. Kroutil, *Angew. Chem. Int. Ed.*, 2014, **53**, 14153–14157.
195 M. Korpak and J. Pietruszka, *Adv. Synth. Catal.*, 2011, **353**, 1420–1424.
196 T. Sehl, H. C. Hailes, J. M. Ward, U. Menyes, M. Pohl and D. Rother, *Green Chem.*, 2014, **16**, 3341–3348.
197 C.-W. Fan, G.-C. Xu, B.-D. Ma, Y.-P. Bai, J. Zhang and J.-H. Xu, *Journal of Biotechnology*, 2015, **195**, 67–71.
198 J. H. Sattler, M. Fuchs, K. Tauber, F. G. Mutti, K. Faber, J. Pfeffer, T. Haas and W. Kroutil, *Angew. Chem. Int. Ed.*, 2012, **51**, 9156–9159.
199 Y. J. Choi and S. Y. Lee, *Nature*, 2013, **502**, 571–574.
200 C. E. Nakamura and G. M. Whited, *Current Opinion in Biotechnology*, 2003, **14**, 454–459.
201 H. Yim, R. Haselbeck, W. Niu, C. Pujol-Baxley, A. Burgard, J. Boldt, J. Khandurina, J. D. Trawick, R. E. Osterhout, R. Stephen, J. Estadilla, S. Teisan, H. B. Schreyer, S. Andrae, T. H. Yang, S. Y. Lee, M. J. Burk and S. Van Dien, *Nature Publishing Group*, 2011, **7**, 445–444.
202 C. J. Paddon, P. J. Westfall, D. J. Pitera, K. Benjamin, K. Fisher, D. McPhee, M. D. Leavell, A. Tai, A. Main, D. Eng, D. R. Polichuk, K. H. Teoh, D. W. Reed, T. Treynor, J. Lenihan, M. Fleck, S. Bajad, G. Dang, D. Dengrove, D. Diola, G. Dorin, K. W. Ellens, S. Fickes, J. Galazzo, S. P. Gaucher, T. Geistlinger, R. Henry, M. Hepp, T. Horning, T. Iqbal, H. Jiang, L. Kizer, B. Lieu, D. Melis, N. Moss, R. Regentin, S. Secrest, H. Tsuruta, R. Vazquez, L. F. Westblade, L. Xu, M. Yu, Y. Zhang, L. Zhao, J. Lievense, P. S. Covello, J. D. Keasling, K. K. Reiling, N. S. Renninger and J. D. Newman, *Nature*, 2013, **496**, 528–532.
203 M. Schrewe, N. Ladkau, B. Bühler and A. Schmid, *Adv. Synth. Catal.*, 2013, **355**, 1693–1697.
204 N. Oberleitner, C. Peters, J. Muschiol, M. Kadow, S. Saß, T. Bayer, P. Schaaf, N. Iqbal, F. Rudroff, M. D. Mihovilovic and U. T. Bornscheuer, *ChemCatChem*, 2013, **5**, 3524–3528.
205 A. Pennec, F. Hollmann, M. S. Smit and D. J. Opperman, *ChemCatChem*, 2014, **7**, 236–239.
206 J.-W. Song, E.-Y. Jeon, D.-H. Song, H.-Y. Jang, U. T. Bornscheuer, D.-K. Oh and J.-B. Park, *Angew. Chem. Int. Ed.*, 2013, **52**, 2534–2537.
207 K. B. Otte, J. Kittelberger, M. Kirtz, B. M. Nestl and B. Hauer, *ChemCatChem*, 2013, **6**, 1003–1009.
208 D. C. Pryde, D. Dalvie, Q. Hu, P. Jones, R. S. Obach and T.-D. Tran, *J. Med. Chem.*, 2010, **53**, 8441–8460.
209 E. Garattini, M. Fratelli and M. Terao, *Cell. Mol. Life Sci.*, 2007, **65**, 1019–1048.
210 E. Garattini, R. Mendel, M. ROMAO, R. Wright and M. Terao, *Biochem. J*, 2003, **372**, 15–32.
211 T. Nishino, *Journal of Biological Chemistry*, 2005, **280**, 24888–24894.
212 T. Nishino, *Journal of Biochemistry*, 1994, **116**, 1–6.
213 M. Neumann, G. Mittelstädt, C. Iobbi-Nivol, M. Saggu, F. Lendzian, P. Hildebrandt and S. Leimkühler, *FEBS Journal*, 2009, **276**, 2762–2774.
214 C. Enroth, B. T. Eger, K. Okamoto, T. Nishino, T. Nishino and E. F. Pai, *Proceedings of the National Academy of Sciences*, 2000, **97**, 10723–10728.
215 R. Huber, P. Hof, R. O. Duarte, J. Moura, I. Moura, M.-Y. Liu, J. LeGall, R. Hille, M. Archer and M. J. Romão, *Proceedings of the National Academy of Sciences*, 1996, **93**, 8846–8851.
216 R. Hille, *Archives of Biochemistry and Biophysics*, 2005, **433**, 107–116.

217 R. Hille, J. Hall and P. Basu, *Chem. Rev.*, 2014, **114**, 3963–4038.
218 W. Ambroziak, G. Izaguirre and R. Pietruszko, *J. Biol. Chem.*, 1999, **274**, 33366–33373.
219 P. C. Ruenitz and X. Bai, *Drug metabolism and disposition*, 1995, **23**, 993–998.
220 B. Rochat, M. Kosel, G. Boss, B. Testa, M. Gillet and P. Baumann, *Biochemical pharmacology*, 1998, **56**, 15–23.
221 H. g. McDaniel, H. Podgainy and R. Bressler, *Journal of Pharmacology and Experimental Therapeutics*, 1969, **167**, 91–97.
222 T. Ghafourian and M. R. Rashidi, *Chemical and pharmaceutical bulletin*, 2001, **49**, 1066–1071.
223 N. E. Austin, S. J. Baldwin, L. Cutler, N. Deeks, P. J. Kelly, M. Nash, C. E. Shardlow, G. Stemp, K. Thewlis, A. Ayrton and P. Jeffrey, *Xenobiotica*, 2001, **31**, 677–686.
224 A. Moriyasu, K. SUGIHARA, K. Nakatani, S. Ohta and S. Kitamura, *Drug metabolism and pharmacokinetics*, 2006, **21**, 485–491.
225 S. Kitamura, K. SUGIHARA and S. Ohta, *Drug metabolism and pharmacokinetics*, 2006, **21**, 83–98.
226 S. Brandänge and L. Lindblom, *Biochemical and biophysical research communications*, 1979, **91**, 991–996.
227 M. Stanulović and S. Chaykin, *Archives of Biochemistry and Biophysics*, 1971, **145**, 27–34.
228 M. Whittlesea and J. Gorrod, *Journal of Clinical Pharmacy and Therapeutics*, 1993, **18**, 357–364.
229 S. I. Jeon, J. W. Hong and H. C. Yoon, *Biotechnol Lett*, 2006, **28**, 1401–1408.
230 J. H. Carter, J. A. Deddens, J. L. Pullman, B. M. Colligan, L. O. Whiteley and H. W. Carter, *Clinical cancer research*, 1997, **3**, 1479–1489.
231 J. B. Rannes, A. Ioannou, S. C. Willies, G. Grogan, C. Behrens, S. L. Flitsch and N. J. Turner, *J. Am. Chem. Soc.*, 2011, **133**, 8436–8439.
232 L. Sun, T. Bulter, M. Alcalde, I. P. Petrounia and F. H. Arnold, *ChemBioChem*, 2002, **3**, 781–783.
233 L. Sun, I. P. Petrounia, M. Yagasaki, G. Bandara and F. H. Arnold, *Protein engineering*, 2001, **14**, 699–704.
234 S. Staniland, B. Yuan, N. Giménez-Agulló, T. Marcelli, S. C. Willies, D. M. Grainger, N. J. Turner and J. Clayden, *Chem. Eur. J.*, 2014, **20**, 13084–13088.
235 Y. Y. Gorbanev, S. Kegnæs and A. Riisager, *Top Catal*, 2011, **54**, 1318–1324.
236 F. van Rantwijk and A. Stolz, *'Journal of Molecular Catalysis. B, Enzymatic'*, 2015, **114**, 25–30.
237 A. Otrelo-Cardoso, M. da Silva Correia, V. Schwuchow, D. Svergun, M. Romão, S. Leimkühler and T. Santos-Silva, *IJMS*, 2014, **15**, 2223–2236.
238 A. Badalyan, E. G. Yoga, V. Schwuchow, S. Pöller, W. Schuhmann, S. Leimkühler and U. Wollenberger, *Electrochemistry Communications*, 2013, **37**, 5–7.
239 P. Galletti, M. Pori, F. Funiciello, R. Soldati, A. Ballardini and D. Giacomini, *ChemSusChem*, 2014, **7**, 2684–2689.
240 C.-S. Goh, D. Milburn and M. Gerstein, *Current Opinion in Structural Biology*, 2004, **14**, 104–109.
241 I. Fridovich, *J. Biol. Chem.*, 1970, **245**, 4053–4057.
242 D. A. Evans, M. D. Ennis and D. J. Mathre, *J. Am. Chem. Soc.*, 1982, **104**, 1737–1739.
243 S. Song, S.-F. Zhu, Y. Li and Q.-L. Zhou, *Org. Lett.*, 2013, **15**, 3722–3725.
244 M. Sakuma, A. Sakakura and K. Ishihara, *Org. Lett.*, 2013, **15**, 2838–2841.
245 T. Uemura, X. Zhang, K. Matsumura, N. Sayo, H. Kumobayashi, T. Ohta, K. Nozaki and H. Takaya, *J. Org. Chem.*, 1996, **61**, 5510–5516.
246 Z.-Y. Li, S. Song, S.-F. Zhu, N. Guo, L.-X. Wang and Q.-L. Zhou, *Chin. J. Chem.*, 2014, **32**, 783–787.
247 K. Bowden, I. M. Heilbron, E. R. H. Jones and B. C. L. Weedon, *J. Chem. Soc.*, 1946, 39.
248 G. T. Suárez and M. Fernández, Oxidation of Primary Alcohols to Carboxylic acids: a

Guide to current Commen Practice, Wilet New York, 1st edn. 2006, 1–4.
249 M. J. Schultz, C. C. Park and M. S. Sigman, *Chem. Commun.*, 2002, 3034–3035.
250 A. Dijksman, A. Marino-González, A. Mairata i Payeras, I. W. C. E. Arends and R. A. Sheldon, *J. Am. Chem. Soc.*, 2001, **123**, 6826–6833.
251 L. Sie Yon, F. N. Gonawan, A. H. Kamaruddin and M. H. Uzir, *Ind. Eng. Chem. Res.*, 2013, **52**, 9441–9453.
252 W. Carruthers and I. Coldham, Modern Methods of Organic Synthesis, Cambridge University Press, UK 2004, 1–4.
253 K. R. Campos, S. Lee, M. Journet, J. J. Kowal, D. Cai, R. D. Larsen and P. J. Reider, *Tetrahedron Letters*, 2002, **43**, 6957–6959.
254 K. Omura and D. Swern, *Tetrahedron*, 1978, **34**, 1651–1660.
255 M. S. Taylor and E. N. Jacobsen, *Angew. Chem. Int. Ed.*, 2006, **45**, 1520–1543.
256 P. G. Wuts and T. W. Greene, 2006, 1–1112.
257 S. Kara, D. Spickermann, J. H. Schrittwieser, A. Weckbecker, C. Leggewie, I. W. C. E. Arends and F. Hollmann, *ACS Catal.*, 2013, **3**, 2436–2439.
258 G. de Gonzalo, G. Ottolina, F. Zambianchi, M. W. Fraaije and G. Carrea, *'Journal of Molecular Catalysis. B, Enzymatic'*, 2006, **39**, 91–97.
259 O. Ulbert, T. Fráter, K. Bélafi-Bakó and L. Gubicza, *'Journal of Molecular Catalysis. B, Enzymatic'*, 2004, **31**, 39–45.
260 C. A. G. N. Montalbetti and V. Falque, *Tetrahedron*, 2005, **61**, 10827–10852.
261 B. M. Trost, S. V. Ley and I. Fleming, 1991, **7**.
262 B. L. Bray, *Nature Reviews Drug Discovery*, 2003, **2**, 587–593.
263 E. Valeur and M. Bradley, *Chem. Soc. Rev.*, 2009, **38**, 606–631.
264 D. J. C. Constable, P. J. Dunn, J. D. Hayler, G. R. Humphrey, J. L. Leazer Jr, R. J. Linderman, K. Lorenz, J. Manley, B. A. Pearlman, A. Wells, A. Zaks and T. Y. Zhang, *Green Chem.*, 2007, **9**, 411.
265 E. Valeur and M. Bradley, *Chem. Commun.*, 2005, 1164.
266 C. L. Allen and J. M. J. Williams, *Chem. Soc. Rev.*, 2011, **40**, 3405.
267 C. Gunanathan, Y. Ben-David and D. Milstein, *Science*, 2007, **317**, 790–792.
268 Y. Zhang, C. Chen, S. C. Ghosh, Y. Li and S. H. Hong, *Organometallics*, 2010, **29**, 1374–1378.
269 A. Nova, D. Balcells, N. D. Schley, G. E. Dobereiner, R. H. Crabtree and O. Eisenstein, *Organometallics*, 2010, **29**, 6548–6558.
270 K. Ekoue-Kovi and C. Wolf, *Chem. Eur. J.*, 2008, **14**, 6302–6315.
271 A. Goto, K. Endo and S. Saito, *Angew. Chem. Int. Ed.*, 2008, **47**, 3607–3609.
272 J. R. Martinelli, D. A. Watson, D. M. M. Freckmann, T. E. Barder and S. L. Buchwald, *J. Org. Chem.*, 2008, **73**, 7102–7107.
273 C. L. Allen, S. Davulcu and J. M. J. Williams, *Org. Lett.*, 2010, **12**, 5096–5099.
274 S.-M. Lu and H. Alper, *J. Am. Chem. Soc.*, 2008, **130**, 6451–6455.
275 B. P. Babu, Y. Endo and J.-E. Bäckvall, *Chem. Eur. J.*, 2012, **18**, 11524–11527.
276 K.-I. Fujita, Y. Takahashi, M. Owaki, K. Yamamoto and R. Yamaguchi, *Org. Lett.*, 2004, **6**, 2785–2788.
277 K.-I. Fujita, W. Ito and R. Yamaguchi, *ChemCatChem*, 2013, **6**, 109–112.
278 D. J. C. Constable, C. Jimenez-Gonzalez and R. K. Henderson, *Org. Process Res. Dev.*, 2007, **11**, 133–137.
279 J. W. Bunting, K. R. Laderoute and D. J. Norris, *Can. J. Biochem.*, 1980, **58**, 394–398.
280 R. B. Morin and M. Gorman, 2014.
281 C. S. Cho, B. T. Kim, T.-J. Kim and S. C. Shim, *Chem. Commun.*, 2001, 2576–2577.
282 Z. Zhang, Y. Liu, L. Ling, Y. Li, Y. Dong, M. Gong, X. Zhao, Y. Zhang and J. Wang, *J. Am. Chem. Soc.*, 2011, **133**, 4330–4341.
283 Y.-R. Zhang, L. He, X. Wu, P.-L. Shao and S. Ye, *Org. Lett.*, 2008, **10**, 277–280.
284 M. R. Linder and J. Podlech, *Org. Lett.*, 2001, **3**, 1849–1851.
285 F. R. Dastoli and S. Price, *Archives of Biochemistry and Biophysics*, 1967, **118**, 163–165.
286 A. Boisen, T. B. Christensen, W. Fu, Y. Y. Gorbanev, T. S. Hansen, J. S. Jensen, S. K.

Klitgaard, S. Pedersen, A. Riisager, T. Ståhlberg and J. M. Woodley, *Chemical Engineering Research and Design*, 2009, **87**, 1318–1327.
287 T. Werpy, G. Petersen, A. Aden, J. Bozell, J. Holladay, J. White, A. Manheim, D. Eliot, L. Lasure and S. Jones, 2004, 1–77.
288 B. Saha, S. Dutta and M. M. Abu-Omar, *Catal. Sci. Technol.*, 2011, **2**, 79.
289 E. Gubbels, L. Jasinska-Walc and C. E. Koning, *J. Polym. Sci. A Polym. Chem.*, 2012, **51**, 890–898.
290 C. H. R. M. Wilsens, Y. S. Deshmukh, B. A. J. Noordover and S. Rastogi, *Macromolecules*, 2014, **47**, 6196–6206.
291 C. Moreau, M. N. Belgacem and A. Gandini, *Top Catal*, 2004, **27**, 11–30.
292 J. N. Chheda, G. W. Huber and J. A. Dumesic, *Angew. Chem. Int. Ed.*, 2007, **46**, 7164–7183.
293 P. Lanzafame, G. Centi and S. Perathoner, *Catalysis Today*, 2014, **234**, 2–12.
294 Y. Y. Gorbanev, S. K. Klitgaard, J. M. Woodley, C. H. Christensen and A. Riisager, *ChemSusChem*, 2009, **2**, 672–675.
295 A. Villa, M. Schiavoni, S. Campisi, G. M. Veith and L. Prati, *ChemSusChem*, 2013, **6**, 609–612.
296 N. K. Gupta, S. Nishimura, A. Takagaki and K. Ebitani, *Green Chem.*, 2011, **13**, 824.
297 S. E. Davis, B. N. Zope and R. J. Davis, *Green Chem.*, 2012, **14**, 143.
298 M. A. Lilga, R. T. Hallen and M. Gray, *Top Catal*, 2010, **53**, 1264–1269.
299 T. Mallat and A. Baiker, *Chem. Rev.*, 2004, **104**, 3037–3058.
300 S. Siankevich, G. Savoglidis, Z. Fei, G. Laurenczy, D. T. L. Alexander, N. Yan and P. J. Dyson, *JOURNAL OF CATALYSIS*, 2014, **315**, 67–74.
301 A. S. K. Hashmi and G. J. Hutchings, *Angew. Chem. Int. Ed.*, 2006, **45**, 7896–7936.
302 B. M. Nestl, S. C. Hammer, B. A. Nebel and B. Hauer, *Angew. Chem. Int. Ed. Engl.*, 2014, **53**, 3070–3095.
303 F. Koopman, N. Wierckx, J. H. de Winde and H. J. Ruijssenaars, *Bioresource Technology*, 2010, **101**, 6291–6296.
304 W. P. Dijkman, D. E. Groothuis and M. W. Fraaije, *Angew. Chem. Int. Ed.*, 2014, **53**, 1-5.
305 J. Carro, P. Ferreira, L. Rodríguez, A. Prieto, A. Serrano, B. Balcells, A. Ardá, J. Jiménez-Barbero, A. Gutiérrez, R. Ullrich, M. Hofrichter and A. T. Martínez, *FEBS Journal*, 2015, 1-12.

Publications